Università degli Studi di Ferrara

DOTTORATO DI RICERCA IN

BIOLOGIA EVOLUZIONISTICA E AMBIENTALE

CICLO XXV

COORDINATORE Prof. Guido Barbujani

Biotechnological potential of microalgae: morpho-physiological and biochemical studies

Settore Scientifico Disciplinare BIO/01

Dottoranda

Dott.ssa Martina Giovanardi

Tutor

Prof.ssa Simonetta Pancaldi

Anni 2010/2012

Table of contents

Abbreviations

A	antheraxanthin
ACCase	acetyl-CoA carboxylase
ATPase	ATP synthase
AWP	apple waste product
BM	brackish medium
BN	Blue Native
Chl	chlorophyll
Car	carotenoids
CTAB	cetyltrimethyl ammonium bromide
Cyt	Cytochrome
DCMU	3-(3,4-dichlorophenyl)-1,1-dimethylurea
div	division
DNS	3,5-dinitrosalicylic acid assay
EDTA	Ethylenediaminetetraacetic acid
ES	Erddekokt Salze medium
F_M	maximum PSII fluorescence in the dark adapted state
F_m	recovered maximum PSII fluorescence in the dark adapted state in a sample previously exposed to high light
F_{mM}	maximum PSII fluorescence in the dark adapted state (in experiments where light-induced PSII photoinhibition is also assessed)
F_t	steady-state fluorescence
F_V	variable fluorescence
F_0	minimal fluorescence
GGPP	geranylgeranyl pyrophosphate
Glu	glucose
HL	high light
HPLC	high performance liquid chromatography
kD	constitutive NPQ constant
kf	fluorescence constant
kp	photochemical rate constant
kNPQ	regulated NPQ constant
LHC	light-harvesting complexes
LL	low light
$NADP^+$	nicotinamide adenine dinucleotide phosphate (oxidised)
NADPH	nicotinamide adenine dinucleotide phosphate (reduced)
NDH	NAD(P)H dehydrogenase
NPQ	non-photochemical quenching
NTPs	ribo-nucleotides
OD	optical density
PAGE	polyacrylamide gel electrophoresis
PAM	pulse amplitude modulation
PAR	photosynthetically active radiation
PCR	polymerase chain reaction
Pheo	pheophytin

PQ	plastoquinone
prt	protein
PSI	photosystem I
PSII	photosystem II
PSY	phytoene synhtase
PUFA	polyunsaturated fatty acids
PVDF	polyvinylidene fluoride
Q_A	primary quinone acceptor
Q_B	secondary quinone acceptor
q_E	energy depending quenching
q_I	photoinhibitory quencing
q_T	state-transition quenching
RC	reaction center
RNAi	RNA interference
ROS	reactive oxygen species
RT	room temperature
RT-PCR	reverse transcription - polymerase reaction chain
RuBisCO	ribulose-1,5-biphosphate carboxylase/oxygenase
SDS	sodium dodecyl sulphate
TAG	triacylglycerol
TAP	Tris – acetate – phosphate medium
TEM	transmission electron microscope
V	violaxanthin
wt	wild type
Y(NF)	quantum yield of thermal dissipation associated with inactivated PSII
Y(NO)	combined yield of fluorescence and constitutive thermal dissipation
Y(npq)	yield of non-photochemical quenching
Y(PSII)	yield of PSII photochemistry
Z	zeaxanthin
2D	second dimension

1. General introduction

During these last few decades the search of new sources of agricultural products t' do not affect the Earth's declining agricultural and energy resources is becoming more and more necessary. In fact, several problems which are all associated with the constant growth of the world population have to be solved, such as the limits of Earth's arable lands, the continuing need for more agricultural products appointed to human food, animal feed, raw materials for industries (Döös et al., 2002; Spolaore et al., 2006; Shneider et al., 2011), together with the necessity of finding new renewable sources to compete with the increasing cost and depletion of fossil fuels (Smith et al., 2010). With this in mind, microalgae have gained considerable importance for their possible use in a wide range of applications, that vary from simple biomass production to valuable products with commercial and ecological implications (Pulz and Gross, 2004).

1.1. Diversity of microalgal groups

Microalgae are photosynthetic microorganisms, with the ability, then, to use solar energy for the synthesis of organic compounds that can be used for food, animal feed, as high-value compounds and potential biofuels (Chisti, 2007). These organisms can be found in all existing Earth ecosystems, both aquatic and terrestrial, and include a big variety of species living in a wide range of environmental conditions, such as fresh, brackish or marine waters, high temperatures, even up to 45°C, and acid or alkaline conditions (Aaronson and Dubinsky, 1982; Hu et al., 2008; Mata et al., 2010). Moreover, they usually have the potential to adapt to diverse habitats, as well as the ability to efficiently modify their metabolism in response to changes in environmental conditions (Gushina and Harwood, 2006; Leonardi et al., 2011).

Taxonomically, microalgae have been classified on the basis of the following main criteria: i) photosynthetic pigments, ii) storage reserves and iii) nature of cell covering (van den Hoek, 1995; Tommaselli, 2004). Moreover, further cytological and morphological characters have been taken into consideration, such as the occurrence of flagellate cells and the structure of flagella, the modality of nuclear and cell division, the presence of an

envelope of endoplasmic reticulum around the chloroplast and the possible connection between the endoplasmic reticulum and the nuclear membrane (Tommaselli, 2004). In 1989 Lee was one of the first scientists that classified these photosynthetic organisms in different groups on the basis of the evolution of the plastid, which sometimes can be surrounded by additional membranes originating from the endoplasmic reticulum (Tommaselli, 2004). In particular:

- *Glaucophyta*, *Rhodophyta* and *Chlorophyta* have the plastid surrounded by only two membranes;
- *Dinophyta* and *Euglenophyta* have the plastid surrounded by one additional membrane;
- *Heterokontophyta* have the plastid surrounded by two additional membranes.

The Division *Chlorophyta* represents one of the greatest group of algae, whose members are widespread in all aquatic environments, with a big morphological variability, ranging from microscopic (with or without flagella) to macroscopic organisms (Tripodi, 2006; Tommaselli, 2004). These microalgae have in common several characteristics other than the chloroplast enclosed by a double membrane:

- chlorophylls (Chl) *a* and *b* as photosynthetic pigments, together with α- and β-carotene, xantophylls and other carotenoids (Car) as accessory pigments (Tripodi, 2006; Leonardi et al., 2011). The photosynthetic pigment profile is very similar to that of higher plants (Deveraux et al., 1990). In fact, green algae and higher plants belong to the same group of *Viridiplantae*;
- starch (α-1,4-linked polyglucane, with α-1,6 ramifications) as storage product, exclusively synthesized and accumulated inside the chloroplast. When a pyrenoid is present, starch is found around this structure, which is frequently crossed by one or more thylakoids. Starch granules can also be present embedded in the stroma (Dodge, 1973);
- cellulose as the main component of the cell wall (Tommaselli, 2004).

The group includes coccoid, unicellular or colonial flagellates, multicellular or multinucleate filaments. Furthermore, a very wide variety in the chloroplast morphology is observed among the different algae, thus the plastid is considered an important taxonomic character (Tripodi, 2006). The *Chlorophyta* are also commonly named “green algae” because of the characteristic bright-green colour that is conferred to the cells by the pigment profile

(Leonardi et al., 2011). However, exceptions can be found in this group. In fact, some microalgae accumulate Car under certain conditions (usually stress conditions) of growth and, for this reason, they acquire a deep red to purple colouring (Tommaselli, 2004). An example is given by *Haematococcus pluvalis (*Fig. 1 a), whose cells are converted to cysts and astaxanthin, which confers an orange-red colour, is accumulated inside the protoplast when the growth conditions become unfavourable (Tommaselli, 2004; Damiani et al., 2010). The Division comprises 4 different Classes. Among them, the *Chlorophyceae* Class is considered the largest taxonomic group in which the microalgae exploited for commercial application can be found. *Chlamydomonas* sp. (Fig. 1 b), for example, is often used in laboratories for molecular biology studies and is considered a model organism (Harris et al., 2001; Leonardi et al., 2011), whereas *Dunaliella* sp. (Fig. 1 c), *Haematococcus* sp. and *Chlorella* sp. (Fig. 1 d) are considered natural sources of industrially useful products (Spolaore et al., 2006).

The *Rhodophyta* Division includes around 4000 species, mainly inhabiting marine waters (Tripodi, 2006). This group of organisms is mainly represented by macroalgae, while the unicellular forms are less common (Tommaselli, 2004). The *Rhodophyceae* are also called "red algae" because of the characteristic colour of the tallus, which is given by accessory pigments, the phycobiliproteins (phycoerythrin and phycocyanin), associated with the Chl *a* (and sometimes the Chl *d*), as well as the presence of α- and β-carotene and xantophylls (Tripodi, 2006). Floridean starch (β-1,4-linked glucan) is accumulated in the cytoplasm as a storage product. The cell wall is composed by a microfibrillar layer of cellulose or xilan, but the main components are amorphous polysaccharides (mucilage), usually agar or carrageenans. The morphology of the plastid is very variable in this group of organisms, however single thylakoids (never differentiated in grana and intergrana; Pancaldi et al., 2011), phycobilisomes and pyrenoids are always present inside the organule (Tommaselli, 2004). Red algae represent the majority of the seaweeds. Commercial exploitation of this group of organisms involves the extraction and employment of the mucilage from the cell wall (Tommaselli, 2004).

The *Dynophyta* Division embraces unicellular biflagellate planktonic algae living in fresh and marine waters. These organisms have the chromosomes always condensed inside the nucleus, starch accumulated outside the chloroplast, Chls *a* and c_2 and Car, including peridinin, as pigments (Tripodi, 2006; Tommaselli, 2004; Pancaldi et al., 2011). A great

variety in morphology and size is present in these group of organisms. They commonly have a cell covering structure (theca) that differentiates them from other algal groups (Tripodi, 2006). Cells can be indeed either armored or unarmored. Armored species have thecae formed by cellulose plates, which are key features used for their identification, surrounding the cell wall (Tommaselli, 2004). The theca can be smooth and simple or laced with spines, pores and/or grooves and can be highly ornamented (Tripodi, 2006). Dynophalgellates are known to produce highly toxic large blooms, and for this reason have attracted a lot of negative attention from the general public (Tripodi, 2006). Moreover, Dynophlagellates are considered an important source of ω-3-unsaturated fatty acid, such as eicosapentaenoic and docosaesaenoic acids (Tommaselli, 2004).

The *Heterokontophyta* Division includes nine classes of organisms (van den Hoek 1995), which differ in pigment composition, cell wall nature and structure of the flagella. When present, they always have unequal lengths (Tripodi, 2006). The *Heterokontophyta* represent a very important group of photosynthetic organisms, as they form most of the marine phytoplankton (Tripodi, 2006). The storage product is chrysolaminarin (β-1,3-linked glucan), but also lipids can be highly accumulated inside the cytoplasm. The chloroplast contains Chls *a* and *c* and Car such as β-carotene and xantophylls, which confer the characteristic "gold-green" colour to the cells (Tripodi, 2006). The *Eustigmatophyceae* and the *Bacillariophyceae* classes include species which are used for commercial applications (Leonardi et al., 2011). The *Eustigmatophyceae* Class embraces unicellular, very small, coccoid organisms that are often mistaken for green-microalgae because of the similarity in morphology, reproduction, cell colour and chloroplast structure. These organisms contain only Chl *a* inside the chloroplast, whereas violaxanthin is the major light-harvesting accessory pigment. Moreover, the structure of the glucidic storage product is unknown (Leonardi et al, 2011). One of the most important microalgae belonging to this Class is *Nannochloropsis* sp., well known for its ability to accumulate polyunsaturated fatty acids, mainly eicosapentaenoic acid, used for biofuel production (Boussiba et al., 1987; Rodolfi et al., 2009; Simionato et al., 2011). The *Bacillariophyceae* Class includes diatoms, a very conspicuous number of golden-brown unicellular microorganism (Tommaselli, 2004) with an immense variety of shapes (Leonardi et al., 2011). They have indeed a siliceous cell wall, the frustule, showing different structures and ornamentations, which are used as key features

for diatom classification. These organisms have often been exploited for commercial applications. In fact, deposits of fossil diatoms are involved in filtration and absorption processes, whereas the employment of these microalgae in aquaculture is pursued because of their ability of accumulating polyunsaturated fatty acids inside living cells (Pohl, 1982; Tommaselli, 2004).

1.2. The relevance of microalgal biotechnology

The biotechnology of microalgae can be considered the youngest branch of algal biotechnology and has gained significant importance in recent decades for the possibility of employing these organisms for different commercial applications (Pulz and Gross, 2004; Harun et al., 2010). The great taxonomic diversity, the usually fast and easy growth, the rapid adaptation of some microalgae which live in extreme conditions to different environments, and so the possibility to control the production of some bioactive molecules by the manipulation of the cultivation systems make these organisms a very interesting natural source of new compounds with biological activity that could be used as functional ingredients (Plaza et al., 2008). Moreover, recent developments in microalgal genetic engineering has opened up the possibility to use these organisms as “green cell- factories”, for the overproduction of traditional algal compounds or the production of new molecules of interest (León-Bañares et al., 2004). Nowadays there are numerous commercial applications of microalgae. They are indeed used to enhance the nutritional value of food and animal feed, they can be incorporated into cosmetics, they are cultivated for the extraction of highly-valuable molecules such as carotenoids, polyunsaturated fatty acids with more than 18 carbons (PUFA; Gill et al., 1997; Certik et al., 1999) and other lipids, which can be converted into biofuels (Spolaore et al., 2006; Harun et al., 2010). Moreover, they are sometimes involved in bioremediation processes (Baumgarten et al., 1999; Torres et al., 2008; Bathnagar et al., 2009; Levine et al., 2011). However, among all the products of microalgal biotechnology the biomass itself represents the most important one in terms of production amount and economic value (Pulz and Gross, 2004).

1.2.1. Algal biomass for human nutrition

The chemical composition of microalgae (and algae in general) gives basic information on the nutritive potential of the algal biomass (Becker, 1988). Microalgae are indeed able to compete with other human food sources such as yeast, meat, milk, rice or soybean (Spolaore et al., 2006) as they are rich in proteins, lipids, carbohydrates, vitamins, pigments and enzymes (Harun et al., 2010). Microalgae for human nutrition are usually available under different forms, such as tablets, capsules and liquids (Pulz and Gross, 2004; Spolaore et al., 2006). The green algae *Chlorella* and *Dunaliella* and the cyanobacterium *Spirulina* (*Arthrospira*) represent the few strains that are currently used for human nutrition (Spolaore et al., 2006; Brennan and Owende, 2010; Harun et al, 2010). *Chlorella* is known to have health-promoting effects thanks to the accumulation inside cells of β-1,3-glucan, which is an active immunostimulator, a free-radical scavenger and a reducer of blood lipids (Spolaore et al., 2006). On the other hand, *Dunaliella salina* is exploited for its ability to accumulate large amounts of β-carotene and is used in powder as an ingredient of dietary supplements and functional food (Spolaore et al., 2006).

1.2.2. Algal biomass for animal nutrition

It has been shown that low amounts of microalgal biomass, in particular derived from the organisms belonging to the genera *Chlorella*, *Scenedesmus* and *Spirulina*, can positively affect the physiology of animals, improving immune responses, fertility, weight control, health skin and coat lustrousness. For this reason, microalgae are usually added as a valuable feed supplement in animal nutrition (Pulz and Gross, 2004; Spolaore et al., 2006; Brennan and Owende, 2010). For example, it has already been reported their exploitation in poultry feed to replace conventional protein sources, because microalgae usually contain up to 5-10% of proteins (Harun et al., 2010). Microalgae are also at the basis of the fish natural food chain and, for this reason, are widely used in aquaculture as a food source for larvae of many species of molluscs, crustaceans and fishes, as well as they are employed for zooplankton production (Pulz and Gross, 2004). Among the several species that are commonly used for these purposes, the green algae *Haematococcus pluvialis* and *Dunaliella salina* are famous for enhancing the colour of mussels and salmonids (Spolaore et al., 2006).

1.2.3. Microalgae as a source of valuable substances

Microalgae can be cultivated for their capability of accumulating high amounts of pure molecules, which can be differently produced depending on the taxonomic position and the physiology of each strain (Pulz and Gross, 2004; Spolaore et al., 2006). Among these molecules, PUFA play an important role as they are known to reduce the risk of cardio-vascular diseases (Ruxton et al., 2004). Microalgae are the first producers of PUFA, in fact animals and higher plants are unable to synthetize these molecules. Despite fishes are considered an important source of PUFA, they also obtain them from the phytoplankton (Spolaore et al., 2006). Microalgal PUFA are already used as additives in infant milk formula. Moreover, chickens are fed with microalgae to produce ω-3- enriched eggs. Currently, docosahexaenoic acid (DHA) is the only algal PUFA that is commercially available, because algal extracts are not yet competitive sources of eicosapentaenoic, ϒ-linoleic and arachidonic acids against other primary sources (Brennan and Owende, 2010). Among polysaccharides, agar agar, alginates and carrageenans are the main available products extracted in particular from *Rhodophyta* and are used in different fields of industry, as well as in cosmetics, because of their rheological gelling or thickening properties (Pulz and Gross, 2004). Moreover, polysaccharides from microalgae also have a pharmaceutical importance for their immune response enhancing activity (Namikoshy, 1996). As microalgae are photosynthetic organisms, they are also very rich in pigments. Chlorophyll is indeed one of the most valuable compounds which are extracted from these organisms, and it is usually employed as a natural food colouring agent and for pharmaceutical purposes, because of its antioxidant and antimutagenic properties (Harun et al., 2010; Hosikian et al., 2010). It is known that most algae cultured under optimum conditions contain about 4% dry weight of Chl (Harun et al., 2010). Car are also normally extracted from microalgae and used for a wide range of applications (Brennan and Owende, 2010). β-carotene, astaxanthin, but also lutein, zeaxanthin, lycopene and bixin (Spolaore et al., 2006) are not only used as a natural food colorant, as additive for animal feed and as a source of pro-vitamin A, but also find application in cosmetics (Del Campo et al., 2000; Spolaore et al., 2006). Moreover, Car are used in pharmaceutical for their intrinsic anti-inflammatory properties and therapeutic chemopreventive anticancer effects, linked to their capability of acting as quencher against reactive oxygen species (Guerin et al., 2003; Spolaore et al., 2006). The commercial

production of carotenoids from microalgae competes with the synthetic production. However, although the synthetic forms are less expensive, Car production from microalgae has the advantage of supplying natural isomers in the natural ratio (Spolaore et al., 2006). Among green algae, *D. salina* is the most suitable source of β-carotene, which is accumulated inside cells at concentrations up to 14% dry weight (Borowitzka and Borowitzka, 1988; Brennan and Owende 2010, Leonardi et al., 2011). *H. pluvialis* is instead the main source of astaxanthin, which is accumulated at concentrations around 1-8% dry weight (Boussiba and Vonshak, 1991; Guerin et al., 2003; Damiani et al., 2010).

1.2.4. Bioremediation with microalgae

For the obtainment of the microalgal biomass and the optimisation of productivity, several cultivation factors must be taken into account, such as available nutrients, pH, light, cultural cell density, temperature and contamination by other microorganisms. Among nutrients, nitrogen and phosphorous are essential (Markou and Georgakakis, 2011). Nitrogen content varies from 1 to 10% in the microalgal biomass and depends upon the amount, the availability and the type of nitrogen source (NO_3^-, NO_2^- or NH_4^+; Grobbelaar, 2004; Markou and Georgakakis, 2011). It has been estimated that the large-scale production of microalgal biomass requires 8-16 tons N/ha as fertilizer. These quantities not only highly affect the costs of the biomass production, but also raise questions about their environmental impact (Levine et al, 2011; Markou and Georgakakis, 2011). Conversely, phosphorous often represents an important growth limiting factor (Grobbelaar, 2004; Markou and Georgakakis, 2011) and has to be supplied in excess because of its scarce bioavailability (Chisti, 2007). However, nutrients for algal production can be supplied from municipal, industrial or agricultural waste and wastewater (Martínez et al., 2000; Levine et al., 2011). The intensification of the agro-industry (Markou and Georgakakis, 2011) and of the industrialisation (Martínez et al., 2000), indeed, has resulted in an excess of waste and wastewater rich in organic and inorganic pollutants, generating problems such as eutrophication, surface and ground water pollution, putridity and odours, gas emissions, as well as their land disposal (Markou and Georgakakis, 2011). Aerobic and anaerobic digestion is often used for the removal of the organic pollutants, however these treatments have a minimal effect on the management of the inorganic pollutants, mainly nitrogen and phosphorous, whose bio-availability is instead increased by these processes (Levine et al.,

2011; Markou and Georgakakis, 2011). As microalgae are able to grow autotrophically at low C/N ratios (Baumgarten et al., 1999), they can be easily cultivated in diluted waste and wastewater, in order to allow growth and simultaneously remove the pollutants in a bioremediation process (Baumgarten et al., 1999; Martínez et al., 2000; Mata et al., 2010; Levine et al., 2011; Markou and Georgakakis, 2011). Among agro-industrial wastes, the most studied are pig and cattle wastes (Markou and Georgakakis, 2011). However, other animal manures such as poultry (Cheung and Wong, 1981; Iyovo et al., 2010) and dairy manure (Wang et al., 2010; Levine et al, 2011) have already been tested for the cultivation of green algae, showing a significant reduction in the nitrogen and phosphate content.

1.3. Microalgae as a promising source of biofuel

The global energy demand is dramatically increasing every day since the beginning of the industrial revolution, in the late 18^{th} century (Mussgnug et al., 2010). Nowadays, the search for new carbon-neutral energy resources has become necessary, because of the constant increase in oil prices, the fossil fuels depleting supplies and, most important above all, the strong global concern about climate change (Chisti, 2007; Smith et al., 2010; Stephens et al., 2010). In recent years, several environment-friendly renewable sources have been investigated as an alternative to fossil fuels (Mussgnug, 2010). Among them, photovoltaic, wind and wave power, geothermal and solar thermal have been designed for the production of electricity (Stephens et al., 2010), whereas feedstock from photosynthetic plants have been used for the production of potential renewable and carbon neutral fuels (biofuel) (Chisti, 2007; Smith et al., 2010; Brennan and Owende, 2010; Mata et al., 2010; Scott et al., 2010; Stephens et al., 2010). Up to now, the most common biofuels are bio-ethanol, obtained from corn starch, sugar cane or sugar beet, and biodiesel from oil crops (Smith et al., 2010; Mata et al., 2010). However, it has been estimated that unsustainably large cultivation areas would be required in order to satisfy the global energy demand (Chisti, 2007; Scott et al., 2010; Stephens et al., 2010). Moreover, the use of plant biomass for energy would enter in competition with food and feed production, which also requires more and more land for the cultivation of food crops, because of the constantly increasing world population (Mussgnug et al., 2010; Stephens et al., 2010). During these last recent

years, however, many research reports and articles have started to focus on microalgae as a potential feedstock for biofuel production (Chisti, 2007; Li et al., 2008a, 2008b; Hu et al., 2008; Schenk, 2008; Smith et al., 2010; Brennan and Owende, 2010; Mata et al., 2010; Mussgnug et al., 2010; Stephens et al., 2010). There are several advantages in using microalgae for the production of biofuel instead of higher plants:

- microalgae have a higher photosynthetic efficiency with respect to higher plants, converting to biomass more than 10% of the solar energy, instead of 0.5% converted by crops (Smith et al., 2010);
- from a practical point of view, microalgae are easy to cultivate and grow very fast (1-3 doublings per day) (Hu et al., 2008; Scott et al., 2010), using limited land resources and avoiding the competition with food crops (Li et al., 2008a; Smith et al., 2010);
- microalgae grow almost everywhere, as only sunlight and some nutrients are required (Mata et al., 2010). Some of them tolerate marginal lands such as deserts and arid lands, not suitable for conventional agriculture (Hu et al., 2008);
- less water is needed to cultivate microalgae as compared to the amount required for oil crops (Li et al., 2008a);
- nutrients such as nitrogen and phosphorus can be recycled from a variety of wastewater sources, coupling biomass and biofuel production to the additional benefit of bioremediation (Hu et al., 2008; Li et al., 2008a);
- CO_2 from flue gases emitted from power plants and other resources can be used by microalgae to enhance grow and obtain biomass, contributing to reduce emission of this greenhouse gas (Hu et al., 2008; Stephens et al., 2010);
- if grown inside photobioreactors, biomass can be produced throughout the year, reaching a theoretical annual productivity ten times higher than that of terrestrial plants (Hu et al., 2008).

Microalgae can be used as feedstock for the production of several biofuels, such as biodiesel, methane, ethanol and hydrogen, based on the algal strains (Mussgnug et al., 2010; Scott et al., 2010) and hence on their efficiency in the production of starch, sugars and oils (Stephens et al., 2010).

1.3.1. Thermochemical and biochemical conversion of the algal biomass

Basically, the microalgal biomass can be converted into energy via thermochemical or biochemical technologies (Brennan and Owende, 2010). Thermochemical conversion includes different processes such as gasification (Hirano et al., 1998), thermochemical liquefaction (Dote et al., 1994) and pyrolysis (Miao and Wu, 2004; Miao et al., 2004), involved in the obtainment of bio-oil burning biomass at different medium-high temperatures and under different pressure conditions, depending on the technology used (Brennan and Owende, 2010). Biomass can also be directly burned in a combustion process in presence of air at high temperatures, converting the stored chemical energy in the biomass into gases (Brennan and Owende, 2010; Scott et al., 2010). On the other hand, biochemical conversion includes processes such as the biomass fermentation, in order to obtain bioethanol, biomethane and bio-hydrogen (Chisti, 2007; Li et al., 2008a; Harun et al., 2010). Bioethanol is obtained by fermentation of the sugars and proteins contained in the biomass. Even if literature on algae fermentation is very rare, the production of bioethanol from microalgae leads to several advantages, such as the very scarce energy consumption and the simple technology. Besides, the CO_2 produced as by-product can be recycled as carbon source for microalgae during the cultivation process (Harun et al., 2010). Biomethane is produced as a by-product of the anaerobic fermentation of the microalgal biomass to obtain biogas (Harun et al., 2010; Mussgnug et al., 2010). Research in this field using microalgae as feedstock is very limited (Mussgnug et al., 2010), however conversion efficiency is estimated to be high because of the low content of cellulose and the absence of lignin inside the biomass (Harun et al., 2010). Unfortunately, higher costs compared with grass and wood, usually employed for the purpose, have been reported, so commercial application have not been implemented yet (Harun et al., 2010). The hydrogen production in green algae has been discovered in 1940s (Gaffron and Rubin, 1942) and concerns the conversion of hydrogen ions into molecular H_2 by hydrogenase enzymes activated under anaerobic conditions (Ghirardi et al., 2000; Brennan and Owende, 2010). Among microalgae, *Chlamydomonas reinhardtii* is one of the most studied for this ability (Kruse et al., 2005; Melis et al., 2000; Mussgnug et al., 2010).

1.3.2. Biodiesel from microalgae

Biodiesel is currently produced by oil crops. However, in order to limit the competition with food crops and so reduce the land surface required for their cultivation, new substrates such as frying and waste cooking oils, tallow, lard and animal oils have recently been taken into consideration for the purpose (Chisti, 2007; Mandal and Mallick, 2009). Nevertheless, the combined production of biofuels from traditional oil crops and these new sources of biodiesel is still not sufficient for the satisfaction of the global energy demand for transportation fuels (Chisti, 2007; Smith et al., 2010). It is known for many years that some microalgae are able to produce biomass yield containing high percentages of oils (Aaronson et al., 1980). These oils are mainly accumulated inside cells in the form of triacylglycerols (TAGs), which can be extracted and used for the production of biodiesel via simple transesterification processes (Smith et al., 2010). As shown in Tab. 1, the oil content is very similar in microalgae and oil crops (Mata et al., 2010). However, the fast and easy growth throughout the year and the high photosynthetic efficiencies allow microalgae to reach higher biomass productivities, resulting in higher lipids yields per land surface unit (Chisti, 2007; Mata et al., 2010). In this way, microalgae seem to be the only source of biodiesel that could compete with the fossil fuel in the really next future (Chisti, 2007; Smith et al., 2010; Mata et al., 2010; Demirbas and Demirbas, 2011). In Tab. 2 microalgae known to accumulate lipids inside cells and the relative percentages of oil on dry weight are reported. Oil levels between 20 and 50% are quite common, although some microalgae, such as *Botryococcus braunii*, are able to accumulate lipids up to 75% (Chisti, 2007), even if biomass yields are consequently lowered (Hu et al., 2008). However, when many microalgae are grown under stress conditions, the lipid production is triggered (Hu et al., 2008). Nitrate depletion is the most commonly reported nutritional-limiting factor known to promote lipid accumulation (Tornabene et al., 1983; Li et al., 2008b; Hu et al., 2008; Pruvost et al., 2009; Leonardi et al., 2011; Pruvost et al., 2011). In fact, when nitrogen is limiting, protein synthesis is inhibited and the excess of carbon and energy produced during photosynthesis is channelled into storage lipids, mainly in the form of TAGs (Scott et al., 2010; Leonardi et al., 2011). Green microalgae are considered the most suitable organisms for the accumulation of lipids (Hu et al., 2008; Demirbas and Demirbas, 2011). This is mainly because they are able to colonize several natural habitats from freshwater to seawater, and moreover because they

can be easily isolated and cultivated under laboratory conditions (Hu et al., 2008). *Chlorella* is considered one of the best candidates for the lipid accumulation, and many studies have been performed with this microalga (Miao and Wu, 2006; Xu et al., 2006; Li et al., 2007; Heredia-Arroyo et al., 2010; Gao et al., 2010). However, many other species are also efficient and productive, and several parameters, such as the ability to grow under specific combination of nutrients or specific environmental conditions have to be taken into consideration during strain selection (Mata et al., 2010). Recently, special attention has been focused on the *Chlorophyta Neochloris oleoabundans* and *Scenedesmus acutus* (Leonardi et al., 2011). In particular, *N. oleoabundans* is well-known for its ability to accumulate up to 50% of lipids, which are TAGs by the 80%, when the microalga is grown under nitrogen starvation (Tornabene et al., 1983; Li et al., 2008b; Leonardi et al., 2011; Baldisserotto et al., 2012; Giovanardi et al., 2013; Popovich et al., 2012).

About the quality of microalgal biodiesel, little information is available in the literature (Francisco et al., 2010). Several parameters have to be considered and, for its acceptability, the microalgal biodiesel have to comply with International Biodiesel Standard for Vehicles (EN14214) in Europe (Chisti, 2007; Leonardi, 2011) and with ASTM Biodiesel Standard D6751 in the United States (Knothe, 2006). In general, the fatty acids mainly findable in the majority of the land plants are palmitic, stearic, oleic, linoleic and linolenic (Miao and Wu, 2006; Knothe, 2008; Leonardi et al., 2011). These fatty acids are well represented in some microalgae recently examined (Leonardi et al., 2011). However, microalgae are also richer than higher plants in PUFA, which are considered more susceptible to oxidation during storage, and so are not suitable for the acceptability of microalgal biodiesel (Chisti, 2007). This problem could be overcome by partial catalytic hydrogenation of the microalgal oil (Jang et al., 2005; Dijkstra, 2006; Chisti, 2007). Currently, some promising microalgal species have been identified (Leonardi et al., 2011). Among them, oils from *S. obliquus* meet all the required specifications, whereas *N. oleoabundans*, *D. tertiolecta* and *C. vulgaris* are suitable candidates if oils are used in mixtures with other oils (Leonardi et al., 2011).

The production of biodiesel from microalgae is not economically feasible yet and considerable investment in technological development and technical expertise is still needed for it to become a reality (Francisco et al., 2010; Mata et al., 2010; Wijffels and Barbosa,

2010). Among challenges which need to be pursued, the most important are obtaining high biomass yields, high lipid contents and adequate fatty acid profiles (Leonardi et al., 2011). In order to reach these targets, a multidisciplinary approach is required, such as the integration of the engineering with discoveries in algal biology (Scott et al., 2010; Wijffels and Barbosa, 2010). The biorefinery concept is also very important in order to reduce the costs of making microalgal biodiesel (Chisti, 2007). In this way, algal biomass could be used after the lipid extraction for animal feed or fermented in order to obtain bio-methane by anaerobic digestion. Moreover, CO_2 from flue gas emissions could be sequestered by cells and nutrient-rich wastewaters could supply all the nutrient required for growth, allowing to reach high biomass yields, matching bioremediation processes and reducing the overall costs (Mata et al., 2010; Scott et al., 2010).

1.4. The difficult binomial biomass production-lipid accumulation and possible strategies to overcome it

At present, the two main areas in which there is a considerable activity in order to optimise the feasibility of the microalgal biodiesel consist in: i) optimising algal growth systems and ii) maximising the rate of TAGs production (Scott et al., 2010). About the first issue, several factors need to be monitored during algal growth. Among these, the most important concern abiotic elements such as light, temperature, nutrient concentration, O_2 and CO_2 availability, pH and salinity and operational elements, such as shear produced by mixing, dilution rate and harvesting frequency (Mata et al., 2010). Conversely, in order to reach high lipid contents, stress conditions, in particular nutrient depletion, are needed (Tornabene et al., 1983, Li et al., 2008a; Li et al., 2008b; Hu et al., 2008; Scott et al., 2010). Obviously, biomass productivity and lipid accumulation are often inversely correlated, as the storage of TAGs inside cells occurs at the expenses of energy used for growth (Wijffels and Barbosa, 2010). Recently, several studies have suggested growth conditions that can be used for the industrial scale-up of lipid production from algae (Scott et al., 2010). For instance, Rodolfi et al. (2009) described a two-stage process in which cells were firstly grown under nutrient-sufficient conditions to allow biomass accumulation, which was subsequently transferred under nutrient depletion in order to induce the lipid synthesis. However,

heterotrophic and mixotrophic growth have also been described as useful tools for obtaining biomass yields rich in lipids (Chisti, 2007; Scott et al., 2010; Brennan and Owende, 2010; Giovanardi et al., 2013), whereas further researches in genetic and metabolic engineering could offer the possibility to improve strains (Wijffels and Barbosa, 2010) and overproduce algal oils (Hu et al., 2008).

1.4.1. Heterotrophic and mixotrophic growth for improving biomass yields

Most of the microalgal cells can be cultured under autotrophic, heterotrophic and mixotrophic conditions (Heredia-Arroyo et al., 2010). Autotrophy is the normal condition of growth, where light is used as energy source in order to fix CO_2 in organic macromolecules. Conversely, heterotrophic cells utilise only organic compounds as carbon and energy source in darkness (Mata et al., 2010; Chen et al., 2011). As has been observed in several studies, biomass accumulation can be highly improved in this way (Chen, 1996; Chen and Wen, 2003; Xu et al., 2006; Chen et al., 2011). Moreover, several studies have shown that high lipid contents were also achieved in some microalgae (Wu et al., 1994; Xu et al., 2006; Heredia-Arroyo et al., 2010; Chen et al., 2011). This effect is mainly due to the alteration of the N:C ratio when the organic carbon source is added to the medium, thus the same effect as if algae were grown under nitrogen depletion (Scott et al., 2010). The heterotrophic cultivation avoids problems concerning the light limitation when algae are grown in large-scale cultivation processes (Chen et al., 2011). Furthermore, the harvesting costs are highly reduced in heterotrophic growth systems because of the high biomass densities achieved (Brenan and Owende, 2010). However, some limitations occur when algae are grown heterotrophically. First of all, not all microalgae are able to grow in the absence of light (Chen and Wen, 2003). Moreover, some high-valuable molecules like pigments are not synthesized in heterotrophic cultures, thus a different type of cultivation needs to be applied for these purposes (Lee et al., 2001). Finally, contaminations occur more easily compared to autotrophic cultures (Scott et al., 2010; Chen et al.,2011). Mixotrophy is termed the condition in which light and organic compounds are simultaneously supplied for growth (Lee, 2001; Xu et al., 2006; Heredia-Arroyo et al., 2010). In this way, photosynthesis and assimilation of the organic carbon proceed concomitantly during the day, whereas during the night less biomass is lost because cells continue to grow using the organic compounds (Lee, 2001; Scott et al., 2010; Stephens et al., 2010). In previous studies, an increase in the

biomass yield has often been observed not only with respect to autotrophic cultures, but also compared with heterotrophic cultures (Ogawa and Aiba, 1981; Martinez and Orus, 1991, Kobayashi et al., 1992; Marquez et al., 1995; Shi and Chen, 1999; Lee, 2001; Yang et al., 2000; Brennan and Owende, 2010). Microalgae can assimilate a variety of organic carbon sources (Chen et al., 2011). Among others, glucose is the preferred, but also acetate, fructose, glycerol and sucrose can be used for growing algae in mixotrophy (Heredia-Arroyo et al., 2010; Chen et al., 2011). However, finding cheaper organic carbon sources is becoming very important in the perspective of limiting costs and allowing feasibility of microalgal exploitation on the large scale (Heredia-Arroyo et al., 2010; Chen et al., 2011). For this reason, several studies are recently focusing on using cheaper organic carbon sources, often coming from high-organic carbon waste products, such as crude glycerol (Liang et al., 2009), corn powder hydrolysed (Xu et al., 2006); molasses (Andrade and Costa, 2007), or organic effluents derived from agri-food industries (Brennan and Owende, 2010; Heredia-Arroyo et al., 2010; Giovanardi et al., 2013). Currently, little information on mixotrophic cultivation of microalgae for the production of lipids is available (Chen et al., 2011). Furthermore, the physiological effects of organic carbon nutrition on photosynthetic activity and on the interaction between autotrophic and heterotrophic metabolism are still partly unknown (Kang et al., 2004; Giovanardi et al., 2013). Then, further studies are needed in order to better understand what is the role of carbon metabolism in energy conversion and improve the performance of microalgal cultures (Yang et al., 2000; Giovanardi et al., 2013).

1.4.2. Metabolic engineering of microalgal physiology

Genetic modification of microalgae has received little attention during the past years, however now it represents a developing area, which can improve biomass productivity and expand the number of microalgal products (León-Bañares et al., 2004; Chisti, 2007; Eriksen, 2008). During the last decade, then, significant advances have been achieved (Radakovits et al., 2010). Molecular engineering can be considered a useful tool that can potentially be targeted to different metabolic pathways of microalgae, in particular in order to (Chisti, 2007):

- increase photosynthetic efficiency for the increment of the biomass yields;
- enhance algae growth rate;
- increase oil content inside cells;
- improve tolerance to environmental variables that can stress or inhibit microalgal growth, such as temperature, pH, salt and other factors (Radakovits et al., 2010);
- alleviate the light saturation phenomenon, reduce photoinhibition and reduce the susceptibility to photooxidation when cells are exposed to high light intensities.

One of the most studied systems for improving the photosynthetic efficiency and/or decreasing the effects of photoinhibition is the reduction of the photosynthetic antenna size (Eriksen, 2008; Radakovits et al., 2010). This approach has two main positive effects: i) reduced antenna size results in lower absorption coefficients per unit of biomass, so that light can penetrate deeply in high-density cultures; ii) as smaller light harvesting complexes (LHC) absorb less light, increased light intensities are needed to saturate each reaction centre, and fewer photons are dissipated as heat and fluorescence (Eriksen, 2008). In this way, cells are also less subjected to photoihnibition (Radakovits et al., 2010). Earlier research by Mussgnug et al. (2007) showed increased biomass productivities under high light when both LHCI and LHCII were knocked down in *Chlamydomonas reinhardtii* by RNAi-based strategy. However, results were referred to laboratory conditions, so it remains to be ascertained how these mutants could perform in large-scale culture conditions (Radakovits et al., 2010).

Metabolic engineering is also being studied for the possibility of modifying the lipid metabolism, in order to enhance the feasibility of algal biodiesel production (Scott et al., 2010). Even if microalgal lipid metabolism has not been studied as much as in terrestrial plants, many genes are homologous, then it can be supposed that at least some of the transgenic strategies used for higher plants could be applied to microalgae as well (Radakovits et al., 2010). In higher plants, several studies have been focused on the overexpression of key enzymes involved in TAGs production, as well as on complementary strategies that reduce lipid catabolism (Scott et al., 2010). In 1995 Dunahay and collaborators overexpressed the native acetyl-CoA carboxylase (ACCase) in the diatom *Cyclotella cryptica*. Despite the activity of the key enzyme was increased by 2-3 folds, no increased lipid production was observed (Eriksen, 2008; Scott et al., 2010), indicating the

complexity in the regulation of this enzyme (Scott et al., 2010). An alternative approach for obtaining increased lipid yields could represent the deletion of metabolic pathways that are involved in the accumulation of high-energy storage compounds, such as starch, in order to let precursor metabolites free and allow their consequent channelling in the desired lipid biosynthetic pathways (Radakovits et al., 2010; Scott et al., 2010). Wang et al. (2009), for instance, have observed an increase in TAGs lipid bodies when two *C. reinhardtii* starch-less mutants were grown under N depletion. Moreover, a starch-less mutant of *Chlorella pyrenoidosa* has also been investigated for its capability of accumulating high amount of PUFA (Ramazanov and Ramazanov, 2006). Genetic engineering of microalgae can be applied not only for the overproduction of lipids for biofuel purposes, but also for the enhancement of the productivity of traditional algal compounds or for the production of new bioactive compounds for industrial and pharmaceutical applications, such as recombinant vaccines, mammalian antibodies and high-valuable compounds such as carotenoids (León-Bañares et al., 2004).

At present, full or near-full genome sequences are available for a very small number of microalgae, and only about 10 different algal species can be transformed (Wijffels and Barbosa, 2010). However, *C. reinhardtii* is the most important species for which most metabolic enginnering tools have been developed (Radakovits et al., 2010; Wijffels and Barbosa, 2010). It can be expected that many other genomes from other important algal strains will be sequenced in the near future, because of the current high interest in the field and of the availability of fast and reliable technologies for genome sequencing (Wijffels and Barbosa, 2010).

1.5. Technologies for microalgal biomass production

Despite the several advantages concerning the use of microalgae instead of higher plants for the production of molecules and biofuel, the cultivation of microalgal biomass is generally more expensive than the cultivation of crops (Chisti, 2007). In fact, several factors can be limiting and need to be constantly controlled, such as temperature, salinity, mixing, light cycle and intensity, pH, gas exchange, cell fragility, cell density and growth inhibition

(Shenk et al., 2008; Mata et al., 2010). At present, open pond and closed photobioreactor technologies have already achieved economic viability (Shenk et al., 2008).

The open pond system has been used since the 1950s and represents the less expensive way to culture microalgae for large scale biomass production (Brennan and Owende, 2010). The most commonly used open pond system is the raceway pond (Fig. 2) (Chisti, 2007; Shenk et al., 2008; Brennan and Owende, 2010). This is usually made of a closed loops, oval shape recirculation channel, 0.15-0.5 m deep, in order to allow light penetration through the water. A paddlewheel is usually placed in order to promote mixing and circulation of both microalgal biomass and nutrients, which are usually introduced in front of it, whereas microalgal biomass is harvested after the whole cycle, behind the paddlewheel (Chisti, 2007; Shenk et al., 2008; Brennan and Owende, 2010). CO_2 is instead provided by the atmosphere. Despite the low costs, several disadvantages affect this system. Biomass productivity is indeed lower compared with closed photobioreactors. This can be attributed to several determining factors, such as evaporative water loss, temperature fluctuation within a diurnal cycle and seasonally, CO_2 deficiency, inefficient mixing and light limitations (Brennan and Owende, 2010). However, the main problem concerns the possibility of contaminations by other undesired algal species and protozoa. Then, sustainable cultivation of a single species in open pond is possible only if extremophiles microalgae are used, such as *D. salina*, an halotolerant *Chlorophyta*, or *Spirulina* sp., which is able to grow in alkaline environments (Shenk et al., 2008).

Closed photobioreactor technology allows to overcome some of the major problems associated with the open pond system (Brennan and Owende, 2010). Tubular, flat plate and column bioreactors (Fig. 3) are typical examples of closed bioreactors (Chisti, 2007; Shenk et al., 2008; Brennan and Owende, 2010). Among them, column photobioreactors are the less expensive, offer the most efficiency mixing, the highest volumetric mass transfer rates and the best controllable growth conditions. In this type of closed bioreactor, the columns are placed vertically, aerated from the flow, usually by gas bubbling, and illuminated through transparent walls by external or internal lights (Erikssen, 2008). However, costs are extremely high compared to the open pond systems. Indeed, in order to avoid the overheating that can occur mainly in summertime, evaporative water cooling systems are necessary. Moreover, artificial illumination is also needed in order to avoid light limitation.

These factors obviously affect the economy of the system (Chisti, 2007; Brennan and Owende, 2010). However, higher costs are compensated by higher productivities, with a consequent decrease in harvesting costs, as lower volume of cultural broth has to be processed to obtain the same quantity of biomass (Chisti, 2007).

1.6. The photosynthetic apparatus in green algae and higher plants

Photosynthetic organisms are obviously influenced by the availability of light for their growth and production performance. When grown in large-scale processes, the quantity of light absorbed from microalgae depends on several factors, such as the position of the cells inside the photobioreactor, the culture density and the cell pigmentation. Different models, all based on the relationship between growth and amount of received light, have been empirically established in order to predict a culture performance. However, most of them do not consider the basic principles of photosynthetic biochemistry, and completely ignore important phenomena that can occur in cells, such as photoinhibition and photoacclimation (Camacho Rubio et al., 2003). Then, a better understanding of the photosynthetic process in microalgae and application of this knowledge in the empirical modelling are required in order to fit all the evaluations.

In plants and green algae, the photosynthetic process occurs inside chloroplast (Fig. 4). This organelle is surrounded by a double membrane mainly composed by phospholipids. Furthermore, a third specialized internal membrane is organised in flattened membranous sacs, creating the thylakoid system. Thylakoids can be usually found stacked, forming the so-called “grana regions”, whereas consecutive grana are linked by non-stacked thylakoids, the “stroma lamellae”. Thylakoids physically separate two different compartments inside chloroplast, the thylakoid lumen, i.e. the space inside thylakoids, and the stroma, the fluid compartment that surrounds the thylakoids (Taiz and Zeiger, 2002; Nelson and Ben-Sherm, 2004).

The overall reaction catalysed during the photosynthetic process is described as follows:

$$6\ CO_2 + 6\ H_2O + \text{light energy} \rightarrow C_6H_{12}O_6 + 6\ O_2$$

O_2, ATP and NADPH are produced as a consequence of the photolysis of water. The so-called light-dependent reactions catalyse the process, which takes place on thylakoids membrane. The high-energy compounds produced are then used during the carbon fixation reactions, or Calvin cycle, which occur in the stroma of the chloroplast and where CO_2 is reduced to sugars (Taiz and Zeiger, 2002).

1.6.1. The role of pigments in photosynthetic membranes

Pigments are used by photosynthetic organisms to harvest light energy, which is then converted to chemical energy and stored to organic macromolecules. On the whole, photosynthetic pigments represent almost the 50% of the total lipids inside thylakoids, whereas the remaining part is represented by galactolipids, small quantities of phospholipids and few sterols (Taiz and Zeiger, 2002). Among photosynthetic pigments, which are associated with proteins to give pigment-protein complexes, Chls are the most important as they are specifically involved in light-energy harvesting. These molecules derive from the δ-aminolevulinic acid and are composed by a tetrapyrrolic ring, with one atom of Mg bound in the centre. Moreover, a long hydrophobic chain composed by phytol allows the molecule fixation inside the thylakoid membrane bilayer. In green algae and higher plants Chl*a* and Chl*b* (Fig. 5) are present. These two molecules differ from each other only for the group bound at carbon atom 3: in the former it is a methyl group, while the latter has a formil group. Chl*a* is the main chlorophyll of green algae and higher plants. It is contained in all reaction centres, but it is also found in light-harvesting complexes. Conversely, Chl*b* is an accessory pigment and it is part of the antenna system.

Car are instead C_{40} tetraterpenes biosynthesized by the central isoprenoid pathway (Fig. 6). They are organised in long polyene chains which present up to 15 carbons conjugated with double bonds. This feature is responsible for their characteristic absorption spectra and their specific photochemical properties (Naik et al., 2003). Car can be distinguished in carotenes, which are hydrocarbons containing only carbon and hydrogen, and xanthophylls, their oxygenated derivatives. The main carotene in photosynthetic membranes is β-carotene, which is mainly found inside the reaction centres, whereas lutein, violaxanthin, zeaxanthin and neoxantin are the main xanthophylls, localized in the antenna systems. Car are accessory pigments, which absorb light and transfer the excitation energy

to Chl. Furthermore, they play an important role for the photoprotection of the photosynthetic membrane, scavenging reactive species of oxygen and limiting the damage caused by photo-oxidation (McCarthy et al., 2004; Szabó et al., 2005).

Plants are able to use only a small fraction of the solar emission spectrum for photosynthesis. This is comprised in the visible region, between 400 and 700 nm, and is called photosynthetically active radiation (PAR). Pigments are indeed able to adsorb only specific wavelengths:

- Chl*a* presents the most intense absorption peak at 440 nm, whereas a second peak is found at 660 nm;
- Chl*b* has a similar absorption spectra, with the first absorption peak at 470 nm and the second at 645 nm;
- Car have characteristic absorption spectra depending on the considered molecule, however all the absorption peaks overlap in the blue region, and so their main absorption can be generalised to be at 470 nm.

Pigments are found in an excited state after they have absorbed a photon. This state in unstable, so the energy is promptly transferred to another molecule in the following ways: i) electron transfer to an acceptor molecule; ii) electron transfer to another pigment by Förster resonance energy transfer process. Chl excitation energy can also be dissipated by i) fluorescence release or ii) energy release as heat (Ruban et al., 2012). Chl*a* is the first electron acceptor in all oxygenic photosynthetic organisms, whereas Chl*b* and Car harvest and transfer light energy to Chl*a* by resonance. Conversely, energy released by heat or fluorescence is considered a side dissipative effect during the photosynthetic process.

1.6.2. The "light-driven" reaction of photosynhtesis

The light reactions are catalysed by four main protein complexes, two photosystems (PSI and PSII), one cytochrome (Cyt) b_6f, and an ATP synthase (ATPase), which are all embedded in the thylakoid membrane and oriented as shown in Fig. 7, so that the water oxidation occurs at the lumen side, whereas the NADPH and ATP produced are released in the stroma (Taiz and Zeiger, 2002). Biochemical composition of these multisubunit protein

complexes has been better elucidated after the invention of the SDS-PAGE technology (Nelson and Ben-Shem, 2004):

- the PSII reaction center (RCII) is composed of two homologous proteins of nearly 40 kDa, D1 and D2. These proteins bind two weakly coupled Chls known as P_{680}, which function as the primary electron donor, one molecule of pheophytin, the Cyt *b559*, required for the correct assembly of the complex, and the plastoquinones (Taiz and Zeiger, 2002). Flanking the reaction center there are two intrinsic light-harvesting proteins, CP43 and CP47, which bind 14 and 16 molecules of Chl*a* respectively. However, most of the Chls which are associated with PSII are located in the peripheral light-harvesting complex II (LHCII). This complex is composed by trimers of Lhcb proteins, which bind around 12-14 Chl*a* and *b* and up to 4 Car each (Nelson and Ben-Shem, 2004). PSII is considered a water-plastoquinone oxidoreductase complex, because its activity is to initiate the photosynthetic electron transfer chain by using light as a driving force and water as the electron source (Daniellson et al., 2006);
- the Cyt b_6f is considered a plastoquinone-plastocyanin oxidoreductase, as its main function is to mediate electron transfer from reduced plastoquinone of PSII to plastocyanin, a small soluble, copper-containing protein of PSI, generating a transmembrane electrochemical proton gradient for ATP synthesis. Cyt b_6f functions as a dimer, and each monomer is composed by 8 subunits: Cyt *f*, Cyt b_6, the Rieske iron-sulfur protein and subunit IV are large subunits, whereas 4 small hydrophobic subunits (PetG, PetL-PetM) are also present (Nelson and Ben-Shem, 2004);
- the PSI RC is composed by 12-14 subunits known as PsaA-PsaL, PsaN and PsaO. The heterodimer PsaA-PsaB forms the heart of PSI and binds a Chl dimer known as P_{700}, the primary electron donor, and 5 electron acceptors, A_0 (Chl *a),* A_1 (phylloquinone) and 3 Fe_4-S_4 iron sulphur centres. The other Psa subunits are involved in binding and coordinating other elements of the reaction centre, such as two further Fe_4-S_4 iron sulphur clusters (PsaC), ferredoxin (PsaC-PsaE) and plastocyanin (PsaF), as well as the LHCI complex (PsaK, PsaG, PsaJ and PsaF) and the LHCII during state transition (PsaH and PsaL). Furthermore, they contribute to the maintenance of PSI integrity (Nelson and Ben-Shem, 2004). LHCI is the extrinsic peripheral light-harvesting complex and is composed by 4 light-harvesting Chl-containing proteins, Lhca1-Lhca4 (Nelson and Ben-Shem, 2004).

Different from LHCII, which contains almost 40-50% of the total pigments in thylakoids, LHCI binds a small part of total pigments, nearly 5-10% (Taiz and Zeiger, 2002);

- ATP synthase (ATPase) is a highly-conserved subunit complex which catalyses ATP synthesis using a transmembrane proton gradient generated by the photosynthetic electron-transport chain. This enzyme is composed by several different subunits, located in stromal and transmembrane regions, called CF_1 and CF_0 respectively. In particular, the whole complex functions as a molecular motor in which there are stationary subunits (I, II, IV, δ, α and β and III) and rotary subunits (ϒ and ε) (Nelson and Ben-Shem, 2004).

During the light-reactions of photosynthesis the electron transfer can be represented in a "Z-scheme" (Fig. 8). At the beginning of the scheme, LHCII complex delivers the light energy that has been absorbed to the RC of PSII (RCII). This excitation energy is funnelled through the antenna pigments, which are organized inside the complex in a descending energy gradient: Car → Chl*b* → Chl*a* → P_{680} of PSII. The consequence of the excitation of P_{680} to P_{680}* is the transfer of an electron to Pheophytin *a*, the primary electron acceptor in RCII:

$$P_{680}^* + Pheo \rightarrow P_{680}^+ + Pheo^-$$

The re-reduction of P_{680}^+ is due to an electron donor, a tyrosine residue of D1 called Y_z, which in turn is reduced by an electron from the water oxidation system: $2H_2O \rightarrow O_2 + 4H^+ + 4e^-$. From $Pheo^-$, the electron is funnelled to the plastoquinone acceptors Q_A and Q_B. After the re-reduction of Q_B with a second electron, 2 protons are retrieved from the stroma side, forming a completely reduced quinone Q_BH_2, which is released into the lipid bilayer of thylakoids and replaced by an oxidized quinone from the membrane quinone pool. Electrons are in this way transported through the Cytb_6f complex to the soluble electron carrier plastocyanin, also located at the lumen side of the thylakoid membrane, and finally plastocyanin provides electrons to the PSI. Solar energy that has been channelled by LHCI allows the excitation of P_{700} to P_{700}*. The primary acceptor in PSI is A_0. From A_0^-, electrons are transferred through a series of carriers to the ferredoxin on the stroma side of the thylakoid membrane and then are used for the reduction of $NADP^+$ to NADPH. The electrochemical proton gradient formed by the photolysis of water and by the plastoquinones which have released protons from the stroma into the lumen side is used for the synthesis of ATP by the ATPase complex (Nelson and Ben-Shem, 2004).

1.7. Non-photochemical quenching induction and role of the xanthopyll cycle on the formation of q_E

Microalgae have evolved the capacity to absorb more PAR light than that needed for their photosynthetic requirements, and so the excess of energy has to be dissipated as heat or fluorescence emission (Müller et al, 2001; Scott et al., 2010). However, under high-light intensities, the photosynthetic RCII becomes progressively saturated (closed), and the energy transfer from the antenna complexes is inhibited because of the lack of electron acceptors, which are all found in the reduced form (Frenkel et al., 2007; Ruban et al., 2012). In this way, potentially harmful excitation energy remains in the photosynthetic membrane and promotes the formation of reactive oxygen species (ROS), causing photooxidative damages to the photosynthetic apparatus, i.e. photoinhibition (Frenkel et al., 2007; Allahverdiyeva and Aro, 2012). In order to avoid photoinhibition, higher plants and green algae have tried to reduce the excess of absorbed energy by means of several mechanisms (Müller et al, 2001; Ruban et al., 2012). Among the short-term regulatory processes which have evolved for the purpose (Ruban et al., 2012), non-photochemical quenching (NPQ) mechanisms, which allow to dissipate energy as heat, have been developed (Müller et al, 2001; Ruban et al., 2012). Three kinetics components contribute to NPQ: i) a rapidly, reversible, ΔpH dependent component, q_E; ii) a state-transition related component, q_T; and iii) a slowly reversible, photoinhibition related component, q_I (Szabó et al., 2005; Allahverdiyeva and Aro, 2012). q_E represents the major component of NPQ. Several studies have demonstrated a correlation between the development of q_E and the accumulation of PsbS, a specific subunits of PSII (Kullheim et al., 2002; Horton et al., 2008). However, the functional role of this subunit and the mechanism involved in the development of q_E are still unclear (Allahverdiyeva and Aro, 2012). Another key component responsible for the formation of q_E is the interconversion of specific xanthophyll pigments mostly bound to LHC, i.e. the xanthophyll cycle (Fig. 9) (Allahverdiyeva and Aro, 2012; Ruban et al., 2012). This cycle is also activated by the decrease in lumen pH due to the excess of light and consists of the conversion from violaxanthin (two epoxide groups) to zeaxanthin (no epoxide groups), which is directly involved in quenching of Chl excitation (Allahverdiyeva and Aro, 2012; Ruban et al., 2012). The accumulation of zeaxanthin is directly correlated with q_E in several plants and under several conditions (Demmig-Adams, 1990; Müller et al, 2001; Ruban et al.,

2012; Allavehrdiyeva and Aro, 2012). Havaux and Kloppstech (2001) showed, in the *Arabidopsis thaliana npq1* mutant, which lacked functional violaxanthin de-epoxidase and so the possibility to convert violaxanthin to zeaxanthin, a reduced q_E under high-light intensities. The strategy adopted by this mutant in order to avoid photoinhibition was to reduce the antenna size to minimize the amount of light that could excite PSII. On the other hand, Rees and colleagues (1992) showed in isolated thylakoids, in which zeaxanthin was accumulated, higher levels of q_E, but only at lumen pH values higher than *in vivo* conditions. However, additional xanthophylls can be involved in q_E formation. Indeed, in the Chlorophyta *Mantoniella squamata*, which presents an incomplete xanthophyll cycle and accumulates antheraxanthin, high levels of q_E are anyway inducible. The role of antheraxanthin has been considered for the explanation of zeaxanthin-indipendent q_E processes also in other studies (Gilmore and Yamamoto, 1993). Therefore, in a given organism, the calculation of the level of de-epoxidation, as the amount of antheraxanthin and zeaxanthin over the total amount of xanthophylls has become a common practice (Müller et al, 2001). Finally, although zeaxanthin is implicated in the formation of q_E, it cannot be considered essential. Indeed, in mutants that accumulate constitutively zeaxanthin, q_E was strictly dependent on the lumen pH (Niyogi et al., 1999), confirming an important role of this factor in the regulation of the xanthophyll cycle (Müller et al., 2001).

1.8. Methods involved in studies of the photosynthetic membranes

In photosynthetic organisms, the correct Chl-protein assembly is necessary in order to have high photosynthetic efficiency. In green microalgae, whose cell volume is usually mainly occupied by the chloroplast, this parameter could be considered an indicator of their wellness conditions, and so an important factor to be taken into account in order to promote the best conditions for obtaining high biomass yields (Simionato et al., 2011; White et al., 2011). Moreover, analyses of the organisation of these complexes and of the interactions between them can be useful to understand their relationships with other metabolic pathways (White et al., 2001). Currently, biophysical and biochemical analyses are used for the purpose. Among the former, the use of Chl*a* fluorescence measurements for the evaluation of the photosynthetic performance in higher plants and green algae is commonly

practised (Baker, 2008). In this thesis, pulse modulation and spectrofluorimetric techniques are considered. Among biochemical techniques, Blue Native polyacrylamide gel electrophoresis (BN-PAGE) has been recently employed to obtain information on the biogenesis and assembly phases of photosynthetic protein complexes in thylakoids and on their native interaction (Eubel et al., 2005; Rokka et al., 2005).

1.8.1. Pulse amplitude modulation (PAM) fluorimetry

PAM fluorimetry is an important fast and non-invasive technique adopted for the measurement of the photosynthetic performance of higher plants and microalgae (White et al., 2011) and concerns the study of the PSII photochemical efficiency based on the amount of light emitted as fluorescence following excitation (Lichtenthaler, 2005; Baker, 2008). Two cases are considered for the study of PSII with PAM fluorimetry: i) dark-adapted samples and ii) light-adapted samples. Dark-adapted samples are incubated in darkness before analysis. In these conditions, Q_A is completely oxidised and PSII is non-saturated, i.e. in the so-called "open" state. If a weak red (650 nm) measuring light is applied, the minimal fluorescence value F_0 is detected. If samples are then exposed to a short pulse of saturating light (typically less than one second at several thousand μmol photons m^{-2} s^{-1}), Q_A is completely reduced and PSII enters the "closed" state. Under these conditions, the maximum fluorescence value F_M is measured (Baker, 2008). The difference between F_M and F_0 is defined the "variable fluorescence", F_V, whereas the ratio F_V/F_M is defined the maximum quantum yield of PSII in the dark-adapted state. In non-stressed plants, F_V/F_M values are generally around 0.8, i.e. the 80% of the absorbed light is used during the photochemical reaction by PSII, whereas the remaining is involved in dissipative processes, fluorescence included (Hendrickson, 2004). Conversely, in non-stressed microalgae the ratio is lower than in higher plants, as was observed by Kromkamp and Peene (1999), around 0.6-0.7 in phytoplankton. Moreover, almost constant F_V/F_M values have been found in non-stressed cultures (White et al., 2011). However, when photosynthetic organisms are exposed to biotic and abiotic stresses, a decrease in the ratio is observed (Baker et al., 2008). For example, White and colleagues (2011) have observed a strong F_V/F_M decrease when *Chlorella* sp. was grown under nitrogen starvation in order to promote lipid accumulation.

Light-adapted samples are instead treated with actinic light. In these conditions, basal fluorescence level increases to F', which rises to the maximal fluorescence level F_M' when a saturating light pulse is given. These parameters allow to measure PSII efficiency under different conditions of light, i.e. the PSII actual quantum yield, Y(PSII) (Genty et al., 1989; Baker, 2008).

According to Hendrickson (2004), the distribution of the energy absorbed by PSII can be described with different kinetic constants which are in competition with each other:

- photochemical rate constant, kp, i.e. the photochemical activity of PSII;
- regulated NPQ constant, kNPQ, i.e. the energy dissipation as heat which is dependent on regulated non-photochemical processes;
- constitutive NPQ constant, kD, i.e. the constitutive thermal energy dissipation which does not depend on regulated non-photochemical processes;
- fluorescence constant, kf, i.e. the energy dissipation as fluorescence.

In order to quantify the importance of each parameter, fluorescence values obtained with PAM fluorimetry can be used in an energy partitioning analysis. With energy partitioning, three different quantum yields are obtained and summed up to unit (Hendrickson, 2004):

$$Y(PSII) + Y(NO) + Y(npq) = 1$$

The energy fraction which is used in photochemical processes is described as quantum yield of PSII and is represented by the following equation:

$$YPSII = \frac{kp}{kp+kNPQ+kD+\mathrm{K}f}$$

The sum of the light fraction which is loss by constitutive thermal dissipation or as fluorescence Y(NO) is described by the following equation:

$$Y(NO) = \frac{kf+kD}{kp+kNPQ+kD+Kf}$$

Finally, non-photochemical yield Y(npq) is described as:

$$Y(npq) = \frac{kNPQ}{kp+kNPQ+kD+kf}$$

1.8.2. 77K and RT microspectrofluorimetry

The organisation of the Chl-protein complexes *in vivo* is usually studied in photosynthetic organisms by low temperature fluorescence emission spectra (77K) (Ferroni et al., 2011) and room temperature (RT, i.e. 295K) microspectrofluorimetry (Pancaldi et al., 2002; Ferroni et al., 2011). At 77K, the spectra show a prominent band between 710 and 740 nm, depending on the species analysed. This emission is assigned to PSI and its antenna LHCI. Moreover, PSII originates two characteristic emissions, usually resolved as two independent peaks, at 685 and 695 nm, which have been assigned to CP43 and CP47 respectively (van Dorssen et al., 1987; Alfonso et al., 1994; Groot et al., 1999; Ferroni et al., 2011). Finally, a shoulder at 680 nm can also be observed. This emission has been attributed to the "free" LHCII, i.e. LHCII complexes not stably associated with PSII to form LHCII-PSII complexes (Hemelrjik et al., 1992; Šiffel and Braunová, 1999; van der Weij-de Wit et al., 2007). In photosynthetic organisms, the adjustment of PSI:PSII stoichiometry represents one of the responses which have been adopted for the maintenance of the maximal levels of energy conversion or for avoiding oxidative damages (Satoh et al., 2002). 77K represents a useful technique for the investigation of energy input processes, calculating the PSI/PSII ratio (F_{714}/F_{685} ratio), which is directly correlated with PSI:PSII stoichiometry (Satoh et al., 2002). Several studies performed on cyanobacteria and green microalgae have indeed demonstrated that light quality and intensity, temperature, salt stress and combinations of these factors affect photosynthetic characteristics such as the PSI/PSII reaction centre ratio, electron transport capacity of the two photosystems, cyclic electron transport activity and 77K fluorescence emission spectrum (Schubert and Hagemann, 1990; Murakami and Fujita, 1993; Maxwell et al., 1994; Hibino et al., 1996; Murakami et al., 1997; Miskiewicz et al., 2000; Satoh et al., 2002).

When spectra are recordered at RT, a different shape than that of spectra at 77K is observed. At RT, indeed, the 90% of the fluorescence emitted originates from PSII (Krause and Weiss, 1991; Pancaldi et al., 2002). Moreover, at RT many Chls belonging to different complexes emit at overlapping wavelengths (Ferroni et al., 2011). This results in a single maximum peak at around 684 nm, attributed mainly to PSII, which emits in the spectral region of 675-695 nm. Moreover, PSI-LHCI and vibrational satellites of PSII originate a very broad shoulder in the region between 710-740 nm (Ferroni et al., 2011). RT emission spectra were only occasionally used in photosynthesis researches because of the partial overlapping contribution of Chls from different complexes (Franck et al., 2005; Ferroni et al., 2009; Lambrev et al., 2010). However, if the registered spectra are resolved in their analytical components, RT bands can be attributed to specific complexes, as it has been demonstrated in several works (Pancaldi et al., 2002; Baldisserotto et al., 2004; Ferroni et al., 2007; Ferroni et al., 2009; Ferroni et al, 2011; Baldisserotto et al., 2012; Giovanardi et al., 2013). In our laboratories RT spectra recorded from single-living cells samples have been elaborated in order to obtain derivative spectra and single emission components (Pancaldi et al., 2002). This allowed to resolve the PSII emission region in three different components at approximately 679, 685 and 695 nm (Pancaldi et al., 2002; Baldisserotto et al., 2004; Ferroni et al., 2007; Ferroni et al., 2009), slightly blue-shifted at 678, 683 and 694 nm in the green microalga *N. oleoabundans* (Baldisserotto et al., 2012; Giovanardi et al., 2013). According with the most recent data of RT fluorescence emission in green algae (Ferroni et al., 2011), the attributions were to free LHCII, main PSII core band and LHCII-PSII functional assemblies respectively. Moreover, further minor components were resolved at 670 nm, assigned to free Chl, and 700 nm, assigned to LHCI-PSI and uncoupled LHCII aggregates (Ferroni et al., 2011).

1.8.3. BN PAGE as a tool in analyses of photosynthetic protein interaction and assembly

The cellular processes require the action of several enzymes, which often contain multiple subunits and are associated with each other in larger protein complexes. The need for the formation of these complexes for their activity is often unclear, so the knowledge of the composition and structure of these protein complexes results in a much deeper understanding of the metabolic pathway and cellular processes (Eubel et al., 2005). About

the photosynthetic apparatus, it is clear that multi-subunit complexes are necessary in order to accomplish all the reactions which occur inside the chloroplast (Kügler et al., 1997). The structure of these complexes has been determined with high resolution (Zouni et al., 2001; Ben-Shem et al., 2003; Kurisu et al., 2003). However, the composition of protein complexes is different among the thylakoid regions considered (Järvi et al., 2011). For instance, it has been shown that the high molecular-mass supercomplexes, composed of PSII dimers and LHCII, represent the most active form of PSII and are mainly located in the granal thylakoid membrane (Danielsson et al., 2006). Conversely, low-molecular PSII monomers have been found in the unstacked region of the thylakoid membrane, where the PSII repair cycle takes place, suggesting that these sub-complexes represent the intermediates of the repair cycle and/or the biogenesis of PSII (Baena-Gonzalez and Aro, 2002; Aro et al., 2005). Moreover, two high-molecular mass PSI megacomplexes, PSI-LHCII and PSI-NDH [NAD(P)H dehydrogenase] have been identified in the stroma thylakoid membrane. These megacomplexes have been shown to be involved in the state transition and NDH-dependent cyclic electron transfer respectively (Peng et al., 2008; Sirpio et al., 2009). This information has been acquired thanks to the development of techniques which allow reliable separation of the protein complexes. Among them, BN-PAGE has been mostly used. This technique has been developed for the first time by Schägger and Vonjagow (1991) for the investigation of the individual components of the respiratory chain in mitochondria. If native gel electrophoresis allows to separate proteins on the basis of their internal charge, hydrophobic proteins, such as the one involved in the respiratory chain or embedded in thylakoids, need an external charge added prior electrophoresis. In BN-PAGE electrophoresis charge is introduced to proteins by incubation with the dye Coomassie blue instead of the highly denaturating detergent sodium dodecyl sulphate (SDS), commonly used in SDS gel electrophoresis, which allows the proteins separation according to their size (Kügler et al., 1997; Eubel et al., 2005). The resolution capacity of BN-PAGE is very high and allows the separation of PSII and PSI, Cyt b_6f complex, ATPase and LHC complexes within a single gel. The technique represents a very reliable method for the molecular mass determination of proteins or protein complexes (Kügler et al., 1997).

BN-PAGE electrophoresis is often coupled with an SDS-gel system for a two-dimensional separation in the so-called 2D BN-SDS PAGE (Eubel et al., 2005). This technique

requires the incubation of native gel strips obtained from BN-PAGE with urea, β-mercaptoethanol and SDS for denaturation. After that, strips are placed horizontally on an SDS-gel system for the separation of the individual subunits which compose the protein complexes (Eubel et al., 2005; Järvi et al., 2011). After that, SDS-gel can be stained for the visualisation of the proteins, or blotted onto nitrocellulose or PVDF membranes for the detection of a specific protein subunit. Alternatively, individual subunits can be cleaved from the gel and used for their identification by mass spectrometry (Eubel et al., 2005).

Tables and figures

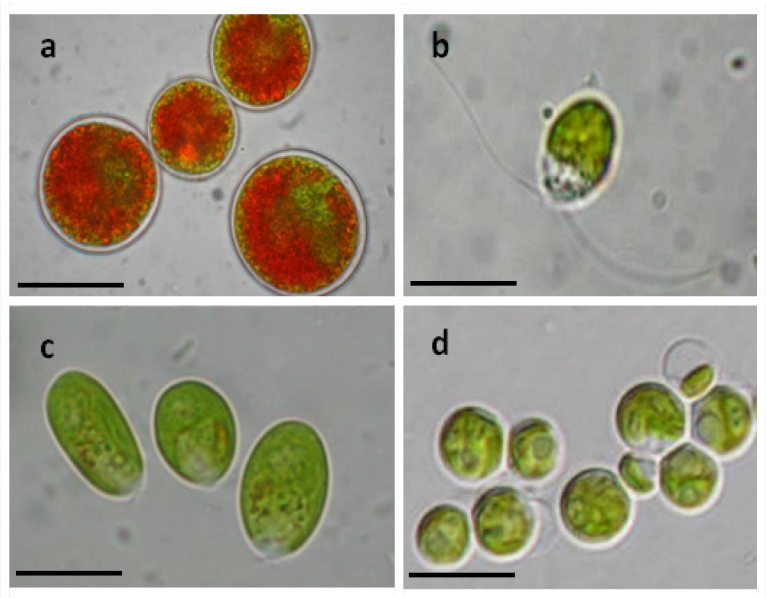

Fig.1: microalgae belonging to the *Chlorophyceae* Class. a) cysts of *Haematococcus pluvialis* in which Car are accumulated, b) *Chlamydomonas reinhardtii*, c*) Dunaliella tertiolecta,* d) *Chlorella sorokiniana.* Bars: 10 µm.

Plant source	% oil by wt in biomass	Oil yield (L oil/ha year)	Land use (m^2 year/kg biodiesel)
Corn/Maize (*Zea mais* L.)	44	172	66
Soybean (*Glycine max* L.)	18	636	18
Jatropha (*Jatropha curcas* L.)	28	741	15
Canola/Rapeseed *(Brassica napus* L.*)*	41	974	12
Sunflower *(Helianthus annuus* L.)	40	1070	11
Palm oil (*Elaeis guineensis*)	36	5366	2
Microalgae (low oil content)	30	58,700	0.2
Microalgae (high oil content)	70	136,900	0.1

Tab 1: comparison between some oleaginous crops and microalgae as biodiesel feedstock in terms of oil accumulation, oil productivity and land surface required. Adapted from Mata et al. (2010).

Microalga	Oil content (% by dry wt)
Botryococcus braunii	25-75
Chlorella sp.	28-32
Dunaliella primolecta	23
Isochrysis sp.	25-33
Nannochloris sp.	20-35
Nannochloropsis sp.	31-68
Neochloris oleoabundans	35-54
Nitzschia sp.	45-47

Tab 2: oil content in some promising microalgae. Adapted from Chisti (2007).

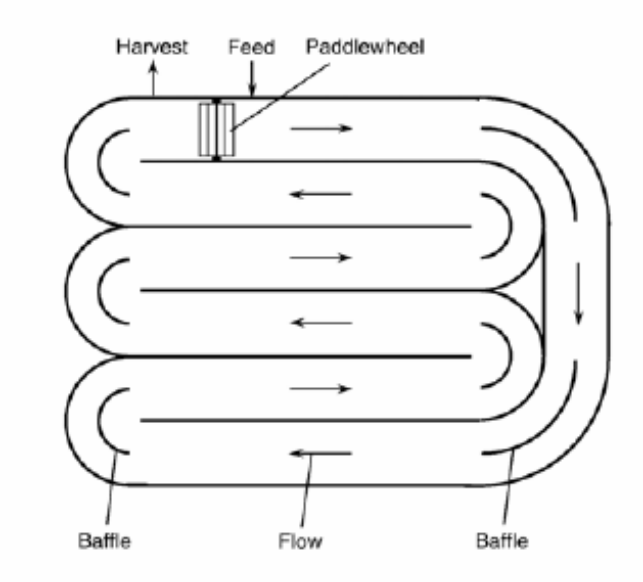

Fig. 2: raceway pond for the production of microalgal biomass. From Chisti (2007).

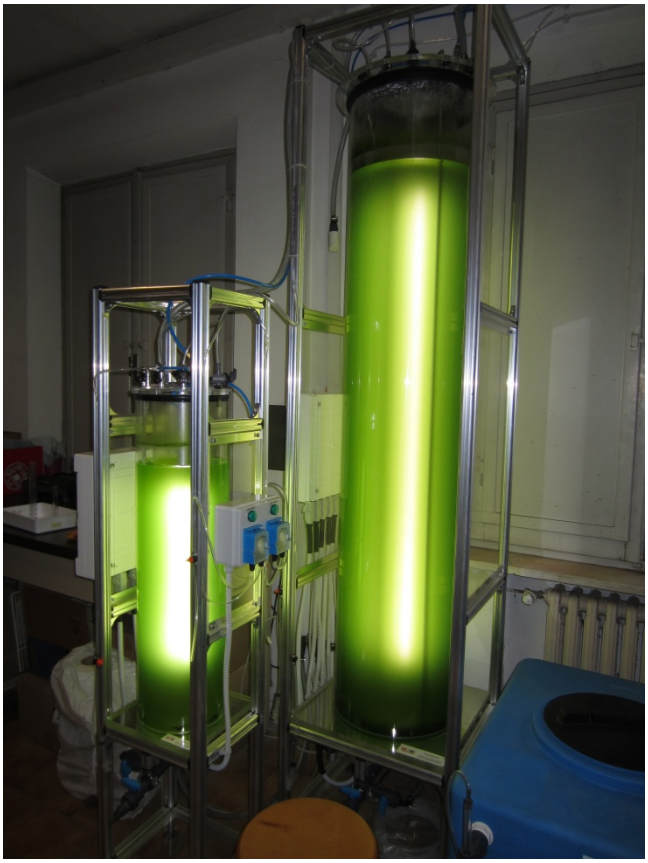

Fig. 3: column bioreactor installed in the Laboratory of Plant Cytophysiology of the University of Ferrara by M2M Engineering Sas.

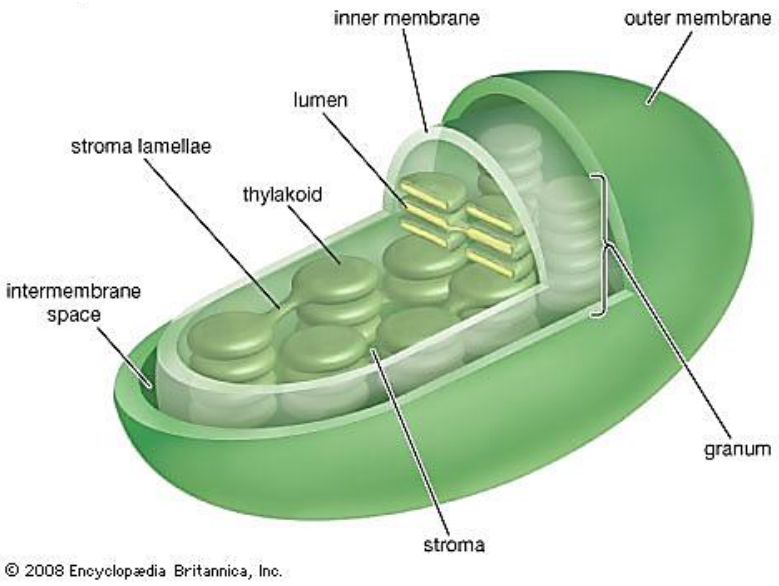

Fig. 4: the structure of the chloroplast. From Encyclopedia Britannica (www.britannica.com).

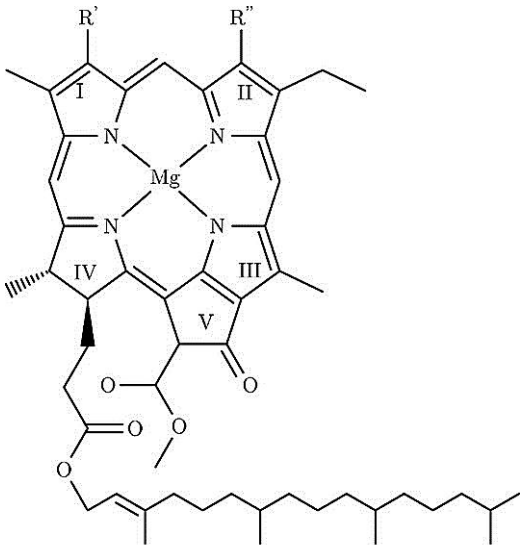

Chl *a*; R' = –CHCH$_2$, R" = –CH$_3$
Chl *b*; R' = –CHCH$_2$, R" = –CHO

Fig. 5: structure of Chl *a* and *b*. Modified from Heimdal et al. (2007).

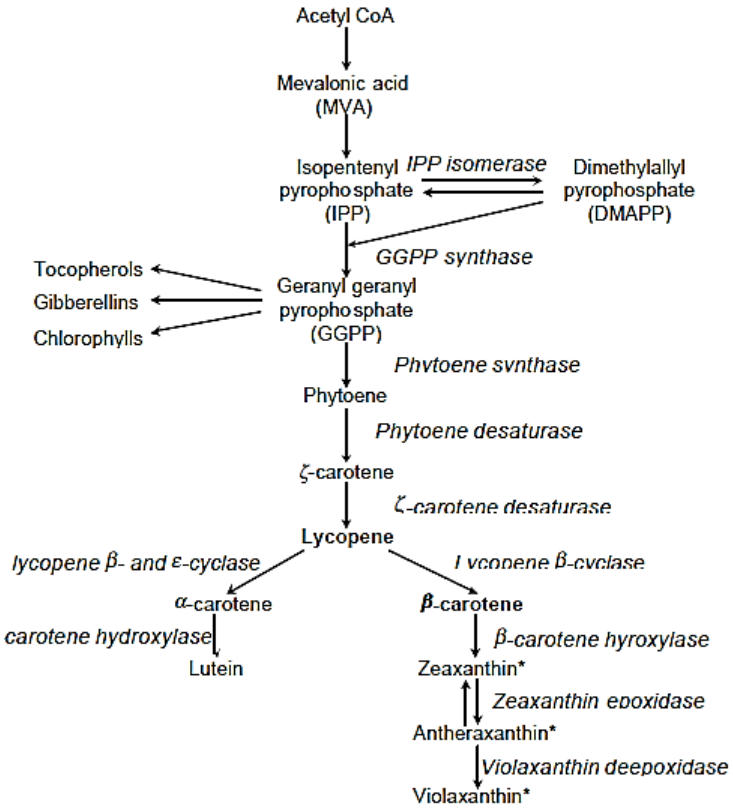

Fig. 6: the Car biosynthetic pathway. From Naik et al. (2003).

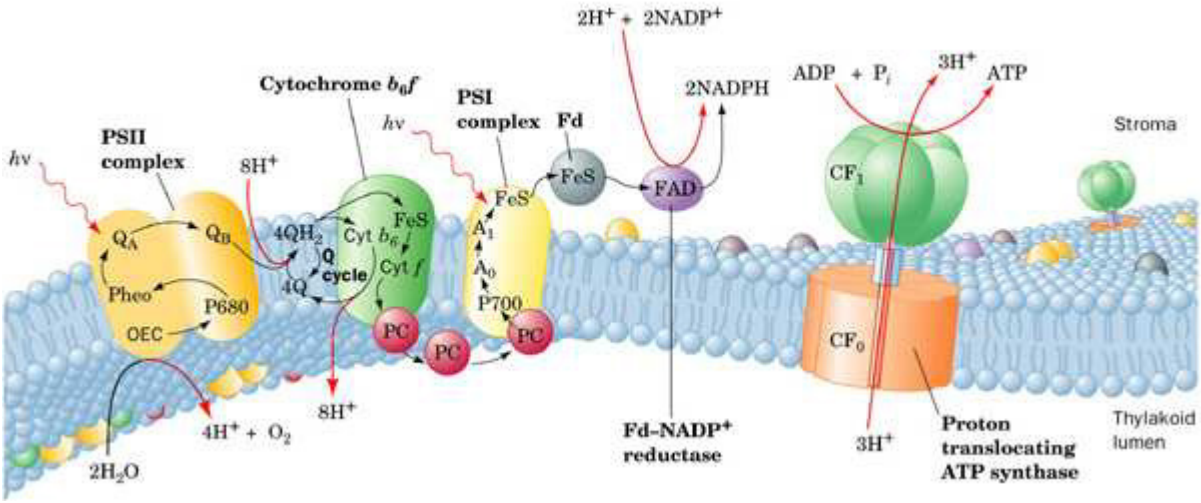

Fig. 7: detailed view of light reaction of photosynthesis.

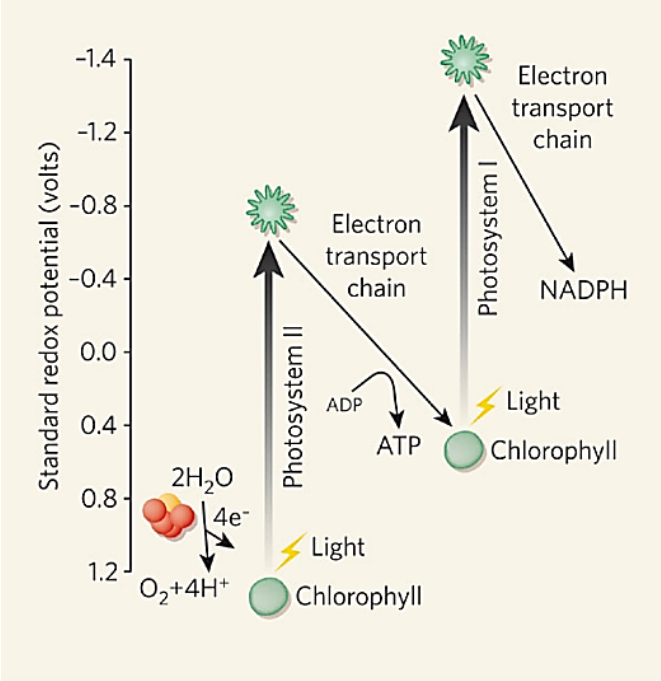

Fig. 8: rappresentation of the «Z-scheme» of electron transfer during light-reactions in photosynthesis. From Allen and Martin (2007).

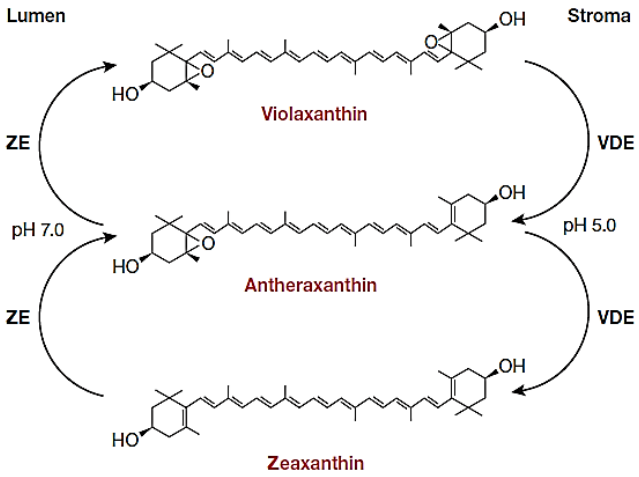

Fig. 9: the xanthophylls cycle. VDE: violaxanthin de-epoxidase; ZE: zeaxanthin epooxidase. From Szabó et al. (2005).

Aim of the work

This Thesis has been developed thank to a grant by the Italian Ministry for University and Research (MIUR) entitled “Energy saving and distributed microgeneration” and concerns a morpho-physiological and biochemical study of microalgae known to be used for biotechnological applications. The aim of the work is also to improve basic knowledge of microalgal physiology, whose current limitation is considered one of the main factors that interfere with the development of processes from the laboratory to the large scale.

This Thesis has been divided in three main sections.

The first is a morpho-physiological study about the effects of mixotrophic growth in the green microalga *Neochloris oleoabundans* on cell growth, photosynthetic efficiency and lipid accumulation. This section has been developed in two main subjects:

1) effects on cell growth, lipid accumulation and photosynthetic efficiency of mixotrophic cultivation of *N. oleoabundans* in presence of different glucose concentrations;
2) mixotrophic cultivation of *N. oleoabundans* in presence of a by-product from an agri-food industry and lipid synthesis induction under nutrient starvation.

In the second section, biochemical and biophysical analyses of the photosynthetic apparatus of *N. oleoabundans* grown in presence of different glucose concentrations were performed to provide new information on photosynthetic metabolism and its interaction with the organic carbon source assimilation. This work was supported by a scholarship granted by the University Institute of High Studies (IUSS)-1931 of Ferrara for PhD students mobility, and experiments were performed at the laboratories of Prof. Eva-Mari Aro (Dept. of Molecular and Food Biology, University of Turku, Finland).

The third section has been part of a Ministerial project PRIN 2007 supported by the Italian Ministry for University and Research (MIUR) entitled “Protein turn-over and accumulation in plants”, performed in collaboration with the University of Pavia and the University of Padua (Italy). In this study, the nuclear transformation of *Chlamydomonas reinhardtii* with two exogenous genes encoding for the phytoene synthase of *Arabidopsis thaliana* (*At*PSY) and *Oryza sativa* (*Os*PSY1) was performed. The effects on the Car

accumulation, Car profiles and photosynthetic performance were studied in transformed cells. This work allowed to gain important knowledge on the genetic engineering of microalgal cells and the methods used might as well be applied to the fatty acid metabolic pathway for the increase in lipid accumulation in a very next future.

Part I

Effects of mixotrophy on cell growth, lipid accumulation and photosynthetic performance of the green microalga Neochloris oleoabundans*: biotechnological implications*

1. Introduction

During these last decades the search for new carbon-neutral energy resources has become essential, considering the constant increase in oil prices, the starting depletion of fossil fuels supplies and the strong global concern about climate change (Chisti, 2007; Smith et al., 2010; Stephens et al., 2010). In this scenario, microalgae have started to receive increasing attention for their possible exploitation in the green energy field, in particular for their capability to accumulate lipids suitable for biodiesel production (Chisti, 2007; Li et al., 2008; Hu et al., 2008; Schenk, 2008; Smith et al., 2010; Brennan and Owende, 2010; Mata et al., 2010; Mussgnug et al., 2010; Stephens et al., 2010). Microalgae are photosynthetic microorganisms able to convert solar energy into chemical energy with higher photosynthetic efficiencies compared to higher plants, because of their simple unicellular structure (Harun et al., 2010). Moreover, they have the ability to easily modify their metabolism in response to changes in environmental conditions (Leonardi et al., 2011). For example, lipid accumulation is induced as an energy storage mechanism when cells are cultivated under stress conditions, such as high-light intensities or nutrient depletion (Hu et al, 2008, Smith et al., 2010; Mata et al., 2010; Li et al., 2011; Popovich et al., 2012). Unfortunately, these conditions of growth usually do not allow to achieve high biomass densities (Li et al., 2008a; Pruvost et al., 2009; Heredia-Arroyo et al., 2010). Biomass productivity and lipid accumulation are often inversely correlated, as the storage of TAGs inside cells occurs at the expense of energy used for growth (Wijffels and Barbosa, 2010). For this reason, the production of biodiesel from microalgae is not economically feasible yet and considerable investment in technological development and technical expertise is still needed for it to become a reality (Francisco et al., 2010; Mata et al., 2010; Wijffels and Barbosa, 2010). Recently, several studies have suggested growth conditions that can be used for the industrial scale-up of lipid production from algae (Scott et al., 2010). Among them, mixotrophic and heterotrophic growth have recently been considered alternative methods for achieving higher biomass densities with respect to autotrophic cultures (Lee, 2001; Xu et al., 2006; Heredia-Arroyo et al., 2010; Scott et al., 2010; Stephens et al., 2010; Giovanardi et al., 2013). Mixotrophy is termed the condition in which organic carbon is supplied in the culture medium together with light, so microalgae can benefit from coupling photosynthetic activity with the organic carbon assimilation for growth (Lee, 2001; Xu et al., 2006; Heredia-

Arroyo et al., 2010; Scott et al., 2010; Stephens et al., 2010; Giovanardi et al., 2013). Previous studies, performed on several mixotrophic microalgal species, have shown a strong increase in biomass yields, not only with respect to autotrophic cultures, but also compared to heterotrophic cultures, which consume only organic carbon for growth (Ogawa and Aiba, 1981; Martinez and Orus, 1991, Kobayashi et al., 1992; Marquez et al., 1995; Shi and Chen, 1999; Lee, 2001; Yang et al., 2000; Brennan and Owende, 2010).

Among the oil-rich microalgae well-known as biofuel producing species, the Chlorophyta *Neochloris oleoabundans* has gained considerable attention since the 1980s, when the first studies showed its capability to accumulate 35-54% of lipids, which were TAGs for up to 80%, when the microalga was cultivated under nitrogen starvation (Tornabene et al., 1983). Many studies have been subsequently performed in order to find out the best conditions for increasing both biomass and lipid productivity, growing the nitrogen-starved microalga in different conditions, i.e. varying the temperature of growth, providing CO_2 insufflation or cultivating the microalga in seawater media (Pruvost et al., 2009; Gouveia et al., 2009; Popovich et al., 2012). The effects of different nitrogen sources supplied to the growth media at different concentrations have also been studied with respect to growth and lipid accumulation (Li et al., 2008b). However, high lipid-enriched biomass productivities were never obtained with *N. oleoabundans*, and several Authors suggested a two-stage cultivation process: during the first one, cell could be grown in nitrogen-sufficient media, to allow biomass production. In a second step, biomass could be harvested and then transferred under nitrogen depletion, to induce lipid accumulation (Gouveia et al., 2009; Davis et al., 2012; Giovanardi et al., 2013; Popovich et al., 2012).

In our recent work, *N. oleoabundans* has been discovered to be a mixotrophic microalga (Giovanardi et al., 2013). The capability of *N. oleoabundans* to grow in presence of a carbon-rich waste product (Apple Waste Product – AWP) derived from an agri-food industry has been investigated, and the results clearly showed an increased biomass yield when the microalga was grown mixotrophically. This was the first work showing the capability of the microalga to use an organic carbon source for growth, as beforehand only the cultivation in presence of wastewaters or anaerobic digestate was tested (Levine et al., 2011; Wang and Lan, 2011; Yang et al., 2011). However, despite the advantage of coupling biomass production with low-cost organic carbon consumption, lipid accumulation was

enhanced only when nitrate was not provided in the culture media (Giovanardi et al., 2013). Furthermore, it was also shown that, among the different sugars present in the mentioned organic carbon source, glucose mainly contributed to growth (Giovanardi et al., 2013). Glucose has been considered the preferred carbon source also in other experiments concerning the mixotrophic cultivation of *Chlorella* sp. (Shi and Chen, 1999; Yang et al., 2001; Xu et al., 2006; Liang et al., 2009; Heredia-Arroyo et al., 2010; Heredia-Arroyo et al., 2011; Wan et al., 2011). Interestingly, when lipid accumulation was investigated, higher yields were always achieved when glucose was added to the growth media (Xu et al., 2006; Liang et al., 2009; Heredia-Arroyo et al., 2010; Heredia-Arroyo et al., 2011; Yang et al., 2011; Wan et al., 2011).

N. oleoabundans is usually described as a freshwater organism, and thus it is often cultivated in Bristol GR^+ or similar freshwater media (Bold, 1949; Lopes da Silva et al., 2009). However, this organism has been originally isolated from the arid soils in Saudi Arabia, and is considered a halotolerant microalga (Chatanachat and Bold, 1962). Experimental studies have shown the capability of *N. oleabundans* to grow from brackish to seawater media (Band et al., 1992; Arredondo-Vega et al., 1995; Baldisserotto et al., 2012; Popovich et al., 2012). Salinity also affected the biochemical composition, the cell size and the cell morphology of the microalga (Band et al., 1992; Arredondo-Vega et al., 1995; Baldisserotto et al., 2012). In a recent work, the growth of *N. oleoabundans* in freshwater and brackish medium (0.6 *vs* 17 ‰ of salinity) has been compared, showing increased cell volume and similar photosynthetic efficiency in the latter samples, and confirming the ability of the microalga to adapt to brackish environments (Baldisserotto et al., 2012). The results obtained are very important. Indeed, under the increased scarcity of freshwater for human consumption, the cultivation of halotolerant species in marine and brackish waters for biodiesel production can be considered an interesting alternative (Popovich et al., 2012). With these purposes, *N. oleoabundans* has recently been cultivated in seawater medium, to determine whether the microalga continued to be a good candidate for green-energy feedstock. The results confirmed its capability to accumulate lipids suitable for biodiesel production, but only when cells were grown under nitrogen depletion conditions (Popovich et al., 2012).

The recent works described above showed that mixotrophic cutivation of *N. oleoabundans* leads to enhanced biomass production, whereas, when cells are grown in brackish medium, increased cells volumes are observed. Then, combining the two conditions of growth might lead to further improved biomass yields with respect to freshwater autotrophic samples. In this first part of this Thesis, the microalga *N. oleoabundans* was cultivated in brackish medium (17‰ salinity), in autotrophic and mixotrophic conditions, in order to compare growth, morphological and physiological aspects, with special attention on the photosynthetic apparatus. In the first section, the cultivation of *N. oleoabundans* was tested in the presence of different glucose concentrations, focusing on parameters that are relevant to biotechnological applications. Growth was estimated in parallel to glucose consumption, whereas lipid accumulation was investigated by staining cells with the specific fluorocrome Nile Red. Pulse amplitude modulated (PAM) fluorimetry was employed in order to monitor the photosynthetic activity during growth and lipid accumulation. White et al. (2011), in fact, have recently suggested that PAM fluorimetry can be a useful tool for the parallel evaluation of photosynthesis, nutritional status of the cells and neutral lipid accumulation inside cells. In the second section, the growth ability of *N. oleoabundans* in a brackish medium with addition of Apple Waste Product (AWP) diluted 1/20 was tested. A two-phases experiment was set up: in the first phase, to obtain basic information on the biology of the microalga grown in mixotrophy, cell growth, lipid accumulation, cell morphology, pigment content and photosynthetic efficiency were monitored during 28 days of growth. Then, in the second phase of the experiment, cells, grown either autotrophically or mixotrophically for 7 days, were transferred to brackish water, under nutrient depletion, to evaluate and to compare the algal ability to accumulate lipids and to obtain new information about growth and morpho-physiological aspects of autotrophic and mixotrophic *N. oleoabundans* cells under starvation. Results were compared with previous works in which the microalga was grown in freshwater medium with AWP (Giovanardi et al., 2013) or in autotrophic brackish medium (Baldisserotto et al., 2012).

2. *Mixotrophic growth of* N. oleoabundans *with glucose as organic carbon source*

2.1 Materials and methods

2.1.1. Algal strain and culture condition

The microalga *N. oleoabundans* UTEX 1185 (syn. *Ettlia oleoabundans*) (Chlorophyta, Neochloridaceae, Sphaeropleales) was obtained from the Culture collection of the University of Texas (UTEX, USA; www.utex.org). Cells were grown and maintained in axenic liquid BM medium (Baldisserotto et al., 2012) in a growth chamber (24 ± 1 °C temperature, 80 $\mu mol_{photons}\ m^{-2}\ s^{-1}$ PAR and 16:8 h of light-dark photoperiod), without shacking and external CO_2 supply. For experiments, cells were inoculated at a density between 0.5 and 0.7 x 10^6 cells mL^{-1} in BM medium containing 0 (control), 2.5 or 5 g L^{-1} of glucose and grown in 500 mL Erlenmeyer flasks (300 mL of total volume) in the same growth chamber described above, with continuous shacking at 80 rpm. For analyses, aliquots of samples were collected at 0, 2, 3, 4, 7, 9, and 11 days of growth. Experiments were performed at least in triplicate.

2.1.2. Growth evaluation

Growth was estimated counting the cells with a Thoma's haemocytometer under the light microscope (Zeiss, model Axiophot). Specific growth rates during the exponential phases were calculated according to Giovanardi et al. (2013).

2.1.3. Glucose consumption evaluation

The glucose intake from cells was measured with the 3,5 dinitrosalicylic acid (DNS) assay for total reducing sugars, according to Miller (1959). Aliquots of 1 mL of samples were centrifuged at 10000 *g* for 5 min, then 0.3 mL of the supernatant were used in a reaction with 1 mL of DNS. When necessary, dilutions with distilled water were made before reaction. Samples were kept at 95˚C for 5 min, after that the optical density (OD) was analysed with a Pharmacia Biotech Ultrospec®2000 UV/vis spectrophotometer (1 nm bandwidth; Amersham Biosciences, Piscataway, NJ, USA) at 540 nm. The OD values were referred to a calibration curve in order to obtain the glucose concentration ($mg_{EqGlu}mL^{-1}$).

2.1.4. Light and fluorescence optical microscopy and Nile Red stained cell observations

Microscopic observations were taken from small aliquots of samples using a Zeiss model Axiophot microscope with conventional or fluorescent attachments. The light source for Chl fluorescence observation was a HBO 100 W pressure mercury vapour lamp (filter set, BP436/10, LP470). The intracellular presence of lipids was evaluated by staining cells with the fluorochrome Nile Red (9-diethylamina-5*H*benzo[α]phenoxazine-5-one, 0.5% dissolved in acetone) (Sigma-Aldrich, Gallarate, Milano, Italy), as described in Giovanardi et al. (2013). After staining, observations were made with the same microscope described above, exiting cells at 485 nm (filter set BP485, LP520). Pictures of cells were taken with a Canon Powershot S40 digital camera (4 megapixels), mounted on the ocular lens through a Leica DC 150 system (Leica camera AG, Solms, Germany).

2.1.5. Pigment extraction and analyses

Pigment extraction was performed according to Giovanardi et al. (2013). Aliquots of cells were collected by centrifugation at 600 *g* and then pigments were extracted at 80˚C for 15 min with 2 mL of 100% methanol. After clarification by centrifugation, the extracts were measured with the same spectrophotometer described above at 666 (Chl*a*), 653 (Chl*b*) and 470 (Car) nm. Quantification was performed according to Wellburn (1994).

2.1.6. PAM fluorimetry

The maximum quantum yield of PSII was determined using an ADC OS1-FL fluorometer (ADC Bioscientific Ltd, Hoddesdon, Hertfordshire, UK). Aliquots of samples were collected by centrifugation at 10000 *g* for 3 min. The pellets were then deposited onto pieces of wet filter paper (Schleicher & Schuell) (Ferroni et al., 2011). After incubation in the dark for 15 min, initial fluorescence (F_0) and maximum fluorescence (F_M) values were measured flashing the samples with a saturating light impulse. These values were used for the calculation of the maximum quantum yield of PSII: Y(PSII) = F_V/F_M, where variable fluorescence is $F_V = (F_M-F_0)$ (Baker et al., 2008; Lichtenthaler et al., 2005).

2.1.7. Data treatment

Data were processed with Microcal Origin 6.0 software (OriginLab, Northampton, MA, USA). In each case means ± standard deviations for *n* number of samples are given. Statistical analyses for comparison of the different data were carried out using Student's *t*-test with a significance level of 0.05.

2.2. Results and Discussion

2.2.1. Effect of different glucose concentrations on *N. oleoabundans* growth

As is shown in Fig. 1, the growth of *N. oleoabundans* was highly promoted when 2.5 and 5 gL^{-1} of glucose were supplied to BM medium, confirming the capability of this microalga to grow mixotrophically. Cell densities and growth rates of autotrophic and mixotrophic samples are reported in Fig. 2. During the first 3 days all samples grew with no differences, irrespective of the presence of glucose, reaching cell densities of about 5 x 10^6 cell mL^{-1} (Fig. 2 a). However, during the following days the growth rate of control samples started to progressively decrease and cells reached the stationary phase after 9 days of growth, with a cell density of about 14 x 10^6 cell mL^{-1}. Conversely, cells grown with 2.5 and 5 gL^{-1} of glucose continued to grow faster after day 3, reaching at day 7 cell densities of about 79 and 63 x 10^6 cell mL^{-1}, respectively. After the 7^{th} day, however, both mixotrophic samples entered the stationary phase, and cell density values started to decrease (Fig. 2 a). Growth rates at the intervals of 0-3 and 3-7 days are shown in Fig. 2 b. During the time interval of 0-3 days, similar growth rates, ranging between 0.9 and 1.1 div day^{-1}, were observed in all samples. During the following interval, growth rates in control cells strongly decreased, confirming the gradual entrance in stationary phase. Conversely, values only slightly decreased in mixotrophic samples, confirming the continuous growth until the 7^{th} day. In cultures grown with 2.5 and 5 gL^{-1} of glucose, the cell densities at the end of the exponential phase were measured to be 3.2 and 2.7 times higher than in the control, respectively ($p < 0.01$ in both cases). Such values are very high as compared to previous works testing different cultivation protocols (Yang et al., 2011; Giovanardi et al., 2013; Baldisserotto et al.,

2012; Popovich et al., 2012), and suggest that the mixotrophic growth with glucose is an alternative way for obtaining high-density cultures of this microalga. Interestingly, initial glucose concentration higher than 2.5 gL^{-1} did not yield higher cell density values. This was also previously observed in preliminary experiments in which the increase in glucose concentration beyond 5 gL^{-1} did not lead to improved cell densities (data not shown). Similar data were obtained in other studies in which *Chlorella* sp. was cultivated supplying different glucose concentrations to the growth media (Ip et al., 2004; Xiong et al., 2008; Heredia-Arroyo et al., 2010; Wan et al., 2011). This effect was attributed to substrate inhibition (Ip et al., 2004; Xiong et al., 2008; Heredia-Arroyo et al., 2010). Moreover, it has been reported that different mixotrophic microalgal species showed different optimal glucose concentrations for growth promotion (Wan et al., 2011). As shown in Fig. 3, in which cell growth of mixotrophic samples and parallel glucose consumption are reported, the optimal glucose concentration for *N. oleoabundans* appeared to be 2.5 gL^{-1}. In that case, indeed, glucose was completely utilized. Conversely, besides growth was not further promoted in the 5 gL^{-1}-supplied medium, an excess of substrate (17%) was also observed at the end of the experiment (Fig. 3). Interestingly, cells started to consume glucose only after 3 days of growth, i.e. when growth was promoted with respect to control. This aspect could be linked to the necessity of cells to adapt to the new glucose-supplied media during the first days of growth. Moreover, in both cases, glucose continued to be assimilated when cells entered the stationary phase of growth. In this way, despite the nutrient limitation conditions prevented the cell growth, the remaining sugar could have been used for providing energy to be addressed towards other metabolic pathways (Wan et al., 2011).

2.2.2. Optical microscopy and Nile red staining observation

The cell morphology of *N. oleoabundans* grown with 0, 2.5 and 5 gL^{-1} of glucose was periodically followed after 3 (exponential phase), 7 (late exponential phase) and 9 (stationary phase) days of growth. After 3 days, control cells were spherical and contained a large red-fluorescent cup-shaped chloroplast which occupied most of the cell volume (Baldisserotto et al., 2012; Giovanardi et al., 2013) (Fig. 4 a, b). Differences between autotrophic and mixotrophic cells already occurred at this time of growth, irrespective of the glucose concentration used. In cells supplied with 2.5 and 5 gL^{-1} of glucose, indeed,

vegetative cells showed slightly bigger dimensions. Moreover, the presence of big sporocysts containing several cells with small dimensions was observed in both mixotrophic samples (Fig. 4 c, d). These sporocysts were previously detected in *N. oleoabundans* grown mixotrophically (Giovanardi et al., 2013) or in presence of different anaerobic digestates added to the medium of growth (Yang et al., 2011). The increase in cell density from the 4th day of growth in mixotrophic samples could be linked to the release of cells from sporocysts. After 7 days of cultivation, more evident differences between control and treated cells occurred. About the former, morphology did not change significantly, except for the increased vacuolisation inside cells (Fig. 4 e), linked to the cell aging (Baldisserotto et al., 2012). Conversely, in mixotrophic samples the chloroplast lost its characteristic cup-shape and translucent globules started to accumulate inside the cytoplasm (Fig. 4 f, g). After 9 days of growth, mixotrophic *N. oleoabundans* cells appeared suffering (Fig. 5 a, b). Most of the cells were slightly flattened, losing their perfect spherical shape, and the translucent globules increased their volume inside cells. Moreover, cells appeared bleached. In order to check if such translucent globules were linked to lipid accumulation, cells were stained with the lipid-specific fluorochrome Nile Red. In fact, this assay is considered a quick method for checking the presence of lipid globules via microscopic observations of stained-cells (White et al., 2011; Popovich et al., 2012; Giovanardi et al., 2013). As expected, the presence of large lipid droplets was confirmed in mixotrophic cells after 9 days of growth, with no differences between the two glucose concentrations (Fig. 5 c, d). Scott and co-workers (2010) reported that growing microalgae under mixotrophic conditions produces an altered N:C ratio towards the carbon source, giving the same effects of nitrogen depletion conditions. In this way, lipid accumulation is induced during the stationary phase, when the nitrogen source has been consumed. On the other hand, the lipid metabolic pathway requires energy for lipid synthesis (Wan et al., 2011). As observed in section 2.2.1., glucose was consumed even when cells entered the stationary phase, providing the additional energy and material.

2.2.3. Effect of glucose on photosynthetic pigment content

The effects of the carbon source supplement on pigment content were monitored throughout cell growth and are shown in Fig. 6. During the first 3 days of growth, no differences in pigment content occurred between autotrophic and mixotrophic cultures.

About Chl content, Chl*a* (Fig. 6 a) and Chl*b* (Fig. 6 b) concomitantly decreased in all the samples, resulting in an overall reduction of more than 70% with respect to time 0 (Fig. 6 c). Differences were observed during the following days of cultivation. In particular, in control samples the trend of total Chl content pointed to a slight increase from day 4 to day 9 of cultivation, and a very strong increase at day 11, when Chl content reached the values recorded at the beginning of the experiment. Chl (and Car) plays, in fact, important roles in light-harvesting complexes and, in high-densities microalgal cultures, an increase in LHC antenna system is needed in order to maximise the light capture efficiency (Shenk et al., 2008). Then, the higher Chl amount at day 0 (inoculum) in all the samples has been attributed to the initial pigment content in the high-density starter cultures that were used for the inocula. Similarly, the higher content in total Chl at the end of the experiment in autotrophic cultures could be linked to the increase in cell densities. In diluted cultures, light penetration is usually higher than in dense cultures (Shenk et al., 2008), then a decrease in Chl content after day 0 could be linked to the effect of dilution. A different trend of Chl content was observed in mixotrophic samples after the 3rd day of growth (Fig. 6 a-c). Despite growth was highly promoted by glucose consumption from day 3 onwards, Chl*a*, Chl*b*, and, thus, total Chl content remained at very low values up to the end of the experiment, with only a slight increase in cells grown with 2.5 gL^{-1} of glucose at day 11. At the end of the experiment, in fact, values were 57% and 74% lower with respect to control for cells grown in 2.5 and 5 gL^{-1} of glucose respectively ($p < 0.05$ in both cases). In effect, in mixotrophic microalgae the pigment content varies depending on the considered species and carbon source supplied to the medium of growth (Liu et al., 2009). Little information on the effects of glucose on pigment content is available, but several studies have shown a decrease in Chl content with respect to autotrophic cultures when the organic carbon source, glucose included, was added to the medium (Yamane et al., 2001; Ip et al., 2004; Liu et al., 2009a). Despite the different trend in autotrophic and mixotrophic samples, the variation of Chl*a* content was linear with that of Chl*b*, resulting in constant Chl*a*/Chl*b* ratio in all samples. However, the ratio tended to be higher in mixotrophic cells, especially in those grown with 5 gL^{-1} of glucose (Fig. 6 d). Car content was shown to be less influenced by the addition of an organic carbon source (Liu et al., 2009a). In the marine diatom *Phaeodactylum tricornutum*, little variations in Car content were observed under glucose supplement, but resulting in lower Chl/Car ratios due to the concomitantly decrease in Chl*a* content (Liu et al., 2009a).

Conversely, in the green microalga *Haematococcus pluvialis* grown mixotrophically, Car concentration strongly increased, reaching higher values with respect to the autotrophic controls (Orosa et al., 2001). In *N. oleoabundans*, variations in Car concentrations during the microalgal growth followed the same trend of Chl content until day 7, irrespective of the presence of glucose (Fig. 6 e). However, different from what observed for Chl, Car content subsequently increased not only in controls (2.4 times more from day 7 to day 11), but also in treated samples (2.3 and 1.9 more from day 7 to day 11 in 2.5 and 5 gL^{-1} glucose-grown cells, respectively), although concentrations as high as those measured for controls were never reached. Considering the effect of glucose intake on microalgal growth and the consequently altered N:C ratio in mixotrophic cells (which simulates the same conditions of nitrogen starvation when microalgae reached the stationary phase) (Scott et al., 2010), in these samples Car might be probably synthesized in response to stress conditions (Berges et al., 1996; Orosa et al., 2001). Increased Car content from day 7 onwards resulted in different Chl/Car ratios, which remained stable for autotrophic cultures, whereas decreased in cells grown with 2.5 (-35%, $p < 0.01$ at 9 days of growth and -23%, $p < 0.05$ at 11 days of growth with respect to control) and 5 gL^{-1} of glucose (-36%, $p < 0.01$ at 9 days of growth and -48%, $p < 0.05$ at 11 days of growth with respect to control), due to the concomitant stabilisation of Chl content at low levels (Fig. 6 f).

2.2.4. Maximum PSII quantum yield determination in autotrophic and mixotrophic samples

Chl *a* fluorescence measurements can be considered a very important tool to study photosynthetic performance and stress conditions in microalgae (Baker, 2008). Among these techniques, PAM fluorimetry is fast and non-invasive and gives important information on the photochemical activity of photosystem II (PSII), which reflects the functionality of the photosynthetic apparatus and so the physiological state of the organisms (Maxwell and Johnson, 2000; Baker et al., 2008; White et al., 2011). The maximum PSII quantum efficiency measured as F_V/F_M ratio has recently been used for the estimation of the effects of nutrient limitation on photosynthetic apparatus of microalgal cells (White et al., 2011). Despite F_V/F_M values in non-stressed higher plants are usually around 0.8 (Baker, 2008), in microalgae values between 0.6 and 0.7 are usually measured (Krompkamp and Peene, 1999; White et al., 2011). The same values were observed when *N. oleoabundans* was grown in freshwater

and brackish medium (Baldisserotto et al., 2012). In agreement with such literature data, F_V/F_M ratios obtained in this work showed a nearly constant values around 0.6-0.7 in control cells throughout the experiment (Fig. 7). Conversely, a completely different trend was observed when glucose was added to the medium. Indeed, cells grown with 2.5 and 5 gL^{-1} of glucose showed a progressively significant increase in the F_V/F_M ratios, which reached the maximum value at 4 days, when approached 0.8 in both cases ($p < 0.01$ with respect to controls). This unusual, very high value, similar to those normally registered in higher plants, indicated a strong photosynthetic performance in mixotrophic samples. There is very little information available about the photosynthetic activity of *N. oleoabundans* under mixotrophic growth (Giovanardi et al., 2013). In other mixotrophic microalgae the organic carbon metabolism has different influences on photosynthesis (Liu et al., 2009a). In many studies, glucose has been shown to play inhibitory effects, reducing the apparent affinity for CO_2 during CO_2 fixation (Lalucat et al., 1984; Martinez and Orus, 1991) or limiting the synthesis of the RubisCO enzyme of the Calvin cycle (Oesterhelt et al., 2007). Reduced photochemical efficiency of PSII has also been observed, indicating that organic carbon depressed the photosynthetic efficiency (Oesterhelt et al., 2007; Liu et al., 2009a). Conversely, in *N. oleoabundans* the glucose supplement seemed to promote photosynthesis. During mixotrophy, photosynthesis and oxidative phosphorylation of the organic substrate simultaneously occur in order to provide energy for growth (Vonshak et al., 2000). Despite several works have supported the theory that, in some mixotrophic microalgae, autotrophic and heterotrophic metabolisms proceed independently (Marquez et al., 1993; Liu et al., 2009a), it has been proved instead that these processes can also be correlated with each other (Vonshak et al., 2000). In particular, in the cyanobacterium *Spirulina platensis* grown mixotrophically in the presence of glucose, maximum efficiency of PSII photochemistry, higher respiration and capacities of recovery after high-light exposures were observed with respect to autotrophic controls, indicating a higher metabolic activity (Vonshak et al., 2000). Then, glucose might have promoted in the same way photosynthetic efficiency also in *N. oleoabundans*. Results were completely different when *N. oleoabundans* cells entered the stationary phase. In fact, at the end of the experimental time, F_V/F_M ratios in 2.5 and 5 gL^{-1} of glucose-grown cells were dramatically decreased to 0.62 and 0.59 respectively, 15% and 20% less than the value recorded for autotrophic samples ($p < 0.01$ in both cases). F_V/F_M decrease has been linked in several cases with the exposure to stress conditions, such as salinity and

irradiance (Shreiber et al., 2002; Baker, 2008). In a recent study, the application of PAM fluorimetry to monitor the effects of nutrient depletion on lipid accumulation showed a strong decrease in F_V/F_M ratio and an overall reduction of the physiological functions in N-starved *Chlorella* sp. cells containing high amount of lipids (White et al., 2011). Also in this study, the decline in the ratio was observed as soon as cells entered the stationary phase and lipid accumulation was induced, confirming a reverse correlation between high photosynthetic efficiencies and lipid synthesis, which occurred in response to the physiological stress caused by nutrient depletion.

3. *Mixotrophic growth of* N. oleoabundans *in a carbon-rich waste product and lipid synthesis induction during nutrient starvation*

3.1. Materials and methods

3.1.1. Culture conditions and experimental design

Neochloris oleoabundans UTEX 1185 axenic cultures, grown and maintained in BM brackish medium (ca. 17‰ of total salinity; for composition see Baldisserotto et al., 2012) were used in this study. Algal cultures were cultivated without shaking in a growth chamber (24 $\pm$ 1°C; 120 $\mu mol_{photons}$ m^{-2} s^{-1} PAR; 16-8 h light-darkness photoperiod). Experimental design involved 2 steps. For step 1, aliquots of cells in the stationary phase of growth (10-12 x 10^6 cells mL^{-1}) were inoculated into Erlenmeyer flasks (500 ml capacity) containing BM medium added with an apple waste product (AWP) at the final dilution of 1:20. The AWP concentration was determined by extending to the present experiments the information already available for this alga cultivated in the low salinity ES medium enriched with the same AWP substrate (Giovanardi et al., 2013). The AWP was obtained from a semi-solid waste derived from the processing of apples in a vinegar production plant from Trentino Alto Adige region (Italy). The crude, semi-solid waste material was then transferred to the laboratory for further processing (sedimentation, to separate the liquid phase from the solid one, followed by harvesting, filtration, clarification, pH adjustment and sterilization of the liquid phase), according to the protocol reported in Giovanardi and coworkers (2013). The resulting AWP substrate contained about 3% of total sugars, thus working as a mixotrophic substate (for AWP composition, see Tab. 1; Giovanardi et al., 2013). Autotrophic cultures in BM medium were kept in parallel as controls. The culture volume was 300 mL, and the initial cell density was between 0.4 and 0.7 x 10^6 cells mL^{-1}. Experiments were performed in triplicate and their duration was 28 days. Samples were harvested weekly for analyses, except for growth kinetics measurements, which were performed also at the 3rd day of experiment. For step 2, cells were previously cultivated for 7 days in BM medium (autotrophic) and in BM medium added with AWP (mixotrophic) as just described. After 7 days, cells from both autotrophic and mixotrophic media were harvested axenically by centrifugation (500 *g*, 10 min) and resuspended in brackish tap water (tap water added with 14.5 gL^{-1} of NaCl, 0.29 gL^{-1} of KCl, 0.48 gL^{-1} of $CaSO_4 \times 2\ H_2O$, 1.27 gL^{-1} of $MgSO_4 \times 7\ H_2O$ to

reach the total salinity of 17‰). Aliquots of samples were harvested for analyses after 1, 3, 7, 10, 14 and 21 days of starvation. Tap water employed for experiments was obtained from the aqueduct serving the city of Ferrara and managed by the local agency for water, energy and environment (HERA - Holding Energia Risorse Ambiente; www.gruppohera.it); its composition, publicly available at the HERA website, is reported in Tab. 2. Experiments were performed in triplicate. Algae from both experimental steps were used for all analyses reported below.

3.1.2. Growth measurements

For step 1, growth kinetics evaluations were carried out on cell samples collected at time 0 (inoculum), and then after 3, 7, 14, 21 and 28 days. For step 2, growth measurements were performed at time 0 (inoculum in autotrophic and mixotrophic media), after 7 d of cultivation in both media, and then at time 0 (just after the algae were resuspended in the nutrient deprived medium), 3, 7, 10, 14 and 21 days of starvation. Growth was estimated measuring the optical density (OD) at 750 nm with a Pharmacia Biotech Ultrospec®2000 UV–vis spectrophotometer (1 nm bandwidth; Amersham Biosciences, Piscataway, NJ, USA). The values were referred to a calibration curve with known cell number, evaluated with a Thoma's counting camera, versus optical density. On the basis of cell density at different times of cultivation, the growth rate of samples was calculated by using the equation reported in Giovanardi and coworkers (2013).

3.1.3. Quantification of reducing sugars in culture media

For step 1, aliquots of culture media were separated from algae by centrifugation at 10000 *g* for 5 min. Media from autotrophic and mixotrophic cultures were analysed weekly using the DNS (3,5 dinitrosalicylic acid) assay for quantification of reducing sugars as reported in Miller (1959), with minor modifications. 0.3 mL of the supernatant were used in a reaction with 1 mL of DNS. When necessary, dilutions with distilled water were made before reaction. Samples were kept at 95˚C for 5 min, after that the OD was analysed at 540 nm with the same spectrophotometer described above. The OD values were referred to a calibration curve in order to obtain the concentration of reducing sugars ($mg_{EqGlu}mL^{-1}$).

3.1.4. Light and fluorescence microscopy

Cell samples were observed using a Zeiss model Axiophot microscope equipped with conventional or fluorescent attachments. The light source for fluorescence examinations was a HBO 100W pressure mercury vapour lamp. Chloroplasts were visualized by Chl autofluorescence with excitation at 436 nm (filter set, BP436/10, LP470). Images were obtained with a Canon Powershot S40 digital camera (4 megapixels) mounted on the ocular lens through a Leica DC150 system (Leica AG, Solms, Germany). For lipid identification inside cells, the fluorochrome Nile Red (9-diethylamina-5*H*benzo[α]phenoxazine-5-one, 0.5% dissolved in acetone; Sigma-Aldrich, Gallarate, Milano, Italy) was employed according to Giovanardi et al. (2013). After incubation at 37°C in darkness for 15 min, cells were observed with the same microscope described above at the excitation of 485 nm (filter set, BP485, LP520) to highlight the presence of intracellular neutral lipids as gold-yellowish spots. Pictures were taken with the camera described above.

3.1.5. Transmission electron microscopy (TEM)

Cells were harvested weekly by centrifugation (500 *g*, 10 min), fixed with glutaraldehyde and postfixed with OsO_4 following the method reported in Giovanardi and coworkers (2013). Dehydration, embedding and staining were performed as described in previous works (Pancaldi et al., 2002; Baldisserotto et al., 2012). Sections were observed with a Hitachi H800 electron microscope (Electron Microscopy Centre, University of Ferrara).

3.1.6. Photosynthetic pigment analysis

Algal cells suspensions were collected by centrifugation and extracted with absolute methanol for 10 min at 80°C (Baldisserotto et al., 2012; Giovanardi et al., 2013). Absorption of extracts was measured at 666 nm (Chl *a*), 653 nm (Chl *b*) and 470 nm (Car) with a Pharmacia Ultrospec 2000 UV-Vis spectrophotometer (1 nm bandwidth) (Amersham Biosciences, Piscataway, New Jersey, USA). Manipulations of pigment extracts were performed under dim green light to avoid photo-degradation. Pigment concentrations were evaluated according to Wellburn (1994).

3.1.7. Fluorescence measurements

Modulated Chl fluorescence

Chl fluorescence analyses were performed with a pulse amplitude modulated fluorimeter (ADC-OS1-FL, ADC Bioscientific Ltd., Herts, UK). In detail, the PSII maximum quantum yield (F_v/F_M) was measured after 20 min of dark adaptation of cell samples; the effective PSII quantum yield $Y(PSII) = (F_M' - F_S)/F_M'$, according to Genty et al. (1989), the quantum yield of regulated energy dissipation $Y(NPQ) = (F_S/F_M') - (F_S/F_M)$ and the combined yield of fluorescence and constitutive thermal dissipation $Y(NO) = (F_S/F_M)$ were measured after 5 min of exposure to high intensity light (1100 $\mu mol_{photons}\ m^{-2}\ s^{-1}$) (Hendrickson et al., 2004). Samples were prepared as reported in Ferroni et al. (2011).

RT microspectrofluorimetric analyses

In order to study the assembly state of the light harvesting complex (LHCII) with photosystem II (PSII) in autotrophic and mixotrophic cells, room temperature (RT) fluorescence emission spectra were recorded using a microspectrofluorimeter (RCS, Firenze, Italy), associated with a Zeiss model Axiophot epifluorescence photomicroscope (Pancaldi et al., 2002). Samples were prepared as described by Ferroni et al. (2011). Groups of living cells (x40 magnification) were excited at 436 nm. Excitation wavelength was provided by a BP436/10 filter (Zeiss), using a 1.6 mm diaphragm. Autolab software (RCS) was employed to set the recording range (620-780 nm), optimize the photomultiplier response and visualize the emission spectra (Ferroni et al., 2009). For each sample, at least 5 spectra were recorded. Microcal Origin 6.0 software (OriginLab, Northampton, MA, USA) was used for elaboration of spectra, which were corrected as described by Ferroni and co-workers (2011). Fluorescence yield of emission bands, whose attribution is shown in Tab. 3, was evaluated as the area subtended under the corresponding Gaussian curves. Moreover, calculation of difference in relative emission between autotrophic and mixotrophic cells was performed during the experimental time.

3.1.8. Statistical analyses

Data were processed with Microcal Origin 6.0 software (OriginLab, Northampton, MA, USA). In each case means ± standard deviations for *n* number of samples are given. Statistical analyses for comparison of the different data were carried out using Student's *t*-test with a significance level of 0.05.

3.2. Results and Discussion

3.2.1. Phase 1: effects of AWP on cell growth, pigment content, photosynthetic efficiency and lipid accumulation

Growth kinetics

Growth kinetics of *N. oleoabundans* cultures in the mixotrophic AWP-added medium was very different to those recorded for cells in BM medium and confirmed the previous results concerning the capability of the microalga to grow mixotrophically (Giovanardi et al., 2013), as is shown in Fig. 8. Growth kinetics of autotrophic control cells was in line with previous experiments in which *N. oleoabundans* was grown in BM medium (Baldisserotto et al., 2012). Indeed, autotrophic samples showed a continuous slight increase in cell densities, without entering the stationary phase and reaching at 28 days of growth values of about 3.5 x 10^6 cells mL^{-1} (Fig. 9). Conversely, cell densities of AWP-treated samples were already doubled with respect to those of controls at the 3rd day of cultivation, but reached a very significant peak at the 7th day, with cell densities of 9.44 x 10^6 cells mL^{-1} *vs* 1.36 x 10^6 cells mL^{-1} of control samples, i.e. about 7-fold higher than in autotrophic cultures, and growth rates of about 0.62 and 0.15 div d^{-1} for AWP-treated samples and controls, respectively. Subsequently, from day 7 up to the end of experiment, mixotrophic cultures entered the stationary phase, and growth rates underwent a strong rundown if compared to growth recorded during the previous time interval and to that of controls (about 0.03 and 0.06 div day^{-1} for AWP-treated and controls, respectively). At the end of the experiment, cell densities in mixotrophic samples were about 14 x 10^6 cell mL^{-1}, 4 times higher than autotrophic samples, but similar to those reported in *N. oleoabundans* in freshwater ES

medium added with AWP (Giovanardi et al., 2013). Baldisserotto and co-workers (2012) compared the microalgal growth in freshwater and brackish media, and the latter samples showed lower cell densities with respect to ES-grown cells, but increased cell volumes. However, the cell-enlargement effect in brackish medium disappears when the cells are routinely grown in BM. Therefore, it can be easily concluded that the cultivation in brackish medium did not lead to higher cell densities, but only AWP is responsible for the increased growth. In fact, AWP always yields higher cell densities with respect to autotrophic cultures, irrespective of salinity, and also with respect to previous works in which *N. oleoabundans* was cultivated in presence of wastewater effluents (Levine et al. 2011; Yang et al. 2011; Wang and Lan 2011), confirming that AWP might be considered a good alternative substrate to highly-expensive glucose. On the other hand, if cell densities obtained in this experiment are compared with *N. oleoabundans* grown in presence of pure glucose, such high values were never reached (see section 2), confirming that glucose remained the preferred carbon source. In that case, agitation might also have contributed to improve the growth rates, as already demonstrated in previous experiments with the dynoflagellate *Crypthecodinium cohnii* (De Swaff et al., 1999).

Glucose consumption kinetics in mixotrophic microalgae

As already shown by Giovanardi et al. (2013), AWP composition resulted in 2.95% of total sugar compounds, whereas the total amount of organic carbon was calculated to be around 3.35%. Therefore, the concentration of the total organic carbon added to BM medium at the 1:20 dilution was around 1.68 gL^{-1}. However, only 0.93 gL^{-1} of organic carbon resulted to be reducing sugar available to the assimilation by the microalga. As is shown in Fig. 10, the concentration of reducing sugars in AWP-media underwent an overall 70% decrease during the 28 day-long experiment, indicating that AWP supplement exceeded the concentration required for total consumption by the microalga. Values, in fact, decreased from 0.93 to 0.31 $g_{EqGlu}L^{-1}$ at the end of the experiment. Interestingly, the consumption of sugars in the culture media by *N. oleoabundans* cells was about 37 mgL^{-1} day^{-1} during the first 7 d of cultivation, then it decreased to about 17 mgL^{-1} day^{-1} during the following 21 day-long experimental interval, suggesting a higher rate of assimilation when cells were in exponential phase of growth. Moreover, despite cells entered the stationary phase after 7 days of growth, glucose consumption continued up to the end of the experiment. This

indicates that microalgae might benefit from the exogenous carbon source not only for growth, but also for the functioning of other metabolic pathways during the stationary phase (Wan et al., 2011).

Effects of AWP on cell morphology and lipid accumulation

Cell morphology of autotrophic and mixotrophic *N. oleoabundans* was monitored throughout the experiment by light and fluorescence microscopy and by submicroscopical observations at TEM. Moreover, the presence of lipid globules was checked by staining the cells with the lipid-specific fluorochrome Nile Red. Observations of autotrophic control cells at the light microscope (Fig. 11 a, b, d, e) showed the typical cell morphology of *N. oleoabundans* grown in BM medium, but cell dimensions remained similar throughout the experiment (Baldisserotto et al., 2012). In fact, independent of the growth period, cells were almost spherical, with a cell diameter of about 3-3.5 µm. Only one cup-shaped chloroplast, containing a large pyrenoid, was present inside cells (Fig. 11 a, b). Only cells from 21-28 days-old autotrophic cultures sometimes showed signs of cytoplasmic vacuolisation (Fig. 11 d-f), which is probably linked to cell ageing of the cultures (Baldisserotto et al., 2012). Submicrosopical observations showed the presence of the nucleus inside cells, containing a nucleolus. Moreover, inside chloroplast the pyrenoid was surrounded by starch and crossed by one or two thylakoids, which were never appressed to form grana and intergrana inside chloroplast (Fig. 11 c, f). Finally, inside the plastid, small stromatic starch grains were sometimes observed (Fig. 11 f), which might be involved in osmoregulation processes (Band et al., 1992). When control cells were stained with Nile Red, lipid droplets were never detected (data not shown). On the other hand, microalgae grown mixotrophically with AWP showed some peculiar features (Fig. 12). In fact, while cell shape and dimension were similar to those of control samples, differences were observed at the chloroplast and cytoplasm levels. At 7 days of growth, several sporocyst were detected, confirming that cells were in active division (Fig. 12 a). In a recent work, the cultivation of *N. oleoabundans* in presence of anaerobic digestates of manures stimulated the periodic formation of sporocysts, which subsequently released cells, resulting in oscillations of the cell densities (Yang et al., 2011). Same effects were observed when *N. oleoabundans* was grown in freshwater medium added with AWP (Giovanardi et al., 2013) or in presence of glucose (see section 2). Therefore, the formation of these sporocysts might be linked to an effect of the addition to the medium of

the carbon-rich product. Moreover, the release and maturation of cells from sporocysts could be linked to the increase in cell density until the 7th day of growth in mixotrophic samples. Indeed, cells with very small dimensions, just released from sporocysts, were also observed at the 7th day of growth, indicating that the microalga was in active division, as also observed by the increase in the cell density. From Nile Red staining of cells at 7 days of growth, no lipid globules were detected in the cytoplasm (Fig. 12 b). At the same time of growth, submicroscopical observations showed a chloroplast with its characteristic cup-shape and the presence of a large pyrenoid, surrounded by starch and crossed in the middle by one or two thylakoids. One nucleus, with a nucleolus inside, and one or more mitochondria were also observed (Fig. 12 c). Interestingly, the chloroplast was also characterised by large and numerous stromatic starch grains, which subsequently decreased becoming similar to those of controls (Fig. 12 c). It is known that many microalgae, in particular green algae, growing under optimal conditions, usually maintain high photosynthetic efficiencies to sustain growth and reproduction. The excess reducing power is then conserved in the form of starch as the primary carbon storage (Li et al., 2011). In 1980, Akazawa and Okamoto demonstrated that in *Chlorella pyrenoidosa* the exogenous organic carbon was partially accumulated as starch without the prior conversion to glyceraldehyde-3 phosphate, whereas the remaining sugar was oxidized through the glycolytic pathways (Akazawa and Okamoto, 1980). The same effect might have been induced by AWP during mixotrophic growth of *N. oleoabundans*. During the first 7 days, when the organic carbon source was assimilated with maximum rate, sugars might be stored in starch granules inside the stroma of the chloroplast, as also previously observed by Giovanardi et al. (2013). In mixotrophic microalgae, the N:C ratio is shifted towards the carbon (Scott et al., 2010). In this way, effects similar to those caused by nitrogen starvation conditions occur, and lipid globules are accumulated when cells enter the stationary phase (Scott et al., 2010). Starch and lipid metabolisms share common precursors in their metabolic pathways (Li et al., 2011). In *Pseudochlorococcum* sp., starch and lipid synthesis were demonstrated to be inter-convertible (Li et al., 2011). Indeed, cells accumulated starch granules during N-repletion cultivation, but, as soon as conditions turned to N-depletion, the organism shifted the fixed carbon towards the fatty acid synthesis, and the conversion of starch to neutral lipids occurred. Thus, in *N. oleoabundans*, the degradation of starch granules after 7 days, when cells entered the stationary phase, might explain a similar

behaviour. Indeed, as also observed in previous works (Giovanardi et al., 2013), cells started to be gradually vacuolated during growth (Fig. 12 d) and assumed a pale-green colour (Fig. 12 g). Nile Red staining showed accumulation of lipid droplets inside cells, observed as gold-yellowish spots, whose volume increased from the 21st day onwards (Fig. 12 e, h). The detection of lipid globules was possible also by submicroscopical observations (Fig. 12 f, i), where lipids were shown as pale grey (electron-negative) globules in the cytoplasm. Finally, in these cells the ultrastructure of the chloroplast gradually degenerated and at 28 days of growth this organelle was no more detectable (Fig. 12 i).

Effect of mixotrophy on photosynthetic pigments

Time course variations of pigment content, Chl*a*/Chl*b* and Chl/Car ratios are shown in Fig. 13. Interestingly, relevant differences occurred between autotrophic and mixotrophic samples. Indeed, a strong increase in Chl*a* (Fig. 13 a), Chl*b* (Fig. 13 b), and thus in total Chl (Fig. 13 c), occurred when AWP was added to the medium of growth, reaching at the end of the experiment values of about 81% ($p < 0.05$), 37% and 67% ($p < 0.05$) higher than in controls respectively. Conversely, in autotrophic cultures no evident variation was observed for Chl*a* content, whereas an increasing trend was found for Chl*b* content, which was about 45% at day 28 with respect to day 0. The pigment content trend found in mixotrophic cells seems unique to the mode of cultivation with AWP in brackish medium. Indeed, in cells grown in freshwater medium with AWP an increase in Chl content was observed only at 21 days of growth (Giovanardi et al., 2013), whereas when cells were cultivated with different glucose concentrations values lower than those measured for autotrophic samples were shown (see section 2), as expected in microalgae grown mixotrophically (Yamane et al., 2001; Ip et al., 2004; Liu et al., 2009a). Very little is known about the effects of the organic carbon source on photosynthetic pigment content (Ip et al., 2004). However, it has been reported than autotrophic microalgae in high-density cultures usually increase their antenna system, in order to maximise light harvesting (Shenk et al., 2008). In this case, it might be supposed that AWP does not affect directly the pigment composition and the increase in Chl content is mainly linked to the increase in cell density. However, this aspect is still controversial, because cells continued to accumulate Chl even when entered the stationary phase and lipid accumulation was induced. The variations in Chl*a* and Chl*b* between mixotrophic and autotrophic samples resulted in different Chl*a*/Chl*b* ratio (Fig. 13 d). In

mixotrophic samples, indeed, the ratio remained almost stable, due to the concomitant increase in both Chls. Conversely, Chl*a*/Chl*b* ratio gradually decreased in autotrophic samples, due to the increase in only Chl*b* during the experiment, reaching at the end of the experiment values 25% lower than in cells grown with BM+AWP. A different trend was observed for Car content (Fig. 13 e), which showed a decrease in both samples at 7 days of growth, after that a gradual increase in both cells grown in BM and in BM+AWP was observed. Such an increase was marked in mixotrophic samples, which showed at the end of the experiment 67% higher values than those measured at day 0, *vs* the 47% higher values measured for controls. Anyway, mixotrophic samples always showed higher Car content with respect to controls, even if differences were less marked compared to Chl content. In a previous work, an increase in Car concentration was observed proportionally with the increasing concentration of the carbon source inside the medium when the microalga *Phaeodactylum tricornutum* was cultivated in mixotrophic conditions (García et al., 2006). The increase in Car content might also be properly linked to the maintenance of the Chl:Car stoichiometry during the increase in both Chl content. Indeed, different proportion of Chl and Car, reflected in the trend of Chl/Car ratio (Fig. 13 f), seemed almost stable in all the samples, except for the value recorded in cells grown in AWP after 7 days. Chl/Car ratio remained always higher for mixotrophic cells (75% higher at 7 days, $p < 0.01$, and 40% folds higher at 14 days, $p < 0.05$, with respect to controls), due to the increase in Chl content compared to autotrophic cultures.

Measurements of photosynthetic parameters in autotrophic and mixotrophic cells

The effects of AWP on photosynthetic efficiency were evaluated by PAM fluorimetry. In particular, maximum quantum yield of PSII, as F_v/F_M ratio, was obtained from samples pre-incubated in darkness for 20 min, while actual yield of PSII, Y(PSII), yield of regulated thermal dissipation, Y(NPQ) and, finally, yield of energy lost by passive dissipation, Y(NO), were obtained in dark-adapted samples exposed to 1100 $\mu mol_{photons}\ m^{-2}s^{-1}$ for 5 min, (Fig. 14).

Time course of PSII maximum quantum yield measured as F_V/F_M ratio in both autotrophic and mixotrophic samples is reported in Fig. 14 a. At time 0 (inoculum), the ratio was stable around 0.6, as observed in previous works (Baldisserotto et al., 2012; Giovanardi

et al., 2013). Interestingly, a different trend was observed in cells grown in BM+AWP with respect to controls. In these latter, indeed, the ratio remained almost stable throughout the experiment, with a decrease only at 28 days. Conversely, mixotrophic samples showed a very higher F_V/F_M ratio at 7 days with respect to BM-grown cells, reaching values of 0.772 *vs* 0.694 ($p < 0.01$). These higher values were previously shown in *N. oleoabundans* when the microalga was grown in the presence of glucose (see section 2), suggesting that this behaviour is typical for the mixotrophic cultivation of this microalga, irrespective of the organic carbon source supplied. However, higher F_V/F_M ratios were never observed in previous works in which several microalgal species were grown mixotrophically (Liu et al., 2009a). The F_V/F_M ratio in cells grown with AWP, however, decreased to values similar to those of controls after 7 days of growth, when cells entered the stationary phase, as already observed in previous works (White et al., 2011) and when *N. oleoabundans* was grown in the presence of glucose (see section 2). F_V/F_M is a very useful parameter which can be used to estimate the maximum quantum yield of photochemistry in PSII. However, the ratio does not provide a rigorous quantitative value, as this simple model requires several assumption, which are not necessarily correct for all the situations (Baker, 2008). Therefore, to obtain further information about the functionality of the photosynthetic apparatus during mixotrophy, measurements of the Chl fluorescence were performed after exposure to 1100 $\mu mol_{photons}\ m^{-2}s^{-1}$ for 5 min. The energy absorbed by PSII can be divided in three fractions, corresponding to competing processes: energy used for photochemistry, Y(PSII); energy dissipated as heat by light-dependent dissipation mechanisms, Y(NPQ); energy constitutively dissipated as heat or fluorescence emission by non-functional PSII, Y(NO) (Genty et al., 1989; Hendrickson et al., 2004; Losciale et al., 2011). Y(PSII) is a useful parameter to evaluate the proportion of potentially active PSII after high-light exposure and can give a measure of the rate of linear electron transport and, thus, an indication of overall photosynthesis (Maxwell and Johnson, 2000). Interestingly, time course of Y(PSII) after 5 min of illumination with saturating-light was similar to that registered for F_V/F_M ratio in both samples (Fig. 14 b). Indeed, control cells maintained an almost stable trend, with a slight increase in the value at 14 days and a subsequent decrease after 21 days of growth. Conversely, cells grown with AWP showed higher Y(PSII) at 7 days of growth with respect to autotrophic cultures, confirming that AWP induced an enhancement of the photosynthetic activity during the exponential phase. Previous works have shown that, under laboratory conditions, Y(PSII) is

directly related to the efficiency of carbon fixation (Maxwell and Johnson, 2000). Here, the role of the enhancement of the photosynthetic efficiency remains unknown, it is indeed very unusual in mixotrophic microalgae (Lalucat et al., 1984; Martinez and Orus, 1991; Oesterhelt et al., 2007; Liu et al., 2009a). However, as soon as cells entered the stationary phase, such values progressively decreased down to levels lower than in controls at 21 and 28 days. Conversely, Y(NO) after 5 min of high-light exposure was always slightly higher in mixotrophic samples with respect to control cells (Fig. 14 c), although differences were significant only at 21 days of growth (+35%, $p < 0.05$), suggesting a lower capability to protect themselves against damage by excess illumination with respect to autotrophic cultures (Klughammer and Schreiber, 2008). To asses if NPQ response was modified in different cultures, Y(NPQ) was measured for each sample after 5 min of actinic high-light exposure (Fig. 14 d). Y(NPQ) is the fraction of energy dissipated as heat by the regulated photo-protective NPQ mechanisms. Interestingly, a decreasing trend was observed in both cultures after 14 days, however in mixotrophic samples the capability to induce NPQ was always lower with respect to controls throughout the experiment ($p < 0.01$ at 7 and 21 days of growth). Under F_0 and F_M conditions, i.e. when the first saturating pulse is applied after a period of dark incubation, the stress-induced damage of the photosynthetic apparatus is usually reflected in an increase of Y(NO) and a decrease in Y(PSII) (Klughammer and Schreiber, 2008). However, during high-light exposure, as long as NPQ mechanisms are not affected, high Y(NPQ) are usually observed to compensate a decrease in Y(PSII) (Klughammer and Schreiber, 2008). In this work, it seems rather that in mixotrophic cultures the decrease in Y(PSII) was not compensated by Y(NPQ), but instead accompanied by an increase in Y(NO). Y(NPQ) was already less inducible at 7 days of growth in cells grown with AWP, probably because they presented higher photosynthetic efficiencies with respect to autotrophic cultures, thus they has a minor need for excess energy dissipation. However, subsequently the increasing trend of Y(NO) and the decreasing trend of Y(NPQ) in mixotrophic cells entering the stationary phase might reflect a suboptimal capacity of photo-protective reactions and an incapability to regulate photochemistry at maximal values (Klughammer and Schreiber, 2008). These results might also be linked with the progressive lipid accumulation inside cells. Indeed, in a recent work, it has been shown that, when lipid accumulation is induced, microalgae are more susceptible to photodamage if exposed to high-light (Simionato et al., 2011).

In order to get more precise information on the origin of fluorescence and estimate if the differences observed by PAM measurements were linked to different assembly state of PSII pigment-protein complexes, RT fluorescence emission spectra analyses were obtained for both cells grown in BM and BM+AWP. Fourth-order derivatives were calculated to find the components to be used for the deconvolution by Gaussian fitting procedure (Ferroni et al., 2011). Gaussian deconvolution of spectra showed three emission peaks assigned to PSII (Tab. 3). Free LHCII emitted at 680 nm, PSII core emitted at 686 nm, while emission at 694 nm was attributed to LHCII-PSII functional assemblies. Moreover, emission at 702 nm was attributed to the contribution of LHCII aggregates and LHCI-PSI complexes, while emissions at 660 and 670.5 nm were assigned to uncoupled Chl (Ferroni et al., 2011). In order to get information on the emission intensities in autotrophic and mixotrophic cells, differences of fluorescence emission spectra were calculated after 7 (Fig. 15 a), 14 (Fig. 15 b), 21 (Fig. 15 c) and 28 (Fig. 15 d) days of growth. Difference spectra showed only minor variations between control and cells grown with AWP. In particular, at 7 days of growth mixotrophic samples gained emission between 687 and 698 nm, indicating an improved assembly of LHCII-PSII. Same effects were observed when *N. oleoabundans* was grown in freshwater medium with AWP (Giovanardi et al., 2013), and were linked to the active synthesis of complexes during cell growth (Ferroni et al., 2004; Giovanardi et al., 2013). Furthermore, a slightly increasing emission at 673 nm, corresponding to emission of free Chl, was observed with respect to control cells at 21 days of growth, and might be linked with the active synthesis of Chl which occurred in mixotrophic samples. However, these differences were not significant, suggesting that mixotrophy did not strongly affect the assembly of PSII pigment-protein complexes.

3.2.2. Phase 2: effects of nitrogen starvation on cell growth, pigment content, photosynthetic efficiency and lipid accumulation in *N. oleoabundans* previously grown autotrophically or in presence of AWP

Growth kinetics of cells transferred to a brackish tap water from autotrophic or mixotrophic media

During phase 1, mixotrophic cells reached their maximum cell density and entered the end of the exponential phase after 7 days of growth. For this reason, a second phase of the experiment was set up: after cultivation for 7 days in autotrophic or AWP-added medium, the cells were harvested and resuspended in brackish tap water (starvation medium). During the first week, cell growth was comparable to that observed during phase 1 both for cells grown with or without AWP. As soon as both samples were transferred to brackish tap water, they immediately entered the stationary phase (Fig. 16). Indeed, growth rates were measured to be around 0.03 and 0.01 div day^{-1} for cells grown previously in BM and BM+AWP medium, respectively. The same results were obtained by Popovich and collaborators (2012). Nitrogen is indeed one of the most important inorganic limiting nutrients required for growth of microalgal cells (Brennan and Owende, 2010) and its deficiency has a great influence on many aspects of their physiology (Merzlyak et al., 2007).

Effect of starvation on cell morphology and lipid synthesis induction of N. oleoabundans *cells*

Cell morphology of samples previously grown in BM and BM+AWP and subsequently transferred to brackish tap water changed dramatically in both samples with respect to cells observed during phase 1. However, no differences between the two samples occurred, and morphology was similar throughout the experiment, with no changes due to the ageing of cultures. Light microscopy observations showed the presence of several cells with larger dimensions, never detected during phase 1 in BM or BM+AWP medium (Fig. 17 a, b). In most of these cells, the characteristic cup-shape of the chloroplast was lost. However, the main characteristic of these cells was the presence of several translucent globules inside the cytoplasm, which were confirmed to be lipid droplets by Nile Red staining (Fig. 17 c, d). These globules were clearly detected as yellowish spots and in the cell occupied a larger volume with respect to those observed in mixotrophic samples during phase 1 (Fig. 12 h).

The lipid droplets were also identified by TEM observations, either as numerous small droplets inside the cytoplasm (Fig. 17 e), or sometimes as converging droplets into few globules with bigger dimensions (Fig. 17 f). Lipid accumulation inside cells under starvation is consistent with previous works in which *N. oleoabundans* was grown either in N-depleted fresh- or marine waters (Tornabene et al., 1983; Li et al., 2008b; Gouveia et al., 2009; Pruvost et al.,2009; Popovich et al., 2012). This is considered the most important carbon and energy storage mechanism which some microalgae use to save the excess of reducing power formed by the concomitant photoassimilation of carbon and inhibition of photosynthetic efficiencies (Li et al., 2011). Interestingly, TEM observations also showed the presence of modified, thickened cell wall (Fig. 17 e, f), a response that has been frequently observed in many microalgae in response to different stresses (Van Donk et al., 1997; Agrawal and Singh, 2001; Ferroni et al., 2007; Baldisserotto et al., 2012). In many microalgae, cell wall thickening appears when cells are grown in nutrient-deficient media. This behaviour has been attributed to the preparation for encystment or to a strategy for limiting the cell growth (van Donk et al., 1997).

Quantification of photosynthetic pigment during growth in brackish tap water

Time-course variation of pigment content was analysed only in the period between 0-14 days after the cells were transferred to brackish tap medium. After 14 days, indeed, the extraction procedures applied during phase 1 became completely inefficient, probably due to the thickening of the cell wall described in previous section, which conferred more resistance to the cell walls. As is shown in Fig. 18, a strong decrease in Chl content occurred in both samples throughout the experiment, irrespective of their previous growth in BM or BM+AWP. Chl*a* content dramatically decreased until reaching at 14 days values of about 65-70% lower with respect to time 0. However, as is shown in Fig. 18 a, the strongest decrease occurred during the first 3 days, when values were 50% lower in both samples with respect to time 0. The same trend was observed for Chl*b* content (Fig. 18 b) in both samples during the first 3 days (-50% compared to day 0). However, the pigment concentration remained stable in control cells during the rest of the experiment, whereas, in cells previously grown with AWP, a further decrease was observed, and at 14 days Chl*b* was measured to be 72% lower than at the beginning of phase 2. The decreasing trend of Chl*a* and Chl*b* in both samples resulted in an overall decay in the total Chl content (Fig. 18 c), which was halved

during the first 3 days of starvation, and then continued to decrease until reaching values between 62% lower in control cells and 70% lower in cells previously grown in AWP with respect to time 0. The same decrease in Chl trend was observed in *N. oleoabundans* grown in N-starved freshwater (Giovanardi et al., 2013). On the whole, nitrogen is essential for the synthesis of protein and Chl, thus, when cells are grown in N-depleted media, loss of these molecules and a consequent decrease in the photosynthetic functions are usually observed (Berges et al., 1996; Young and Beardall, 2003; Giovanardi et al., 2013). Because of the simultaneous decrease in both Chl*a* and Chl*b* content, Chl*a*/Chl*b* ratio remained stable in both samples throughout the time (Fig. 18 d). However, the values in samples previously grown mixotrophically was slightly higher with respect to that of control cells, probably due to slightly higher levels of Chl*a*. Differences were significant only at 14 days ($p < 0.01$), probably linked to the stronger decrease in Chl*b* content with respect to controls during starvation. On the other hand, Car content was less affected by starvation with respect to Chl in both the samples (Fig. 18 e). In cells previously grown autotrophically, a decrease of about 45% occurred during the first 3 days, after that the values remained stable at 0.08 nmol 10^{-6} cell. Conversely, in cells previously grown with AWP, the Car content was lower than that measured in controls at time 0 and, even if small fluctuations occurred throughout the experiment, values did not show significant variations from day 0 to day 14. Chl is more sensitive to N-deficiency with respect to Car (Young and Beardall, 2003). In previous works, the persistence of higher relative proportions of Car has been related to the reorganisation of the photosynthetic apparatus, in order to maximise light harvesting during N-deficiency (Herzig and Falkowski, 1989; Sosik and Michell, 1991). However, as probably in the case of our starved *N. oleoabundans*, the higher relative proportion of Car with respect to the Chl concentration has also been linked with an enhanced photoprotection in N-starved cells, which usually showed a smaller or completely degenerated chloroplast and a minor photosynthetic efficiency in comparison with cells grown in N-repleted media (Merzlyac et al., 2007). The concomitant decrease in Chl content resulted in strongly decreasing Chl/Car ratio in both samples (Fig. 18 f), which varied from 32% to 58% lower values at 14 days of growth with respect to time 0 for controls and cells previously grown in AWP, respectively, as also observed in *N. oleoabundans* grown in N-starved freshwater (Giovanardi et al., 2013) and in other microalgae grown under nutrient depletion (Berges et al., 1996; Young and Beardall, 2003; Merzlyac, 2007).

F_V/F_M ratio in starved N. oleoabundans cells previously grown autotrophically and mixotrophically

Time course of F_V/F_M ratio of cells previously grown in BM and BM+AWP and then transferred to brackish tap water is shown in Fig. 19. As was observed during phase 1 of experiment, after 7 days of growth cells in BM+AWP showed 13% ($p < 0.05$) higher values with respect to cells grown in BM. PSII is mainly affected to nitrogen starvation, probably because the rapid turnover of D1 and D2 proteins of RCII is limited by the decline in protein synthesis (Berges et al., 1996). Conversely, the reaction center of PSI (RCI) has been shown to be more stable during these stress conditions (Plumbey et al., 1989). In previous works in which several microalgae were grown under N-depletion, a decrease in maximum quantum efficiency of PSII was always observed (Geider et al., 1993, 1998; Berges et al., 1996; Young and Beardall, 2003; White et al., 2011). Interestingly, in this study, when cells were transferred to nitrogen starvation, the trend of F_V/F_M ratio was very different between the two types of samples. Indeed, in control cells the value dramatically decreased by 43% within the first 3 days of starvation, after that it became stable around 0.4 up to the end of experiment. Conversely, cells previously grown in BM+AWP maintained higher values with respect to control cells and, after a slight decrease by 14% during the first day of starvation, values remained stable around 0.6 throughout the experiment, i.e. 75% higher than the corresponding values measured for cells previously grown autotrophically ($p < 0.01$ after the first day of starvation, $p < 0.05$ for the other experimental times). These results might indicate that when samples are previously grown in AWP, which induces growth promotion, photosynthetic pigment accumulation and enhanced photosynthetic efficiency, the capability to maintain higher maximal quantum yields of PSII with respect to controls is ensured also when the samples are transferred under N-starvation. The reason of this physiological behaviour is still unknown.

4. Conclusion

During these last recent years, the studies concerning the cultivation of *N. oleoabundans* for biofuel purposes have become more and more numerous, in relation to the capability of this microalga to accumulate lipids when grown under nutrient starvation. In this work, the mixotrophic cultivation of *N. oleabundans* in a brackish medium added with different organic carbon sources has been tested, with the aim of studying the effects on cell density, cell morphology, photosynthetic efficiency and lipid accumulation inside cells. With this purpose, the experiments were organized in two different sections.

In a first experiment, cells were grown adding to the medium different glucose concentrations. Glucose, indeed, is considered one of the preferred carbon sources which are assimilated by heterotrophic and mixotrophic microalgae (Heredia-Arroyo et al., 2010), and in a previous work in which *N. oleoabundans* was grown in presence of AWP, it was found to give the major contribution to growth (Giovanardi et al., 2013). Results showed that growth of *N. oleoabundans* was highly enhanced by the addition of glucose in the culture medium, reaching cell densities never observed before (Yang et al., 2011; Baldisserotto et al., 2012; Popovich et al., 2012; Giovanardi et al., 2013). Agitation of the flasks might also have contributed to increase the cell concentration. Among the different glucose amounts used in the experiments, the concentration of 2.5 gL^{-1} was the optimal, whereas higher concentrations did not lead to higher cell densities. This is very important, because a glucose supplement at low concentration may be an effective way to improve the economic feasibility of mixotrophic microalgal cultures. After 3 days of growth, biomass was highly promoted by the glucose supplement in mixotrophic cultures, which also showed higher photosynthetic efficiency. However, after 7 days the cells entered the stationary phase and decreased their photosynthetic efficiency in response to stress conditions, together with strong promotion of lipid accumulation. This study confirmed that glucose can be considered a very suitable substrate for the obtainment of high-lipid enriched *N. oleoabundans*.

Despite glucose allowed to obtain very high cell densities, it is considered a very-expensive substrate. For this reason, the capability of mixotrophic microalgae to grow in the presence of organic carbon waste sources, which can be recycled with zero or negative

costs, is often investigated, in order to lower the costs of the process during scaling-up and provide the additional benefit of bioremediation (Heredia-Arroyo et al., 2010). Then, in a second experiment, *N. oleoabundans* was grown in the presence of AWP, a carbon-enriched by-product derived from the agri-food industry, which was already shown to promote cell growth (Giovanardi et al., 2013). AWP was added to a brackish medium (Baldisserotto et al., 2012), in order to test if the effects of enhanced growth and increasing cell volumes could be usefully combined. However, the characteristics observed in *N. oleoabundans* cells grown in brackish medium during the experiment performed by Baldisserotto et al. (2012) were not so emphasized in this experiment, probably because of the acclimation of the cells to the brackish medium during long-lasting cultivation in BM medium. However, the same cell densities observed when cells were grown in freshwater medium + AWP were reached in mixotrophic samples, suggesting that salinity did not interfere with cell growth. The ability to grow in media with different salinity allows the microalga to be acclimatable to different environments (Baldisserotto et al., 2012). This is very important in this scenario in which freshwater supply is limiting (Popovich et al., 2012). Moreover, it is known that the cultivation in brackish or marine media allows to prevent or minimize contaminations by other microorganisms (Das et al., 2011), which is also very important in the perspective of a scale up to the industrial process. Therefore, the results confirmed that *N. oleoabundans* can be cultivated in brackish media without affecting any characteristic which makes it a very suitable candidate for biofuel purposes. In a first phase of the experiment, higher cell densities, higher photosynthetic pigment synthesis and higher photosynthetic performance were observed during the exponential phase of mixotrophic samples. The enhanced photosynthetic efficiency when cells are grown mixotrophically is a very unusual characteristic of *N. oleoabundans*, and further experiments would be required in order to better understand how mixotrophy modulates pigment-protein complexes in the thylakoid membranes of the chloroplast. Differences with respect to autotrophic samples occurred also at the morphological level, with starch accumulation inside the plastid, which was subsequently degraded when cells entered the exponential phase. Interestingly, after 21 days of growth, cells started to accumulate lipid globules, which increased over time, occupying the majority of the cell volume at the end of the 28-days experiments. During the second phase of the experiment, as soon as cells were transferred under nutrient depletion, block of cell growth, decrease in pigment content and alteration of the cell morphology were

observed in response of the stress. However, the concomitant accumulation of lipid globules, which occupied the majority of the cell volume, occurred.

On the whole, to study the most suitable condition, which might allow to obtain high *N. oleoabundans* biomass enriched in lipids, promoting at the same time the economic feasibility and allowing to scale up the process from the laboratory to the industrial scale, three different strategies should be considered:

1. the cultivation of *N. oleoabundans* in presence of glucose as organic carbon source, reaching very high biomass densities enriched in lipids in a single, short-time step;
2. the long-term, single step cultivation of *N. oleoabundans* in presence of AWP as organic carbon source, reaching higher biomass of cells enriched in lipids with respect to autotrophic samples. This strategy might be coupled with the necessity of agri-food industries to dispose their waste products still enriched in nutrients with zero or negative costs;
3. the short-term, two step cultivation of *N. oleoabundans*, at first in presence of AWP as organic carbon source, in order to obtain high cell densities during the first days of growth. Cells might be then transferred in N-limited conditions, such as simple tap or marine water, to induce lipid accumulation in a few days. This strategy would require a double amount of water with respect to the single-step strategies described above. However, the problem might be partially solved by recycling the water used in the first phase of cultivation.

Tables and Figures

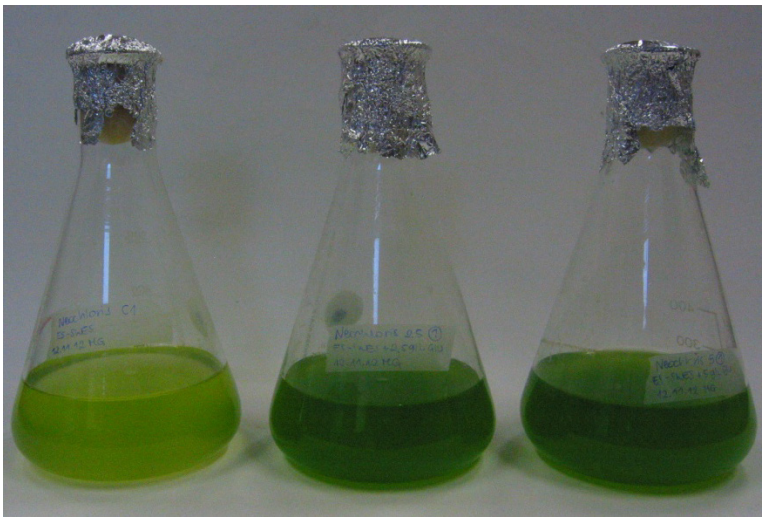

Fig. 1: autotrophic and mixotrophic *N. oleoabundans* cultures after 7 days of growth (0, 2.5 and 5 gL^{-1} of glucose added from left to right).

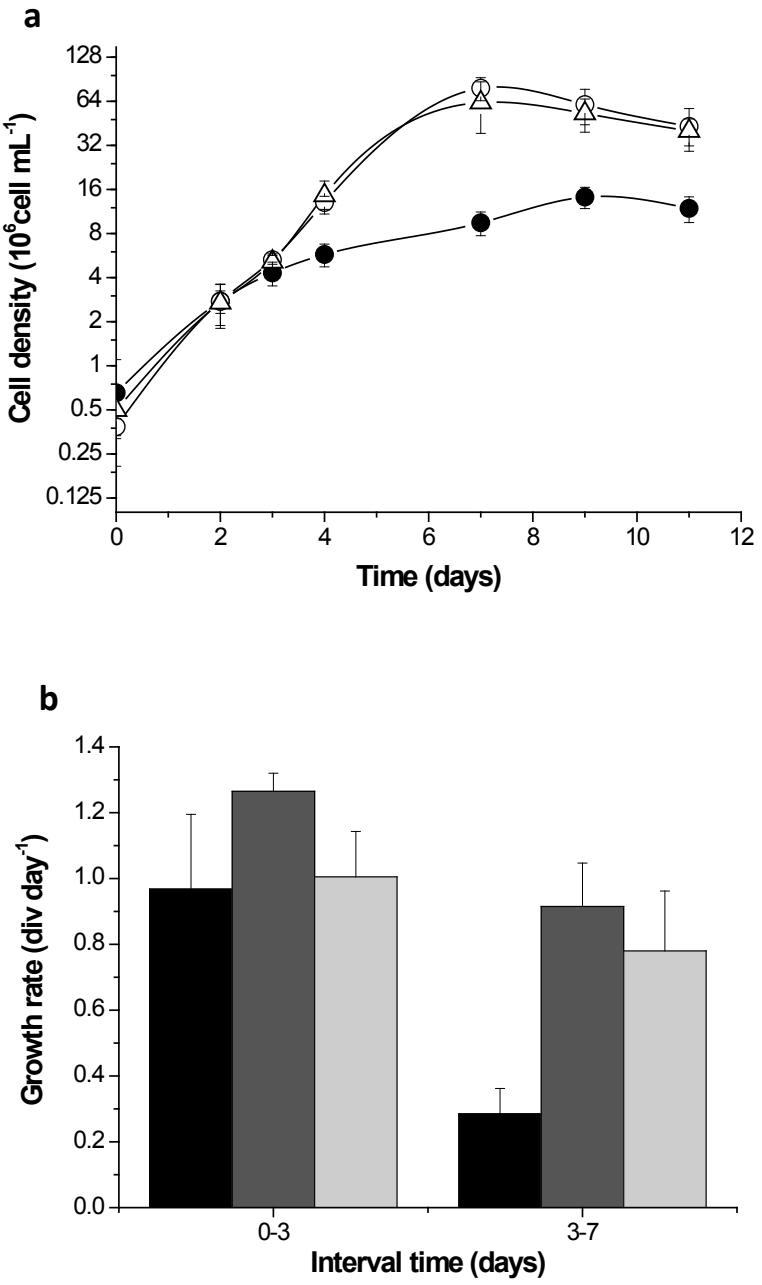

Fig. 2: a) growth kinetics of *N. oleoabundans* in media containing 0 (filled circles), 2.5 (empty circles) and 5 (empty triangles) gL^{-1} of glucose. b) growth rates calculated during the exponential phase after 0-3 and 4-7 days in cells grown with 0 (black), 2.5 (dark grey) and 5 (light grey) gL^{-1} of glucose. For each sample, values are means ± s.d. (n > 3).

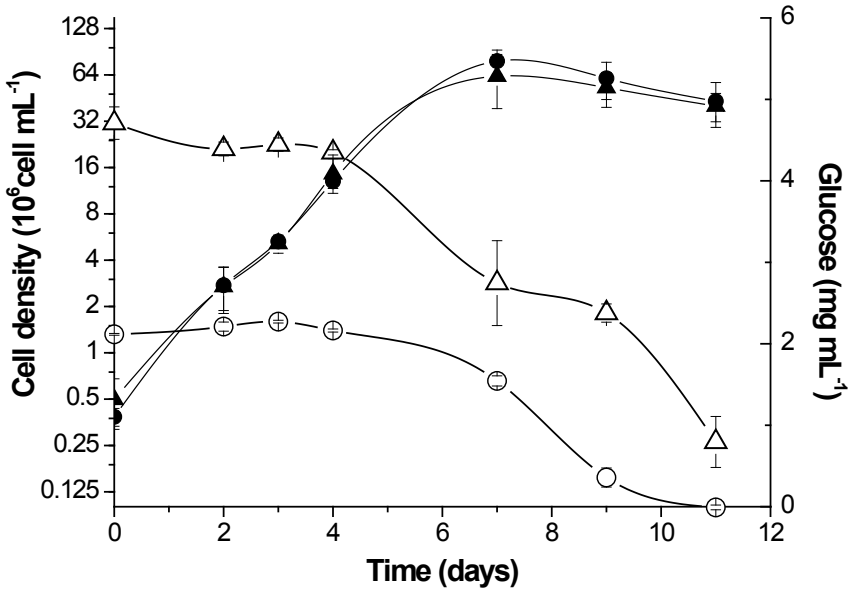

Fig.3: growth kinetics of *N.oleoabundans* in presence of 2.5 (filled circles) and 5 (filled triangles) gL^{-1} of glucose and corresponding glucose consumption (empty circles and empty triangles respectively). For each sample, values are means ± s.d. (n > 3).

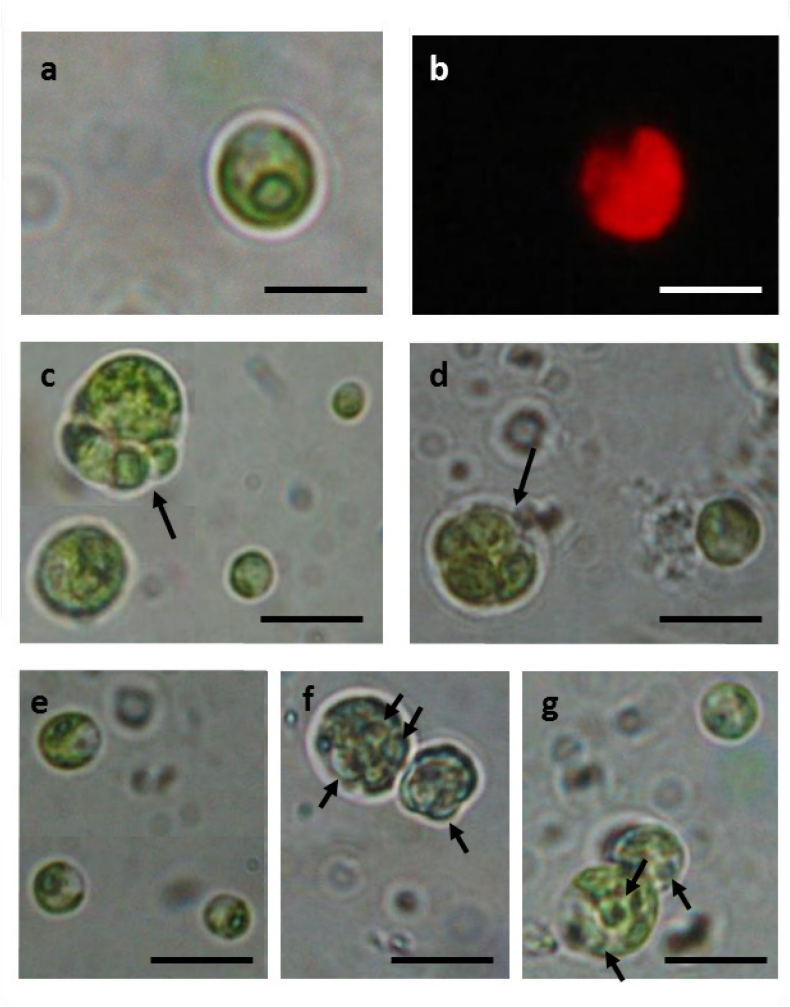

Fig. 4: cell morphology of *N. oleoabundans*. a) control cells at 3 days of growth and b) corresponding fluorescence of the chloroplast.Bars: 3 µm. c) cells grown in 2.5 gL^{-1} and d) in 5 gL^{-1} of glucose at 3 days of growth showing sporocysts (arrows) in the cell population. Bars: 6 µm. e) control cells after 7 days of growth. Bar: 6 µm. f) cells grown in 2.5 gL^{-1} and g) 5 gL^{-1} of glucose after 7 days of growth. The presence of translucent globules is indicated with arrows. Bars: 4 µm.

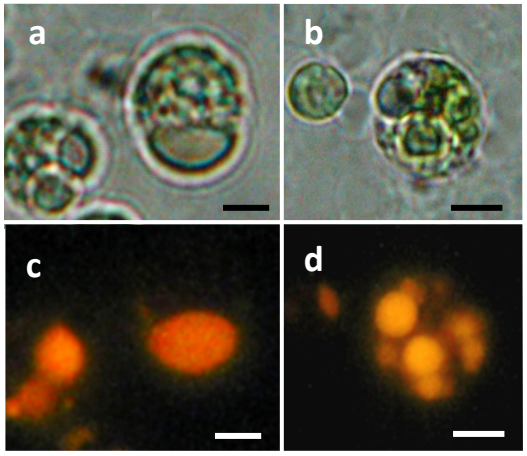

Fig. 5: light and epifluorescence photomicrographs of *N. oleoabundans* cells after 9 days of growth. a) Cells grown in 2.5 gL^{-1} and b) 5 gL^{-1} of glucose and their corresponding Nile Red-staining observation (c, d). Bars: 2 µm.

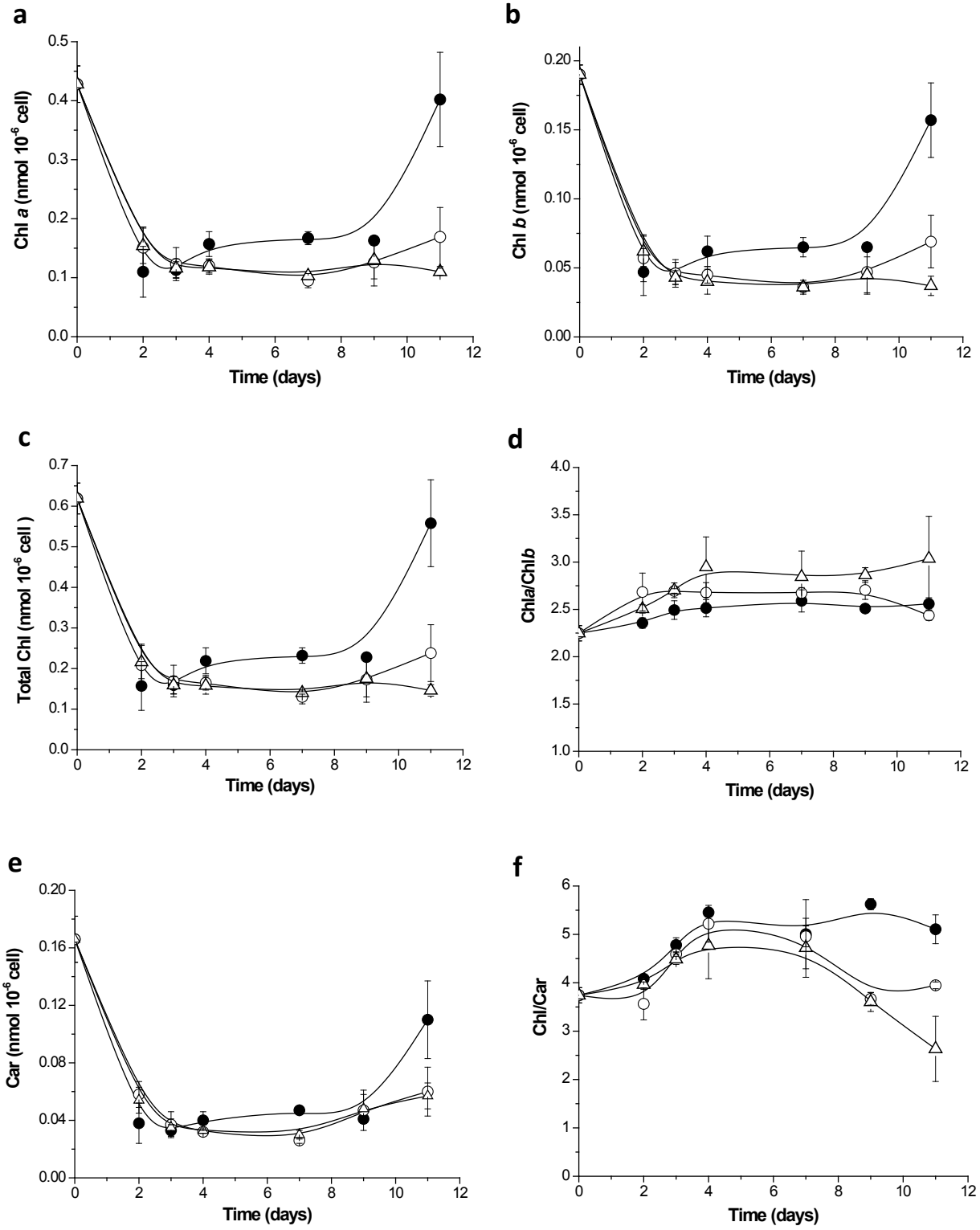

Fig. 6: time-course variations of Chl*a* content (a), Chl*b* content (b), total Chl content (c), Chl*a*/Chl*b* ratio (d), Car content (e) and Chl/Car ratio (f) of *N. oleoabundans* grown in presence of 0 (filled circles), 2.5 (empty circles) and 5 (empty triangles) gL^{-1} of glucose. For each sample, values are means ± s.d. (n > 3).

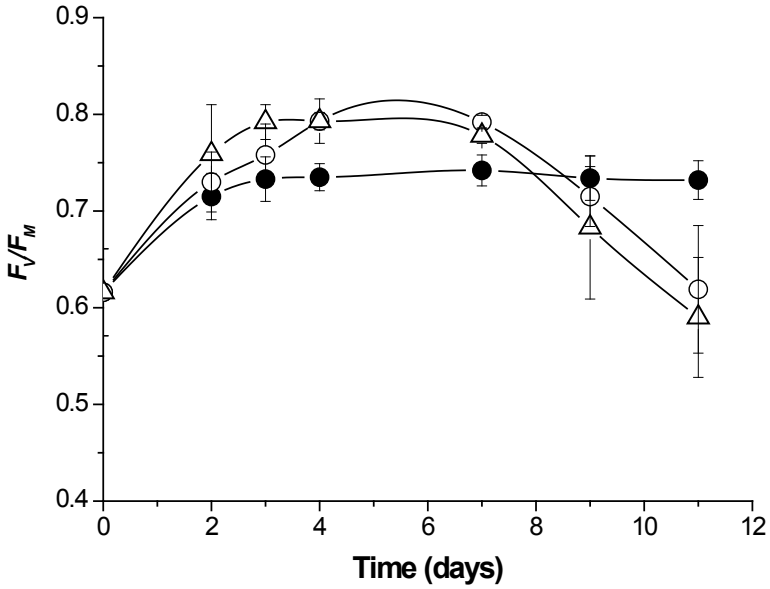

Fig. 7: time course of PSII maximum quantum yield F_V/F_M in *N. oleoabundans* grown with 0 (filled circles), 2.5 (empty circles) and 5 (empty triangles) gL^{-1} of initial glucose. For each sample, values are means ± s.d. (n > 3).

pH	5.72
Carbohydrates	g/100 ml
Glucose	0.75
Fructose	1.75
Sucrose	0.45
Acids	g/100 ml
Malic acid	0.30
Lactic acid	0.05
Acetic acid	0.05
Alcohols	mg/l
Ethanol	0.02

Tab.1: chemical composition of AWP. From Giovanardi et al. (2013).

Parameters	**Units**	**Average values**
pH	pH	7.6
Hardness	mmol$CaCO_3$ L^{-1}	190
Cl^-	mgL^{-1}	24
F^-	mgL^{-1}	<0.01
NH_4^+	mgL^{-1}	< 0.02
NO_3^-	mgL^{-1}	8.0
NO_2^-	mgL^{-1}	< 0.02
CO_3^{2-} and HCO_3^-	mgL^{-1}	245
Na^+	mgL^{-1}	14
K^+	mgL^{-1}	2.7

Tab. 2: chemical composition of the tap water used for the preparation of nutrient deprived media. Values were available in HERA website (www.gruppohera.it) and are referred to a monthly average registered at the time when experiments were executed.

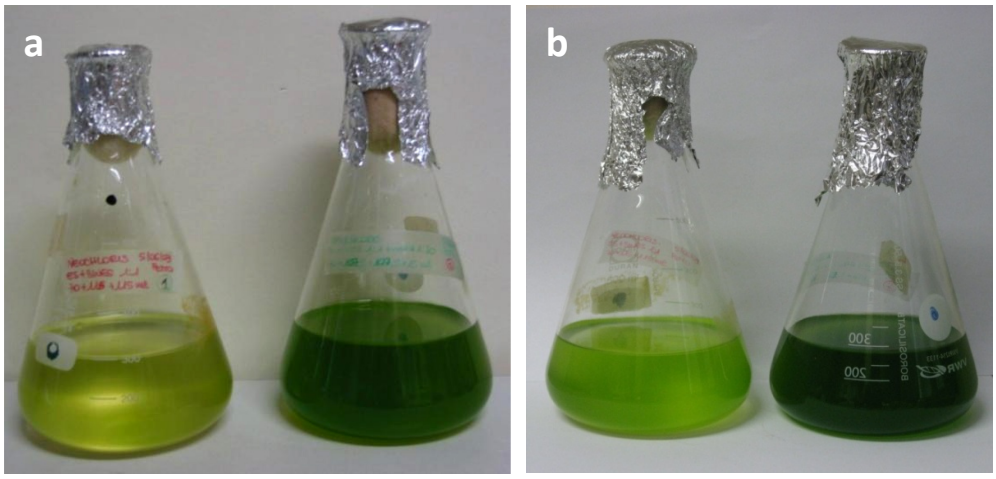

Fig. 8: *N. oleoabundans* cells grown in BM medium (pale green cultures) and in BM + AWP (dark green cultures) after 7 (a) and 28 (b) days of growth.

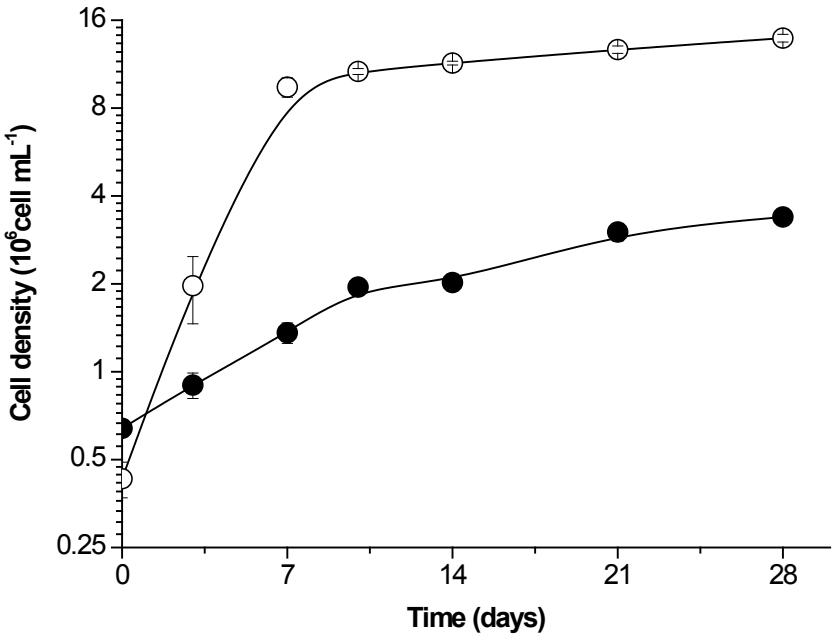

Fig. 9: growth kinetics of *N. oleoabundans* in BM medium (filled circles) and BM+AWP medium (empty circles). Values are means ± s.d. (n = 3).

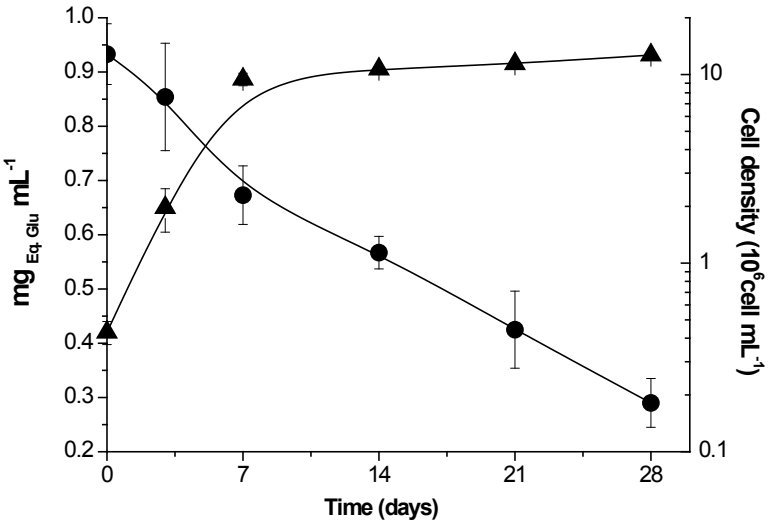

Fig. 10: growth kinetics of *N.oleoabundans* in BM+AWP medium (triangles) and corresponding glucose consumption (circles). For each sample, values are means ± sd (n > 3).

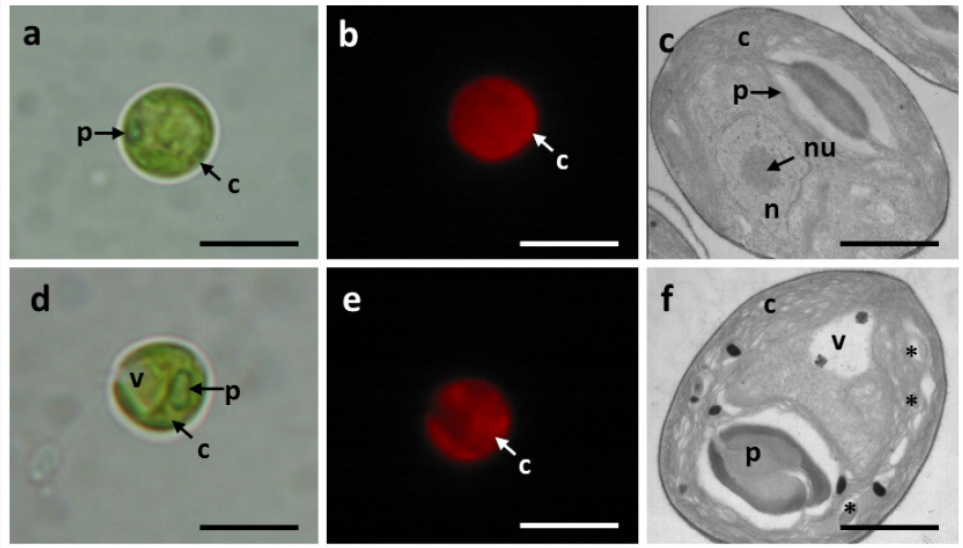

Fig. 11: cell morphology of *N. oleoabundans* grown in BM medium after 7 (a-c) and 28 (d-f) days. a, b, d, e) light and fluorescence microscopy images. Bars: 3.5 µm. c, f) submicroscopical views. Bars: 1 µm. p: pyrenoid, c: chloroplast, n: nucleus, nu: nucleolus, v: vacuolisations, asterisks: starch granulations inside the chloroplast.

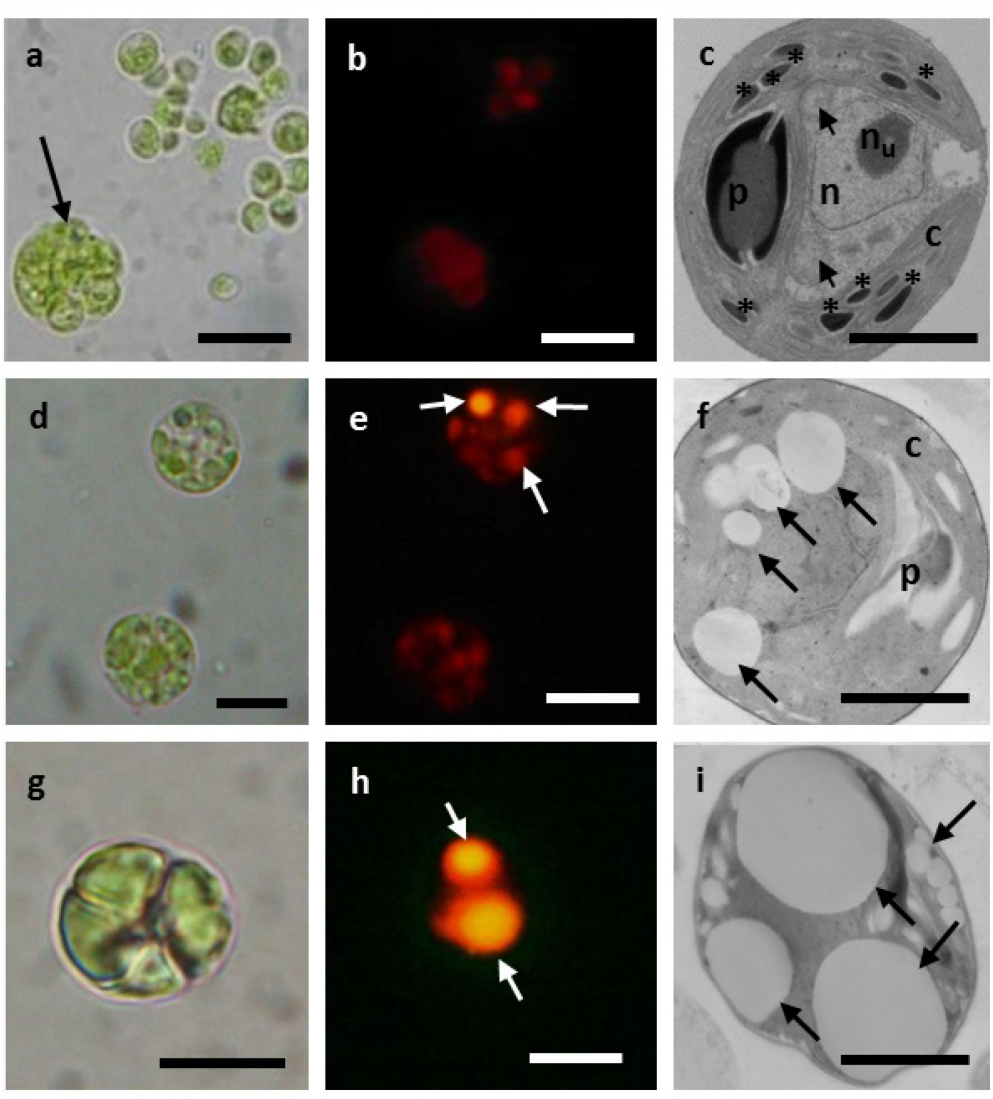

Fig. 12: cell morphology of *N. oleoabundans* grown in BM+AWP medium. a-c) aspects of cells at 7 days of growth. a) observations under the light microscope. Bar: 3 µm, arrow: sporocyst. b) epifluorescence micrograph of Nile Red-stained cells. Bar: 3.5 µm. c) transmission electron micrograph. Bar: 1.5 µm. Arrows: mitochondria, n: nucleus and n_u: nucleolus, c: chloroplast, p: pyrenoid, asterisks: starch granules. d-f) cells at 21 days of growth. d) light microscopy observations. Bar: 3 µm. e) Nile Red-stained cells. Bar: 3 µm, arrows: lipid globules inside cells. f) submicroscopical observations. Bar: 1.5 µm. Arrows: lipid globules, c: chloroplast, p: pyrenoid. g-i) cells at 28 days of growth. g) light microscopy. Bar: 3 µm. h) Nile Red-stained cells. Bar: 3 µm, arrows: lipid globules detected inside cells. i) submicroscopical observations. Bar: 1.5 µm, arrows: lipid globules.

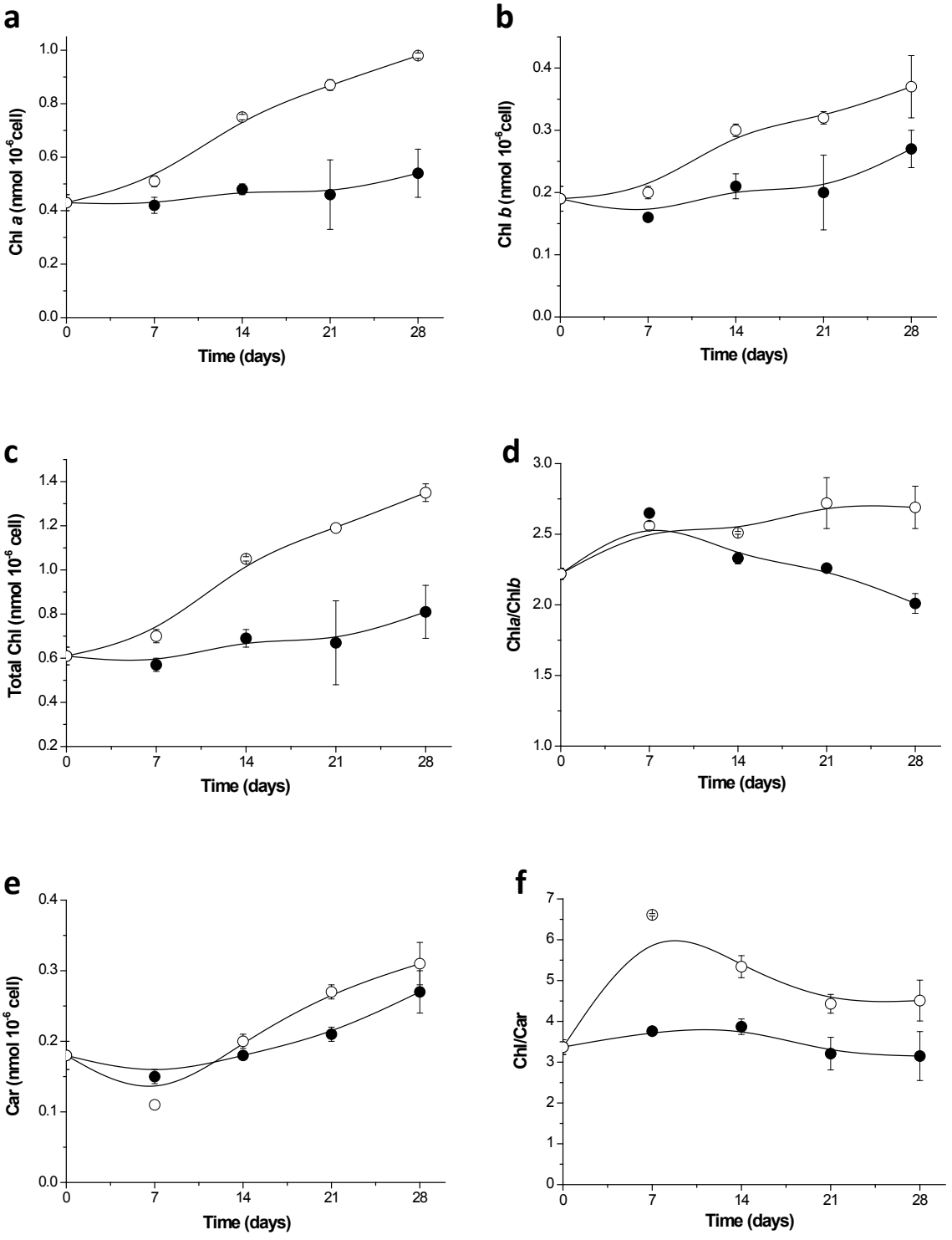

Fig. 13: time-course of Chl*a* (a), Chl*b*(b), total Chl (c), Chl*a*/Chl*b* ratio (d), Car (e) and Chl/Car ratio in *N. oleoabundans* cells grown in BM (filled circles) and BM+AWP medium (empty circles). For each samples, values are means ± s.d. (n = 3).

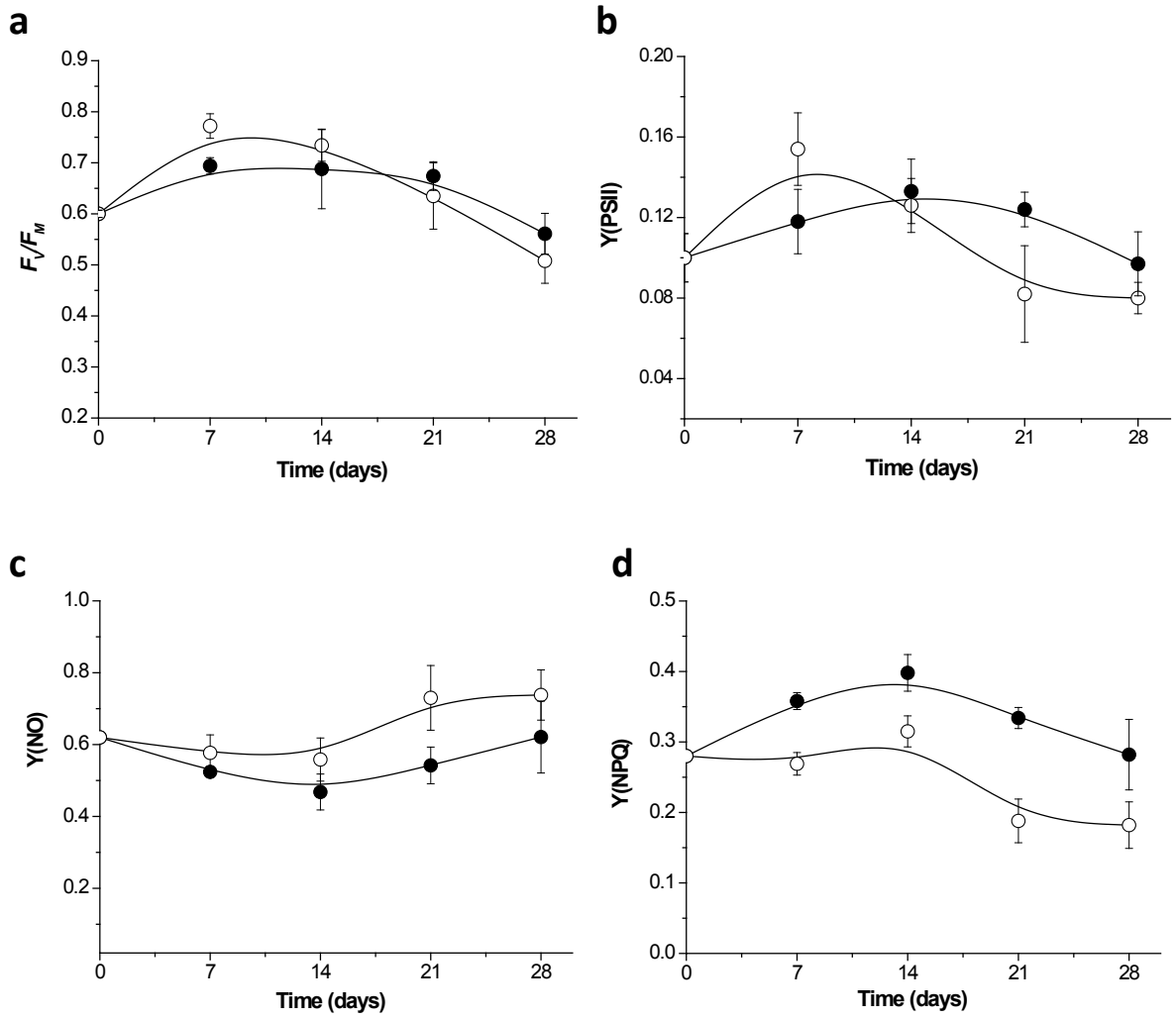

Fig. 14: time-course of F_V/F_M ratio (a), actual yield of PSII [Y(PSII)] (b), yield of constitutive thermal dissipation and fluorescence emission [Y(NO)] (c) and yield of non-photochemical quenching [Y(NPQ)] (d) in *N. oleoabundans cells* grown in BM (filled circles) and BM+AWP medium (empty circles). Values are means ± s.d. of 3 replicates.

λ (nm)	Attribution
660-670.5	uncoupled Chl
680	free LHCII
686	PSII core
694	LHCII-PSII functional assemblies
702	LHCII aggregate

Tab. 3: attribution of fluorescence emission bands by PSII in *N. oleoabundans* cells, according to Ferroni et al. (2011).

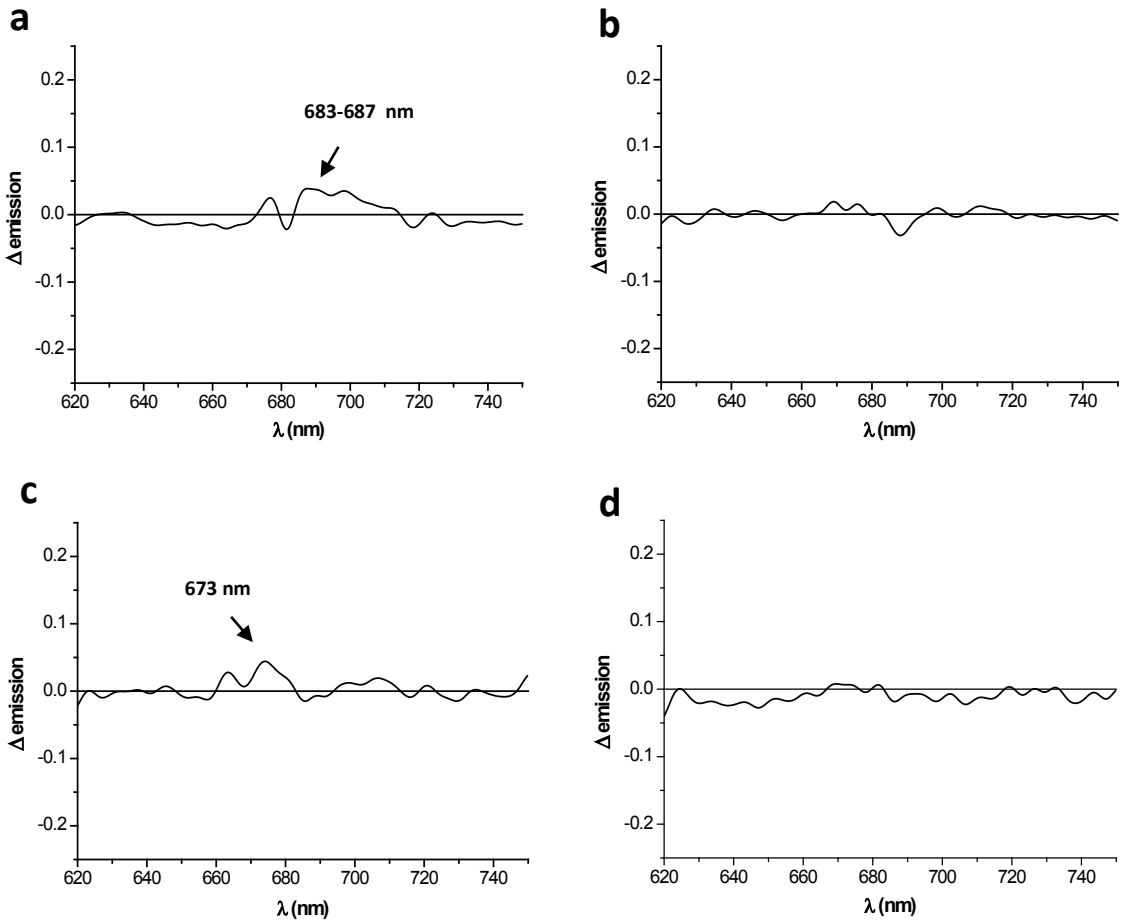

Fig. 15: differences between normalized fluorescence emission spectra recorded from *N. oleoabundans cells* grown in BM+AWP and BM medium after 7 (a), 14 (b), 21 (c) and 28 (d) days of growth.

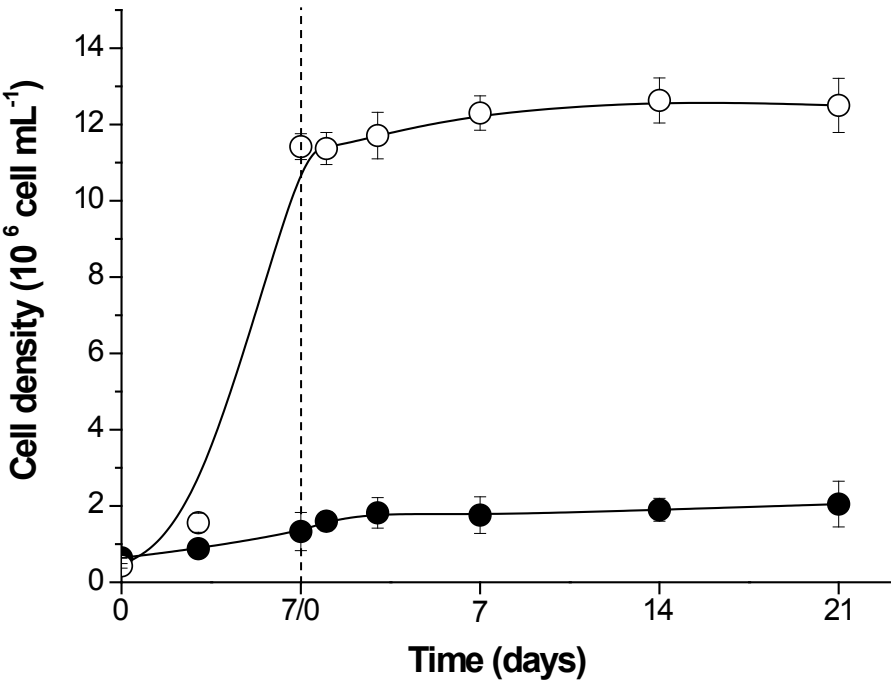

Fig. 16: growth kinetics of *N. oleoabundans* cells transferred in brackish tap water after 7 days of growth in BM (filled circles) or BM+AWP medium (empty circles). Dashed vertical line indicates the moment when cells were transferred to brackish tap water. Values are means ± s.d. of at least 3 replicates.

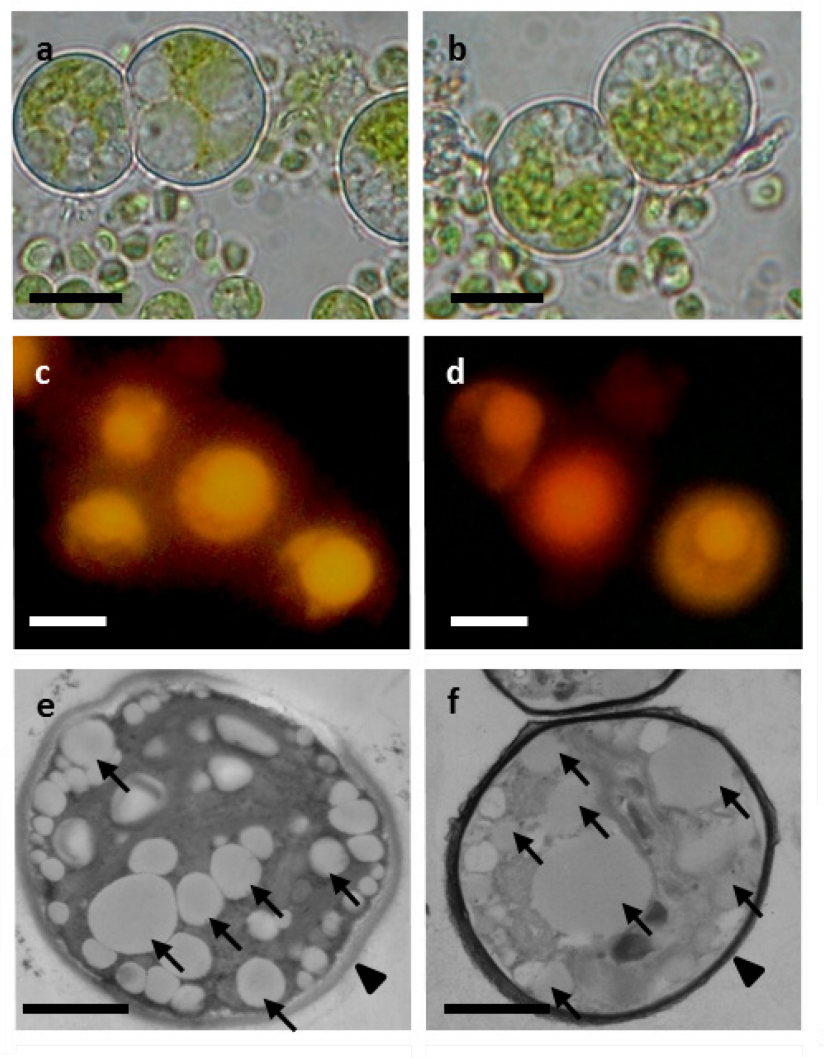

Fig. 17: representative images of *N. oleoabundans* grown in brackish tap water for 21 days. a) cell morphology of samples previously grown autotrophically or b) mixotrophically. Bars: 3 µm. c) epifluorescence micrographs of Nile Red-stained cells previously grown autotrophically or d) mixotrophically. Bars: 3 µm. e) transmission electron micrographs of cells previously grown autotrophically or d) mixotrophically. Arrows indicate some of the lipid globules that are present inside cells. Black arrowhead: thickening of the cell wall. Bars: 1.5 µm.

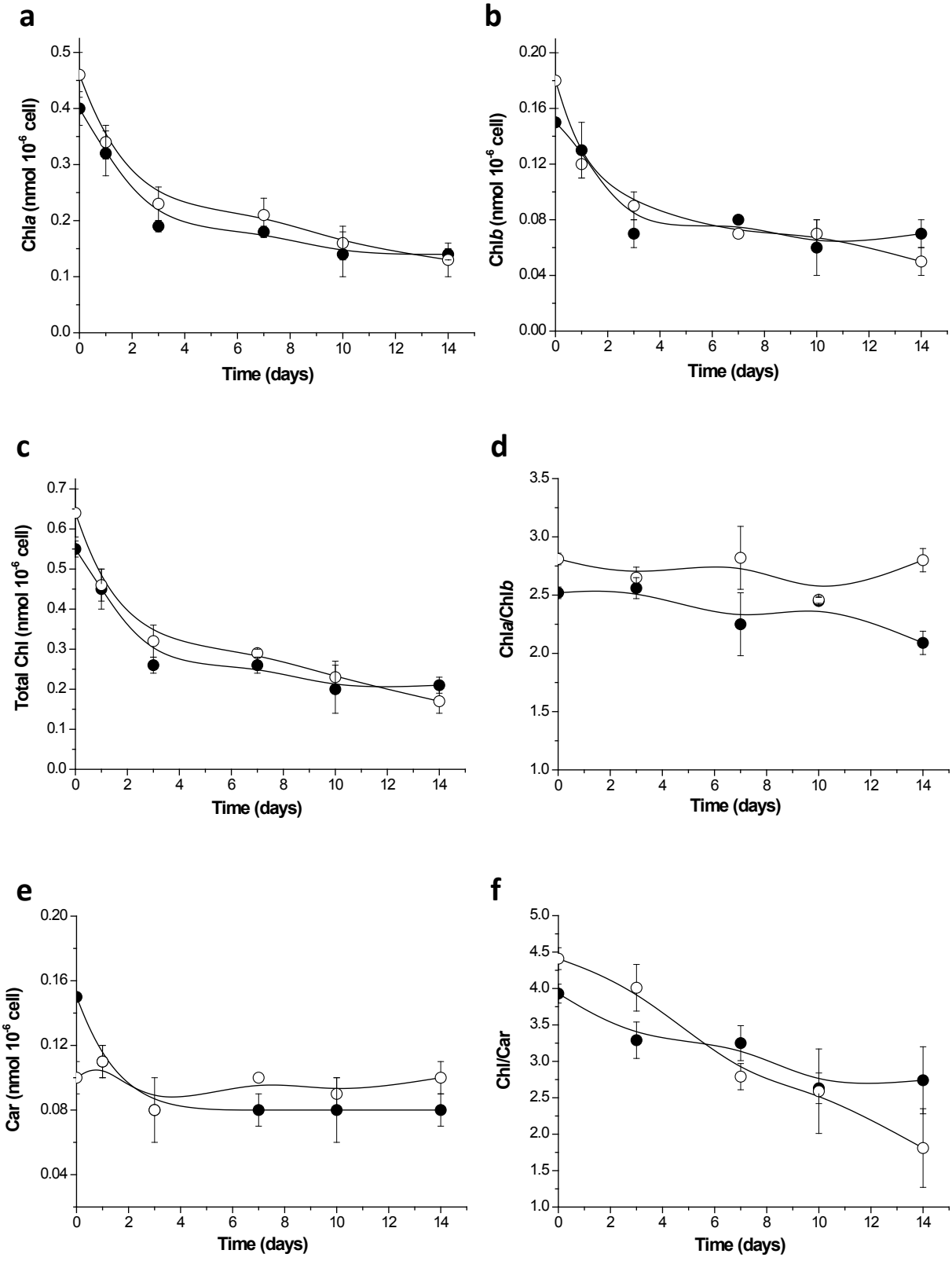

Fig. 18: time-course of Chl*a* (a), Chl*b* (b), total Chl (c), Chl*a*/Chl*b* ratio (d), Car (e) and Chl/Car ratio (f) in *N. oleoabunans* maintained in brackish tap water after 7 days of cultivation in BM (filled circles) or BM+AWP medium (empty circles). Values are means ± s.d. of 3 replicates.

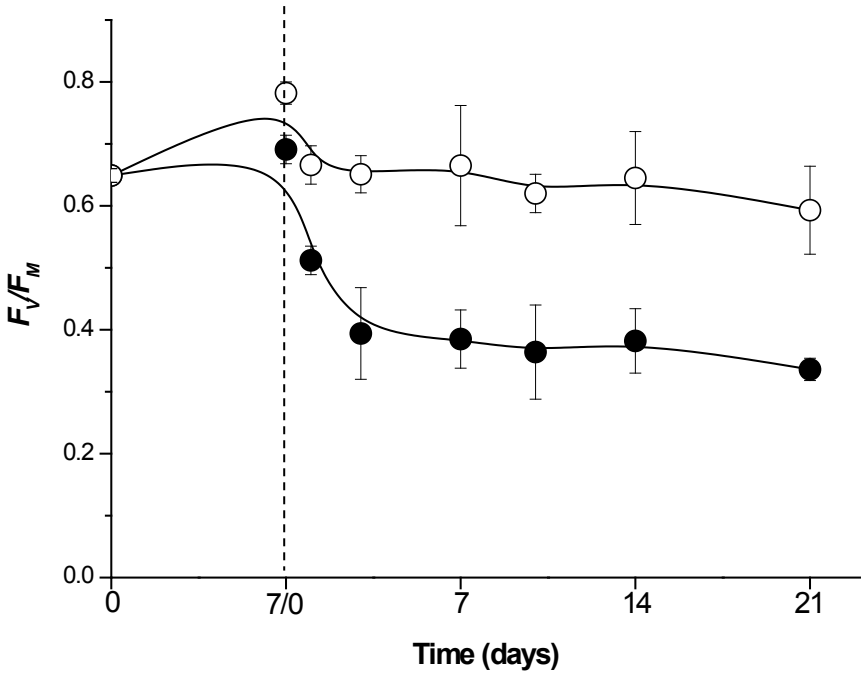

Fig. 19: F_V/F_M ratio in *N. oleoabundans* grown autotrophically (filled circles) or mixotrophically (empty circles) during the first 7 days of growth and subsequently transferred to brackish tap water. Values are means ± s.d. (n = 3).

Part II

Effects of glucose on the organisation of the photosynthetic apparatus in the microalga **N. oleoabundans**

1. Introduction

Photosynthesis is one of the most ancient biochemical processes which supports almost all life on Earth. This process involves several light-dependent reactions, which start with the absorption of light energy for the synthesis of NADPH and ATP as intermediate energy compounds (Geider and MacIntyre, 2002). The obtained reducing power is then used during the Calvin cycle for CO_2 fixation in sugars (Falkowski and Raven, 1997). On the whole, the important features of the light reactions of photosynthesis are: i) the collection of photons by light-harvesting antennae; ii) the migration of excitation energy from absorbed photons to the reaction centers; iii) the electron transfer from H_2O to $NADP^+$ and iv) the generation of ATP by a trans-thylakoid pH gradient driving force, which is formed as a consequence of the electron transfer (Geider and MacIntyre, 2002). Energy transduction in photosynthesis is mediated by four multi-subunit membrane-protein complexes, which are embedded in the thylakoid membranes of the chloroplast (Dekker and Boekema, 2005). PSII, a water-plastoquinone oxidoreductase complex, starts the photosynthetic electron transfer chain from water to plastoquinone using light as a driving force (Chow et al., 1990; Minagawa et al., 2004; Daniellson et al., 2006). The electrons from plastohydroquinone reach PSI via the Cyt b_6f complex and plastocyanin. PSI is involved in a light-dependent electron transport to ferredoxin and to $NADP^+$ (Chow et al., 1990). Finally, ATP synthase (ATPase) is a highly-conserved complex which catalyses ATP synthesis using the trans-membrane proton gradient generated by the photosynthetic electron-transport chain (Nelson and Ben-Shem, 2004). Moreover, PSII and PSI are flanked by light-harvesting pigment-protein complexes (LHC), which deliver the light energy that has been absorbed to the RC of the two photosystems (Minagawa et al., 2009).

The photosynthetic process cannot be understood without a detailed knowledge of the structure of its single components (Dekker and Boekema, 2005). The application of biophysical, biochemical and physiological techniques has provided a good understanding of the multi-subunit complexes, as well as of the events which drive the electron transfer processes with water oxidation (Barber, 2002; Nelson and Yocum, 2006). In particular, all the protein complexes are composed by several protein subunits coordinating a large number of cofactors (Minagawa et al., 2004, 2009). Moreover, these complexes show the tendency to

form higher-order associations, the so-called supercomplexes (Dekker and Boekema, 2005). The dynamic organisation of the pigment-protein complexes in the thylakoid membrane and their flexibility may play important roles in maintaining an optimal photosynthetic efficiency in several conditions (Anderson et al., 1995). Indeed, the photosynthetic process can be affected by a variety of environmental stresses, such as different light regimes (Chow et al., 1990), but also temperature and nutrient limiting conditions (Anderson et al., 1995). For example, in aquatic environments the CO_2 availability may become limiting, and photosynthetic organisms need to evolve adaptative mechanisms in order to maintain the light-harvesting and the carbon fixation capacities (Badger and Spalding, 2000). One of the strategies is to assimilate an external organic carbon source, shifting the metabolism from autotrophic to mixotrophic (Heifetz et al., 2000).

During these recent years, mixotrophic microalgae have been largely investigated for their capability to highly increase their biomass content, benefiting from the exogenous organic carbon source assimilation together with light harvesting and CO_2 fixation for growth (Marquez et al. 1993; Lee, 2001; Xu et al., 2006; Scott et al., 2010; Stephens et al., 2010). This approach, indeed, can be considered an important strategy for the industrial scale-up of lipid production from microalgae (Scott et al., 2010). However, the optimization of the process is still far from being commercially available. At present, this is due not only to technical limitations, but also, and maybe more relevantly, to an incomplete knowledge about the effects of organic carbon nutrition on the photosynthetic activity in mixotrophic cells (Rubio et al., 2002; Scott et al., 2010; Wijffels and Barbosa, 2010). Thus, further studies need to be performed, in order to improve basic knowledge of the microalgal physiology, leading to advantageous growth conditions and so to increased biomass densities (Wijffels and Barbosa, 2010). Several works support the theory that, in some mixotrophic microalgae, autotrophic and heterotrophic metabolisms proceed independently (Marquez et al., 1993; Liu et al., 2009a). Conversely, in other studies they have been shown to be linked to each other (Vonshak et al., 2000). In many studies glucose caused inhibitory effects, reducing the apparent affinity for CO_2 during CO_2 fixation (Lalucat et al., 1984; Martinez and Orus, 1991) or limiting the synthesis of the RuBisCO of the Calvin cycle (Oesterhelt et al., 2007). Reduced photochemical efficiency of PSII has also been observed, indicating that organic carbon depresses the photosynthetic efficiency (Valverde et al., 2005; Oesterhelt et al., 2007; Liu et

al., 2009a). About the interaction of organic carbon assimilation and photosynthetic activity in *N. oleoabundans*, very little or no information is available. However, in previous works described in this Thesis (see Part I), mixotrophy promoted the activity of the photosynthetic apparatus, with very high PSII maximum quantum efficiency, never observed in other mixotrophic microalgal species (Yamane et al., 2001; Ip et al., 2004; Liu et al., 2009a). However, the maximum quantum yield of PSII, usually measured as F_V/F_M ratio, should not be considered a rigorous quantitative value, because, as a simple model, it admits a number of assumptions which might not be correct in all situations (Baker et al., 2008). In this work, the effects of different glucose concentrations supplied in the culture media were assessed in order to provide new information on the photosynthetic metabolism and its interaction with the organic carbon source assimilation in *N. oleoabundans*. Several approaches have been used to this purpose. Immunodetection with antibodies against different subunits of thylakoid multi-protein complexes was employed to identify differences in their abundance between autotrophic and mixotrophic samples, whereas Blue-Native polyacrylamide gel electrophoresis (BN-PAGE) has been employed to obtain information on native interactions of photosynthetic protein complexes in thylakoids (Hippler et al., 2001; Eubel et al., 2005; Rokka et al., 2005). In parallel, Chl fluorescence measurements were performed *in vivo* on freshly-collected samples to identify differences in the modulation of the photosynthetic electron transport and in PSI/PSII stoichiometry in autotrophic and mixotrophic cells.

2. Materials and methods

2.1. Algal strain and culture condition

The microalga *N. oleoabundans* UTEX 1185 (syn. *Ettlia oleoabundans*) was obtained from the Culture collection of the University of Texas (UTEX, USA; www.utex.org). Cells were grown and maintained in axenic liquid BM medium (Baldisserotto et al., 2012) in a growth chamber (24 ± 1 °C temperature, 80 $\mu mol_{photons}$ m^{-2} s^{-1} PAR and 16:8 h of light-darkness photoperiod), without shacking and external CO_2 supply. For experiments, cells were inoculated at a density between 0.5 and 0.7 x 10^6 cells mL^{-1} in BM medium containing 0 (control), 2.5 or 5 g L^{-1} of glucose and grown in 500 mL Erlenmeyer flasks (300 mL of total volume) in the same growth chamber described above, with continuous shacking at 80 rpm. For each glucose concentration, at least 3 replicates were set up. Growth was estimated measuring the optical density at 750 nm with a Pharmacia Biotech Ultrospec®2000 UV–vis spectrophotometer (1 nm bandwidth; Amersham Biosciences, Piscataway, NJ, USA), sampling periodically 1 mL of culture. The values were referred to a calibration curve with known cell number, evaluated with a Thoma's haemocytometer, versus optical density.

2.2. Thylakoid isolation from microalgal cells

Thylakoid membranes were isolated according to Pantaleoni et al. (2009), with modifications. For extraction, 300 mL of culture in late-exponential phase of growth were harvested by centrifugation at 600 *g* for 10 min. Pellets were transferred to an ice-cold mortar containing sand quartz. The extraction was performed grinding cells with liquid N_2, then the lisate was resuspended in the grinding buffer (330 mM sorbitol, 50 mM Tricine-NaOH pH 7.5, 2 mM Na_2EDTA pH 8.0, 1 mM $MgCl_2$, 5 mM ascorbate, 0.05% bovine serum albumin, 10 mM NaF) and transferred to 15 mL tubes. Samples were centrifuged at 300 *g* for 5 min at 4°C and then at 700 *g* for 5 min at 4°C, in order to remove sand quartz and cell debries. Pellets were discarded and the thylakoids present in the supernatant were collected by centrifugation at 7000 *g* for 10 min at 4°C. The supernatant was discarded and thylakoids were resuspended in 1 mL of shock buffer (5 mM sorbitol, 50 mM Tricine-NaOH pH 7.5, 2 mM Na_2EDTA, 5 mM $MgCl_2$, 10 mM NaF) and centrifuged at 7000 *g* for 10 min at 4°C. After that, the supernatant was removed and around 100 µL of storage buffer (100 mM sorbitol,

50 mM Tricine-NaOH pH 7.5, 2 mM Na_2EDTA pH 8.0, 5 mM $MgCl_2$, 10 mM NaF) were added to the pellet. The samples were rapidly frozen in liquid nitrogen and stored at -80°C until further analyses. Manipulation of samples was always performed on ice and in very dim safe light. Quantification of Chl and proteins in thylakoid samples was performed according to Porra (1989) and Lowry (1951), respectively.

2.3. SDS-PAGE and immunoblotting

Thylakoid proteins were separated by SDS-PAGE according to Laemmli (1970) on a 15% acrylamide resolving gel containing 6 M urea. After electrophoresis, proteins were visualised by Coomassie staining overnight (0.1% Coomassie Brilliant Blue R250, 7% acetic acid, 40% MeOH in distilled water), followed by destaining (7.5% acetic acid, 25% MeOH) for 5 h, or blotted onto a PVDF membrane (Millipore, Watford, Hertforshire, U.K.). Western blotting with enhanced chemiluminescence detection was performed with standard techniques using protein-specific antibodies against D1-DE loop of D1 protein, PsaB subunit of PSI, ATP-β subunit of ATPase, and antibodies raised against the entire LHCII complexes. For immunodetection of D1-DE loop and PsaB, 0.5 μg of Chl were loaded in each lane, whereas, for detection of ATP-β, samples were also loaded on a protein basis (40 μg in each lane). Finally, for LHCII detection, 0.25 μg of Chl were loaded in each lane. Protein amount was quantified with Image J software.

2.4. BN-PAGE and second dimension (2D) electrophoresis

BN-PAGE was performed according to Rokka et al. (2005) with small modifications. Thylakoids containing 5 μg Chl were resuspended in medium A (25mM BisTris-HCl, pH 7.0, 20% w/v glycerol and 0.25 mg mL^{-1} Pefabloc) to a final concentration of 1 μg μL^{-1} Chl. After that, an equal volume of 2% (w/v) dodecyl β-D-maltoside (Sigma), freshly prepared in medium A, was added. Thylakoids were then solubilised on ice for 15 min and centrifuged at 18000 *g* at 4°C for 15 min. The supernatant was supplemented with 1/10 volume of SB buffer (100 mM BisTris-HCl, pH 7.0, 0.5 M ε-amino-*n*-caproic acid, 30% w/v sucrose and 50 mg mL^{-1} Serva Blue G) and loaded on gel with 5-12.5% gradient of acrylamide in the separation gel. Electrophoresis was performed with a Hoefer Mighty Small system (Amersham Biosciences) at 0°C for 3.5 h by gradually increasing the voltage from 75 to 200 V. For comparison, thylakoids from *A. thaliana* were included in the analyses. Quantification

of band volume was performed with Image J software. After BN-PAGE, the lanes were cut out and incubated in 10%-sodium dodecyl sulphate (SDS) Laemmli buffer containing 5% (v/v) β-mercaptoethanol for 1.5 h, followed by separation of the protein subunits of the complexes with SDS-PAGE (12% polyacrylamide) and 6M urea. After electrophoresis, proteins were visualised by silver staining.

2.5. Fluorescence measurements

For *in vivo* biophysical analyses, samples were collected from the different cultures of *N. oleoabundans* grown with 0, 2.5 and 5 gL^{-1} of glucose. In particular, mixotrophic samples were compared with control samples either at the same cultivation time (after 7 days of growth), or at the same phase of growth, i.e. in late exponential phase, when control samples reached the same cell density observed in mixotrophic cultures after 7 days.

Flash-induced Chl fluorescence relaxation kinetics

The single flash-induced increase in Chl*a* fluorescence yield and its subsequent relaxation in darkness (FF-relaxation) were measured with a double-modulation fluorimeter (Photon System Instruments, Brno, Czech Republic). For analyses, 1 mL of samples containing 8 µg mL^{-1} Chl was incubated in darkness for 10 min and then Q_A^- reoxidation kinetics was recorded after a single-saturating flash (10 µs), provided by red LED, in the 150 µs - 100 s time range. Analyses were carried out either in the presence or absence of DCMU 5 µM (Allahverdiyeva et al., 2007). For each sample, measurements from at least 3 biological replicates were obtained. For easier comparison, the fluorescence relaxation curves were averaged and normalised to the same amplitude. Elaboration of data was carried out with Origin 6.0 software (OriginLab, Northampton, MA, USA). Since the fluorescence yield is not linearly correlated with the amount of Q_A^-, the relative Q_A^- concentration was estimated according to the model of Joliot using 0.5 for the value of the energy-transfer parameter between PSII units (Joliot and Joliot, 1964). Multicomponent deconvolution of the relaxation curves was performed by using a fitting function with two exponential and one hyperbolic components:

$$F(t) - Fo = A1\, e^{-t/T1} + A2\, e^{-t/T2} + \frac{A3}{1 + t/T3}$$

where $F(t)$ is the variable fluorescence yield, Fo is the basic fluorescence level before the flash, $A1$-$A3$ are the amplitudes, $T1$-$T3$ are the time constants from which the half-lifetimes can be calculated via $t_{1/2} = \ln 2T$ for the exponential components, and $t_{1/2}$ is the T for the hyperbolic component (Vass et al., 1999). For comparison between samples, statistical analyses were carried out with Student's *t*-test, with a significance level of 0.05.

Slow kinetics of PSII fluorescence

Experiments were carried out from liquid cultures containing 15 µg mL^{-1} pre-incubated in darkness for 10 min. Samples were subsequently exposed to actinic light. The following program was triggered: 90 $\mu mol_{photons}\ m^{-2}s^{-1}$, 11 min; dark, 11 min; 1000 $\mu mol_{photons}\ m^{-2}s^{-1}$, 15 min; dark, 5 min. Light saturating pulses were given every 40 s. Time course of Chl fluorescence parameters F_M', i.e. the maximum fluorescence in the light-adapted state measured applying the pulse, and F_t, i.e. the steady state fluorescence yield, were determined with a DUAL-PAM-100 (Waltz, Germany). Fluorescence curves were recorded from at least 3 replicates for each sample. Elaboration of data was carried out with Origin 6.0 software (OriginLab, Northampton, MA, USA).

77K fluorescence emission spectrum

Fluorescence emission spectra measured *in vivo* from samples containing 8 µg mL^{-1} Chl were recorded at 77 K with a diode array spectrophotometer (S2000; Ocean Optics, Dunedin, FL, USA) equipped with a reflectance probe as described in Keranen et al. (1999). Fluorescence excitation was obtained with light below 500 nm, defined using LS500S and LS700S filters (Corion, Holliston, MA, USA) placed in front of a slide projector, and the emission was recorded between 600 and 800 nm. Experiments were carried out on at least 3 replicates for each sample, and the emission spectra obtained for each replica were averaged. Elaboration of the spectra was performed with Microsoft Excel™.

3. Results

3.1. Characterisation of Chl-protein complexes in thylakoids membranes of autotrophic and mixotrophic *N. oleoabundans*

Chl and protein quantification in thylakoid membranes

Quantification of Chl and protein amounts in thylakoids of *N. oleoabundans* grown in the presence of 0, 2.5 and 5 gL^{-1} are reported in Tab. 1. Total Chl quantified in thylakoids was compared with the corresponding protein amount to obtain Chl/protein ratios (Chl/prt). The values obtained were different between control and mixotrophic samples. Interestingly, in the cultures grown in 2.5 and 5 gL^{-1} of glucose, indeed, Chl/prt was halved with respect to autotrophic samples. About the Chl *a*/*b* molar ratio, instead, it was observed that the values were higher in mixotrophic than in autotrophic samples.

When SDS-gels were visualized by Coomassie staining, analyses showed differences in the thylakoid protein pattern between autototrophic and mixotrophic samples (Fig. 1). In particular, when lanes were loaded on an equal Chl basis, both samples from mixotrophic cells showed an important enrichment of the entire protein pattern, irrespective of the amount of glucose added to the medium of growth (Fig. 1 a). Conversely, when samples were loaded on a protein basis, less intense bands just below 25 kDa, which correspond to LHCII proteins (Bennet, 1991), were observed in mixotrophic samples. Therefore, in the thylakoids of mixotrophic cells the lower Chl/prt ratio corresponded to a decrease in LHCII, which hosts most of the Chl. On the other hand, in mixotrophic samples a protein below 17 kDa seemed to be more abundant than in autotrophic samples (Fig. 1 b). Some of the key proteins which belong to major thylakoid complexes were detected and quantified by immunoblot analyses (Fig. 2). Interestingly, differences in the protein amounts occurred between autotrophic and mixotrophic samples. Indeed, on a protein basis, lower amounts of ATP-β were detected in samples grown with 2.5 (-19%) and 5 (-23%) gL^{-1} of glucose with respect to control cells. For analysis of subunits belonging to Chl-protein complexes, the gels were instead run on a Chl basis. Decreasing amounts of PsaB were also measured with the increase in glucose concentrations. Indeed, about 59 and 40% of the PsaB control level were detected in 2.5 and 5 gL^{-1} of glucose-grown cells, respectively. Relative LHCII protein amount also decreased when glucose concentration increased in the medium of growth. Indeed, in

cells grown with 2.5 gL^{-1} and of 5 gL^{-1} of glucose the amounts were about 10 and 13% lower than in controls, respectively. Conversely, D1 protein was detected in higher amounts in 2.5 (+47%) and 5 (+29%) gL^{-1} of glucose with respect to autotrophic samples, but no direct correlation with the glucose amount added to the media of growth was observed.

Organisation and assembly of thylakoid complexes

In order to obtain the separation of the thylakoid membrane complexes from autotrophic and mixotrophic *N. oleoabundans*, a BN-PAGE system was optimised. In a first analysis, the pattern of protein complexes in autotrophic *N. oleoabundans* was compared to that of the model organism *A. thaliana* (Fig. 3 a). Since in the BN-PAGE the apparent molecular mass of the protein complexes from *N. oleoabundans* corresponded to the predicted molecular masses known for *A. thaliana*, each complex was recognised based on the same molecular mass. Despite this, evident differences in the pattern of complexes occurred between the two samples. Autotrophic *N. oleoabundans* lacked PSII-LHCII supercomplexes and also LHCII assemblies with respect to *A. thaliana*. Moreover, in the microalgal samples the PSI-LHC complexes (including PSI core, LHCI and LHCII) and PSII dimers were resolved as separate bands. Finally, PSI-LHC, PSII dimers and PSII monomers had higher molecular weight, while LHCII trimers and monomers were lighter as compared to *A. thaliana*.

After this first analysis, membrane protein complexes from autotrophic and mixotrophic *N. oleoabundans* were separated by BN-PAGE with the same procedure (Fig. 3 b). A different pattern of protein complexes was resolved in BN gels of thylakoids from different samples. In particular, although the two mixotrophic samples did not yield exactly the same profile, in general it was found that: i) all complexes in mixotrophic samples had slightly higher molecular weight compared to controls; ii) the mixotrophic samples had visibly lower amount of PSII dimer (about -25%) and more PSII monomer (about +25% in both cases) with respect to control. Moreover, in thylakoids from cells grown with 5 gL^{-1} of glucose, less PSI-LHC supercomplexes and LHCII monomers were also shown with respect to mixotrophic samples grown with 2.5 gL^{-1} of glucose. In order to support the identification of the PSII and LHCII protein complexes and to resolve their composition, each stripe from the BN-PAGE was further analysed by SDS-PAGE in the 2D, enabling the separation of different

protein complexes into constituting subunits (Fig. 4). In each 2D image in Fig. 4, the first conspicuous band from the left, corresponding to PSI-LHC complexes, contained Psa A/B subunits of PSI and some LHCI proteins. Confirming the Western Blot analyses which showed decreased levels of PSI in mixotrophic samples, PsaA and B appeared less abundant in thylakoids from 2.5 and 5 gL^{-1} of glucose-grown cells (Fig. 4 a, b). Moreover, PSI-LHCII complexes were also observed in all the samples, but amounts appeared lower in mixotrophic with respect to autotrophic cells. Interestingly, only in 2.5 gL^{-1} of glucose-grown samples some PSII subunits were bound to PSI (Fig. 4 a). This was not observed in control and in sample grown with 5 gL^{-1} of glucose. The second band, corresponding to the PSII dimers, contained the Chl-binding proteins CP47 and CP43, as well as D1 and D2 subunits of PSII core, in the dimeric form. When thylakoids from 2.5 (Fig. 4 a) and especially 5 (Fig. 4 b) gL^{-1} of glucose-grown samples were compared with controls, it was clearly evident that all the subunits belonging to PSII dimer were less abundant. Conversely, when the 2D resolution of the 4^{th} band, corresponding to PSII monomers and containing the same PSII subunits as in dimers, were compared between samples, it was clearly visible that all the subunits were more abundant in both mixotrophic samples with respect to thylakoids from control cells. Cyt b_6f was co-migrating with the PSII monomers, but no obvious difference was observed in its subunits between samples. Finally, the resolution of bands corresponding to LHCII trimers and monomers did not show any relevant difference between autotrophic and mixotrophic cells as well.

3.2. Fluorimetric analyses on *in vivo* autotrophic and mixotrophic *N. oleoabundans*

Effects of different glucose concentrations on reoxidation kinetics of Q_A

The effects of mixotrophy on the activity of both quinone components of the quinone-iron acceptor complex, Q_A and Q_B, can be studied by measuring flash-induced changes in the yield of Chl fluorescence (Vass et al., 2002). The reduction of Q_A upon flash excitation results in a prompt increase of Chl fluorescence yield, which is followed by a dark decay in the range of 100 µs – 10 s time range due to the reoxidation of Q_A by various pathways (Vass et al., 2002). The fluorescence relaxation is dominated by a fast component (few-hundred µs), arising from Q_A^- to Q_B electron transfer in RCII, which had an oxidised or

semi-reduced plastoquinone (PQ) molecule in the Q_B pocket at the time of flashing. The middle phase (few ms), arises from Q_A^- reoxidation in centers which had an empty Q_B site in darkness and had to bind PQ from the pool. Finally, the slow phase of flash-induced fluorescence relaxation curve (few s) shows the recombination of the S2 state of the water oxidising complex with Q_B^- via the $Q_A^- Q_B \leftrightarrow Q_A Q_B^-$ equilibrium (Vass et al., 1999; Vass et al., 2002; Allahverdiyeva et al., 2005).

When mixotrophic samples were compared with autotrophic cultures at 7 days of growth, analyses of the kinetics of the flash-induced fluorescence relaxation showed that the fast phase of decay was slightly accelerated in samples grown with 2.5 (-3%) and 5 (-10%) gL^{-1} of glucose with respect to control (ca. 570 μs of time constant) (Tab. 2; Fig. 5 a). Conversely, the relative amplitude of the fast relaxation phase slightly increased with the increase in glucose concentration (+7% and +14% in 2.5 and 5 gL^{-1} of glucose-grown cells, respectively, as compared to control; Tab. 2). However, these results were not significant. When middle phases of decay were compared, the time of decay was highly accelerated in 5 gL^{-1} of glucose-grown cells (-47%, $p < 0.01$), whereas no differences in relative amplitudes or time of decay were observed between 2.5 gL^{-1} of glucose-grown cells and control (Tab. 2; Fig. 5 a). These results indicated a tendency to modify the Q_A-to-Q_B electron transfer in mixotrophic cells and to fasten PQ binding to the Q_B pocket, especially in cells grown in 5 gL^{-1} of glucose. The slow phase of fluorescence relaxation, originating from $S_2(Q_A Q_B)^-$ recombination, showed an increase in relative amplitude in both mixotrophic cells (around +12,5%, $p < 0.01$) and a minor time constant in 5gL^{-1} of glucose-grown cells (-41% with respect to control cells, $p < 0.01$) (Tab. 2; Fig. 5 a).

When mixotrophic samples were instead compared with autotrophic controls at the same phase of growth (Fig. 5 b), the time of decay of the fast phase was further accelerated both in 2.5 (+26%) and especially in 5 (+31%, $p < 0.01$) gL^{-1} of glucose-grown cells with respect to control samples (Tab. 2). Moreover, relative amplitude dramatically increased, i.e. was doubled, in cells grown with the highest concentration of glucose ($p < 0.01$). In these samples, time of decay of the middle phase was also significantly different compared to controls (+69%, $p < 0.01$) (Tab. 2).

In the presence of DCMU, which blocks the reoxidation of Q_A^- by forward electron transfer, the fluorescence relaxation indicates the status of the PSII donor side due to recombination of Q_A^- with donor side components. In a functional PSII complex, the recombination partner of Q_A^- is the S2 state of the water oxidising complex. Interestingly, analysis of these decay curves showed that in the mixotrophic samples a fast-decaying component dominated the decay, confirming the results previously described in the absence DCMU. When mixotrophic samples were compared with controls at 7 days of growth (Fig. 5 c), this fast phase was clearly evident especially in 5 gL^{-1} of glucose-grown cells, whereas when control cells in late exponential phase were used for comparison (Fig. 5 d), the fast-decay was more evident in both mixotrophic samples.

Slow kinetics of Chla fluorescence

In order to clarify the effects of glucose on the dynamics of photosynthetic electron transfer reactions, PAM fluorescence trace in freshly-collected samples of autotrophic and mixotrophic cultures was monitored, measuring the time-course of Chl fluorescence parameters F_M', i.e. the maximum fluorescence in the light-adapted state, measured applying a saturation pulse, and F_t, i.e. the steady state fluorescence yield in the light-adapted state. Samples were pre-incubated in darkness for 10 min before analysis and then the initial F_M and F_0 values were determined by applying a saturation pulse. In Fig. 6 typical *Chla* fluorescence kinetics were represented for control (Fig. 6 a), 2.5 (Fig. 6 b) and 5 (Fig. 6 c) gL^{-1} of glucose-grown cells. Interestingly, no differences occurred between autotrophic samples obtained from cultures with different age from the inoculum and different stage of growth. On the whole, differences between control and mixotrophic samples instead occurred. In particular:

- no differences in the minimal level of fluorescence F_0 were observed before turning on the actinic light, indicating that same amount of PSII in the "open state" was present;
- during the sequence 90 $\mu mol_{photons}\ m^{-2}s^{-1}$ - darkness of the triggered program, in control cells fluorescence F_M' increased to values higher than the initial F_M. Conversely, F_M' decreased during the subsequent dark period (Fig. 6 a). On the other hand, in mixotrophic samples the F_M' increase effect in the light was not

always observed and, when it occurred, the fluorescence increase was not as marked as in controls. Moreover, during the subsequent dark period, after a temporary decrease in F_M, the value increased to the initial F_M value, as expected (Fig. 6 b, c);

- when cells were exposed to 1000 $\mu mol_{photons}\ m^{-2}s^{-1}$, an initial rise in the basal fluorescence F_t was observed in controls, followed by a strong decrease. Conversely, these two phases were less marked in mixotrophic samples and a less evident "hump" was observed with respect to controls at the beginning of the high-light exposure period. Moreover, basal fluorescence F_t remained higher during high-light exposure, suggesting that mixotrophic samples were more sensitive to light than autotrophic samples. The effect was proportional to the increase in glucose concentration;
- when cells were subsequently exposed to darkness, maximum fluorescence gradually increased with no differences between samples. However, as soon as the actinic light was turned off, in controls an evident decrease in the basal fluorescence value was observed even with the weak measurement light, followed by a rise. In mixotrophic samples, instead, this decrease-rise sequence was less evident.

77K fluorescence emission ratio and PSI/PSII stoichiometry in autotrophic and mixotrophic samples

77K spectra were recorded from aliquots of samples containing 8 μgmL^{-1} Chl, frozen and maintained in liquid N_2 before analyses. In Fig. 7 a, mixotrophic samples were compared to controls at 7 days of growth. No differences were observed, indeed spectra almost overlapped. In particular, the peak at around 684 nm was attributed to PSII, while the peak at 714 nm was attributed to PSI-LHCI (Ferroni et al., 2011). Moreover, a broad shoulder between 692 and 703 nm was observed. Emission around 700 nm can be attributed to LHCII aggregates (Horton et al., 1991). When mixotrophic samples were compared to controls at the same stage of growth (Fig. 7 b), spectra were instead very different. In fact, peaks were slightly shifted in control, at 683 nm for PSII and 713 nm for PSI-LHCI. Moreover, the shoulder at 692-703 nm was not observed between PSII and PSI emission regions. It is possible that this emission was not evident because of the higher emission from PSI-LHCI in

control samples. More information was obtained calculating the PSI/PSII emission ratio. As expected, no differences were observed between control and mixotrophic samples when comparison was carried out on cells sampled at the same time from the inocula. Conversely, when samples were compared at the same phase of growth, the ratio measured for controls was interestingly higher with respect to that measured for 2.5 (-8%, $p < 0.05$) and 5 (-10%) gL^{-1} of glucose grown-cells. This confirmed the decrease in the PSI amount over PSII in mixotrophic *vs* autotrophic cells when cultures were in almost stationary phase of growth (Fig. 8).

4. Discussion

The green microalga *N. oleoabundans* is considered a very promising organism to be exploited in the green-energy field because of its capability to accumulate lipids when grown under nutrient starvation (Tornabene et al., 1983; Li et al., 2008b; Pruvost et al., 2009; Popovich et al., 2012; Giovanardi et al., 2013). Unfortunately, very low biomass densities are reached in these conditions of growth. In the work previously discussed in this Thesis - part I, the mixotrophic growth of *N. oleoabundans* in presence of different glucose concentrations allowed to obtain not only very high biomass densities at the end of the exponential phase, but also lipid accumulation when cells entered the stationary phase of growth. Moreover, in those experiments, higher PSII maximum quantum yield, which is considered a very reliable indicator for overall photosynthetic efficiency (Baker et al., 2008), was always observed in mixotrophic cells with respect to autotrophic samples. Very little is known about the effects of the organic carbon source on the activity of the photosynthetic apparatus in mixotrophic microalgae; however, several studies indicated a down-regulation of the photosynthetic apparatus, either in terms of PSII activity (Valverde et al., 2005; Liu et al., 2009a), or with respect to the light-indipendent reactions, linked to a minor synthesis of RuBisCO enzyme, or to a reduced affinity for CO_2 (Oesterhelt et al., 2007). In this work, a comparison of thylakoid-protein assembly in autotrophic and mixotrophic samples of *N. oleoabundans* grown in presence of 2.5 and 5 gL^{-1} of glucose was performed, with particular emphasis on the organisation of PSII and PSI and focussing also on the interaction which occurs between the two photosystems.

For biochemical analyses, thylakoids from autotrophic and mixotrophic samples were isolated from cells at the late-exponential phase of growth, i.e. when samples had the same cell density. Chl/prt ratio already showed differences between thylakoids from autotrophic and mixotrophic cultures. Indeed, thylakoids from mixotrophic cells showed a halved ratio with respect to controls. These different values might be probably related to a lower content of Chl-protein complexes in thylakoids. Indeed, in previous experiment (see part I), a strong decrease in the Chl content was observed in mixotrophic samples with respect to controls. Now it emerges that such decrease can be the effect of both a net loss of thylakoids per cell and changed abundance of Chl-protein complexes in the photosynthetic membranes. These results are also confirmed by Coomassie-staining of SDS-PAGE gels, which showed, in lanes loaded on the basis of the same protein amount, a decreased amount of LHCII proteins. Moreover, Chl*a*/Chl*b* ratio was also higher. As Chl*b* is mostly located in LHCII complexes (Anderson et al., 1995), this result further supports a reduced content of LHCII complexes. In fact, on a Chl basis, immunodetection of LHCII proteins showed a reduced amount with respect to autotrophic cultures, as also observed in previous work concerning other mixotrophic microalgae (Kobáks et al., 2000). However, mixotrophic samples were mainly characterised by a strong increase in D1 protein subunit of PSII and a dramatic decrease in PsaB subunit of PSI, also verified in the bidimensional protein profiles obtained by BN/SDS-PAGE. These results are contrary to what previously observed in the few works in which the effects of an organic carbon source on the light energy distribution between the two photosystems were studied (Kováks et al., 2000; Valverde et al., 2005; Oesterhelt et al., 2007). Indeed, irrespective of the organic carbon source supplied in the medium and of the microalgal species analysed, the Authors always observed reduced amounts of D1 protein and increasing levels of RCI proteins (Kováks et al., 2000; Valverde et al., 2005; Oesterhelt et al., 2007). On the other hand, in this study analyses of the supramolecular organisation of PSII complexes by BN-PAGE and its corresponding silver-stained SDS-PAGE second dimension revealed that in mixotrophic samples PSII was mostly in the monomeric form. For many years, there has been a long-standing discussion about the assembly of PSII components into functional multimeric protein complexes in green algae and higher plants (Minagawa et al., 2004; Dekker and Boekema, 2005). Currently, it is widely accepted that functional PSII is normally organised as a dimer and concentrated in the stacked, appressed regions of grana, whereas PSI monomers are usually found in the unstacked thylakoid membranes (Kruse et

al., 2000; Minagawa et al., 2004; Dekker and Boekema, 2005; Daniellson et al., 2006). This distribution has been linked to the dissociation of PSII dimers into monomers to facilitate the PSII repair cycle, which occurs in the stroma-exposed membranes (Dekker and Boekema, 2005). However, in some cases PSII monomers have been shown to be fully active and also located both in grana cores and margins (Dekker and Boekema, 2005; Daniellson et al., 2006; Takahashi et al., 2009).

As concerns LHCII complexes, they were found to mostly as free trimers in *N. oleoabudans*, irrespective of the mode of cultivation (Kügler et al., 1997; Minagawa et al., 2004; Dekker and Boekema, 2005). Immunoblot detection showed decreased amounts of LHCII in thylakoids from 2.5 and 5 gL^{-1} of glucose-grown cells, however this did not cause major differences in the pigment-protein complexes assembly in comparison to autotrophic samples, although silver staining of 2D-BN/SDS-PAGE gels cannot be used to obtain accurate quantitative information (Daniellson et al., 2006). Finally, in mixotrophic samples less LHCII-PSI complexes were found with respect to autotrophic cells. LHCII is the major antenna of PSII, but can serve either PSII or PSI via state transition, which allows the balance of the light-harvesting capacity of the two photosystems to optimize the efficiency of the photosynthetic process (Allen et al., 1981; Allen and Forsberg, 2001; Iwai et al., 2008; Tikkanen et al., 2008). When the plastoquinone pool is reduced (Allen et al., 1981), a protein kinase is activated through the Cyt b_6f complex (Verner et al., 1997), and phosphorylation of LHCII apoproteins occurs, inducing a strong affinity between LHCII and PSI, so that LHCII works as a peripheral antenna for PSI (State 2) (Allen and Forsberg, 2001; Iwai et al., 2008; Tikkanen et al., 2008). Conversely, oxidation of the plastoquinone pool induces the opposite effect and recovers state 1 (Bennett, 1980). Then, the decreased amount of the state transition-specific LHCII-PSI complexes in mixotrophic samples might be related to a less effective capability to induce state transitions with respect to autotrophic samples. One of the reasons might be the presence of differences in the redox state of the plastoquinone pool in mixotrophic samples (Kováks et al., 2000).

Chl *a* fluorescence induction techniques are the most frequently used measurements for the investigation of light energy distribution and state transition (Kováks et al., 2000). For biophysical analyses, mixotrophic samples were compared with autotrophic cultures analysed either at the same day of growth (7 days) or with the same cell density, i.e. when

controls approached the stationary phase. The effects of mixotrophy on the activity of the forward electron transfer form Q_A^- to Q_B were studied by flash-induced fluorescence kinetics mediated by a single-saturating flash pulse (Vass et al., 2002; Allahverdiyeva et al., 2005, 2007). Differences were present comparing mixotrophic cells with both autotrophic samples mentioned above, although the effects were more marked if mixotrophic cells were compared to controls with the same cell density. Moreover, differences were emphasised with the highest glucose concentration. In thylakoids from mixotrophic cells, the relaxation of flash-induced fluorescence was characterised by minor time constants and increased relative amplitudes during fast and middle phases of fluorescence decay with respect to autotrophic cells. Interestingly, these results suggest a faster electron transfer from Q_A^- to Q_B during the fast phase of decay, with a following faster rebinding of PQ to the Q_B pocket and, then, an overall faster electron transfer in PSII of mixotrophic cells, in particular when glucose concentration is the highest. Moreover, DCMU was effective in blocking the Q_A^- to Q_B electron transfer both in autotrophic and mixotrophic cells, hence modifications in the binding site of Q_B can be excluded in all samples (Allahverdiyeva et al., 2005). However, also the recombination of Q_A^- with S2 states of the water oxidising complex was faster. It appears, then, that the redox proprieties of Q_A might be changed in mixotrophic samples with respect to autotrophic cells (Allahverdiyeva and Aro, personal communication), and might also be linked with the presence of a higher proportion of PSII (non-functional?) monomers. In fact, a minor proportion of functional PSII capable of reducing the primary acceptor Q_A might cause in turn the presence of an overall less reduced PQ pool. The high fraction of oxidized PQ would be more easily available for the reoxidation of Q_A^- after flash induction. Decreased antenna size has also been shown to decrease the rate of Q_A reduction (Takahashi et al., 2009). Another explanation could concern a promoted oxidation of PQ because of modified photosynthetic electron flow in mixotrophic microalgae, although the only report on the subject actually suggests a down-regulated electron transport (Valverde et al., 1995). However, these hypotheses remain conjectural, because no information about such changes in mixotrophic microalgae is available in literature. Further analyses to determine the possible occurrence of increased energy dissipation due to a higher proportion of non-functional PSII in mixotrophic samples, would be required, as well as to understand the role of state transitions and electron flow. However, previous results

obtained in *N. oleoabundans* grown mixotrophically in the presence of AWP (see part I), seem to support these hypotheses.

Before measurements of Chl*a* fluorescence induction by PAM fluorimetry, cells are dark-adapted in order to fully oxidize Q_A and measure the minimal fluorescence level F_0. After that, the first light-saturating pulse is applied, Q_A becomes completely reduced and the maximum fluorescence level F_M is reached (Krause and Weiss, 1984; Baker, 2008). However, in some algae, some accumulation of reduced Q_A can occur during the dark adaptation as well, owning to non-photochemical reduction of plastoquinone by chlororespiration (Baker et al., 2008). Q_A reduction promotes association of LHCII complexes to PSI mediating transition to state 2 (Krause and Weiss, 1984; Finazzi et al., 1999). A similar behaviour is observed in autotrophic *N. oleoabundans* cells, which indeed showed increasing F_M' values under normal growth light conditions, linked to the transition from state 2 to state 1 of LHCII complexes during the linear electron flow (Finazzi et al., 1999; Kováks et al., 2000). Conversely, this behaviour was not observed in mixotrophic cells, and F_M' only rarely exceeded F_M values. The absence of PQ reduction in dark-incubated mixotrophic cells might be linked, again, to differences in state transitions, which might not be as effective as in controls. Furthermore, in the light of these results, it is grounded to suppose that in previous experiments (part I) the mixotrophic samples showed higher F_V/F_M ratio actually because the F_M levels of autotrophic samples were underestimated. Therefore, the samples grown in the presence of glucose do not hold improved photosynthetic efficiency, but rather experience important effects on state transition of LHCII and redox properties of quinones. Moreover, when exposed to high-light conditions, mixotrophic cells showed increased basal fluorescence emission F_t, linked to major susceptibility to photodamage (Baker, 2008). Finally, 77K emission spectra showed decreased emission of PSI over PSII in mixotrophic samples with respect to controls, but only when autotrophic cells in the same late-exponential phase were used for comparison. This resulted in lower PSI/PSII fluorescence ratio, in accordance with immunodetection of D1 and PsaB protein subunits. A similar change in PSI/PSII ratio was found in other mixotrophic microalgae and was put in relation with a down-regulation of photosynthesis (Valverde et al., 1995; Oesterhelt et al., 2007).

In summary, based on the study of organisation and assembly of thylakoid-protein complexes, the effects of glucose on the photosynthetic membrane of *N. oleoabundans*

resulted in decreased amounts of LHCII and, above all, PSI protein subunits. The slight reduction in ATP-β subunit of ATPase might be linked to some interaction with glucose metabolism and ATP production (Kováks et al., 2000). Conversely, increased PSII amounts were found, but mainly present in the monomeric form, which have been frequently considered non-functional, although contrasting opinions can be found in literature (Tikkanen et al., 2008; Takahashi et al., 2009). The 77K spectra also supported a different PSI/PSII stoichiometry, but only if autotrophic cells at the late-exponential growth phase were considered as control. Based on fluorescence relaxation and slow fluorescence induction kinetics, it can be proposed that Q_A presents different redox properties with respect to autotrophic cultures, maybe linked to decreased reduction rates, resulting in a more rapid linear electron flow in mixotrophic cultures. However, the decrease in reduction rate might also be caused by a major proportion of non-functional PSII, i.e. unable to efficiently reduce Q_A. Finally, less effective state transition capability was suggested in mixotrophic samples with respect to control cells, for some reasons which still appear unclear. This may derive from a reducedcapability of chlororespiration in darkness. Collectively, it can be hypothesised an increased susceptibility to photodamage when mixotrophic cells are exposed to high-light conditions. Thus, it can be concluded that mixotrophic cells does not show enhanced photosynthetic activities with respect to control cells, but the higher F_V/F_M values would actually be linked to different redox properties of quinones and less capability to promote state transitions. However, at present, the results collected in this work point to the unique features of the photosynthetic membrane assembled under mixotrophy, but remain difficult to interpret because of their novelty with respect to the available literature. Further investigation on the interplay between photosynthetic light reactions and carbohydrates metabolism need to be pursued in order to identify how glucose consumption interferes with the photosynthetic apparatus of *N. oleoabundans*.

5. Conclusion

The genome of *N. oleoabundans* is not sequenced and moreover very little is known about its physiology and photosynthetic metabolism even when cells are grown autotrophically. The capability of the microalga to grow mixotrophically has been discovered only recently (Giovanardi et al., 2013), thus improvement in the knowledge of the glucose effects on the organisation, assembly and activity of the photosynthetic apparatus might be useful to understand the microalgal metabolism. The results obtained in this work suggest that dramatic changes in photosystems organisation and electron flow occur in mixotrophic samples, with probable modifications in state-transition capability and possibly reduced photosynthetic performance. However, further investigation is needed to provide a complete background. For this reason, this work can be considered a starting point from which further research can be developed.

Tables ans Figures

Samples	Chl (µg µL^{-1})	Prt (µg µL^{-1})	chl/prt	Chl*a* (µg µL^{-1})	Chl*b* (µg µL^{-1})	chl *a*/*b* ratio
0 gL^{-1} glucose	3.380	24.294	0.139	2.623	0.757	3.467
2.5 gL^{-1} glucose	1.650	25.768	0.064	1.325	0.324	4.086
5.0 gL^{-1} glucose	1.820	27.955	0.065	1.449	0.367	3.953

Tab. 1: Chl *a*, *b* and total Chl amounts, protein amounts and corresponding ratios in thylakoids extracted from *N. oleoabundans* grown with 0, 2.5 and 5 gL^{-1} of glucose.

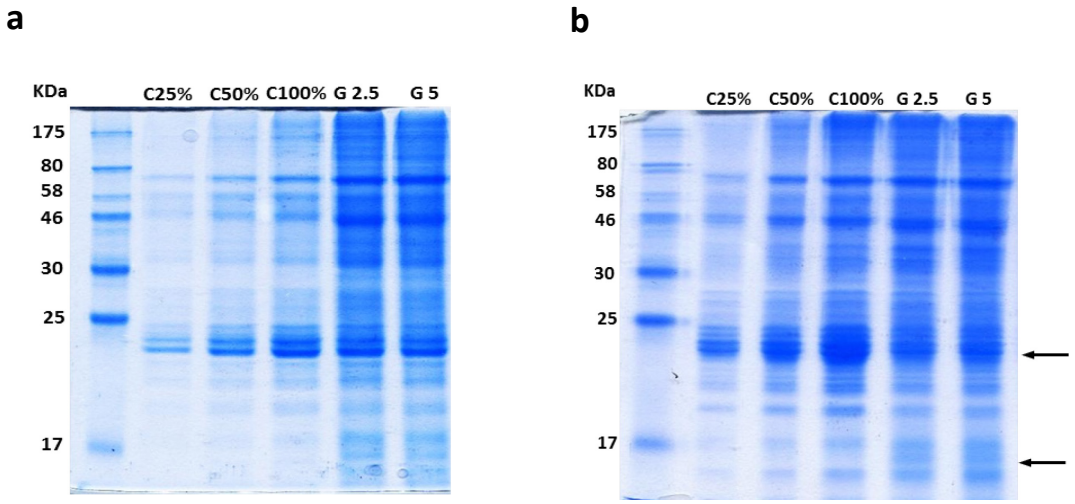

Fig. 1: Coomassie-stained SDS-PAGE of thylakoids membrane proteins from *N. oleoabundans* grown with 0 (C), 2.5 (G 2.5) and 5 (G 5) gL^{-1} of glucose. On each lane, 2 µg of Chl (a) and 20 µg of proteins (b) were loaded. Major differences in the protein profile between different samples are marked by arrows. For comparison, three different amounts of thylakoids from control sample were loaded. Molecular weight marker is reported on the left in each gel.

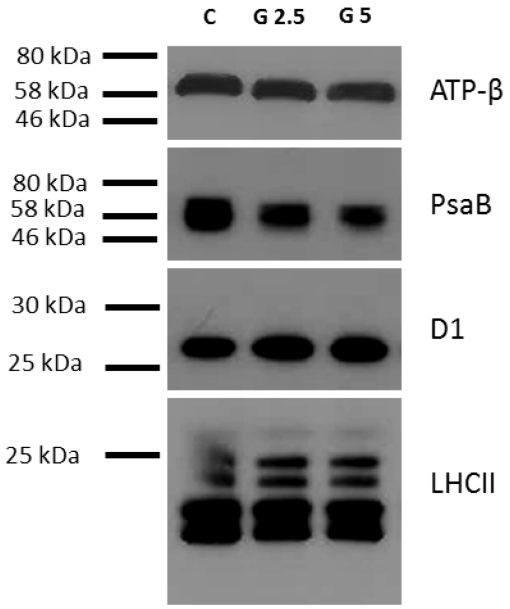

Fig. 2: immunoblot detection of ATPβ (40 µg of protein loaded in each lane), PsaB (0.5 µg of Chl loaded in each lane), D1-DE loop (0.5 µg of Chl loaded in each lane) and LHCII (0.25 µg of Chl loaded in each lane) in thylakoid membranes of *N. oleoabundans* grown with 0 (C), 2.5 (G 2.5) and 5 (G 5) gL^{-1} of glucose.

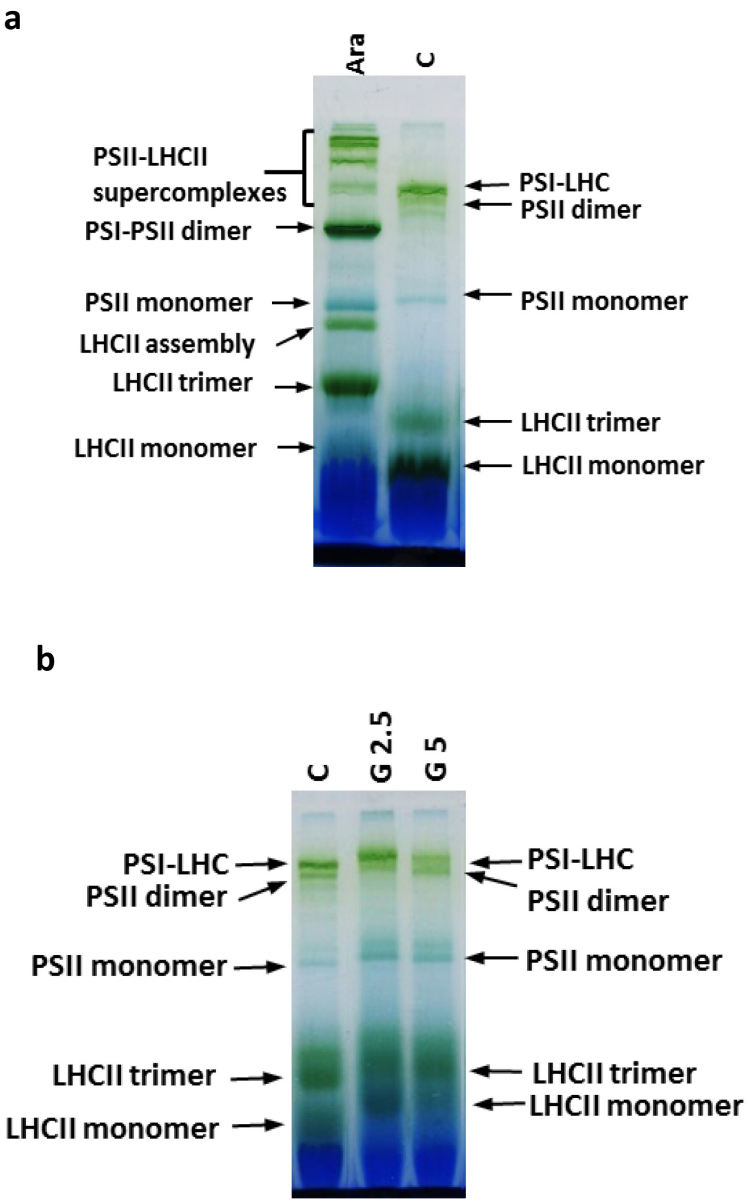

Fig. 3: distribution of different protein complexes in BN/SDS PAGE profile of thylakoids membranes. a) Representative BN-PAGE profile of thylakoids from *Arabidopsis thaliana* (Ara) and autotrophic *N. oleoabundans* (C). b) Representative BN-PAGE profiles of thylakoids from *N. oleoabundans* grown with 0 (C), 2.5 g/L glucose (G2.5) and 5g/L glucose (G 5). For each lane, 5 µg of Chl were loaded.

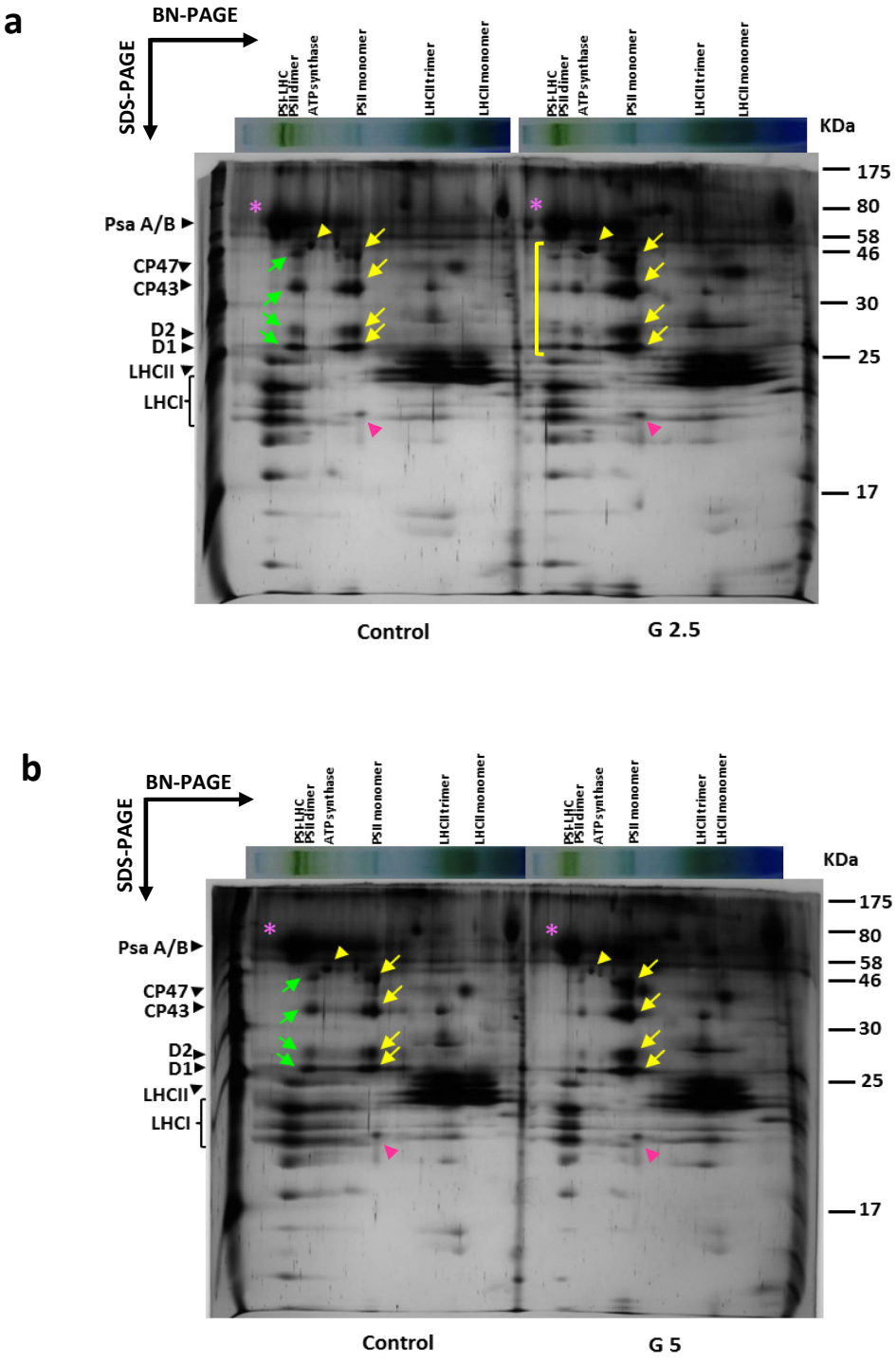

Fig. 4: 2D-BN/SDS-PAGE of protein complexes in thylakoid membranes from autotrophic and mixotrophic *N. oleoaunbans*. a) comparison between cells grown with 0 (C) and 2.5 gL^{-1} of glucose (G 2.5). b) comparison between cells grown with 0 (C) and 5 gL^{-1} of glucose (G 5). The BN-PAGE strips were loaded horizontally on the SDS-PAGE. 5 µg of Chl were loaded in each BN well. The highlighted silver-stained spots corresponded to Psa A/B (purple asterisk), PSII subunits associated with PSI (yellow square bracket), CP47, CP43, D1 and D2 subunits of PSII dimer (green arrows) and PSII monomer (yellow arrows), ATP synthase (yellow arrowhead), Cyt b_6f (purple arrowhead).

	Total Amp (%)	Fast phase *T*/Amp (ms/%)	Middle phase *T*/Amp (ms/%)	Slow phase *T*/Amp (s/%)
C 7 days	100	0.57 ± 0.08 / 85.83 ± 2.60	13.50 ± 4.76 / 7.69 ± 1.30	2.07 ± 0.67 / 6.48 ± 1.37
C late exp	100	0.74 ± 0.08 / 76.11 ± 2.17	17.35 ± 6.98 / 13.56 ± 0.98	3.22 ± 0.82 / 10.33 ± 1.19
G 2.5	100	0.55 ± 0.12 / 84.83 ± 4.47	11.73 ± 3.66 / 7.89 ± 2.19	1.81 ± 0.58 / 7.27 ± 2.33
G5	100	0.51 ± 0.03 / 86.84 ± 0.88	7.18 ± 1.66 / 6.93 ± 0.25	1.22 ± 0.26 / 6.23 ± 0.92

Tab. 2: characteristics of flash-induced Chl fluorescence relaxation in *N. oleoabundans* control cells at 7 days of growth, control cells in late-exponential phase of growth, cells grown in presence of 2.5 (G 2.5) and 5 (G 5) gL^{-1} of glucose. Values are time of decay and relative amplitudes in percent of total variable fluorescence obtained after the fired flash. Numbers are means of at least three replicates ± s.d.

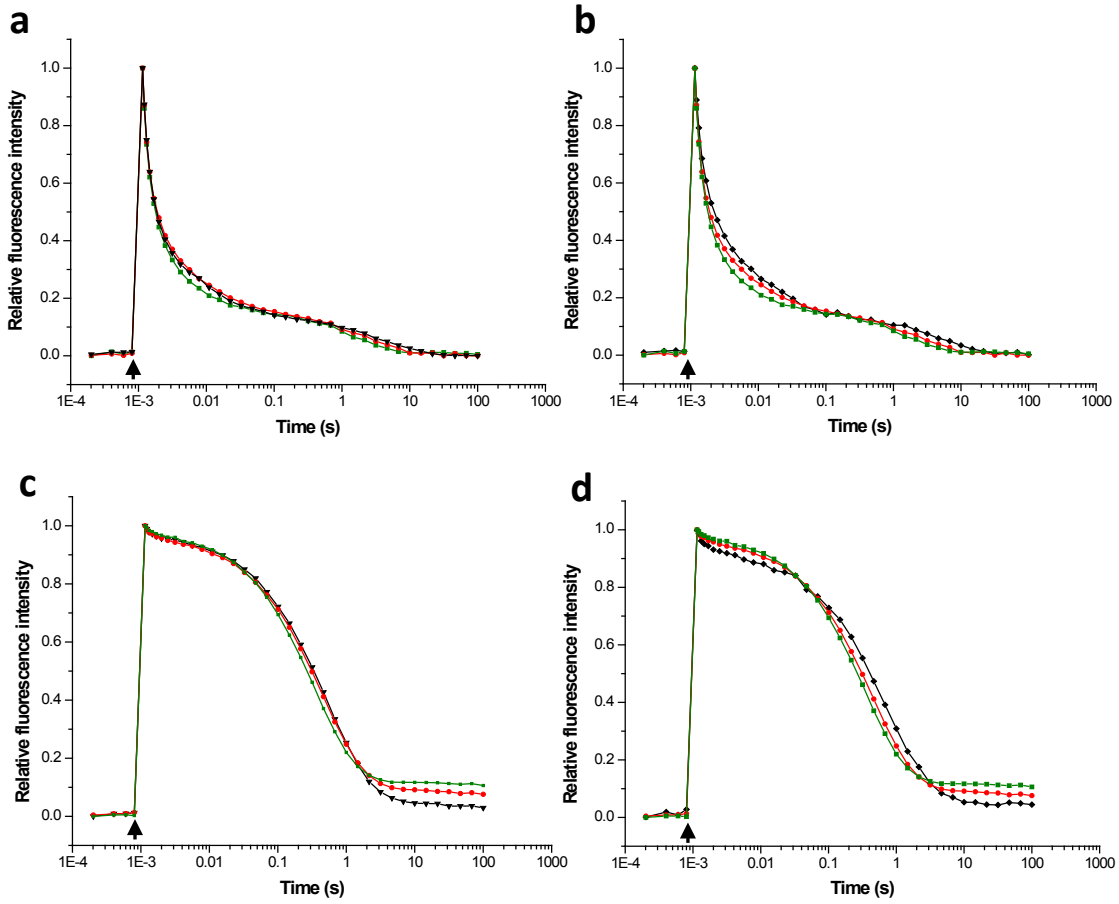

Fig. 5: relaxation of the flash-induced fluorescence in *N. oleoabundans* cells grown with 0 (black line), 2.5 (red line) and 5 (green line) gL^{-1} of glucose. a, c) control cells sampled after the same time of growth (7 days) of mixotrophic samples were used. In c) relaxation as occurring in presence of 5 µM DCMU. b, d) control cells sampled at the same stage of growth (late-exponential) of mixotrophic samples were used. In d) DCMU was added. Curves are average of at least 3 different biological replicates and are normalised to the same amplitude. Arrows: saturating-light pulse.

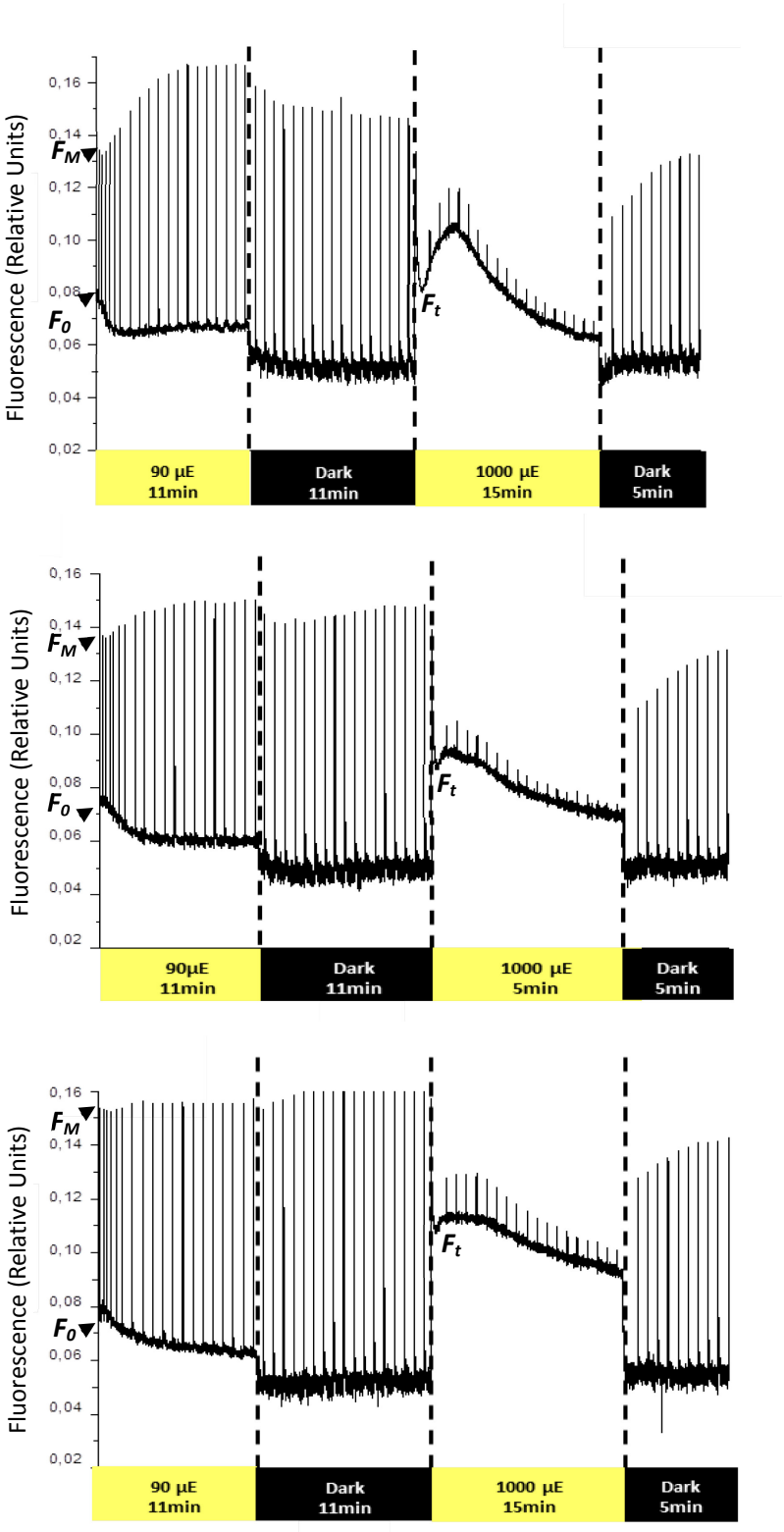

Fig. 6: representative curves of slow Chl*a* fluorescence kinetics in response to changing light intensities in *N. oleoabundans* cells grown with 0 (a), 2.5 (b) and 5 (c) gL^{-1} of glucose. The measurements were started after 10 min of incubation in darkness by turning on the actinic light, and the fluorescence parameters F_M and F_t were monitored triggering the samples with different light intensities as indicated in "Material and methods" section. µE is equivalent of $\mu mol_{photons} m^{-2} s^{-1}$.

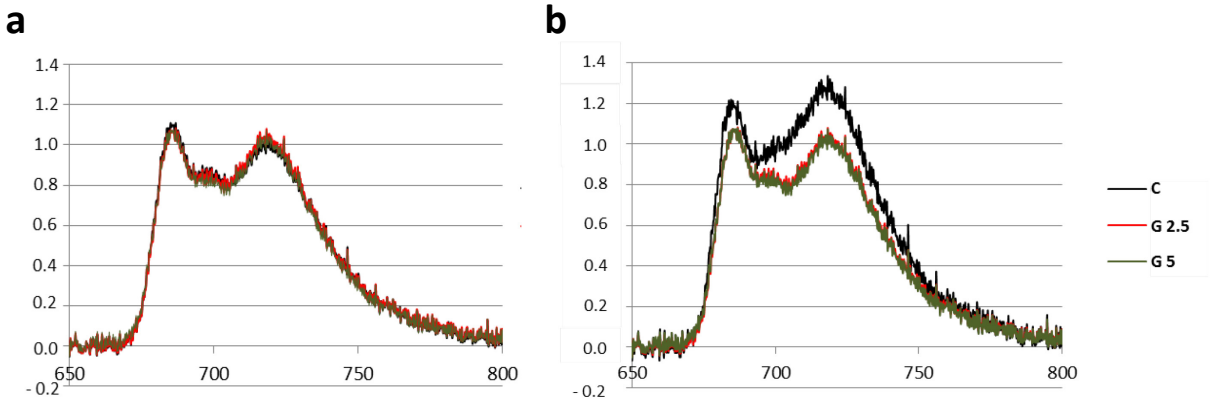

Fig. 7: 77 K fluorescence emission spectra of *N. oleoabundans* grown with 0 (black), 2.5 (red) and 5 (green) gL^{-1} of glucose. a) comparison between mixotrophic samples and control cells with the same time of growth. b) comparison between mixotrophic samples and control cells at the same phase of growth. The 77 K spectra were recorded from cell suspensions with 8 µg mL^{-1} (excitation, 440 nm). For easier comparison, spectra were each normalized to their maximum peak, except for C in figure b), which showed different peak positions.

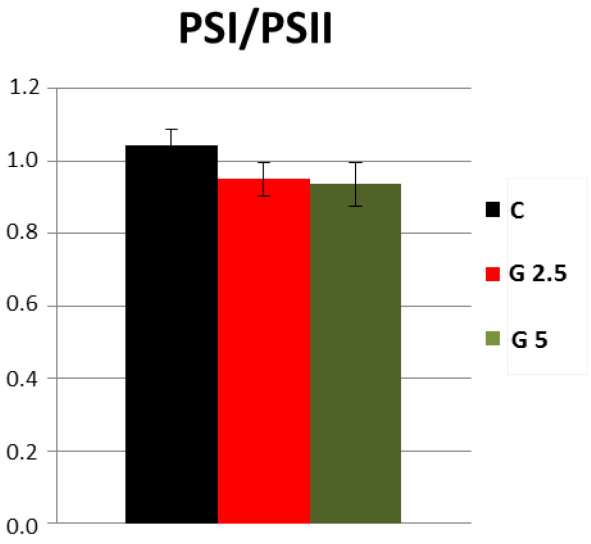

Fig. 8: PSI/PSII fluorescence emission ratio in *N. oleoabundans* grown with 0 (black), 2.5 (red) and 5 (green) gL^{-1} of glucose. Samples are compared on the basis of the same stage of growth. Values are means of at least 3 replicates ± s.d.

Part III

Effects of the expression of two phytoene synthase exogenous genes on carotenoid accumulation and photosynthetic performances in the green microalga **Chlamydomonas reinhardtii**

1. Introduction

Microalgae are unicellular photosynthetic organisms able to convert solar energy into chemical energy for growth (Chisti, 2007). Thanks to their chemical composition, mainly enriched in proteins, lipids, carbohydrates, vitamins, pigments and enzymes (Harun et al., 2010), these organisms are often considered an important source of natural products (Becker, 1988; León-Bañares et al., 2004; Pulz and Gross, 2004; Spolaore et al., 2006). Microalgae present a pronounced metabolic plasticity, which allows them to rapidly adapt to different environments (Gushina and Harwood, 2006). This also permits the production of some bioactive molecules by the manipulation of the cultivation systems, making these organisms very interesting to be exploited in biotechnological applications (León-Bañares et al., 2004; Plaza et al., 2008). Furthermore, during the last recent years, advances in molecular engineering have allowed to induce in microalgae the expression of heterologous genes, opening up the possibility of producing new heterologous proteins or overproducing traditional algal compounds for commercial and research purposes (León-Bañares et al., 2004; Walker et al., 2005; Del Campo et al., 2007). The idea of using microorganisms as bioreactors for the synthesis of recombinant proteins is not new, but has usually involved bacteria and yeast fermentation (Walker et al., 2005). However, limitations in using these microorganisms occur, as bacteria are unable to perform post-transcriptional and post-translational modifications, which are essential for the expression of eukaryotic proteins (Walker et al., 2005), whereas yeast present a different pattern of glycosylation with respect to that of higher plants (Fisher et al., 1999). Microalgae, instead, combine the fast and easy growth of bacteria and other microorganisms with the typical properties of higher plants, such as the same glycosylation pattern and the efficient oxygenic photosynthesis (Walker et al., 2005; Del Campo et al., 2007). Other advantages such as the easy protein purification, due to their simpler structure, and the consideration of green microalgae as GRAS (generally regarded as safe) organisms ensure their exploitation in large-scale production of commercially important proteins (Walker et al., 2005; León et al., 2007). One of the most successful branch of microalgal biotechnology is the Car production (Del Campo et al., 2007). Car are C_{40} tetraterpene pigments synthesised by all photosynthetic organisms, as well as by some non-photosynhtetic bacteria and some fungi (Jin et al., 2003; McCarthy et al., 2004; Cordero et al., 2011). The main classes of Car are two: carotenes are represented by linear or

cyclized hydrocarbons, whereas oxygen derivative of carotenes are called xanthophylls (Jin et al., 2003). In plants and green algae, the synthesis of Car occur inside chloroplast from the precursor geranylgeranyl pyrophosphate (GGPP), generated from isopentenyl pyrophosphate and dimethylallyl pyrophosphate by the action of GGPP synthase (Fig. 6 in "General introduction" section). The condensation of two molecules of GGPP yields the first Car of the biosynthetic pathway, the phytoene. The reaction is catalysed by the phytoene synthase (PSY), which has been considered a rate limiting key-enzime of the biosynthetic pathway, thus an important control point for the regulation of the carbon flux into and through the pathway (Shewmaker et al., 1999; Fraser et al., 2002; Sandmann et al., 2006; Couso et al., 2011). From phytoene, 4 sequential desaturation and one isomerization yield to lycopene, from which α- and β-carotene are obtained. The hydroxylation of β-carotene allows to obtain zeaxanthin, which is epoxidated to form antheraxanthin and violaxanthin, whereas neoxanthin is obtained by a different rearrangement of violaxanthin (Richmond et al., 1990). On the other hand, lutein and its derivative loroxanthin are generated from hydroxilation of α-carotene (Baroli et al., 2003). In microalgae and higher plants, Car are important constituent of the photosynthetic apparatus. In particular, two β-carotenes are found in the RCII, whereas the xanthophylls lutein, violaxanthin, zeaxanthin and neoxanthin are accessory pigments in the antenna system LHCII (Depka et al., 1998; Jin et al., 2003; McCarthy et al., 2004). Thus, in addition to their participation in light-harvesting processes, main functions of Car are to maintain structure and function of photosynthetic complexes, to dissipate the excess of light energy absorbed by the antenna pigments and to play an important role in the protection of photosynthetic apparatus from photooxidative damage (McCarthy et al., 2004). Their antioxidant properties are also important in the human health care, and are used in pharmaceutical, exerting intrinsic antinflammatory properties, prevention against oxidative stress and therapeutic chemopreventive anticancer effects, among others (Guerin et al., 2003; Spolaore et al., 2006; León et al., 2007). With these purposes, natural carotenes are usually preferred as they are a mixture of *cis* and *trans* molecules, thus Car production from biological sources, like microalgae, is promoted (Del Campo et al., 2007). Despite microalgae are the most important source of Car, literature about the genetic manipulation of the Car biosynthetic pathway in these microorganisms is very rare and related to few microalgae species, such as *Dunaliella* (Sun et al., 2007), *Haematococcus* (Steinbrenner and Sandmann, 2006) and *Chlamydomonas* (León et al., 2007;

Vila et al., 2007; Cordero et al., 2011; Couso et al., 2011). Among them, *C. reinhardtii* is considered a model organism, during the past years it has been well characterised (Harris et al., 2001; Walker et al., 2005) and its nuclear genetic manipulation is easy and well established. Then, *C. reinhardtii* can be considered the best candidate for the expression of foreign genes involved in the carotenogenic pathway (León et al., 2007; Cordero et al., 2011). In a recent work, the transformation of *C. reinhardtii* with a foreign β-carotene oxygenase gene induced the production of a new ketocarotenoid, even if in very small quantities and without any further changes in the Car profile (León et al., 2007). Many progresses have been achieved transforming the microalga with two exogenous PSY genes from *D. salina* (Couso et al., 2011) and *C. zofingensis* (Cordero et al., 2011). In both cases, accumulation of Car was observed in some transformants, confirming the possibility of employing molecular engineering for commercial purposes, as well as improving the knowledge about the carotenogenic pathway, not fully understood yet (Couso et al., 2011). However, no information about the effects of the transformation on the physiology of these microorganisms are still available. In this study, the effects of the expression of two exogenous PSY genes from *Arabidopsis thaliana* (*AtPSY*) and *Oryza sativa* (*OsPSY1*) in the green microalga *C. reinhardtii* has been studied, with particular regards to the responses of the photosynthetic apparatus. With these purposes, fluorimetric analyses have been performed on positive transformants which expressed a different phenotype compared to that of wt cells, in order to observe if eventual modification of the carotenogenic pathway would lead to different behaviour to exposition to different light regimes.

2. Materials and Methods

2.1. Strain and culture conditions

The *Chlamydomonas reinhardtii* cell-wall deficient strain cc-3491 was obtained from the *Chlamydomonas* Genetics Center (Duke University, Durham NC, USA). Cultures were maintained on solid Tris acetate/phosphate medium added with 10 gL^{-1} of sorbitol (TAP-S)(www.chlamy.org) in a growth chamber (24±1°C, 100 $\mu mol_{photons} m^{-2} s^{-1}$ PAR, 16-8 h light-darkness photoperiod). For physiological analyses of positive transformants, liquid cultures were prepared in 100 mL Erlenmeyer flasks (50 mL total volume) and shaken continuously at

90 rpm. For experiments at different light exposures, cells were grown in the same growth chamber as described above at: a) 30 $\mu mol_{photons}\ m^{-2}s^{-1}$ PAR (low-light cultures - LL); b) 150 $\mu mol_{photons}\ m^{-2}s^{-1}$ PAR (high-light cutures - HL). Experiments were always carried out in triplicates and growth was always monitored by measurement of optical density (OD) at 750 nm with a PharmaciaBiotech Ultrospec® 2000 UV-Vis (1 nm bandwidth; Amersham Biosciences,Piscataway, NJ, USA). OD was referred to a calibration curve with known cell number, previously estimated by cell counting with a Thoma's counting camera, versus optical density. *Escherichia coli* strain TOP10 (Invitrogen) was used and transformed by heat shock with the plasmids constructed as follows.

2.2. Construction of the expression vector for *C. reinhardtii* transformation

Gateway Technology (Invitrogen) was used in order to obtain expression vectors to be used for *C. reinhardtii* transformation. Different entry vectors were firstly created to obtain each expression construct. The coding sequences of *Phytoene Synthase* (*PSY*) of *Arabidopsis thaliana* (At5g17230), and *Oryza sativa 1* (Os06g0729000) were kindly provided by Dr. Ralf Welsh (University of Freiburg, Germany). *AtPSY* and *OsPSY1* sequences were amplified using HotStart HiFidelity DNA Polymerase (QIAGEN) following the manufacturer's instruction, using primers flanked by AttB1 and AttB2 sequences, as indicated in Tab. 1. The obtained PCR products were subsequently used for BP recombination with pDONR221 (Invitrogen). A second entry clone contained the *C. reinhardtii* β2-tubulin gene promoter, which had been selected to drive the expression of both *AtPSY* and *OsPSY1* in the microalga, in combination with the first intron of small subunit of ribulose bisphosphate carboxylase (*rbcS2*). This sequence was amplified by PCR using pHyg3 (Berthold et al., 2002), with primers flanked by AttB4 and AttB1R (Tab. 1) and subsequently recombined in *pDONR P4-P1R* (Invitrogen). Finally, the *C. reinhardtii* 3' untranslated region of small subunit of *rbcS2* gene was amplified from pHyg3 (Berthold et al, 2002) using specific primers flanked by AttB2R and AttB3 sequences (Tab. 1), and PCR products were used for BP recombination with pDONRP2R-P3 (Invitrogen). This 3'end contains 230bp of the 3' untranslated region of the *C. reinhardtii rbcS2* gene (Goldschmidt-Clermont and Rahire, 1986) with a functional TGTAA polyadenylation signal. The Destination vector was generated subcloning the multisite recombination cassette (R4-Cm^r-ccdB-R3) of pKm43GW,0 (Karimi et al, 2002) in pUC19 multiple cloning site (*HindIII/KpnI*). Then, hygromycin resistance cassette was excided

from pHyg3 (Berthold et al, 2002) with *HindIIII* and subcloned upstream of Gateway cassette (Invitrogen), to allow selection of transformed individuals. The obtained Destination vector was named pHyg6. Two versions of pHyg6 (B-D) were obtained by mean of two distinct multiple LR recombination reactions with pDONR vectors carrying sequences of interest (Tab. 2; Fig. 1). Nucleotide sequences of all PCR products were confirmed by sequencing both strands (Macrogen Inc.).

2.3. Glass beads nuclear transformation and screening of trasformants

Nuclear transformation was carried out using glass beads method as described by Kindle et al. (1990), with some modifications. Cells were grown until they reached the density of 1-2 x 10^6 cell mL^{-1} and subsequently harvested by centrifugation (5000 *g*, 5 min), resuspended in 1/100 of the original volume and incubated in continuous shaking (50 rpm) at room temperature for 2-4 hours. 0,3 mL of this cell suspension was added to a glass tube containing 0,3 g of sterilized glass beads (0,3 mm Ø), 100 µL of 20% polyethylene glycol (MW 8000) and 2 µg of Phyg6-B or Phyg6-D plasmid. Cells were then vortexed at maximum speed for 30 seconds and incubated o/n in 10 mL of TAP-S. The day after aliquots of 7,5 and 15 x 10^6 cells mL^{-1} were spread onto solid TAP-S containing 10 µg mL^{-1} Hygromycin B. Colonies were visible after 10-14 days.

The genomic DNA extraction from colonies grown in selective medium was performed as described in previous works (Murray and Thompson, 1980; Rogers and Bendich, 1985), with modifications. One loop full of cells was scrapped and cultured in 3 mL of TAP-S with 10 µg mL^{-1} Hygromycin B. After 3 d of growth cells were harvested by centrifugation at 10000 *g* for 5 min and pellet was grinded in liquid nitrogen. 400 µL of CTAB extraction buffer (100 mM Tris-HCl pH 8.0, 50 mM Na_2EDTA pH 8.0, 500 mM NaCl, 2% CTAB w/v, 1% β-mercaptoethanol v/v) and 100 µL of 0,5% 30.000 PVP where then added. DNA extraction was firstly performed with 850 µL of 1:1 phenol/chloroform. Top phase was harvested and extracted with phenol. DNA contained in the following top phase was precipitated adding 0.7 volumes of isopropanol and incubating at -20°C for 4 hours. After washing with 70% ethanol for three times, the obtained pellet was resuspended in 30 µL of 5mM Tris-HCl pH 8.0. Samples were kept at -20°C. PCR reaction was carried out in order to detect the presence of the transgene. The specific primer pairs AtPSY RTfor - attb3-rbcS2 rev

and OsPSY1 RTfor - attb3-rbcS2 rev (Tab. 1) were used. 1 µL of 1:10 diluted genomic DNA was added to 25 µL of total volume reaction containing 1µL of each primer (10 µM), 2.5 µL of 10x Dream Taq™ Green Buffer including 20 mM $MgCl_2$, 0.2 mM $dNTP_s$ and 0.625 U of Dream Taq™ DNA polymerase. All reagents were obtained from FERMENTAS®. Cycling conditions were: denaturation 5 min at 95°C, melting 30 s at 95 °C, annealing 30 s at 60 °C and final extension 45 sec at 72 °C in order to complete all the amplicons. The amplification products were analysed by electrophoresis on 1% agarose gel. The sizes of amplified products were estimated by comparison with 1kb DNA ladder (Applichem).

2.4. RNA extraction, cDNA synthesis and Reverse transcription-PCR (RT-PCR).

RNA extraction was performed using freshly collected algae from 1ml of liquid culture in TAP-S medium with 10 µg mL^{-1} hygromycin. Samples were grinded with liquid nitrogen and then processed using Aurum RNA Fatty and Fibrous kit (Bio-Rad). RNA integrity was evaluated by 1% agarose gel electrophoresis. A 9 µL sample of the extracted RNA was retro-transcribed using the ImProm-II reverse transcription system (Promega) with an oligo(dT) primer, following the manufacturer's instruction. qRT-PCR was performed with GoTaq® Flexi DNA Polymerase (Promega) following the manufacturer's instructions. Reaction mixtures were set up in duplicate, using 0.5 µL of cDNA 1:4 diluted and 0.5 µL of each primer (0.5 mM final concentration for each) in a 20 µL final volume. Primers were AtPSY RT for and AtPSY RT rev (Tab. 1). A no-template control reaction was also performed.

2.5. Pigment extraction and analysis

For pigment extraction, aliquots of 1mL of cell suspension were harvested by centrifugation at 600 *g* for 10 min. 2 mL of methanol were added to the pellet and incubated at 80°C for 15 min in the dark (Ferroni et al., 2007). The extracts were clarified by centrifugation and analyzed with a UV/Vis Spectrophotometer (Pharmacia Biotech Ultrospec® 2000) (1 nm resolution). For Chl*a*, Chl*b* and Car quantification, the extracts were measured at 750 nm, 666 nm (Chl*a*), 653 nm (Chl*b*) and 470 nm (Car). The quantification was performed according to Wellburn (1994).

For HPLC analyses, 1 mL samples were harvested by centrifugation and pigments were extracted with 1 ml acetone 80% over night at -20°C. The extracts were analysed by

HPLC (Agilent Zorbax ODS-C18 4.6 x 250 mm, 5 µm column), as described in Färber and Jahns (1998). Car were identified by retention times and absorption spectra, and quantification was referred to total Chl.

2.6. Fluorimetric analyses

Modulated Chl fluorescence

Pulse amplitude modulated (PAM) fluorescence was analysed with an ADC OS1-FL fluorometer (ADC Bioscientific Ltd, Hoddesdon, Hertfordshire, UK). Aliquots of cell suspensions from wt and transformed cells were centrifuged at 10000 *g* for 3 min and the pellets were deposited onto pieces of wet filter paper (Schleicher & Schuell)(Ferroni et al., 2011). After 15 min of dark adaptation, initial fluorescence (F_0) and maximum fluorescence (F_{mM}) values were measured and used to calculate the maximum quantum yield of PSII, i.e. F_v/F_{mM} ratio, where $F_v=F_{mM}-F_0$ (Lichtenthaler et al., 2005). After the determination of F_v/F_{mM}, the samples were exposed to 1200 $\mu mol_{photons}\ m^{-2}s^{-1}$ for 5 min. At the end of induction, the steady state fluorescence yield was measured (F_t) and a saturation pulse was applied for the determination of the maximum fluorescence in the light-adapted state (F_m'). Subsequently, cells were allowed to recover in darkness for 5 min and a pulse was applied for the determination of F_m. The fluorescence parameters were used in preliminary experiments to calculate the yield of PSII photochemistry in the light-adapted state as $Y=((F_m'-F_t)/F_m')$ (Genty et al., 1989). The quantum yield of thermal dissipation associated with inactivated PSII after the light induction was determined as $Y(NF) = 1-((F_v/F_m)/(F_v/F_{mM}))$ (Hikosaka et al., 2004).

In HL and LL cultures, for a detailed analysis of the energy partitioning in a mixed population of active and photoinactivated PSII complexes, the measuring sequence described above was applied, but calculation of quantum yields was performed following Hendrickson et al. (2005), with modifications. In particular, the total absorbed energy fraction was partitioned in Y(PSII), Y(NO), Y(npq) and Y(NF). In this procedure, each quantum yield described by Hendrickson et al. 2004 was corrected for a factor which is directly proportional to the remaining active fraction of PSII capable of photochemical activity after a photoinhibitory light treatment $((F_v/F_m)/(F_v/F_{mM}))$ (Hendrickson et al., 2005). Consequently, the following equations were used:

$Y(PSII)=[(F_m'-F_t)/F_m'] [(F_v/F_m)/(F_v/F_{mM})]$ (yield of PSII photochemistry)

$Y(NO)= (F_t/F_{mM}) [(F_v/F_m)/(F_v/F_{mM})]$ (combined yield of fluorescence and constitutive thermal dissipation)

$Y(npq)= (F_t/F_m'-F/F_m) [(F_v/F_m)/(F_v/F_{mM})]$ (yield of regulated thermal dissipation)

The sum of the 4 yields is the unity. Experiments were carried out in triplicates.

RT Microspectrofluorimetry

In order to study the assembly state of the light harvesting complex (LHCII) with photosystem II (PSII) in transformed and wt cells, room temperature (RT) fluorescence emission spectra were recorded using a microspectrofluorimeter (RCS, Firenze, Italy), associated with a Zeiss model Axiophot epifluorescence photomicroscope (Pancaldi et al., 2002). Samples were prepared as described by Ferroni et al. (2011). Groups of living cells (x40 magnification) were excited at 436 nm. Excitation wavelength was provided by a BP436/10 filter (Zeiss), using a 1.6 mm diaphragm. Autolab software (RCS) was employed to set the recording range (620-780 nm), optimise the photomultiplier response and visualize the emission spectra (Ferroni et al., 2009). Spectra were recorded from wt and transformed cells both in normal growth conditions and after photoinhibition treatment (5 min exposure to 1200 $\mu mol_{photons}\ m^{-2}s^{-1}$, followed by 5 min of recovery in darkness). For each sample, at least 5 spectra were recorded. Microcal Origin 6.0 software (OriginLab, Northampton, MA, USA) was used for elaboration of spectra, which were corrected as described by Ferroni et al. (2011). The Gaussian fitting procedure was carried out as described in previous works (Böddi and Franck, 1998; Šiffel and Braunová, 1999; Ferroni et al., 2009, 2011). Fluorescence yield of emission bands, whose attribution is shown in Tab. 3, was evaluated as the area subtended under the corresponding Gaussian curve. Moreover, calculation of difference spectra between photoinhibited samples and their relative emission in normal cells was performed.

2.7 Data treatment

Data were processed with Microsoft Excel™ and Microcal Origin 6.0 (OriginLab, Northampton, MA, USA) softwares, means±standard deviations (SD) for n (number of samples) are given in each case. Statistical analyses were carried out with Student's *t*-test, with a significant level of 0.05.

3. Results

3.1. Screening of transformants and transformation efficiency

Cells of *C. reinhardtii* cc-3491 cw-less strain were transformed with plasmids pHyg6-B and pHyg6-D, obtained as described in "Materials and methods" section. These plasmids contained the cDNA sequence encoding *AtPSY* and *OsPSY1* respectively (Welsch et al., 2008). Sequences were flanked by the constitutive β-tubulin promoter in combination with the first intron of *rbcS2* and the 3' untranslated terminator region of *C. reinhardtii rbcS2* gene. Moreover, the plasmids contained the Hygromycin-resistance cassette excised from pHyg3 (Berthold et al., 2002), with the *aphVII'* gene that confers resistance to eucariotic antibiotic Hygromycin B. Hygromycin-resistant colonies were identified based on their growth on selective medium, with a frequency of 0.22 x 10^{-6} cells for pHyg6-B and 0.26 x 10^{-6} cells for pHyg6-D. Afterwards, the integration of the recombinant genes was confirmed by PCR screening. The combination of primers showed in Tab. 1 was used and fragments of 1.118 and 1.242 kb were amplified for pHyg6-B and D respectively. Among the transformants grown in selective medium, the 60% of colonies contained pHyg6-B (Fig. 2 a), whereas 67% of colonies transformed with pHyg6-D showed the insertion of the transgene (Fig. 2 b). Then, Hygro-PSY positive colonies were inoculated in liquid TAP-S with 10 μg mL^{-1} of Hygromycin and further analysed. Among the positive colonies, only one transformant with pHyg6-B construct (hereafter named B3 colony) showed an increased content of Car of about 40% with respect to the control in late stationary phase of growth (Data not shown). RT-PCR analyses confirmed the transcription of the relevant mRNA, and thus the expression of *AtPSY* gene (Fig. 2 c). Subsequently, further physiological analyses were then focused on this transformant.

3.2. Phenotypic characterisation of B3: preliminary analyses

In order to better identify the effects of the nuclear transformation for the expression of the exogenous *AtPSY* in *C. reinhardtii*, new cultures of the Hygro-PSY positive colony B3 were set up and compared with wt cells. Physiological analyses were performed at 4, 11 and 30 days of growth on cells cultured in liquid medium at 100 $\mu mol_{photons}\ m^{-2}s^{-1}$ of light intensity.

Pigment content

The trends of pigment content are shown in Fig. 3. During the experimental time, a decreasing trend of total Chl content was observed both in wt and B3 cells (Fig. 3 a). However, in wt a strong decrease in total Chl occur from 11 to 30 days of growth (-53%), while in B3 the decrease was less marked, resulting in higher concentrations at 30 days of growth with respect to control (+62%, $p < 0.01$). Same decreasing trend was observed for Car concentration in both samples (Fig. 3 b). As concerns the transformed cells, Car content was significantly higher already at 4 days of growth ($p < 0.05$). Increased concentrations were observed also at 30 days of growth with respect to wt cells, despite difference was not significant at this point ($p = 0.06$). The simultaneous variations of Chl and Car contents led to a gradual increase in the Chl/Car ratio in B3 cells, whereas in wt cells the ratio remained stable, except at 30 days of growth, when a slight decrease was observed (Fig. 3 c).

PAM fluorimetry

The effects of the transformation on photosynthetic efficiency were evaluated by PAM fluorimetry. In particular, maximum quantum yield of PSII, as F_v/F_{mM} ratio, actual yield of PSII (Y(PSII)) and yield of dissipation in photoinactivated PSII (Y(NF)) were obtained from samples exposed to 1200 $\mu mol_{photons}\ m^{-2}s^{-1}$ for 5 min, followed by 5 min of dark recovery (Fig. 4). F_v/F_{mM} ratios appeared significantly different between wt and B3 cells after the 4^{th} day of growth (Fig. 4 a). In wt cells the ratio was maintained around 0.55, while in B3 cells a decreasing trend from ca. 0.6 to ca. 0.35 was observed during the experimental time, reaching 37% lower values with respect to wt at 30 days of growth ($p < 0.05$ at 11 days and $p < 0.01$ at 30 days). Y(PSII) is a useful parameter to evaluate the proportion of potentially active PSII after high-light exposure. Despite the lower F_v/F_{mM} ratios, unexpectedly in B3 cells

Y(PSII) was always higher, with values varying from 0.09 at 4 days to 0.12 at 30 days of growth (Fig. 4 b). Conversely, in wt cells this percentage varied from 0.036 at 4 days to 0.055 at 30 days, thus was always lower at the same experimental time (-61% and -53% respectively, $p < 0.05$). Finally, Y(NF) is the ratio between PSII actual quantum yield after light induction and PSII maximum quantum yield at time 0, thus indicated the proportion of inactivated PSII after light induction. Despite increasing trends were observed for both wt and B3 cells during the time, transformed cells always showed a minor proportion of inactivated PSII with respect to wt cells (Fig. 4 c). In these latter samples, percentages of photoinactivated PSII varied from 24 to 34%, whereas in transformed cells the values never exceeded 21% ($p < 0.05$).

RT Microspectruofluorimetric analysis and comparison with photoinhibited cells

RT Fluorescence emission spectra analyses were obtained for both wt and B3 cells grown in liquid medium at 100 $\mu mol_{photons}\ m^{-2}s^{-1}$ of light exposure after 15 days of growth. The spectra showed a typical peak at 683 nm, assigned to the PSII emission (Franck et al., 2002), and a broad shoulder at 710-740 nm, which correspond to PSI-LHCI emission, with the contribution of vibrational satellites (Franck et al., 2005) (Fig. 5 a, b). In order to get more precise information on the origin of fluorescence, fourth-order derivatives were calculated to find the components to be used for the deconvolution by Gaussian fitting procedure (Ferroni et al., 2011). Gaussian deconvolution of spectra showed three emission peaks assigned to PSII. Free LHCII emitted at 680 nm, PSII core emitted at 686 nm, while emission at 694 nm was attributed to LHCII-PSII functional assemblies. Moreover, emission at 702 nm was attributed to the contribution of LHCII aggregates and LHCI-PSI complexes, while emissions at 660 and 670.5 nm were assigned to uncoupled Chl (Tab. 3) (Ferroni et al., 2011). No differences in the peak positions were observed between wt and B3 cells. However, differences in the relative intensities of the emission bands were present, as demonstrated by the different dimension of areas subtended the different peaks (Fig. 5 a, b). In particular, B3 cells showed increased emissions from uncoupled Chl (F660, ca. +82%) and LHCII-PSII functional assemblies (F694, ca. +26%), whereas decreased emission from PSII core (F686, ca. -17%) and LHCII aggregates (F702, ca. -21%) were shown with respect to wt cells. After photoinhibition treatment, RT microspectrofluorimetric spectra were recorded both for wt and B3 cells, and difference spectra with their relative non-photoinhibited

samples were calculated. Analyses showed differences in emission intensities in both photoinhibited samples with respect to their relative non-photoinhibited controls. In photoinhibited wt, increased emission at 677 nm and decreased emission at 683 nm were observed in comparison with spectra of wt cells grown in normal light conditions (Fig. 5 c). Conversely, photoinhibited B3 cells did not show such strong variations with respect to non-photoinhibited B3 cells, except for a decrease in the emission range between 667 and 687 nm (Fig. 5 d).

3.3. Phenotypic characterisation of B3 to different light intensities: effects of the transformation

Despite Car accumulation occurred only in slightly higher amounts in transformed cells with respect to wt cells and in stationary phase of growth, preliminary experiments on B3 phenotype showed increased characteristics of photoprotection when samples were subjected to photoinhibition treatments (see sections 3.2.2. and 3.2.3.). In order to characterise this physiological response and investigate if and how photoprotection could be related with the nuclear transformation with the exogenous *AtPSY*, liquid cultures were set up and grown under contrasting light regimes, such as 30 $\mu mol_{photons}\ m^{-2}s^{-1}$ as low-light intensity (LL cultures; Fig. 6 a) and 150 $\mu mol_{photons}\ m^{-2}s^{-1}$ as high-light intensities (HL cultures; Fig. 6 b). Growth was monitored after 4, 11, 21 and 31 days from the inoculum, showing no differences between control and transformed cells, irrespective of the light intensity, except for B3 grown under LL conditions, which showed reduced cell density at 11 and 21 days, though it reached the same values as the other samples at 31 days (Fig. 6 c). Parallel to growth measurements, photosynthetic pigment analyses and PAM fluorimetry were performed. Moreover, samples were analysed by HPLC at 4 and 31 days of growth and compared, in order to investigate in transformation induced changes in the composition of Car profile when transformed cells were exposed at different light regimes.

Effects of transformation on photosynthetic pigments amount and Car profile in LL and HL conditions

Different trends of photosynthetic pigments were observed based on the growth light intensities in wt and B3 cells (Fig. 7). About total Chl content in LL cultures, similar

effects as described in section 3.2.1. were observed, even if less marked (Fig. 7 a). Indeed, Chl concentration in wt cells slightly diminished during the experimental time, reaching at the end values 30% lower than those measured at 4 days of growth. Conversely, no variation occurred in transformed cells during the time, thus at 31 days of growth values 21% higher than those measured for wt were detected ($p < 0.05$). About total Chl content in HL cultures (Fig. 7 b), a very evident decreasing trend was observed in wt cells, which showed at the end of the experimental time values 55% lower than at 4 days. Interestingly, in transformed cells the Chl content was constant throughout the experiment, except at 31 days of growth, when lower values were measured. However, very reduced values were detected already at 4 days of growth with respect to wt (-42%, $p < 0.01$). In this case, the Chl concentration in B3 cells did not exceed that of wt 31 days of growth, but similar values were measured in the two samples. Differences between wt and B3 cells in LL and HL conditions were observed also for Car content. About wt-LL cultures (Fig. 7 c), a slightly decreasing trend was found, less marked than that described previously for Chl content. Conversely, transformed cells showed a nearly constant content of Car, thus from 21 days onwards higher concentrations were measured with respect to wt cells, with an increase by ca. 33% at 31 days of growth ($p < 0.05$). In HL cultures, instead, no significant variations were observed throughout the experiment for both wt and B3 cells (Fig. 7 d). Simultaneous variations in Chl and Car content led to Chl/Car ratios between 5 and 6.5 throughout the experiment in LL cultures, with no differences between wt and transformed cells (Fig. 7 e). Conversely, in HL cultures higher values were measured in wt cells only at 4 days of growth ($p < 0.05$), after that no differences between samples were observed (Fig. 7 f).

HPLC analyses of samples grown in LL conditions showed modifications of the Car profile in transformed cells, especially after 4 days of growth (Tab. 4). Despite the total xanthophyll concentration was similar, at this time of growth intracellular levels of zeaxanthin, which were not detected in wt-LL cells, were measured in transformed cells, whereas 2-fold higher levels of antheraxanthin were found with respect to control cells ($p < 0.01$). Conversely, the presence of neoxanthin was 0.7-fold lower following the expression of exogenous *AtPSY* ($p < 0.05$). After 31 days of growth, the effect of transformation did not strongly alter the Car profile, which only showed a decrease in β-carotene content (-21%; $p < 0.05$) in transformed cells with respect to wt. A weak accumulation of violaxanthin was

found in B3 cells, despite differences were not significant (Tab. 4). As shown in Tab. 5, the effects of transformation on the Car profile was emphasized when cells were grown in high-light. No differences in Car concentration between wt- and B3-HL cells at 4 days of growth were found, and in both cases lutein represented the major proportion of Car. Despite this, transformed cells showed 2-fold higher levels of β-carotene ($p < 0.05$), 4.5-fold higher levels of antheraxanthin ($p < 0.01$) and 1,2-fold higher levels of violaxanthin ($p < 0.05$) with respect to wt cells. Moreover, zeaxanthin, not detected in wt cells, was also found. The increased content of these xanthophylls occurred at the expense of neoxanthin and loroxanthin, whose sum was halved as compared to wt cells ($p < 0.01$). This resulted in an unchanged xanthophyll content. Even at 31 days of growth, strong variations in the Car profile occurred. In particular, 6.12- and 3.68- higher folds of zeaxanthin and antheraxanthin were accumulated in transformed cells with respect to wt ($p < 0.01$ in both cases), at the expense of β-carotene (-26%; $p < 0.05$), violaxanthin (-33%, $p < 0.01$), the sum of neoxanthin and loroxanthin (-37%; $p < 0.01$) and lutein (-17%). This resulted in higher concentration of total xanthophylls in wt cells. These concentrations were used to calculate some parameters which were useful for understanding the effect on photoacclimation with the expression of *AtPSY* under low-light and high-light conditions. In wt-LL cells, the total xanthophylls/β-Carotene ratio, as a result of the Car balance between antenna and reaction centers, decreased during the time, mainly because of the major increase in β-carotene with respect to total xanthophylls. In wt-HL cultures, instead, the strong decrease in β-carotene at 4 days of growth resulted in a higher ratio, which then decreased because of the accumulation of this Car upon xanthophylls, despite an increase in them was also observed. On the other hand, in LL and HL transformed cells no strong variations occurred in total xanthophylls/β-Car ratio, irrespective of the light intensity and time of growth. Moreover, different xanthophylls profile among different samples allowed to measure the (zeaxanthin+antheraxanthin)/violaxanthin ratio [(Z+A)/V)], indicative of the de-epoxidation level. In LL-cultures, the ratio was indeed 2.2 times higher in B3 cells with respect to wt at 4 days of growth, mainly due to the higher concentrations of the de-epoxidised xanthophylls. In HL-cultures, the ratio increased throughout the experiment both in wt and B3 cells, but values of the latter were ca. 5 and 7 times higher compared to wt cells at 4 and 31 days of growth, respectively.

Energy partitioning of absorbed light energy in LL and HL cultures

In this work, the partitioning of the absorbed excitation energy in PSII was described between 4 fundamental pathways, according to different approaches (Hendrickson et al., 2005). The first component is the fraction of energy which can be photochemically converted in PSII, the PSII quantum yield, i.e. Y(PSII). The other components represented the total quantum yield of all dissipative processes. In particular, Y(npq) is the fraction of energy passively dissipated in form of heat by the regulated photoprotective NPQ mechanisms, Y(NF) is the fraction of energy dissipated as heat by photo-inhactivated PSII and Y(NO) is the fraction of energy constitutively dissipated in form of heat and fluorescence emission, mainly due to emission of closed PSII.

In wt cells of *C. reinhardtii* cc-3491 grown under LL conditions, only 5% of the energy absorbed by PSII was consumed via photochemistry (Fig. 8 a). This proportion remained constant throughout the experiment. Among all dissipative processes, most of the energy fraction was passively dissipated, in fact Y(NO) represented 40% of total energy during the entire experimental time. Same proportion was observed at day 4 for the energy fraction dissipated by inactive PSII, Y(NF). However, this proportion decreased from 40 to 35% after 11 days, and then it increased again until reaching 45% at 31 days. The trend of Y(NF) was inversely linked to that of Y(npq), which increased from 12 to 20% at 11 days of growth and subsequently decreased to 6% at the end of the experiment. Confirming the observations as in section 3.2.3, B3-LL always showed higher proportion of Y(PSII), which varied in a range between 6 and 13%, with respect to wt cells (Fig. 8 b). Moreover, lower percentage of energy dissipated by inactive PSII, Y(NF), which varied between 32 and 16%, were observed as well. The absorbed energy fraction which was dissipated by NPQ mechanisms, instead, increased from 6% at day 4 to 19% at day 11, after that it slightly decreased until it reached 14% at 21 and 31 days of growth. Interestingly, despite the higher proportion of PSII quantum yield and the lower fraction of Y(NF), B3-LL cells showed a higher percentage of constitutive energy dissipation, Y(NO), which varied from 60% at day 4 to 48% at day 11 and reached the 50% at the end of the experimental time. When cells were grown under HL conditions, different partitioning of absorbed energy was observed both in wt and B3 cells. In wt cells (Fig. 8 c), the proportion of PSII quantum yield was slightly higher with respect to wt-LL cultures, and variable between 6 and 8%, as well as the fraction of energy

constitutively dissipated, Y(NO), which was the 60% at 4 days, decreased to 45% at 21 days and then increased again to 57% at the end of the experiment. About the energy fraction dissipated by inactivated PSII, Y(NF), a gradual increasing trend was observed during the experiment. Finally, Y(npq) remained almost constant until day 31. At the end of the experiment, indeed, the energy loss as heat or fluorescence was exclusively dissipated by the contribution of Y(NO) and Y(NF), whereas NPQ mechanisms contributed only for 1%. Same situation was observed at 4 days of growth in B3-HL cultures, when the absorbed energy fraction was dissipated for the 90% by the only contribution of Y(NO) (70%) and Y(NF) (20%), while the remaining 10% was the fraction of energy used in photochemistry. However, Y(npq) subsequently increased to around 10%, whilst the energy fraction dissipated by non-NPQ mechanisms remained stable at 70%. An increase in the latter fraction at 31 days of growth was linked to a decrease in Y(PSII) fraction from 10 to 6%. When energy partitioning diagrams in LL and HL cultures were compared with each other, an interesting observation was made between wt-HL and B3-LL. In fact, energy partitioning in transformed cells grown at LL conditions after 4 days was the same of that measured in wt cells grown in HL conditions for 31 days, showing the same unusual characteristics of photoacclimation to high-light conditions.

4. Discussion

Microalgae represent one of the most important biological sources of natural compounds which can be used for biotechnological applications (León-Bañares et al., 2004). Among the several products that can be obtained from microalgae, carotenoids play an important role for their possible exploitation in pharmaceutical, cosmetic, and medical fields, thanks to their intrinsic antioxidant, anti-inflammatory and anticancer properties (Del Campo et al., 2007; Liu et al., 2009b). Phytoene synthase (PSY) is the first key-enzyme involved in the Car biosynthetic pathway, catalysing the condensation of two GGPP molecules to generate phytoene. This enzyme is considered rate-limiting in the pathway and determines the carbon flux towards Car production (Shewmaker et al., 1999; Fraser et al., 2002; Sandmann et al., 2006; Couso et al., 2011). For this reason, the first step of the Car biosynthetic pathway has often been the target of genetic engineering in order to induce Car

accumulation in many crop plants (Fray et al., 1995; Hauptmann et al., 1997; Fraser et al., 2002; Lindgren et al., 2003; Ducreux et al., 2005). However, the regulation of the carotenogenic pathway in plants and green algae is not fully understood, and this causes limitations for the application of protocols of the genetic engineering (Couso et al., 2011). As a model organism, *Chlamydomonas reinhardtii* is considered an excellent host for foreign genes encoding for enzymes involved in the carotenogenesis (Cordero et al., 2011; Couso et al., 2011). The genome of this microalga is completely sequenced, thus the nuclear manipulation is easy and well-established (Harris et al., 2001). Then, this organism could offer an excellent tool to unravel the Car biosynthetic pathway and, at the same time, to obtain its modification and promote the accumulation of Car with commercial interest.

In this study, the cDNA sequences encoding for *Arabidopsis thaliana* PSY (*At*PSY) and the first isoform of *Oryza sativa* PSY (*Os*PSY1) were expressed in the cc-3491 cell wall-less strain of *C. reinhardtii*. The PSY gene products are targeted to the chloroplast. The nuclear transformation efficiencies were very low for both cases, and not all the colonies grown on selective medium showed the presence of the transgenes. It is well-documented that transgene expression is often lowered by silencing of exogenous DNA by a host system, with a consequent direct influence on the stability of transformant phenotype (De Wilde et al., 2000). However, also a fragmented integration of the plasmids inside the genome, as well as deletions caused by recombination events, could explain the absence of the DNA sequences of interest, in spite of the capability of colonies to grow in presence of Hygromycin-B (Berthold et al., 2002). Despite the low number of positive colonies, the transformation of *C. reinhardtii* with both *AtPSY* and *OsPSY1* generated stable transformants. However, only one colony, B3, showed in late stationary phase of growth a 40% higher content of Car if compared with the parental strain. This different phenotype was confirmed to be linked to the expression of *AtPSY* by the detection of the corresponding *PSY* transcript. It is known that stable transformants of *C. reinhardtii* integrate different copies of exogenous DNA inside the nucleus by heterologous recombination mechanisms (Harris, 2001) and that difficulties in the expression of heterologous genes could be related both with the insertion position in the genome and the gene copy number. However, the functional expression of the exogenous PSY and consequent Car accumulation could have been prevented in the positive transformants that did not exhibit the phenotype by some unknown post-

transcriptional or post-translational inhibition mechanisms, although these possibilities have not been further investigated.

In previous works, the capability to accumulate Car as a consequence of the transformation with carotenogenic genes in *C. reinhardtii* did not take into consideration the variability in pigment content linked with the phase of growth (León et al., 2007; Cordero et al., 2011; Couso et al., 2011). For this reason, in this study wt and B3 cells have been monitored during cell growth up to the late stationary phase. In wt cc-3491 strain grown in normal light intensities, the amount of Chl and Car decreased indeed during the experiment, without affecting the F_v/F_{mM}. Interestingly, such decrease in pigments was less marked in B3 cells, leading to higher amounts with respect to wt cells at the end of the experiment. However, B3 showed a decreasing trend of F_v/F_{mM}. Decreasing levels of maximum quantum efficiency of PSII have been linked to exposure of photosynthetic organisms to biotic or abiotic stresses in the light (Baker, 2008). However, identification of the intrinsic causes of such decreases can often be difficult. Moreover, a decrease in maximum quantum yield is often linked with photo-inactivation of PSII reaction centres, which dissipate excitation energy as heat rather than using it for photochemistry (Melis, 1999). Conversely, in B3 cells the decreased F_v/F_{mM} was accompanied by higher actual quantum yield of PSII and lower yield of photo-inactivated PSII after a short exposure to high-light, supporting the idea that the decrease in the F_v/F_{mM} is not caused by stress conditions induced by the expression of *At*PSY. Different organisation of PSII in these samples was shown by deconvoluted RT emission spectra. Indeed, higher F694, indicative of LHCII-PSII functional assemblies (Ferroni et al., 2011), confirms that PSII activity is not compromised in B3 cells. Moreover, alteration of the fluorescence spectra after photoinhibition treatments is much less marked in B3 cells than in wt. These preliminary results strongly suggested that B3 could exhibit an interesting phenotype with respect to photoacclimation. For these reasons, new cultures were set up and exposed to two contrasting light regimes. The trend of pigment content from LL to HL was analysed first in wt cells in order to obtain a photoacclimation sequence that could be used for comparison with B3 cells. This sequence includes a transition from wt-LL at 4 days of growth through wt-HL at 4 days of growth and, finally, to wt-HL at 31 days of growth. Following this sequence, decrease in total Chl, total Car and Chl/Car ratio were observed in wt. It is well-known that in photosynthetic organisms photoacclimation to high light induces

a decrease in the LHCII pigment-protein complexes and PSII reaction centres in order to avoid photoinhibition (Fujita et al., 1989; Durnford et al., 2002). The decreasing trend of total Chl content observed in this study was in line with previous experiments performed in *C. reinhardtii* cells, which showed a 50% lower amount of Chl and a decline by 40% of LHC abundance when LL-acclimated cells were exposed to HL (Durnford et al., 2002). Car content was also affected by HL exposure, but the decreasing trend from LL to HL acclimation were less marked. Indeed, only lower amounts of neoxanthin were detected, while lutein, total amount of violaxanthin, antheraxantin and zeaxanthin, as well as the de-epoxidized fraction of xanthophylls (A+Z)/V, were increasing in wt-HL cells. Despite xanthophylls are mainly bound to the Lhc proteins of PSI and PSII (Bassi et al., 1993), only neoxanthin plays the single role of accessory antenna pigment (Demmig-Adams, 1998), whereas violaxanthin, zeaxanthin and lutein are involved in dissipation of excess-light energy (Dall'Osto et al., 2006; Jahns and Holzwarth, 2012). The pigment trends characterising wt cells provided the framework for understanding how B3 had changed its photoacclimation properties. On the whole, a reduction in the pigment content was observed in transformed cells, similar to wt. However, Chl and Car amounts in HL cells were already lower at 4 days of growth with respect to wt, indicating an anticipation of photoacclimation to HL. For this reason, the accumulation of Car in transformed cells was not observed, differentfrom what was shown in previous works where microalgae and higher plants were transformed with exogenous PSY (Shewmaker et al., 1999; Fraser et al., 2002; Ducreaux et al., 2005; Cordero et al., 2011; Couso et al., 2011). Then, the expression of *At*PSY did not induce an absolute Car accumulation, but the amount of each single Car varied to determine a different Car profile. On the whole, in a young (4 days) B3 culture grown in LL conditions: i) Chl amount was reduced like in a HL-photoacclimated wt; ii) the amount of neoxanthin was already lower than that of wt-HL at 31 days, indicating a high reduction of the antenna function; iii) accumulation of violaxanthin, zeaxanthin and antheraxanthin was enhanced, as well as a high amount of de-epoxidized xanthophylls was observed. Under physiological conditions *in vivo*, zeaxanthin occurs only in trace amounts within the LHC (Ruban et al., 1994; Lee and Thornber, 1995; Verhoeven et al., 1996) and is usually formed upon de-epoxidation of violaxanthin during high-light exposure through the operation of the reversible xanthophyll cycle (Yamamoto, 1979, 1985). Therefore, B3 resembles pre-adapted to HL conditions even when grown in LL conditions. However, these characteristics were lost at 31 days of growth,

when the concentration of neoxanthin increased and the level of de-epoxidation decreased dramatically to 0. When B3 was grown in HL conditions, photoacclimation was further enhanced if compared to wt-HL even at 31 days, with further reduction in neoxanthin content until reaching halved levels and highly increased levels of zeaxanthin and antheraxanthin. Accumulation of zeaxanthin and other xanthophylls such as lutein and violaxanthin was also previously observed in other experiments with transgenic *C. reinhardtii* transformed with exogenous PSY from *Dunaliella salina* and *Haematococcus pluvialis* (Cordero et al., 2011; Couso et al., 2011).

Energy partitioning is a useful methods which allows to better understand how photosynthetic organisms use or dissipate the absorbed light energy through several mechanisms, in order to maximize photosynthetic carboxylation and limit the formation of reactive oxygen species and other photooxidative risks (Nyogi, 1999; Losciale et al., 2011). According to Hendrickson et al. (2005), the light energy absorbed by PSII can be quantified in i) fraction used for photochemistry [Y(PSII)]; ii) fraction of energy quenched by light-dependent [Y(npq)] or light-indipendent [Y(NO)] thermal dissipation; iii) fraction of energy dissipated by photo-inactivated PSII [Y(NF)]. In wt-LL, Y(NO) and the sum of energy fractions which are dissipated by light-dependent mechanisms [Y(NF)+Y(npq)] were constant throughout the experiment. Among the latter components, Y(NF) progressively prevailed over Y(npq). Y(NF) is a slowly reversible protective mechanism (Losciale et al., 2011), which might be promoted in cells in stationary phase either by the cell ageing or by the capacity of developing long-term responses during photoacclimation. In wt-HL cells, an increase in the amount of Y(NO) and a decrease in [Y(NF)+Y(npq)] were observed with respect to LL-cells. The decrease in Y(npq) component was enhanced in HL cells and progressively reached the 0 level. This is in line with what observed by Casper-Lindley and Björkman (2008), i.e. that LL-grown algae have a smaller pool of xanthophyll-cycle pigments per Chl, but develop more NPQ during exposure to high-light than cells grown in medium light, probably because of a lower lumen acidification inside thylakoids with respect to LL-cultures (Casper-Lindley and Björkman, 2008).

Differences in the energy partitioning observed between B3-LL cells and wt-LL at 4 days of growth are probably linked to the constitutive accumulation of lutein and zeaxanthin in transformants. In B3-LL cells, indeed, light-dependent mechanisms of energy dissipation

were reduced, with a strong component of Y(NF) and the almost absence of Y(npq), but a higher proportion of Y(NO) with respect to wt-LL. In *A. thaliana* mutants which contained constantly high zeaxanthin levels, maximal quenching was similar to that of wt plants, indicating that an excess of zeaxanthin does not effectively contribute to NPQ (Tardy and Havaux, 1996). Moreover, it has been demonstrated that NPQ can be mediated by pigments already present in darkened cells (Casper-Lindley and Björkman, 1998). Thus, the cabability of developing low NPQ when B3-LL cells at 4 days of growth are exposed to saturating light might be linked to the constitutive presence of de-epoxidized xanthophylls, which led instead to the increase in the constitutive dissipation energy fraction Y(NO). Again, energy partitioning in B3-LL at 4 days of growth resembles much more that of a wt-HL than of a wt-LL. This photoacclimation to HL is clearly not functional in cells grown in LL conditions, in fact the reduced cell growth confirmed the ineffectiveness of light capturing and use. Several compensation mechanisms appear to have been subsequently developed in order to emphasise light harvesting, with increase in neoxanthin concentrations, reaching the same amounts as in wt, and decrease in de-epoxidized xanthophylls during time. In this way, Y(npq) was allowed to increase and light harvesting was promoted to support growth. In B3-HL at 4 days of growth, the photoacclimation to HL was highly emphasised, not only with respect to wt-HL, but also to B3-LL. Indeed, the increased amounts of violaxanthin and de-epoxidized xanthophylls, as well as decreased amounts of neoxanthin, resulted in increased Y(NO) and decreased energy dissipation by light-dependent mechanisms, exclusively represented by Y(NF). However, these characteristics of enhanced long-term photoprotection are probably not required during exposition to such light intensity, as photoacclimation of *C. reinhardtii* to light intensities higher than that used in this study was shown (Durnford et al., 2002). Then, despite at 31 days of growth the effects of transformation were further enhanced, with continuous increase in xanthophylls and decrease in neoxanthin concentration, light-dependent energy dissipation mechanisms were activated in order to try to compensate a de-regulated system and use energy in a more efficient way.

On the whole, these results suggest that the expression of *At*PSY in B3 colony promotes accumulation of dissipative Car, such as zeaxanthin and its intermediate antheraxanthin, inducing the (de-)regulation of the carotenogenesis towards

photoacclimation to HL. When transformed cells are grown in LL, a feed-back mechanisms acting on the endogenous metabolic pathway might be gradually activated, avoiding further de-epoxidation of violaxanthin and inducing accumulation of neoxanthin to improve light harvesting. On the other hand, if transformed cells are grown in HL, this feed-back mechanism might be not sufficient, and other mechanisms of energy-dissipation might be activated by cells in order to compensate the excessive increase in de-epoxidized xanthophylls.

5. Conclusion

In this work, the genetic transformation of the microalga *C. reinhardtii* with *At*PSY and *Os*PSY1 was performed. The expression of the transgenes was confirmed in only one transformant with *At*PSY, which showed increased amounts of Car. However, by further experiments in which cells were grown in different light regimes, it was shown that Car accumulation was light-dependent, while a different Car profile, with initial increased amounts of zeaxanthin, antheraxanthin, violaxanthin and lutein, was always observed. This altered Car profile caused a different use of light during photosynthesis, with differences in the partitioning of absorbed energy towards constitutive energy dissipation fraction Y(NO) and highly reduced Y(npq). In LL cultures, a feed-back mechanism might be activated in order to avoid growth inhibition and promote light-harvesting. Conversely, the accumulation of de-epoxidized xanthophylls was further enhanced in HL, then mechanisms of energy dissipation might be increased in order to compensate the de-regulated accumulation of zeaxanthin. In order to optimize exogenous Car production in microalgae like *C. reinhardtii*, basic knowledge of the Car biosynthetic pathway and its regulation needs to be improved. However, this work shows how genetic engineering together with detailed physiological studies could offer the possibility to obtain a more complete picture of this complex metabolic pathway.

Tables and Figures

Primer	Sequence (5' → 3')
Primers for AtPSY amplification	
attB1-AtPSY1 for	GGGGACAAGTTTGTACAAAAAAGCAGGCTTAATGTCTTCTTCTGTAGCA
attB2-AtPSY1 rev	GGGGACCACTTTGTACAAGAAAGCTGGGTAGGATCMTATCGATAGTCTTGA
Primers for OsPSY1 amplification	
attB1-OsPSY1 for	GGGGACAAGTTTGTACAAAAAAGCAGGCTTAATGGCGGCCATCACGCTC
attB2-OsPSY1 rev	GGGGACCACTTTGTACAAGAAAGCTGGGTAGGATCMCTTCTGGCTATTTCTC
Primers for β-tubulin gene promoter amplification	
attB4-B tub for	GGGGACAACTTTGTATAGAAAAGTTGCTCTTTCTTGCGCTATGACA
attB1-B tub promo intro rev	GGGGACTGCTTTTTTGTACAAACTTGCGCCAGCGGCTGCAAATGGAAACGG
Primers for 3' untranslated region of small subunit of rbcS2 amplification and C.reinhardtii transformation	
attB2-rbcS2 for	GGGGACAGCTTTCTTGTACAAAGTGGCTTAAGGATCCCCGCTCCGTGTA
attb3-rbcS2 rev	GGGGACAACTTTGTATAATAAAGTTGCGGTACCCGCTTCAAATACG
AtPSY1 RT for	TTTGCTTATGACACCCGAAA
AtPSY RT rev	ATAACCGGAACGCTCATCAA
OsPSY1 RT for	AACCACACACCATTCCCATC

Tab. 1: nucleotide sequences of primer pairs used for PCR amplifications.

Plasmid version	Promoter	CDS	Terminator
pHyg6 - B	β2-tubulin promoter + rbcS2 1st intron	At*PSY*	rbcS2 3' UTR
pHyg6 - D	β2-tubulin promoter + rbcS2 1st intron	Os*PSY1*	rbcS2 3' UTR

Tab. 2: Plasmid description.

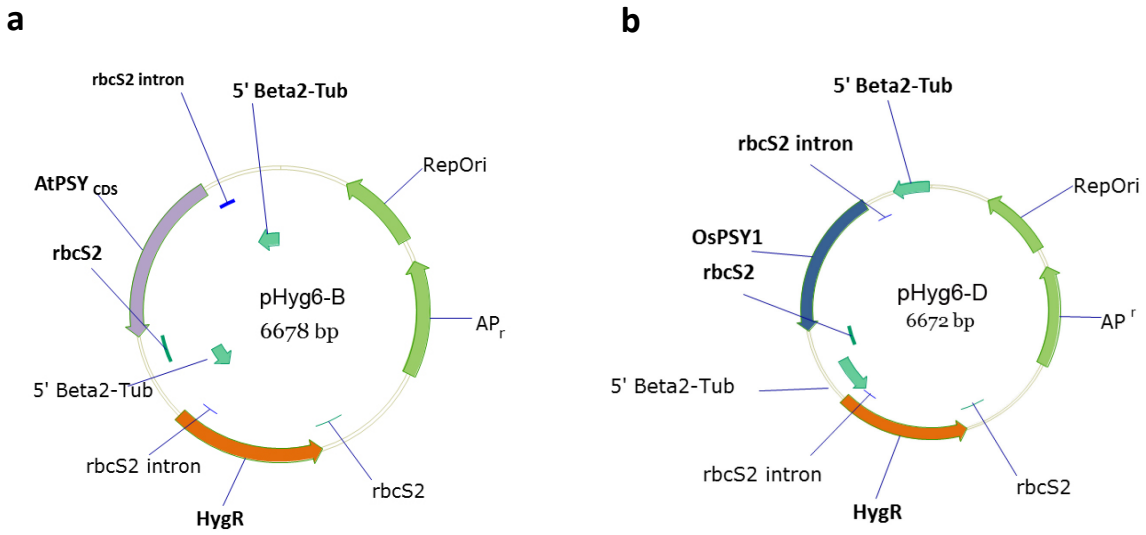

Fig. 1: pHyg6 plasmidic vectors obtained using Gateway Technology recombination. a)pHyg6-B, carrying the coding sequence for *AtPSY* and b) pHyg6-D, containing the coding sequence for *OsPSY1* (Welsh et al., 2008).

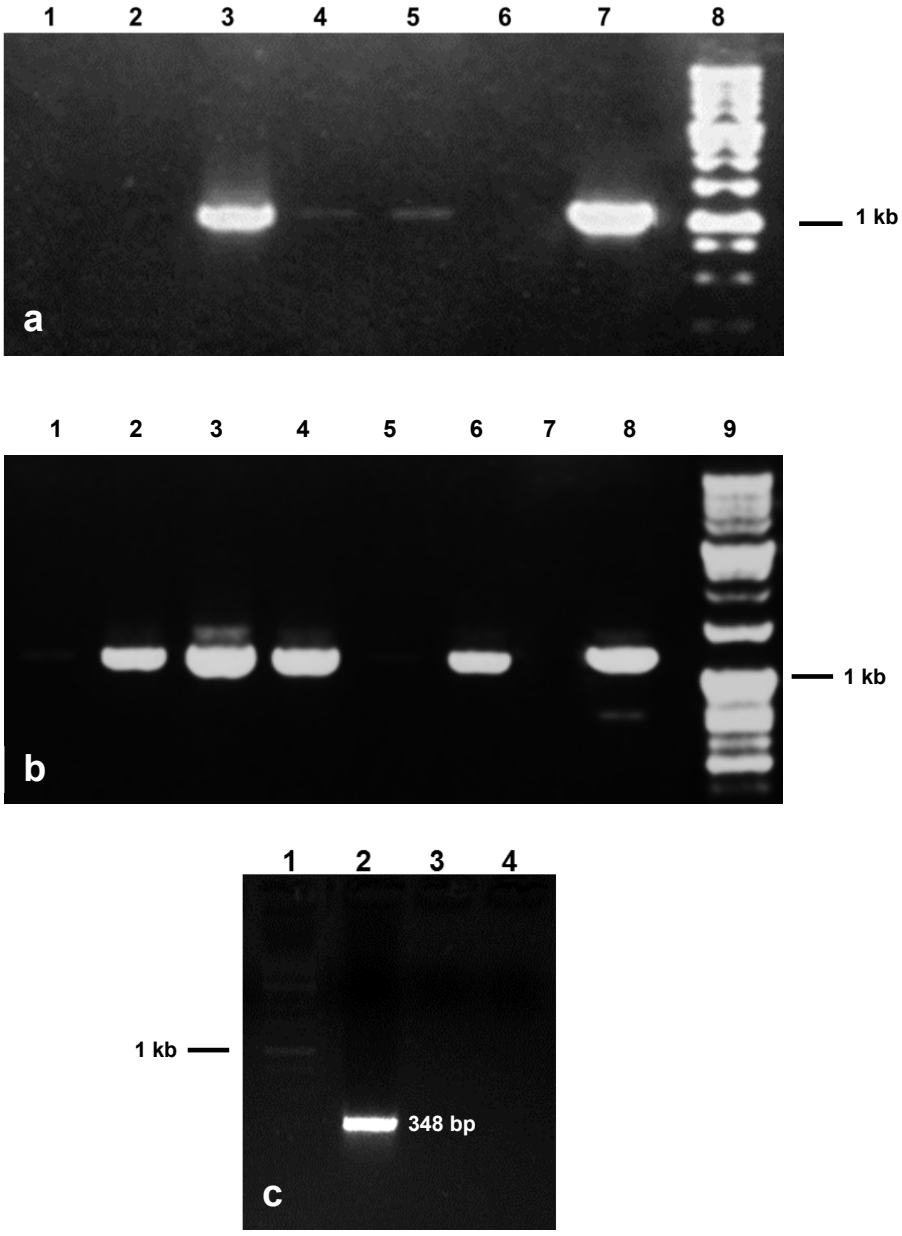

Fig. 2: a) PCR analysis of *C. reinhardtii* transformed with pHyg6-B. 1-5 lines are transformants analysed, line 6 is wild type strain of *C. reinhardtii* and line 7 is pHyg6-B vector. Line 8 is 1 kb DNA ladder (0.1-10 kb, Applichem) Amplified fragments were 1.118 kb length. b) PCR analysis from genomic DNA of *C. reinhardtii* transformed with pHyg6-D. 1-6 lines are transformants analysed, line 7 is wild type strain of *C. reinhardtii* and line 8 is pHyg6-D vector. Line 9 is 1 kb DNA ladder. Amplified fragments were 1.242 kb length. c) RT-PCR Analysis on cDNA from *C. reinhardtii* transformed with pHyg6. Line 1 is 1 kb DNA ladder (0.1-10 kb, Applichem). Line 2 is cDNA from B3 colony, line 3 is wild type strain of *C. reinhardtii*, line 4 is MQ water. Amplified fragments was 348 bp length.

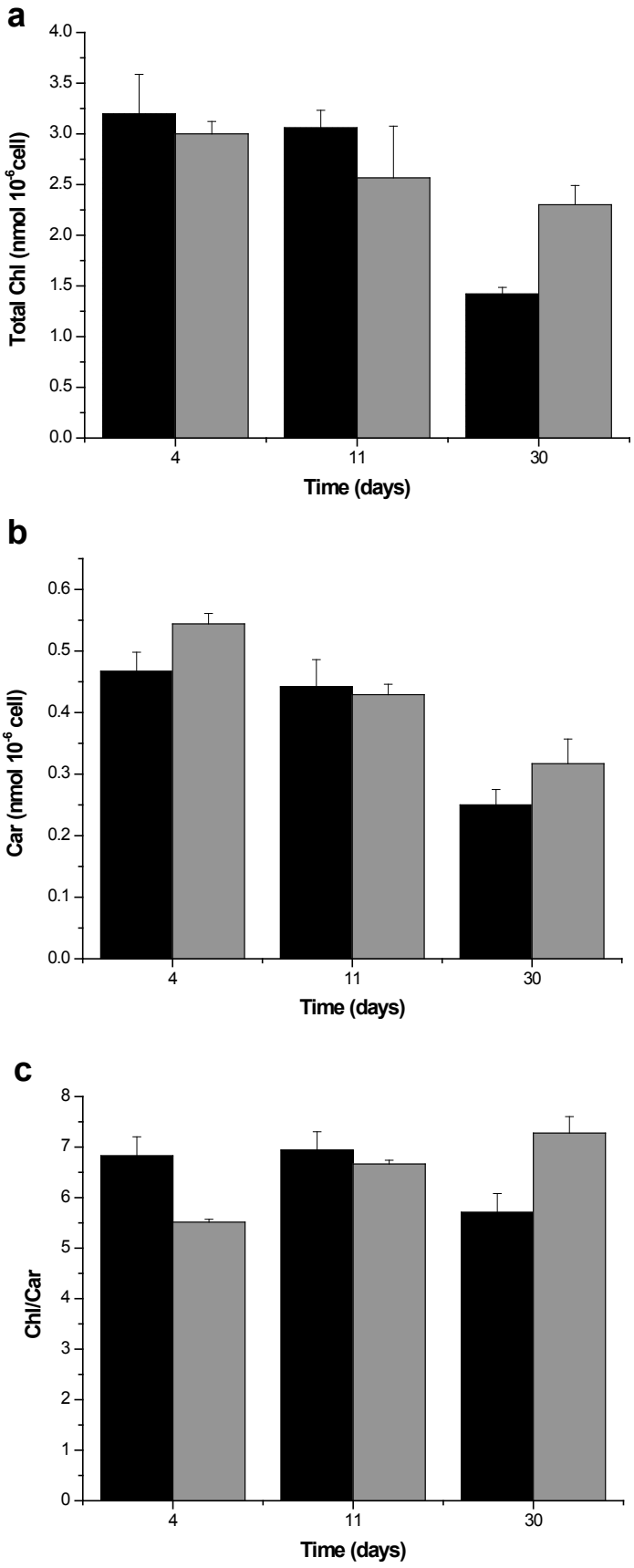

Fig. 3: time course of total Chl (a), Car (b) and Chl/Car ratio (c) during the experimental time in *C. reinhardtii* wt (black) and transformed cells from B3 colony (grey) (n=3 ± s.d.).

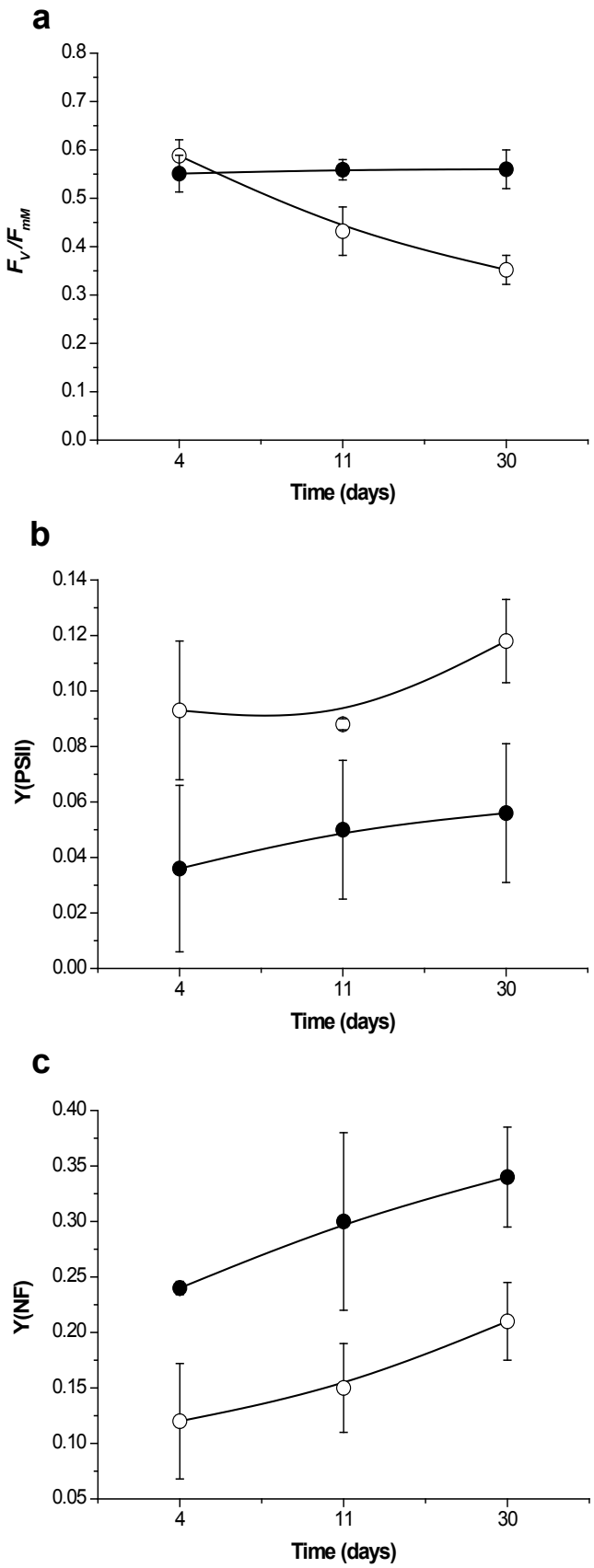

Fig. 4: time courses of F_V/F_{mM} ratio (a), PSII actual quantum yield (b) and yield of photoinactivated PSII (YNF; c) in *C.reinhardtii* wt (filled circles) and transformed cells from B3 colony (empty circles) n=3 ± s.d.).

λ (nm)	Attribution
660-670.5	uncoupled Chl
680	free LHCII
686	PSII core
694	LHCII-PSII functional assemblies
702	LHCII aggregate

Tab. 3: attribution of fluorescence emission bands by PSII in *C. reinhardtii* wt cells, according to Ferroni et al. (2011).

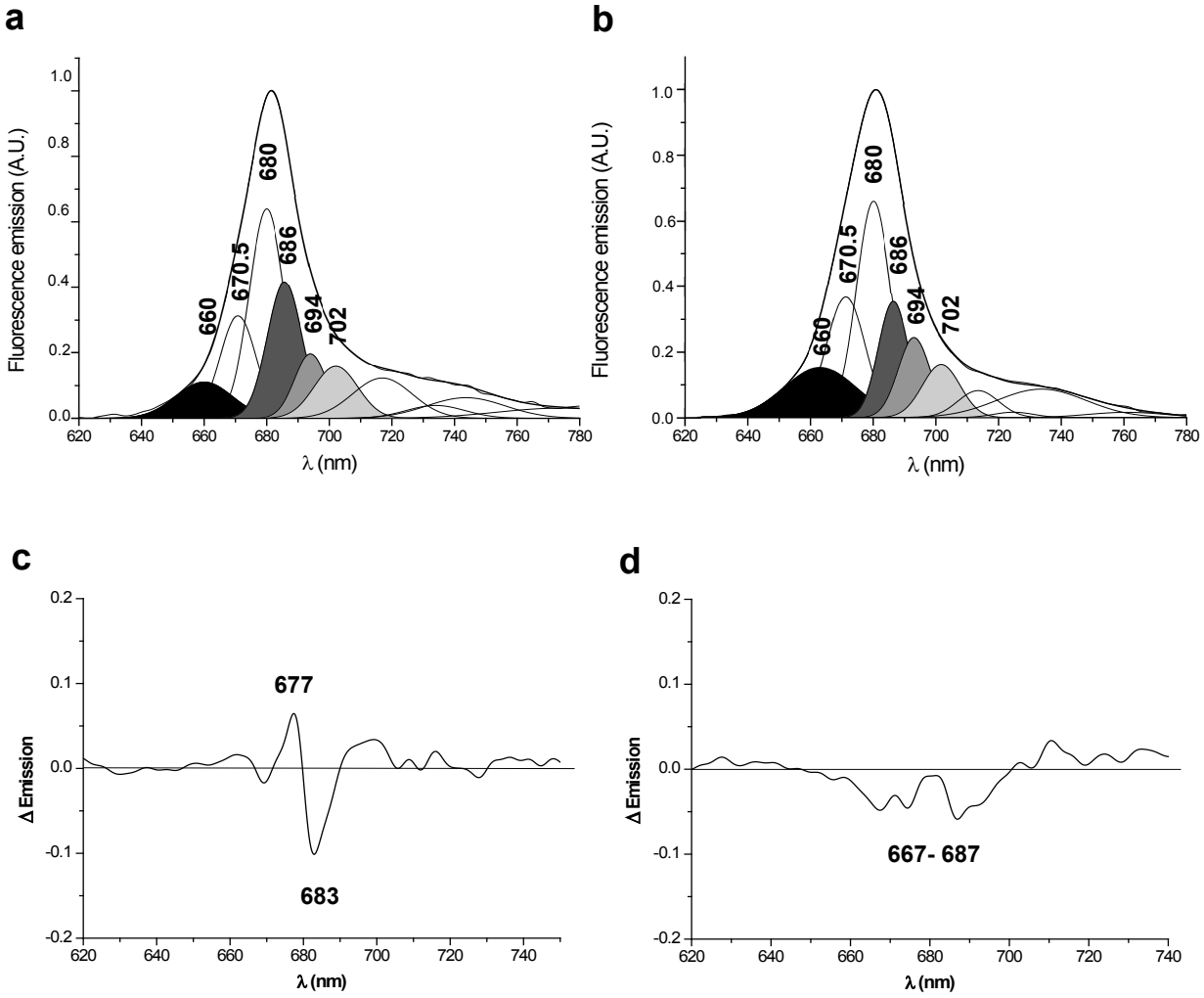

Fig. 5: Gaussian deconvoluted RT emission spectra of wt (a) and B3 (b) *C. reinhardtii* cells. The emission wavelength contributing to PSII region are indicated and different areas subtending the curves have been coloured. c, d: calculation of difference emission spectra between photoinhibited and not-photoinhibited cells of *C. reinhardtii* wt (c) and B3 (d) cells. The emission wavelength altered by photoinhibition treatment are indicated. Deconvoluted spectra derives by the average of at least 5 spectra recorded for each sample.

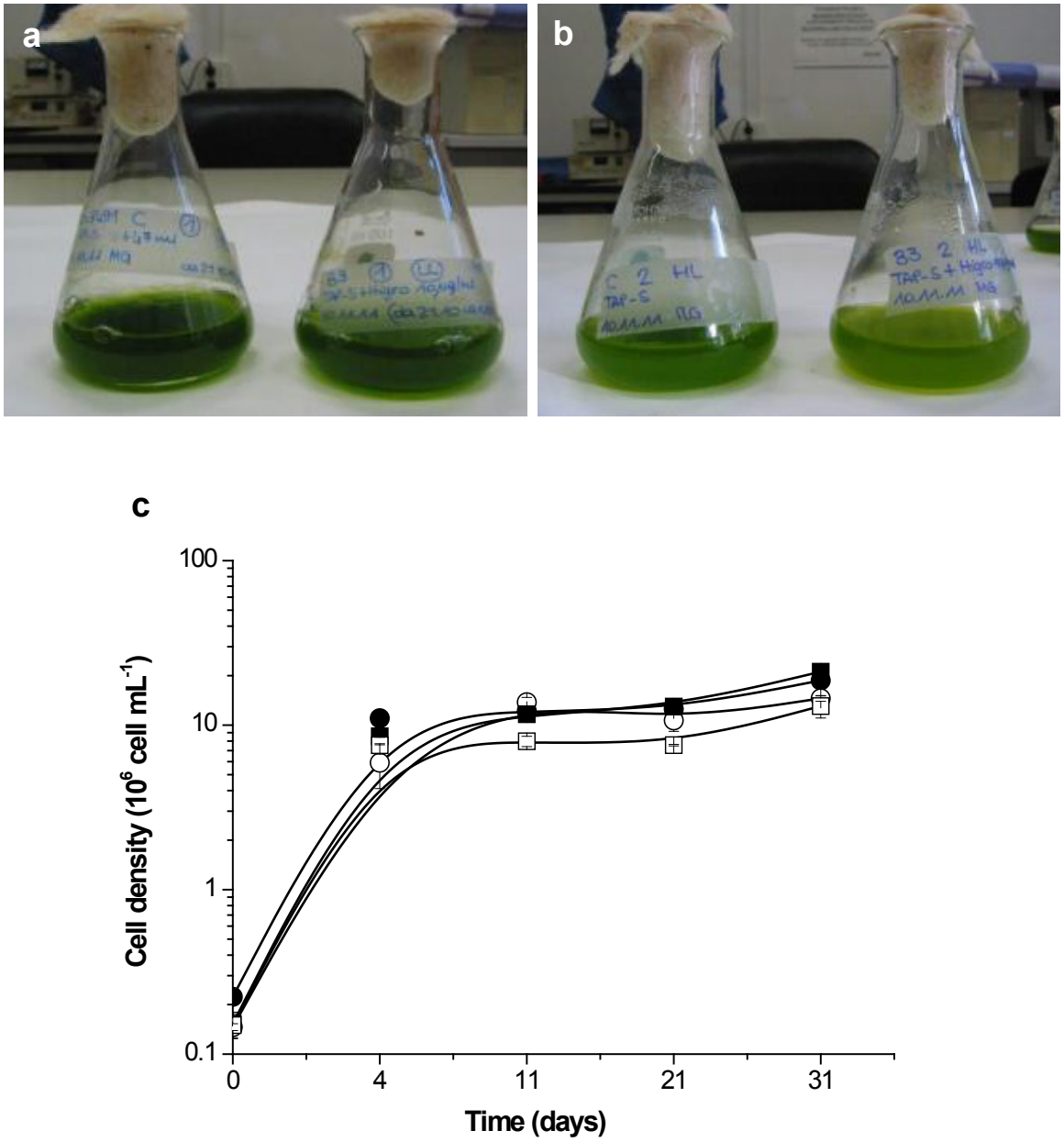

Fig. 6: a) *C. reinhardtii* wt and transformed cells grown at 30 $\mu mol_{photons}\ m^{-2}s^{-1}$ (LL cultures) and b) 150 $\mu mol_{photons}\ m^{-2}s^{-1}$ (HL cultures). c) cell densities of *C. reinhardtii* wt (filled symbols) and B3 (empty symbols) grown in LL (squares) and HL (circles) conditions (n=3 ± s.d.).

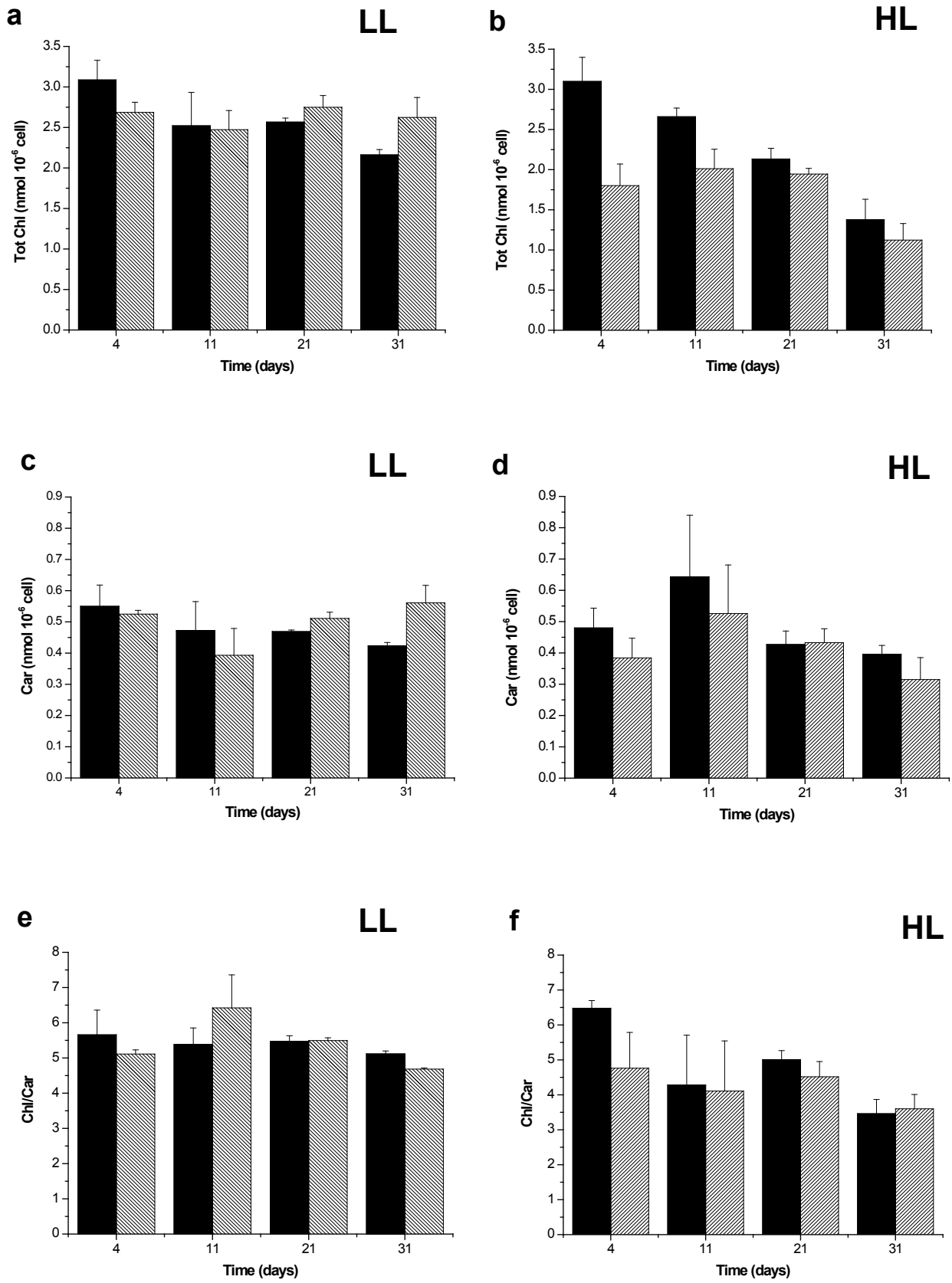

Fig. 7: time-course variations of total Chl (a, b), Car (c, d) and Chl/Car ratio (e, f) in *C. reinhardtii* wt (dark) and B3 (stripes) cells grown at 30 $\mu mol_{photons}\ m^{-2}s^{-1}$ (LL-cultures) and 150 $\mu mol_{photons}\ m^{-2}s^{-1}$ (HL-cultures) of light intensities (n = 3 ± s.d.).

	LL 4 days		LL 31 days	
Car content	**wt**	**B3**	**wt**	**B3**
Total Car	26.30 ± 0.12	25.11 ± 1.01	29.76 ± 1.59	28.23 ± 1.37
β-Carotene	4.46 ± 1.09	3.85 ± 0.56	6.49 ± 0.45	5.12 ± 0.35
Zeaxanthin	n.d.	0.13 ± 0.02	n.d.	n.d.
Antheraxanthin	0.20 ± 0.05	0.42 ± 0.04	n.d.	n.d.
Violaxanthin	4.13 ± 0.38	4.86 ± 0.97	4.34 ± 0.62	5.27 ± 0.60
Neoxanthin+Loroxanthin	9.25 ± 0.80	6.79 ± 0.61	9.22 ± 0.92	8.71 ± 0.94
Lutein	8.26 ± 0.70	9.05 ± 1.58	9.91 ± 1.05	9.27 ± 0.72
Total xanthophylls	21.84	21.85	23.47	23.25
Total xanthophylls/β-Carotene	4.90	5.52	3.62	4.54
(Z+A)/V	0.05	0.11	0	0

Tab. 4: Car content in *C. reinhardtii* wt and transformed cells grown in LL conditions after 4 and 31 days. Car are normalized per 100 chl (n = 3 ± s.d.).

	HL 4 days		HL 31 days	
Car content	**wt**	**B3**	**wt**	**B3**
Total Car	26.80 ± 0.47	28.39 ±4.06	39.19 ± 2.30	31.67 ± 2.06
β-Carotene	2.55 ± 0.98	5.15 ± 1.22	8.08 ± 0.,72	5.99 ± 0.32
Zeaxanthin	n.d.	0.36 ± 0.12	0.25 ± 0.08	1.53 ± 0.65
Antheraxanthin	0.13 ± 0.02	0.58 ± 0.07	0.35 ± 0.01	1.29 ± 0.39
Violaxanthin	4.75 ± 0.40	5.79 ± 0.40	6.21 ± 0.70	4.14 ± 0.30
Neoxanthin+Loroxanthin	8.81 ± 0.55	4.35 ± 0.21	6.98 ± 1.04	4.42 ± 0.59
Lutein	10.56 ± 0.94	12.16 ± 0.73	17.41 ± 1.78	14.4 ± 1.77
Total xanthophylls	24.25	23.24	31.2	25.78
Total xanthophylls/β-Carotene	9.51	4.51	3.86	4.30
(Z+A)/V	0.03	0.16	0.10	0.68

Tab. 5: Car content in *C. reinhardtii* wt and transformed cells grown in HL conditions after 4 and 31 days. Car are normalized per 100 Chl (n = 3 ± s.d.).

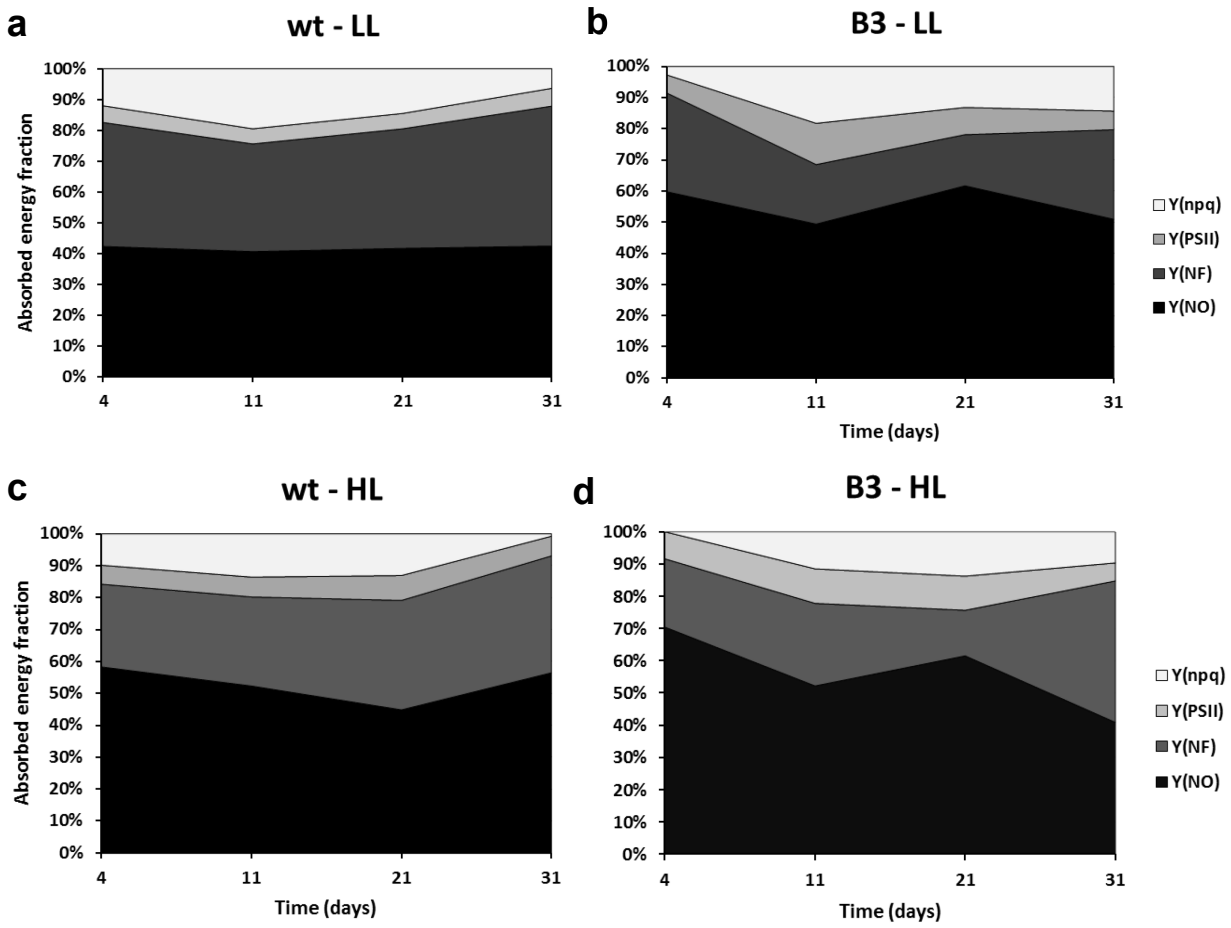

Fig. 8: estimated fraction of the absorbed irradiance 1200 $\mu mol_{photons} m^{-2} s^{-1}$ partitioned in photochemistry [as yield of PSII; Y(PSII)] and in quantum yield of all dissipative processes, such as yield of non-photochemical quenching [Y(npq)], fraction of energy which is constitutively dissipated in form of heat and fluorescence by closed PSII [Y(NO)] and quantum yield of thermal dissipation in inactive PSII [Y(NF)] in *C. reinhardtii* wt and B3 cells grown under LL and HL conditions.

Concluding remarks

During the last few years an increased number of Laboratories have started to develop researches in which microalgae are involved as source of biomass to be exploited for biofuel production (Brennan and Owende, 2010; Mata et al., 2010; Leonardi et al., 2011; Singh et al., 2011; Smith et al., 2010). In this Thesis, research was aimed at increasing the knowledge of microalgal physiology, in order to obtain new useful information for the improvement of culture performance in the perspective of large-scale cultivation (Scott et al., 2010; Wijffels and Barbosa, 2010). In detail, it has been demonstrated that mixotrophy can be considered the best cultivation system for increasing the biomass concentration in the promising microalga *N. oleoabundans*. Several additional advantages in mixotrophic cultivation can be considered, such as the lipid accumulation when cells enter the stationary phase, the possibility of using waste products as organic carbon source and the reduced risks of contamination, which nearly unavoidably mine the success of heterotrophic cultivation (Scott et al., 2010; Chen et al., 2011). With the perspective of transferring the microalgal cultivation process on the large scale, the Laboratory of Plant Cytophysiology (University of Ferrara, Italy, Supervisor: Prof. Simonetta Pancaldi) is now optimising the cultivation of *N. oleoabundans* in two tubular photobioreactors of 20 and 100 L of capacity, respectively.

This Thesis provides also advanced insights in the organization of the thylakoid protein complexes which characterize the photosynthetic membranes when *N. oleoabundans* is grown mixotrophically. Indeed, very little is known about this topic, but investigation in mechanisms which regulate photosynthetic light reactions and carbohydrate metabolisms might be useful for the scaling up of mixotrophic microalgal cultivation, for instance to plan the most fruitful type of illumination.

Finally, it has been demonstrated that molecular engineering, together with detailed physiological studies, can be considered a useful tool which can be targeted to different metabolic pathways of microalgae, such as that leading to neutral lipid accumulation. This might offer the possibility to obtain a more complete picture of this complex metabolic pathway and to allow the overproduction of lipids for biofuel purpose inside microalgal cells.

References

Aaronson S., Berner T., Dubinsky Z. (1980) Microalgae as a source of chemicals and natural products. In "Algal Biomass" (ed. by Shelef G. and Soeder C.J.). Elsevier/North Holland Biomedical Press, pp. 575-601

Aaronson S., Dubinsky Z. (1982) Mass production of microalgae. Experientia 38: 36-40

Agrawal S.C., Singh V. (2001) Viability of dried cells, and survivability and reproduction under water stress, low light, heat, and UV exposure in *Chlorella vulgaris*. Israel Journal of Plant Sciences 1: 27-32

Akazawa K., Okamoto K. (1980) Biosynthesis of sucrose. In "The Biochemistry of plants: a comprehensive treatise" (ed. by Preiss J,.). Academic, New York, vol. 3, pp 199–218

Alfonso M., Montoya G., Cases R., Rodriguez R., Picorel R. (1994) Core antenna complexes, CP43 and CP47, of higher plant photosystem II. Spectral properties, pigment stoichiometry, and amino acid composition. Biochemistry 33: 10494-10500

Allahverdiyeva Y., Mamedov F., Mäenpää P., Vass I., Aro E.M. (2005) Modulation of photosynthetic electron transport in the absence of terminal electron acceptors: Characterization of the *rbcL* deletion mutant of tobacco. Biochimica and Biophysica Acta 1709: 69-83

Allahverdiyeva Y., Mamedov F., Suorsa M., Styring S., Vass I., Aro E. M. (2007) Insights into the function of PsbR protein in *Arabidopsis thaliana*. Biochimica and Biophysica Acta 1767: 677- 685

Allahverdiyeva Y., Aro E.M. (2012) Photosynthetic responses of plants to excess light mechanisms and condition for photoinhibition, excess energy dissipation and repair. In "Photosynhtesis: plastid biology, energy conversion and carbon assimilation. Advances in photosynthesis and respiration" (ed by Eaton-Rye J.J., Tripathy B.C. and Sharkey T.D.). Springer, Netherlands 34: 275-297

Allen J.F., Horton P. (1981) Chloroplast protein phosphorylation and chlorophyll fluorescence quenching. Activation by tetramethyl-p-hydroquinone, an electron donor to plastoquinone. Biochimica et Biophysica Acta - Bioenergetics 638: 290-295

Allen J.F., Forsberg J. (2001) Molecular recognition in thylakoid structure and function. Trends in Plant Science 6: 317-326

Allen J.F., Martin W. (2007) Evolutionary biology - Out of thin air. Nature 445: 610-612

Anderson J.M., Chow W.S., Park Y.I. (1995) The grand design of photosynthesis: Acclimation of the photosynthetic apparatus to environmental cues. Photosynthesis Research 46: 129-139

Andrade M.R., Costa J.A.V. (2007) Mixotrophic cultivation of microalga *Spirulina platensis* using molasses as organic substrate. Aquaculture 264:130-134

Aro E.M., Suorsa M., Rokka A., Allahverdiyeva Y., Paakkarinen V., Saleem A., Battchikova N., Rintamäki E. (2005) Dynamics of photosystem II: a proteomic approach to thylakoid protein complexes.Journal of Experimental Botany 56: 347–356

Arredondo-Vega B.O., Band-Schmidt C.J., Vazquez-Duhalt R. (1995) Biochemical composition of *Neochloris oleoabundans* adapted to marine medium. Cytobios 83: 201–205

Badger M.R., Spalding M.H. (2000) CO_2 acquisition, concentration and fixation in cyanobacteria and algae. In "Photosynthesis: Physiology and Metabolism" (ed. by Leegood R.C., Sharkey T.D., von Caemmerer S.). Kluwer Academic Publishers, Dordrecht, The Netherlands, pp. 369-397

Baena-González E., Aro E.M. (2002) Biogenesis, assembly and turnover of photosystem II units. Philos Trans R. Soc. Lond. B. Biol. Sci. 357: 1451-1459

Bahtnagar A., Chinnasamy S., Singh M., Das K.C. (2011) Renewable biomass production by mixotrophic algae in the presence of various carbon sources and wastewaters. Applied Energy 88: 3425-3431

Baker, N.R. (2008). Chlorophyll fluorescence. A probe of photosynthesis in vivo.Annual Review of Plant Biology 59: 89–113

Baldisserotto C., Ferroni L., Moro I., Fasulo M.P., Pancaldi S. (2004) Modulations of the thylakoid system in snow xanthophycean alga cultured in the dark for two months: comparison between microspectrofluorimetric responses and morphological aspects. Protoplasma, 226: 125-135

Baldisserotto C., Ferroni L., Giovanardi M., Pantaleoni L., Boccaletti L., Pancaldi S. (2012) Salinity promotes growth of freshwater *Neochloris oleoabindans* UTEX 1185 (Sphaeropleales, Neochloridaceae): morpho-physiological aspects. Phycologia 51: 700-710

Band C.J., Arredondo-Vega B.O., Vazquez-Duhalt R., Greppin H. (1992) Effect of a salt-osmotic upshock on the edaphic microalga *Neochloris Oleoabundans*. Plant Cell and Environment 15: 129-133

Barber J. (2002) Photosystem II: a multisubunit membrane protein that oxidises water. Current Opinion in Structural Biology 12: 523-530

Baroli I., Do A.D., Yamane T., Nyogi K. (2003) Zeaxanthin accumulation in the absence of a functional xanthophyll cycle protects *Chlamydomonas reinhardtii* from photooxidative stress. The Plant Cell 15: 992-1008

Bassi R., Pineau B., Dainese P., Marquardt J. (1993) Carotenoid-binding proteins of photosystem-II. European Journal of Biochemistry 212: 297-303

Baumgarten E., Nagel M., Tishner L. (1999) Reduction of the nitrogen and carbon content in swine waste with algae and bacteria. Applied microbiology and biotechnology 52:281-284

Becker E.W. (1988) Micro-algae for human and animal consumption. In "Micro-algal biotechnology" (ed by M.A.Borowitzka and L.J. Borowitzka) Cambridge University Press, Cambridge, pp 222-256

Bennett J. (1980) Chloroplast phosphoproteins. Evidence for a thylakoid-bound phosphoprotein phosphatase. European Journal of Biochemistry 104: 85-89

Bennett,J. (1991) Protein phosphorylation in green plant chloroplasts. Annual Review of Plant Physiology 42: 281-311

Ben-Shem A., Frolow F., Nelson N. (2003) Crystal structure of plant photosystem I. Nature (London) 426: 630-635

Berges J.A., Charlebois D.O., Mauzerall D.C., Falkowski P.G. (1996) Differential Effects of Nitrogen Limitation on Photosynthetic Efficiency of Photosystems I and II in Microalgae. Plant Physiology 110: 689-696

Berthold P., Schmitt R., Mages W. (2002) An engineered *Streptomyces hygroscopicus aph 7''* gene mediates dominant resistance against Hygromycin B in *Chlamydomonas reinhardtii*

Bold H.C. (1949) The morphology of *Chlamydomonas chlamydogama* sp. nov. Bulletin of the Torrey Botanical Club 76: 101-108

Borowitzka M.A., Borowitzka L.J. (1988) *Dunaliella*. In: "Micro-algal biotechnology" (ed. by Borowitzka M.A. & Borowitzka, L.J.) Cambridge University Press, Cambridge, pp. 27-58

Boussiba S., Vonshak A., Cohen Z., Avissar I., Richmond A. (1987) Lipid and biomass production from the halotolerant microalga *Nannochloropsis salina.* Biomass 12:37-47

Boussiba S., Vonshak A. (1991) Astaxanthin accumulation in the green alga *Haematococcus pluvialis*. Plant Physiology 3: 1077-82

Brennan L., Owende P. (2010) Biofuels from microalgae - A review of technologies for production, processing, and extractions of biofuels and co-products. Renewable and Sustainable Energy Reviews 14: 557–577

Casper-Lindley C., Björkman O. (2008) Fluorescence quenching in four unicellular algae with different light-harvesting and xanthophyll-cycle pigments. Photosynhtesis Research 56: 277-289

Chantanachat S., Bold H.C. (1962) Phycological studies. II. Some algae from arid soils. university of texas publications 6218: 1-74

Chen F. (1996) High cell density culture of microalgae in heterotrophic growth. Trends in Biotechnology, 14: 421-6

Chen F., Wen Z. (2003) Heterotrophic production of eicosapentaenoic acid by microalgae. Biotechnology Advances 21: 273-294

Chen C.Y., Yeh K.L., Aisyah R., Lee D.J., Chang J.S. (2011) Cultivation, photobioreactor design and harvesting of microalgae for biodiesel production: A critical review. Bioresource Technology 102: 71-81

Chow W.S., Melis A., Anderson J.M. (1990) Adjustments of photosystem stoichiometry in chloroplasts improve the quantum efficiency of photosynthesis. Proc. Nat. Acad. Sci. USA 87: 7502-7506

Certik M., Shimizu S. (1999) Biosynthesis and regulation of microbial polyunsaturated fatty acid production. Journal of Bioscience and Bioengineering 87: 1-14

Cheung Y.H., Wong M.H. (1981) Properties of animal manures and sewage sludges and their utilisation for algal growth. Agricultural Wastes 3: 109-122

Chisti Y. (2007) Biodiesel from microalgae. Biotechnology Advances 25: 294-306

Cordero B.F., Couso I., León R., Rodríguez H., Vargas M.Á. (2011) Enhancement of carotenoids biosynthesis in *Chlamydomonas reinhardtii* by nuclear transformation using a phytoene synthase gene isolated from *Chlorella zofingiensis*. Applied Microbiology and Biotechnology 91: 341-351

Couso I., Vila M., Rodriguez H., Vargas M.A., León R. (2011) Overexpression of an exogenous phytoene synhtase gene in the unicellular alga *Chlamydomonas reinhardtii* leads to an increase in the content of carotenoids. Biotechnology Progress 27: 54-60

Dall'Osto L., Lico C., Alric J., Giuliano G., Havaux M., Bassi R. (2006) Lutein is needed for efficient chlorophyll triplet quenching in the major LHCII antenna complex of higher plants and effective photoprotection *in vivo* under strong light. BMC Plant Biology 6: 32

Damiani M.C., Popovich C.A., Costenla D., Leonardi P.I. (2010) Lipid analysis in *Haematococcus pluvialis* to assess its potential use as a biodiesel feedstock. Bioresource Technology 101: 3801-3807

Danielsson R., Suorsa M., Paakkarinen V., Alpertsson P.Å, Styring S., Aro E.M., Mamedov F. (2006) Dimeric and monomeric organisation of photosystem II. Journal of Biological Chemistry 281: 14241-14249

Das P., Aziz S.S., Obbard J.P. (2011) Two-phase microalgae growth in the open system for enhanced lipid productivity. Renewable Energy 36: 2524-2528

Davis R.W., Volponi J.V., Jones H.D.T., Carvalho B.J., Wu H., Singh S. (2012) Multiplex fluorometric assessment of nutrient limitation as a strategy for enhanced lipid enrichment and harvesting of *Neochloris oleoabundans*. Biotechnology and Bioengineering 109: 2503-2512

De Swaff M.E., de Rijk T.C., Eggink G., Sijtsma L. (1999) Optimisation of docosahexanoic acid production in batch cultivation by *Crypthecodinium cohnii*. Progress in Industrial Microbiology 35: 185-192

De Wilde C., Van Houdt H., De Buck S., Angenon G., De Jaeger G., Depicker A. (2000) Plants as bioreactors for protein production: avoiding the problem of transgene silencing. Plant Molecular Biology 43: 347-359

Dekker J.P., Boekema E.J. (2005) Supramolecular organisation of thylakoid membranes proteins in green plants. Biochimica and Biophysica Acta 1706: 12-39

Del Campo J.A., Moreno J., Rodríguez H., Vargas M.A., Rivas J., Guerrero M.G. (2000) Carotenoid content of Chlorophycean microalgae: factors determining lutein accumulation in *Muriellopsis* sp. (Chlorophyta). Journal of Biotechnology 76:51-59

Del Campo J.A., García-González M., Guerrero M.G. (2007) Outdoor cultivation of microalgae for carotenoid production: current state and perspective. Applied Microbiology and Biotechnology 74: 1163-1174

Demirbas A., Demirbas M.F. (2011) Importance of algae oil as a source of biodiesel. Energy Conversion and Management 52: 163-170

Demmig-Adams B. (1990) Carotenoids and photoprotection in plants: a role for the xanthophyll zeaxanthin. Biochimica and Biophysica Acta 1020: 1-24

Demmig-Adams B. (1998) Survey of thermal energy dissipation and pigment composition in sun and shade leaves. Plant and Cell Physiology 39: 474-482

Depka B., Jahns P., Trebst A. (1998) β-Carotene to zeaxanthin conversion in the rapid turnover of the D1 protein of photosystem II. FEBS Letters 424: 267-270

Devereux R., Loeblich A.R., Fox G.E. (1990) Higher plants origins and the phylogeny of green algae. Journal of Molecular Evolution 31: 18-24

Dijkstra A.J. (2006) Revisiting the formation of trans isomers during partial hydrogenation of triacylglycerol oils. European Journal of Lipid Science and Technology 108: 249-264

Dodge J.D. (1973) The fine structure of algal cells. Academic Press London and New York, 116

van Donk E., Lurling M., Hessen D.O., Lokhorst G.M. (1997) Altered cell wall morphology in nutrient-deficient phytoplankton and its impact on grazer. American Society of Limnology and Oceanography 42: 357-364

Döös B.L. (2002) Population growth and loss of arable lands. Global Environmental Change 12:303-311

van Dorssen R.J., Breton J., Plijter J.J., Satoh K., van Gorkom H.J., Amesz J. (1987) Spectroscopic properties of the reaction centre and of the 47kDa chlorophyll protein of photosystem II. Biochimica and Biophysica Acta 893: 267-274

Dote Y., Sawayama S., Inoue S., Minowa T., Yokoyama S-y (1994) Recovery of liquid fuel from hydrocarbon-rich microalgae by thermochemical liquefaction. Fuel 73: 1855-1857

Ducreux J.M., Morris W.L., Hedley P.E., Sheperd T., Davies H.V., Millan S., Taylor M.A. (2005) Metabolic engineering of high carotenoids potato tubers containing enhanced levels of β-carotene and lutein. Journal of Experimental Botany 56: 81-89

Durnford D.G., Price J.A., McKim S.M., Sarchfield M.L. (2002) Light-harvesting complex gene expression is controlled by both transcriptional and post-transcriptional mechanisms during photoacclimation in *Chlamydomonas reinhardtii*. Physiologia Plantarum 118: 193-205

Eubel H., Braun H.P., Millar A.H. (2005) Blue-native PAGE in plants: a tool in analysis of protein-protein interactions. Plant Methods 1:11

Falkowski P.G., Raven J.A. (1997) Aquatic photosynthesis. Blackwell

Färber A., Jahns P. (1998) The xanthophyll cycle of higher plants: influence of antenna size and membrane organization. Biochimica and Biophysica Acta 1363: 47-58

Ferroni L., Baldisserotto C., Fasulo M.P., Pagnoni A., Pancaldi S. (2004) Adaptive modifications of the photosynhtetic apparatus in *Euglena gracilis* Klebs exposed to maganese excess. Protoplasma 224: 167-177

Ferroni L., Baldisserotto C., Pantaleoni L., Billi P., Fasulo M.P:, Pancaldi S. (2007) High salinity alters chloroplast morpho-physiology in a freshwater *Kirchneriella* species (*Selenastraceae*) from Ethiopian Lake Awasa. American Journal of Botany, 94: 1973–1983.

Ferroni L., Baldisserotto C., Pantaleoni L., Fasulo M.P:, Fagioli P., Pancaldi S. (2009) Degreening of the unicellular alga *Euglena gracilis*: thylakoid composition, room temperature fluorescence spectra and chloroplast morphology. Plant Biology 11: 631-641

Ferroni L., Baldosserotto C., Giovanardi M., Pantaleoni L., Morosinotto T., Pancaldi S. (2011) Revised assignment of room-temperature chlorophyll fluorescence emission bands in single living cells of *Chlamydomonas reinhardtii*. Journal of Bioenergy and Biomembranes 43: 163-173

Finazzi G., Furia A., Barbagallo R.P., Forti G. (1999) State transitions, cyclic and linear electron transport and photophosporylation in *Chlamydomonas reinhardtii*. Biochimica and Biophysica Acta 1413: 117-129

Fisher R., Liao Y.C., Hoffmann K., Schillberg S., Ermans N. (1999) Molecular farming of recombinant antibodies in plants. Biological Chemistry 380: 825-839

Francisco E.F., Neves D.B., Jacob-Lopes E., Franco T.T. (2010) Microalgae as feedstock for biodiesel production: Carbon dioxide sequestration, lipid production and biofuel quality. Journal of Chemistry, Technology and Biotechnology 85: 395-403

Franck F., Dewez D., Popovic R. (2005) Changes in the Room-temperature Emission Spectrum of Chlorophyll During Fast and Slow Phases of the Kautsky Effect in Intact Leaves. Photochemistry and Photobiology 81: 431-436

Fraser P.D., Römer S., Shipton C.A., Mills P.B., Kiano J.W., Misawa N., Drake R.G., Schuch W., Bramley P.M. (2002) Evaluation of transgenic tomato plants expressing an additional phytoene synthase in a fruit specific-manner. Proc. Nat. Acad. Sci. USA 99: 1092-1097

Fray R.G., Wallace A., Fraser P.D., Valero D., Hedden P., Bramley P.M., Grierson D. (1995) Constitutive expression of a fruit phytoene synthase gene in transgenic tomatoes causes dwarfism by redirecting metabolites from the gibberellin pathway. The Plant Journal 8: 693-701

Frenkel M., Bellafiore S., Rochaix J., Jansson S. (2007) Hierarchy amongst photosynthetic acclimation responses for plant fitness. Physiologia Plantarum 129: 455-459

Fujita Y., Iwama Y., Ohki K., Murakami A., Hagiwara N. (1989) Regulation of the size of light-harvesting antennae in response to light intensity in the green alga *Chlorella pyrenoidosa*. Plant and Cell Physiology 30: 1029-1037

Gaffron H., Rubin J. (1942) Fermentative and photochemical production of hydrogen in algae. The Journal of General Physiology 20: 219-240

Gao C., Zhai Y., Ding Y., Wu Q. (2010) Application of sweet sorghum for biodiesel production by heterotrophic microalga *Chlorella protothecoides*. Applied Energy 87: 756-761

García M.C.C., Camacho F.G., Mirón A.S., Sevilla J.M.F., Chisti Y., Grima E.M. (2006) Mixotrophic production of marine microalga *Phaeodactylum tricornutum* on various carbon sources. Journal of Microbiology and Biotechnology 16: 689-694

Geider R.J., La Roche J., Greene R.M., Olaizola M. (1993) Response of the photosynthetic apparatus of *Phaeodactylum tricornutum* (Bacillariophyceae) to nitrate, phosphate, or iron starvation. Journal of Phycology 29:755–66

Geider R.J., MacIntyre H.L., Graziano L.M., McKay R.M.L. (1998) Responses of the photosynthetic apparatus of *Dunaliella tertiolecta* (Chlorophyceae) to nitrogen and phosphorus limitation. European Journal of Phycology 33: 315-32

Geider R.J., MacIntyre H.L. (2002) Physiology and Biochemistry of photosynthesis and algal carbon acquisition. In "phytoplankton productivity and carbon assimilation in marine and freshwater ecosystems (ed. by Williams P.J.Leb, Thomas D.R. and Reynolds C.S.) Blackwell Science, London

Genty B., Briantais J.M:, Baker N.R. (1989) The relationship between the quantum yield of photosynthetic electron transport and quenching of chlorophyll fluorescence. Biochimica and Biophysica Acta 990: 87-92

Ghirardi M.L., Zhang J.P., Lee J.W., Flynn T., Seibert M., Greenbaum E., Melis A. (2000) Microalgae: a green source of renewable H2. Trends in Biotechnology 18: 506-511

Gill I., Valivety R. (1997) Polyunsaturated fatty acids, part 1: occurrence, biological activities and applications. Trends in biotechnology 15:401-409

Gilmore A.M., Yamamoto H.Y. (1993) Linear models relating xanthophylls and lumen acidity to non-photochemical fluorescence quenching: evidence that antheraxanthin explains zeaxanthin-independent quenching. Photosynthesis Research 35: 67–78

Giovanardi M., Ferroni L., Baldisserotto C., Tedeschi P., Maietti A., Pantaleoni L. & Pancaldi S. (2013) Morpho-physiological analyses of *Neochloris oleoabundans* (Chlorophyta) grown mixotrophically in a carbon-rich waste product. Protoplasma 250: 161-174

Goldschmidt-Clermont M., and Rahire M. (1986) Sequence, evolution and differential expression of the two genes encoding variant small subunits of ribulose bisphosphate carboxylase/oxygenase in *Chlamydomonas reinhardtii*. Journal of Molecular Biology 191: 421-432

Gouveia L., Marques A.E., Lopes da Silva T., Reis A. (2009) *Neochloris oleabundans* UTEX #1185: a suitable renewable lipid source for biofuel production. Journal of Industrial Microbiology and Biotechnology 36: 821-826

Grobbelaar J.U. (2004) The microalgal cell. In "Handbook of microalgal culture: Biotechnlogy and Applied Phycology" (ed. Amos Richmond).Oxford: Blackwell Pubblishing Ltd, pp. 97-115

Groot M.L., Frese R.N., de Weerd F.L., Bromek K., Pettersson A., Petermann E.J.G., van Stokkum I.H.M., van GrondelleR., Dekker J.P. (1999) Spectroscopic properties of the CP43 core antenna protein of photosystem II. Biophysical Journal 77: 3328-3340

Guerin M., Huntley M.E., Olaizola M. (2003) *Haematococcus* astaxanthin: applications for human health and nutrition. Trends in Biotechnology 21:210-216

Gushina I.A., Harwood J.L. (2006) Lipids and lipid metabolism in eukaryotic algae. Progress in Lipid Research 45:160-186

Harris E.H. (2001) *Chlamydomonas* as a model organism. Annual Review of Plant Physiology and Molecular Biology 52: 363-406

Harun R., Singh M., Forde G.M., Danquah M.K. (2010) Bioprocess engineering of microalgae to produce a variety of consumer products. Renewable and Sustainable Energy Reviews 14:1037-1047

Hauptmann R., Eschenfeldt W.H., English J., Brinkhaus F.L. (1997) Enhanced carotenoid accumulation in storage organs of genetically engineered plants. US Patent 5: 618-988

Havaux M., Kloppstech K. (2001) The protective functions of carotenoids and flavonoid pigments against excess visible radiation at chilling temperature investigated in *Arabidopsis npq* and *tt* mutants. Planta 213: 953-966

Heifetz P.B., Förster B., Osmond C.B., Giles L.J., Boynton J.E. (2000). Effects of acetate on facultative autotrophy in *Chlamydomonas reinhardtii* assessed by photosynthetic measurements and stable isotope analyses. Plant Physiology 122: 1439-1446

Hendrickson L., Furbank R.T., Chow W.S. (2004) A simple alternative approach to assessing the fate of absorbed light energy using chlorophyll fluorescence. Photosynthesis Research 82: 73-81

Hendrickson L., Förster B., Pogson B.J., Chow W.S. (2005) A simple chlorophyll fluorescence parameter that correlates with the rate coefficient of photoinactivation of Photosystem II. Photosynhtesis Research 84: 43-49

Heredia-Arroyo T., Wei W., Hu B. (2010) Oil accumulation via heterotrophic/mixotrophic *Chlorella prototecoides*. Applied Biochemistry and Biotechnology 162: 1978-1995

Heredia-Arroyo T., Wei W., Ruan R., Hu B. (2011) Mixotrophic cultivation of *Chlorella vulgaris* and its potential application for the oil accumulation from non-sugar materials. Biomass and Bioenergy 35: 2245-2253

Herzig R., Falkowski P.G. (1989) Nitrogen limitation in *Isochrysis galbana* (Haptophyceae). I. Photosynthetic energy conversion and growth efficiencies. Journal of Phycology 25:462–71

Hibino T., Lee B.H., Rai A.K.,Ishikawa H., Kajima H., Tawada M., Shimoyama H., Takebe T. (1996) Salt enhances photosystem I content and cyclic electron flow via NAD(P)H dehydrogenase in the halotolerant cyanobacterium *Aphanothece halophytica*. Australian Journal of Plant Physiology 23: 321-330

Hikosaka K., Kato M.C., Hirose T. (2004) Photosynthetic rates and partitioning of absorbed light energy in photoinhibited leaves. Physiologia Plantarum 121: 699-708

Hippler M., Klein J., Fink A., Allinger T., Hoerth P. (2001). Towards functional proteomics of membrane protein complexes: analysis of thylakoid membranes from *Chlamydomonas reinhardtii*. The Plant Journal 28: 595-606

Hirano A., Hon-Nami K., Kunito S., Hada M., Ogushi Y. (1998) Temperature effect on continuous gasification of microalgal biomass: theoretical yield of methanol production and its energy balance. Catalysis Today 45: 399-404

Horton P., Ruban A.V., Rees D., Pascal A.A., Noctor G., Young A.J. (1991) Control of the light-harvesting function of chloroplast membranes by aggregation of the LHCII chlorophyll-protein complex. Journal of Federation of European Biochemical Societies 292: 1-4

Horton P., Johnson M.P., Perez-Bueno M.L., Kiss A.Z., Ruban A.V. (2008) Photosynthetic acclimation: does the dynamic structure and macro-organisation of photosystem II in higher plant grana membranes regulate light harvesting states? Journal of Federation of European Biochemical Societies 275: 1069-1079

Hosikian A., Lim S., Halim R.,Danquah M.K. (2010) Chlorophyll extraction from microalgae: A review on the process engineering aspects. International Journal of Chemical Engineering 1: 11

Hu Q., Sommerfeld M., Jarvis E., Ghirardi M., Posewitz M., Seibert M., Darzins A. (2008): Microalgal triacylglycerol as feedstocks for biofuel production: perspective and advances. The Plant Journal, 54: 621-639

Ip P.F., Wong K.H., Chen F. (2004) Enhanced production of astaxanthin by the green microalga *Chlorella zofingiensis* in mixotrophic culture. Process Biochemistry 39: 1761-1776

Iwai M., Takahashi Y., Minagawa J. (2008) Molecular remodeling of photosystem II during state

transitions in *Chlamydomonas reinhardtii*. The Plant Cell 20: 2177-2189

Iyovo G.D., Du G., Chen J. (2010) Poultry manure digestate enhancement of *Chlorella vulgaris* biomass under mixotrophic condition for biofuel production. Journal of Microbial and Biochemical Technology 2:51-57

Jahns P., Holzwarth A.R. (2012) The role of the xanthophyll cycle and of lutein in photoprotection of photosystem II. Biochimica and Biophysica Acta 1817: 182-193

Jang E.S., Jung M.Y., Min D.B. (2005) Hydrogenation for low trans and high conjugated fatty acids. Comprehensive reviews in Food Science and Food Safety 4: 22-30

Järvi S., Suorsa M., Paakkarinen V., Aro E.M. (2011) Optimized native gel system for separation of thylakoid protein complexes: novel super- and mega- complexes. Biochemical Journal 439: 207-214

Jin E., Polle J.E., Lee H.K., Hyun S.M., Chang M. (2003) Xanthophylls in microalgae: from biosynthesis to biotechnological mass production and application. Journal of Microbiology and Biotechnology 13: 165-174

Joliot A. and Joliot P. (1964) Etude Cinétique de la reaction photochimique libérant l'oxigène au cours de photosynhtèse. Comptes rendus de l'Académie des Sciences 258: 4622-4625

Kang R, Wang J, Shi D, Cong W, Cai Z, Ouyang F (2004) Interactions between organic and inorganic carbon sources during mixotrophic cultivation of *Synechococcus* sp. Biotechnology Letters 26: 1429-1432

Karimi M., Inzé D., Depicker A. (2002) GATEWAY vectors for *Agrobacterium*-mediated plant transformation. Trends in Plant Science 7*:* 193-195

Keranen M., Aro E.M., Tyystjarvi E. (1999) Excitation-emission map as a tool in studies of photosynthetic pigment-protein complexes. Photosynthetica 37: 225-237

Kindle K. (1990) High-frequency nuclear transformation of *Chlamydomonas reinhardtii*. Proc Natl Acad Sci USA 87: 1228-1232

Klughammer C., Shreiber U. (2008) Complementary PSII quantum yields calculated from simple fluorescence parameters measured by PAM fluorimetry and the Saturation Pulse methods. PAM Application Notes 1: 27-35

Knothe G. (2006) Analyzing biodiesel: standards and other methods. Journal of the American Oil Chemists' Society 83: 823-833

Knothe G. (2008) “Designer” biodiesel: optimizing fatty ester composition to improve fuels properties. Energy Fuel 22: 1358-1364

Kováks L., Wiessner W., Kis M., Nagy F., Mende D., Demeter S. (2000) Short- and long-term redox regulation of photosynthetic light energy distribution and photosystem stoichiometry by acetate metabolism in the green alga, *Chlamydobotrys stellata*. Photosynthesis Research 65: 231-247

Kobayashi M., Kakizono T., Yamaguchi K., Nishio N., Nagai S. (1992) Growth and astaxanthin formation of *Haematococcus pluvialis* in heterotrophic and mixotrophic conditions. Journal of Fermentation and Bioengineering 74: 17-20

Krause G.H., Weiss E. (1984) Chlorophyll fluorescence as a tool in plant physiology. II. Interpretation of the fluorescence signals. Photosynthesis Research 5: 1139-157

Kromkamp J., Peene J. (1999) Estimation of phytoplankton photosynthesis and nutrient limitation in the Eastern Scheldt estuary using variable fluorescence. Aquatic Ecology 33: 101-104

Kruse O., Hankamer B., Konczak C., Gerle C., Morris E., Radunz A., Schmid G.H., Barber J. (2000) Phosphatidylglycerol is involved in the dimerization of photosystem II. The Journal of Biological Chemistry 275: 6509-6514

Kruse O., Rupprecht J., Mussgnug J.H., Dismukes G.C., Hankamer B. (2005) Photosynthesis: a blueprint for solar energy capture and biohydrogen production technologies. Journal of Photochemical and Photobiological Sciences 4: 957-70

Kügler M., Jänsch L., Kruft V., Schmitz U.K., Braun H.P. (1997) Analysis of the chloroplast protein complexes by blue-native polyacrylamide gel electrophoresis (BN-PAGE). Photosynthesis Research 53: 35-44

Kurisu G., Zahng H., Smith J.L., Cramer W.A. (2003) Structure of the cytochrome b6f complex of oxigenic photosynthesis: tuning the cavity. Science 302: 1009-1014

Laemmli U. (1970) Cleavage of structural proteins during the assembly of the head of bacteriophage T4. Nature 227: 680-685

Lalucat J., Imperial J., Pares R. (1984) Utilization of light for the assimilation of organic matter in *Chlorella* sp. VJ79. Biotechnology and Bioengineering 26: 677-681

Lambrev P.H., Nilkens M., Miloslavina Y., Jahns J., Holzwarth A.R. (2010) Kinetic and spectral resolution of multiple nonphotochemical quenching components in *Arabidopsis* leaves. Plant Physiology 152: 1611-1624

Lee Y (2001) Microalgal mass culture systems and methods: their limitation and potential. Journal of Applied Phycology 13: 307-315

Lee A.I., Thornber J.P. (1995) Analysis of the pigment stoichiometry of pigment-protein complexes from barley *(Hordeum vufgaue).*The xanthophyll cycle intermediates occur mainly in the light harvesting complexes of photosystem I and photosystem II**.** Plant Physiology 107: 565-574

León-Bañares R., González-Ballester D., Galván A., Fernández E. (2004) Transgenic microalgae as green cell-factories. Trends in Biotechnology 22: 45-52

León R., Couso I., Fernández E. (2007) Metabolic engineering of ketocarotenoids biosynthesis in the unicellular microalga *Chlamydomonas reinhardtii*. Journal of Biotechnology 130: 143-152

Leonardi P.I., Popovich C.A., Damiani M.C. (2011) Feedstocks for second-generation biodiesel: microalgae's biology and oil composition. In "Economic Effects of Biofuel Production" (ed. by Dos Santos Bernardes M.A.). Published under CC BY-NC-SA 3.0 licence, pp. 317-346

Levine R.B., Costanza-Robinson M.S., Spatafora G.A. (2011) *Neochloris oleoabundans* grown on anaerobically digested dairy manure for concomitant nutrient removal and biodiesel feedstock production. Biomass and Bioenergy 35: 40-49

Li X., Xu H., Wu Q. (2007) Large-scale biodiesel production from microalga *Chlorella protothecoides* through heterotrophic cultivation in bioreactors. Biotechnology and Bioengineering 98: 764-771

Li Y., Horsman M., Wang B., Wu N., Lan C.Q. (2008a) Biofuels from microalgae. Biotechnology Progress 24: 815-820

Li Y., Horsman M., Wang B., Wu N., Lan C.Q. (2008b) Effect on nitrogen sources on cell growth and lipid accumulation of green alga *Neochloris oleoabundans*. Applied Microbiology and Biotechnology 81: 629-636

Li Y., Han D., Sommerfeld M., Hu Q. (2011) Photosynthetic carbon partitioning and lipid production in the oleaginous microalga *Pseudochlorococcum* sp. (Chlorophyceae) under nitrogen-limited conditions. Bioresource Technology 102: 123-129

Liang Y, Sarkany N, Cui Y (2009) Biomass and lipid productivities of *Chlorella vulgaris* under autotrophic, heterotrophic and mixotrophic growth conditions. Biotechnology Letters 31: 1043-1049

Lichtenthaler H.K., Buschmann C., Knapp M. (2005) How to correctly determine the different chlorophyll fluorescence parameters and the chlorophyll fluorescence decrease ratio R_{Fd} of leaves with the PAM fluorometer. Photosynthetica 43: 379-393

Lindgren L.O., Stalberg K.G., Höglund A.S. (2003) Seed-specific overexpression of an endogenous *Arabidopsis* phytoene synthase gene results in delayed germination and increased levels of carotenoids, chlorophyll, and abscissic acid. Plant Physiology 132: 779-785

Liu X., Duan S., Li A., Xu N., Cai Z., Hu Z. (2009a) Effects of organic carbon sources on growth, photosynhtesis, and respiration of *Phaeodactylum tricornutum.* Journal of Applied Phycology 21: 239-246

Liu G.N., Zhu Y.H., Jiang J.G. (2009b) The metabolomics of carotenoids in engineered cell factory. Applied Microbiology and Biotechnology 83: 989-999

Lopes da Silva T., Reis A., Medeiros R., Oliveira A.C., Gouveia L. (2009) Oil production towards biofuel from autotrophic microalgae semicontinuous cultivations monitorized by flow cytometry. Applied Biochemistry And Biotechnology 159: 568-578

Losciale P., Hendrickson L., Grappadelli L.C., Chow W.S. (2011) Quenching partitioning through light-modulated chlorophyll fluorescence: A quantitative analysis to assess the fate of the absorbed light in the field. Environmental and Experimental Botany 73: 73-79

Lowry O.H., Rosenbrough N.J., Farr A.L., Randall K.J. (1951). Protein measurement with the Folin phenol reagent. Journal of Biological Chemistry 193: 265-275

Mandal S., Mallick N: (2009) Microalga *Scenedesmus obliquus* as a potential source for biodiesel production. Applied Microbiology and Biotechnology 84: 281-291

Markou G., Georgakakis D. (2011) Cultivation of filamentous cyanobacteria (blue-green algae) in agro-industrial wastes and wastewaters: A rewiev. Applied Energy 88: 3389-3401

Marquez F.J., Sasaki K., Kakizono T., Nishio N., Nagai S. (1993) Growth characteristics of *Spirulina platensis* in mixotrophic and heterotrophic conditions. Journal of Fermentation and Bioengineering 5: 408-410

Marquez F.J., Nishio N., Nagai S., Sasaki K. (1995) Enhancement of biomass and pigment production during growth of *Spirulina platensis* mixotrophic culture. Journal of Chemical Technology and Biotechnology 62: 159-164

Martinez F., Orus M.I. (1991) Interactions between glucose and inorganic carbon metabolism in *Chlorella vulgaris* strain UAM101. Plant Physiology 95: 1150-1155

Martínez M.E., Sánchez S., Jiménez J.M., El Yousfy F., Muñoz L. (2000) Nitrogen and phosphorus removal from urban wastewaters by the microalga *Scenedesmus obliquus*. Bioresource Technology 73: 263-272

Mata T.M., Martins A.A., Caetano N.S. (2010) Microalgae for biodiesel production and other applications: A review. Renewable and Sustainable Energy Reviews 14: 217-232

Maxwell D.P., Falk S., Trik C.G., Huner N.P.A. (1994) Growth at low temperatures mimics high-light acclimation in *Chlorella vulgaris*. Plant Physiology 105: 535-543

Maxwell K., Johnson G.N. (2000) Chlorophyll fluorescence - a pratical guide. Journal of Experimental Botany 51: 659-668

McCarthy S.S., Kobayashi M.C., Niyogi K.K. (2004) White mutants of *Chlamydomonas reinhardtii* are defective in phytoene synthase. Genetics 168: 1249-1257

Melis A. (1999) Photosystem-II damage and repair cycle in chloroplasts: what modulates the rate of photodamage *in vivo*? Trends in Plant Sciences 4: 130-135

Melis A., Zhang L., Forestier M., Ghirardi M.L., Seibert M. (2000) Sustained photobiological hydrogen gas production upon reversible inactivation of oxygen evolution in the green alga *Chlamydomonas reinhardtii*. Plant Physiology 122: 127-136

Merzlyak M.N., Chivkunova O.B., Gorelova O.A., Reshetnikova I.V., Solovchenko A.E., Khozin-Goldberg I., Cohen Z. (2007) Effect of nitrogen starvation on optical properties, pigments, and arachidonic acid content of the unicellular green alga *Parietochloris incisa* (Trebouxiophyceae, Chlorophyta). Journal of Phycology 43: 833-843

Miao X., Wu Q.Y. (2004) High yield bio-oil production from fast pyrolysis by metabolic controlling of *Chlorella prototheco*ides. Journal of Biotechnology 110: 85-94

Miao X., Wu Q., Yang C. (2004)Fast pyrolysis of microalgae to produce renewable

Fuels. Journal of Analytical and Applied Pyrolysis 71: 855-863

Miao X., Wu Q. (2006) Biodiesel production from heterotrophic microalgal oil. Bioresource Technology 97: 841-846

Miller G.L. (1959) Modified DNS method for reducing sugars. Analytical Chemistry 31: 426-428

Minagawa J., Takahashi Y. (2004) Structure, function and assembly of Photosystem II and its light-harvesting proteins. Photosynthesis Research 82: 241-263

Minagawa J. (2009) Light-harvesting proteins. In: "*Chlamydomonas* sourcebook" (ed. by Stern D., Witman G.B., Harris E.H.). Elsevier, Amsterdam, pp 503-540

Miskiewicz E., Ivanov A.G., Williams J.P., Khan M.U., Falk S., Huner N.P.A. (2000) Photosynthetic acclimation of the filamentous cyanobacterium, *Plectonema boryanum* UTEX 485 to temperature and light. Plant Cell Physiology 41: 767-775

Müller P., Li X.P., Nyogi K.K. (2001) Non-photochemical quenching. A response to excess light energy. Plant Physiology 125: 1558-1566

Murakami A., Fujita Y (1993) Regulation of stoichiometry between PSI and PSII in response to light regime for photosynthesis observed with *Synechocystis* PCC6714: Relationship between redox state of Cyt b_6-f complex and regulation of PSI formation. Plant cell Physiology 34: 1175-1180

Murakami A., Kim S.J., Fujita Y. (1997) Changes in photosystem stoichiometry in response to environmental conditions for cell growth observed with the cyanophyte *Synechocystis* PCC6714. Plant Cell Physiology 38: 392-397

Murray M., Thompson W.F. (1980) Rapid isolation of molecular weight plant DNA. Nucleic Acid Research 8: 4321-5

Mussgnug J.H., Klassen V., Schluter A., Kruse O. (2010) Microalgae as substrates for fermentative biogas production in a combined biorefinery concept. Journal of Biotechnology 150: 51-56

Naik P.S., Chanemougasoundharam A., Paul Khurana S.M., Kalloo G. (2003) Genetic manipulation of carotenoid pathway in higher plants. Current Science 85: 1423-1430

Namikoshi M. (1996) Bioactive compounds produced by cyanobacteria. Journal of Internetianl Microbiology and biotechnology 17:373-384

Nelson N., Ben-Shem A. (2004) The complex architecture of oxigenic photosynthesis. Nature reviews Molecular cell biology 5: 971-982

Nelson N., Yocum C.F. (2006) Structure and Function of Photosystems I and II. Annual Review of Plant Biology 57: 521-565

Niyogi K.K. (1999) Photoprotection revisited: genetic and molecular approaches. Annual Review of Plant Physiology, Plant Molecular Biology 50: 333–359

Oesterhelt C., Schmalzlin E., Schmitt J.M., Lokstein H. (2007) Regulation of photosynthesis in the unicellular acidophilic red alga *Galdieria sulphuraria*. The Plant Journal 51: 500-511

Ogawa T, Aiba S (1981) Bioenergetic analysis of mixotrophic growth in *Chlorella vulgaris* and *Scenedesmus acutus*. Biotechnology and Bioengineering 23: 1121-132

Orosa M., Franqueira D., Chid A., Abalde J. (2001) Carotenoid accumulation in *Haematococcus pluvialis* in mixotrophic growth. Biotechnology Letters 23: 373-378

Pancaldi S., Baldisserotto C., Ferroni L., Bonora A. e Fasulo M.P. (2002): Room temperature microspectrofluorimetry as a useful tool for studying the assembly of the PSII chlorophyll-protein complexes in single living cells of etiolated *Euglena gracilis* Klebs during the greening process. Journal of Experimental Botany, 53: 1753-1763

Pancaldi S., Baldisserotto C., Ferroni L., Pantaleoni L. (2011) Fondamenti di Botanica generale. Ed. by McGraw-Hill, Milano (Italy).

Pantaleoni L., Ferroni L., Baldisserotto C., Aro E.M., Pancaldi S. (2009) Photosystem II organisation in chloroplasts of *Arum italicum* leaf depends on tissue location. Planta 230: 1019-1031

Peng L., Shimizu H., Shikanai T. (2008) The chloroplast NAD(P)H dehydrogenase complex interacts with photosystem I in *Arabidopsis*. Journal of Biological Chemistry 283: 34873-34879

Plaza M., Cifuentes A., Ibáñez E. (2008) In the search of new functional food ingredients from algae. Trends in Food Science & Technology 19: 31-39

Plumley F.G., Douglas S.E., Switzer A.B., Schmidt G.W. (1989) Nitrogen-dependent biogenesis of chlorophyll-protein complexes. In "Photosynthesis" (ed. by Briggs W.R.). . AR Liss, New York, USA, pp 311-329

Pohl P. (1982) Lipids and fatty acids in microalgae. In "Handbook of biosolar resource" (ed. by Zaborsky O.R.). CRC press, Boca Raton, USA, Vol 1, pp. 383-404

Popovich C.A., Damiani M.C., Constenla D., Martínez A.M., Giovanardi M., Pancaldi S., Leonardi P.I. (2012) *Neochloris oleoabundans* grown in natural enriched seawater for biodiesel feedstock: Evaluation of its growth and biochemical composition. Bioresource Technology 114: 287-293

Porra R.J., Thompson W.A., Kriedemann P.E. (1989) Determination of accurate extinction coefficients and simultaneous-equations for assaying chlorophyll-a and chlorophyll-b extracted with 4 different solvents: verification of the concentration of chlorophyll standards by atomic-absorption spectroscopy. Biochimica and Biophysica Acta 975: 384-394

Pruvost J., Van Vooren G., Cogne G., Legrand J. (2009) Investigation of biomass and lipids production with *Neochloris oleoabundans* in photobioreactor. Bioresource Technology 100: 5988-5995

Pruvost J., van Vooren G., Le Gouic B., Couzinet-Mossion A., Legrand J. (2011) Systematic investigation of biomass and lipid productivity by microalgae in photobioreactors for biodiesel application. Bioresource Technology 102: 150-158

Pulz O., Gross W. (2004) Valuable Products from biotechnology of microalgae. Applied Microbiology and Biotechnology 65: 635-648

Rees D., Noctor G., Ruban A.V., Crofts J., Young A., Horton P. (1992) pH-dependent chlorophyll fluorescence quenching in spinach thylakoids from light treated or dark adapted leaves. Photosynthesis Research 31: 11-19

Richmond A. (1990) Large scale microalgal culture and applications. In "Round" (ed. by Chapman M. and Chapman S.). Progress in Phycological Research 7, pp. 269-330. Biopress, Bristol

Rodolfi L., Chini Z.G., Bassi N., Padovani G., Biondi N., Bonini G., Tredici M.R. (2009) Microalgae for oil: strain selection, induction of lipid synthesis and outdoor mass cultivation in a low-cost photobioreactor. Biotechnology and Bioengeneering 102: 100-112

Rogers S.O., Bendich A.J. (1985) Extraction of DNA from milligram amounts of fresh, herbarium and mummified plant tissues. Plant Molecular Biology 5: 69-76

Rokka A., Suorsa M., Saleem A., Battchikova N., Aro E.M. (2005) Synthesis and assembly of thylakoid protein complexes: multiple assembly steps of photosystem II. Biochem Journal 388: 159-168

Ruban A.V., Young A.J., Pascal A.A., Horton P. (1994) The effects of illumination on the xanthophyll composition of the photosystem II light-harvesting complex of spinach thylakoid membranes. Plant Physiology 104: 227-234

Ruban A.V., Johnson M.P., Duffy C.D.P. (2012) The photoprotective molecular switch in the photosystem II antenna. Biochimica and Biophysica Acta 1817: 167-181

Rubio C.F., García Camacho F., Fernández Sevilla J.M., Chisti Y., Molina Grima E. (2003) A mechanistic model of photosynthesis in microalgae. Biotechnology and Bioengineering 81: 459-473

Ruxton C.H.S., Reed S.C., Simpson M.J.A., Millinghton K.J. (2004) The health benefits of omega-3 polyunsaturated fatty acids: a review of the evidence. Journal of Human nutrition and Dietetics 17:449-459

Sandmann G., Römer S., Fraser P.D. (2006) Understanding carotenoid metabolism as a necessity for genetic engineering of crop plants. Metabolic Engineering 8: 291-302

Satoh A., Kurano N., Senger H., Miyachi S. (2002) Regulation of energy balance in photosystems in response to changes in CO_2 concentrations and light intensities during growth in extremely-high CO_2-tolerant green microalgae. Plant and Cell Physiology 43: 440-451

Schneider U.A., Havlik P., Schmid E., Valin H., Mosnier A., Obersteiner M., Bottcher H., Skalsky´ R., Balkovič J., Sauer T., Fritz S. (2011) Impacts of population growth, economic development, and technical change on global food production and consumption. Agricultural Systems 104: 204-215

Schreiber U., Muller J.F., Haugg A., Gademann R. (2002). New type of dual-channel PAM chlorophyll fluorometer for highly sensitive water toxicity biotests. Photosynthesis Researches 74: 317-330

Scott S.A., Davey M.P., Dennis J.S., Horst I., Howe C.J., Lea-Smith D.J., Smith A.G. (2010) Biodiesel from algae: challenges and prospects. Current Opinion in Biotechnology 21: 277-286

Shenk P.M., Thomas-Hall S.R., Stephens E., Marx U.C., Mussgnug J.H., Posten C., Kruse O., Hankamer B. (2008) Second generation biofuels: high-efficiency microalgae for biodiesel production. Bioenergy Resources 1: 20-43

Shewmaker C.K., Sheehy J.A., Daley M., Colburn S., Ke D.E. (1999) Seed-specific overexpression of phytoene synthase: increase in carotenoids and other metabolic effects. The Plant Journal 20: 401-412

Shi X. M., Chen F. (1999): Production and rapid extraction of lutein and the other lipid-soluble pigments from *Chlorella protothecoides* grown under heterotrophic and mixotrophic conditions. Nahrung 43, 109-113.

Šiffel P., Braunová Z. (1999): Release and aggregation of the light harvesting complex in intact leaves subjected to strong CO2 deficit. Photosynthesis Research 61: 217-226

Simionato D., Sforza E., Corteggiani Carpinelli E., Bertucco A., Giacometti G.M., Morosinotto T. (2011) Acclimation of *Nannochloropsis gaditana* to different illumination regimes: Effects on lipids accumulation. Bioresource Technology 102: 6026-6032

Sirpio S., Allahverdiyeva Y., Hölmstrom M., Khrouchtchova A., Haldrup A., Battchikova N., Aro E.M. (2009) Novel nuclear-encoded subunits of the chloroplast NA(P)H dehydrogenase complex. Journal of Biological Chemistry 284: 905-912

Smith V.H., Sturm B.S.M., deNoyelles F.J., Billings S.A. (2009) The ecology of algal biodiesel production. Trends in Ecology and Evolution 25: 301-309

Sosik H. M., Mitchell B. G. (1991) Absorption, fluorescence, and quantum yield for growth in nitrogen-limited *Dunaliella tertiolecta*. American Society of Limnology and Oceanography 36: 910-21

Spolaore P., Joannis-Cassan C., Duran E., Isambert A. (2006) Commercial applications of microalgae. Journal of Bioscience and Bioengineering 101: 87-96

Steinbrenner J., Sandmann G. (2006) Transformation of the green alga *Haematococcus pluvialis* with a phytoene desaturase for accelerated astaxanthin biosynthesis. Applied and Evironmental Biotechnology 72: 7477-7484

Stephens E., Ross I.L., Mussgnug J.H., Wagner L.D., Borowitzka M.A., Posten C., Kruse O., Hankamer B. (2010) Future prospects of microalgal biofuel production systems. Trends in Plant Science 15: 554-564

Sun G., Zhang X., Sui Z., Mao Y. (2007) Inhibition of PDS gene expression via the RNA interference approach in *Dunaliella salina* (Chlorophyta). Marine Biotechnology 10: 219-226

Szabó I., Bergantino E., Giacometti G.M. (2009) Light and oxygenic photosynthesis: energy dissipation as a protection mechanism against photo-oxidation. European Molecular Biology Organisation 6: 629-634

Taiz L., Zeiger E. (2002): Fisiologia vegetale. Ed. Piccin, Padova, pp. 187-232

Takahashi T., Inoue-Kashino N., Ozawa S., Takahashi Y., Kashino Y., Satoh K. (2009) Photosystem II complex in vivo is a monomer. Journal of Biological Chemistry 284: 15598-15606

Tardy F., Havaux M. (1996) Photosynthesis, chlorophyll fluorescence, light-harvesting system and photoinhibition resistance of a zeaxanthin-accumulating mutant of *Arabidopsis thaliana*. Journal of Photochemistry and Photobiology B 34: 87–94

Tikkanen M., Grieco M., Kangasjiärvi S., Aro E.M. (2008) Thylakoid protein phosphorylation in higher plant chloroplasts optimizes electron transfer under fluctuating light. Plant Physiology 152: 723-735

Tommaselli L. (2004) The microalgal cell. In “Handbook of microalgal culture: Biotechnlogy and Applied Phycology” (ed. Amos Richmond). pp. 3-19

Tornabene T.G., Holzer G., Lien S., Burris N. (1983) Lipid composition of the nitrogen starved green alga *Neochloris oleoabundans*. Enzyme Microbiology and Technology 5: 435-440

Torres M.A., Barros M.P., Campos S.G., Pinto E., Rajamani S., Sayre R.T., Colepicolo P. (2008) Biochemical biomarkers in algae and marine pollution: a review. Ecoxitology and Environmental safety 71: 1-15

Tripodi G. (2006) Introduzione alla botanica sistematica (ed. EdiSES S.r.l)

Valverde F., Ortega J.M., Losada M., Serrano A. (1995) Sugar-mediated transcriptional regulation of the Gap gene system and concerted photosystem II functional modulation in the microalga *Scenedesmus vacuolatus*. Planta 221: 937-952

Vass I., Kirilovsky D., Etienne A.L. (1999) UV-B radiation-induced donor- and acceptor-side modifications of photosystem II in the cyanobacterium *Synechocystis* sp. PCC 6803, Biochemistry 39: 12786-12794.

Vass I., Turcsányi E., Touloupakis E., Ghanotakis D., Petrouleas V. (2002) The mechanism of UV-A radiation-induced inhibition of photosystem II electron transport studied by EPR and Chlorophyll Fluorescence. Biochemistry 41: 10200-10208

Vassiliev I.R., Kolber Z., Wyman K.D., Mauzerall D., Shukla V.K., Fallowsky P.G. (1995) Effects of iron limitation on photosystem II composition and light utilization in *Dunaliella tertiolecta*. Plant Physiology 109: 963-972

Verhoeven A.S., Adams W.W.I., Demmig-Adams B. (1996) Close relationship between the state of the xanthophyll cycle pigments and photosystem II efficiency during recovery from winter

stress. Physiologia Plantarum 9: 567-576

Vila M., Couso I., León R. (2007) Carotenoid content in mutants of the chlorophyte *Chlamydomonas reinhardtii* with low expression levels of phytoene desaturase. Process Biochemistry 43: 1147-1152

Vonshak A., Cheung S.M., Chen F. (2000) Mixotrophic growth modifies the response of *Spirulina* (*Arthrospira*) *platensis* (Cyanobacteria) cells to light. Journal of Phycology 36: 675-679

Walker T.L., Purton S., Becker D.G., Collet C. (2005) Microalgae as bioreactors. Plant Cell Reports 24: 629-641

Wan M., Liu P., Xia J., Rosenberg J.N., Oyler G.A., Betenbaugh M.J., Nie Z., Qiu G. (2011) The effect of mixotrophy on microalgal growth, lipid content, and expression levels of three pathway genes in *Chlorella sorokiniana*. Applied Microbiology and Biotechnology 91: 835-844

Wang L., Li Y., Chen P., Min M., Chen Y., Zhu J., Ruan R.R. (2010) Anaerobic digested dairy manure as a nutrient supplement for cultivation of oil-rich green microalgae *Chlorella* sp. Bioresource Technology 101: 2623-2628

Wang B., Lan C. (2011) Biomass production and nitrogen and phosphorus removal by the green alga *Neochloris oleoabundans* in simulated wastewater and secondary municipal wastewater effluent. Bioresource Technology 102: 5639-5644

Wellburn A.R. (1994) The spectral determination of Chlorophylls *a* and *b*, as well as total carotenoids, using various solvents with spectrophotometer of different resolution. Plant Physiology 144: 307-313

Welsh R., Wüst F., Bär C., Al-Babili S., Beyer P. (2008) A third phytoene synthase is devoted to abiotic stress-induced abscisic acid formation in rice and defines functional diversification of phytoene synthase genes. Plant Physiology 147: 367-380

White S., Anandraj A., Bux F. (2011) PAM fluorometry as a tool to assess microalgal nutrient stress and monitor cellular neutral lipids. Bioresource Technology 102: 1675-1682

Wijffels R.H., Barbosa M.J. (2010) An outlook on microalgal biofuels. Science 329: 796-799

Wu Q., Yin S., Sheng G., Fu J. (1994) New discoveries in study on liquid hydrocarbons from thermal degradation of heterotrophically yellowing algae. Science in China (B) 37: 326-335

Xiong W., Li X., Xiang J., Wu Q. (2008) High-density fermentation of microalga *Chlorella protothecoides* in bioreactor for microbio-diesel production. Applied Microbiology and Biotechnology 78: 29-36

Xu H., Miao X., Wu Q. (2006) High-quality biodiesel production from a microalga *Chlorella prototecoides* by heterotrophic growth in fermenters. Journal of Biotechnology 126: 499-507

Yamamoto, H.Y. (1979) Biochemistry of violaxanthin cycle in higher plants. Pure and Applied Chemistry 51: 639-648

Yamamoto H.Y. (1985). Xanthophyll cycles. Methods in Enzymology 110: 303-312

Yamane Y.I., Utsunomiya T., Watanabe M., Sasaki K. (2001) Biomass production in mixotrophic culture of *Euglena gracilis* under acidic condition and its growth energetics. Biotechnology Letters 23: 1223-1228

Yang C, Hua Q, Shimizu K (2000) Energetics and carbon metabolism during growth of microalgal cells under photoautotrophic, mixotrophic and cyclic light-autotrophic/dark-heterotrophic conditions. Biochemical Engineering Journal 6: 87-102

Yang Y., Xu J., Vail D., Weathers P. (2011) *Ettlia oleoabundans* growth and oil production on agricultural anaerobic waste effluents. Bioresource Technology 102: 1675-1682

Young E.B., Beardall J. (2003) Photosynthetic function in *Dunaliella tertiolecta* (Chlorophyta) during a nitrogen starvation and a recovery cycle. Journal of Phycology 39: 897-905

Zouni A., Witt H.T., Kern J., Fromme P., Krauss N., Saenger W., Orth P. (2001) Cristal structure of photosystem II from *Synechococcus elongatus* at 3.8 Å resolution. Nature (London) 409: 739-743

Websites

www.britannica.org

www.chlamy.org

www.gruppohera.it

www.utex.org

Ringraziamenti

Giunta al termine di questo mio lungo percorso di studi trovo necessario e doveroso ringraziare coloro che mi hanno formato, assistito, aiutato e supportato durante questi anni.

Ringrazio innanzitutto il mio Tutore, la Prof.ssa Simonetta Pancaldi, per avermi dato la possibilità di intraprendere questo percorso, riponendo in me e nel mio lavoro una ferma fiducia, seguendomi costantemente con estrema professionalità, umanità e pazienza.

Un grazie ai miei cari colleghi, la Dott.ssa Costanza Baldisserotto ed il Dott. Lorenzo Ferroni, con i quali ho condiviso ogni giornata del mio lavoro. Li ringrazio non solo per ciò che mi hanno insegnato, permettendo il raggiungimento di una mia autonomia in laboratorio, ma anche per la loro cordialità, allegria ed amicizia. Non posso non scusarmi con loro per la pazienza che hanno avuto nei momenti in cui, un po' sotto pressione, risultavo alquanto brontolona..

Ringrazio inoltre il Prof. Rino Cella (Università di Pavia) per avermi ospitato più volte presso il suo Laboratorio, permettendomi di acquisire nuove competenze che hanno portato all'ottenimento di risultati descritti in questa Tesi. Un grazie anche al Dott. Paolo Longoni e alla Dott.ssa Laura Pantaleoni, anche per la sua ospitalità, come sempre impeccabile. Al Dott. Tomas Morosinotto (Università di Padova) va invece il mio ringraziamento per il supporto prestato durante la rielaborazione dei dati ottenuti all'HPLC, ed a Stefania Basso per avermi affiancato durante le analisi. Infine, un grazie particolare alla Prof.ssa Eva-Mari Aro (Università di Turku, Finlandia) per avermi dato la possibilità di frequentare i suoi Laboratori durante la scorsa estate, permettendomi di vivere un'esperienza unica sia dal punto di vista lavorativo che personale, alla Dott.ssa Yagut Allahverdiyeva, per i suoi insegnamenti e la critica discussione dei dati ottenuti e a Maija Hölstrom, per il suo prezioso affiancamento durante la mia permanenza a Turku.

Come non ringraziare, poi, tutti coloro che da casa mi hanno incoraggiata e sostenuto, soprattutto durante quest'ultimo anno, particolarmente difficile per tutti. Ai miei amici, il ringraziamento per la loro comprensione durante i periodi di assenza nei loro confronti. A tutta la mia famiglia, a Valeria e Renzo per avermi aiutata, supportata, confortata e anche.. ospitata facendomi sentire come a casa.

Ai miei genitori, a cui dedico questa Tesi, per il loro infinito aiuto, senza il quale forse non ce l'avrei fatta. Vedermi realizzata è uno dei loro desideri più grandi, non finirò mai di ringraziarli per tutto ciò che fanno per me ogni giorno.

Infine, ringrazio Mirco, immensamente paziente, compagno di vita, di avventure.. e di sventure!